

Predicting the tactile properties of fabrics from vision and touch

Qinyuan Li

Submitted in accordance with the requirements for the degree of
Doctor of Philosophy

The University of Leeds
School of Design

April 2025

The candidate confirms that the work submitted is his/her own, except where work which has formed part of jointly-authored publications has been included. The contribution of the candidate and the other authors to this work has been explicitly indicated below. The candidate confirms that appropriate credit has been given within the thesis where reference has been made to the work of others.

The following publications were produced in the course of this research:

Li, Q., Xiao, K., & Mao, N. 2024. An investigation of the perceived tactile properties using fabric images, videos, and real fabrics. In CEUR Workshop Proceedings (CEUR-WS. org). CEUR Workshop Proceedings. Referred to Chapter 3 and Chapter 5.

Li, Q., Xiao, K., Pointer, M., & Mao, N. 2023. The Role of Colour and Texture on Fabric Image Preference. In Color and Imaging Conference (Vol. 31, No. 39, pp. 221-226). Society for Imaging Science & Technology. Referred to Chapter 3.

Li, Q., Xiao, K., Pointer, M., & Mao, N. 2023. The correlation of tactile properties of fabrics between visual and touch. *Journal of Vision*, 23(9), 5109-5109. Referred to Chapter 3 and Chapter 4.

Li, Q., Xiao, K., Mao, N., & Pointer, M. 2022. Visual judgement of the tactile properties of fabrics by altering colours. In: Proceedings of the AIC 15th Congress 2022 International Colour Association (AIC). Referred to Chapter 3 and Chapter 4.

One work has been submitted to *Transactions on Applied Perception* and is under reviewing by the time of submission:

Li, Q., Xiao, K., Pointer, M., Mao, N. 2024 November. Perceiving the tactile properties of the fabrics using fabric images, fabric videos, and real fabrics. *Transactions on Applied Perception*. Referred to Chapter 3 and Chapter 5.

Acknowledgement

Firstly, I would like to express my sincere gratitude to my supervisor, Professor Kaida Xiao. With his constant support, guidance, and encouragement, I have a deeper understanding what is research and what is the appropriate attitude towards research. I also would like to thank my co-supervisor Professor Ningtao Mao, for his great contribution and guidance in building the database. I feel so lucky to be the student of them.

A special thank goes to Dr Michael Pointer, who endlessly help and encourage me since the very start of my research career. His book Measuring Colour, and all his lectures greatly helped me build a systematic view of colour science. I am always touched and inspired by his patience to younger generation and his passion towards colour science. I also would like to appreciate Professor Ming Ronnier Luo, who encouraged my study on colour science when I was in Zhejiang University. Appreciate also goes to Dr Yan Lu and Dr Ruili He. Their attitude in PhD research continuously inspired me during these years.

I would like to express my deepest appreciate to my parents for their unconditional love and support. I am so fortunate to be their daughter and be in a lovely family. I also wish both of my grandfathers will be proud of me on the other side.

Lastly, I would like to thank Mr Peifan Xin, for his love, patience, and support. Every day I spend with you brings me so much happiness.

Abstract

Fabric is one of the biggest markets in the world, as nearly everyone is a consumer of fabrics. Tactile properties of fabrics convey vital information and influence consumer decision and satisfaction. With the rapid development of online shopping, consumers face new challenges, including predicting the tactile properties based on fabric images presented on displays and bridging the gap between visual perception and actual tactile perception. Moreover, the understanding of the tactile properties remains uncomplete due to the multiple tactile properties, the various conditions under which they are assessed, various influencing factors, and the limited efforts made on prediction.

The aim of the present study is to provide a consumer-friendly investigation of the perception of fabric tactile properties. A Leeds Fabric Tactile Database was developed and used in a series of psychophysical experiments to achieve the aim. The database consisted of two parts: Part I included colour-rendered fabric images (flat and draped) along with the corresponding real fabrics, and Part II included real fabric images (flat and draped), fabric rotation videos, and the corresponding real fabrics.

Experiment Phase I was carried out using Part I, evaluating flexible-stiff, smooth-rough, soft-firm, spongy-crisp, and warm-cool under the conditions of flat fabric images, draped fabric images, and touching the fabrics without seeing them (touch-only). The effect of individual fabrics, colour, and experiment conditions was analysed, together with the correlations among experiment conditions and among tactile properties.

Following the experiment Phase I, the experiment Phase II was conducted using database Part II. The experiment conditions were expanded to cover all real-life scenarios of human-fabric interaction, with newly added conditions including fabric rotation videos, viewing the fabrics but not touching them (vision-only using real fabrics), and viewing the fabrics while simultaneously touching them

(vision+touch). In addition to the analyses of factors and correlations, predictors were extracted from fabric images and videos to model the perception of fabric tactile properties.

All the psychophysical experiments in the present study applied the method of categorical judgement. The analyses were carried out in alignment with the categorical judgement framework, where each score carried a specific perceptual meaning. Taken together, the present study demonstrated a comprehensive investigation of the perception of fabric tactile properties. By using the fabric images and videos, good prediction can be achieved for the perception of fabric tactile properties.

Table of Content

Acknowledgement	iii
Abstract	iv
Table of Content	vi
List of Tables	xiv
List of Figures	xvi
Chapter 1 Introduction	1
1.1 Background	2
1.2 Aim and objectives	4
1.3 Outline of the thesis.....	5
Chapter 2 Literature review.....	8
2.1 Overview	9
2.2 The perception of fabric tactile properties	10
2.2.1 Tactile perception VS visual-tactile perception.....	10
2.2.2 Description of fabric tactile properties	12
2.2.2.1 Instrument-based description	12
2.2.2.2 Perceptual-based description.....	14
2.2.3 Fabric appearance	18
2.2.3.1 Structure difference	18
2.2.3.2 The effects of colours	21
2.3 Fabric database.....	22
2.4 CIE colorimetry.....	26
2.4.1 CIE standard illuminants	27
2.4.2 CIE colour-matching functions and standard observers.....	27
2.4.3 CIE standard geometric condition	30
2.4.4 CIE tristimulus values XYZ and chromaticity diagram.....	32
2.4.5 CIE uniform colour space	33

2.4.5.1	CIE u' , v' chromaticity diagram	33
2.4.5.2	CIELAB and CIELUV colour space	34
2.4.6	Colour difference formulae	36
2.5	Colour characterisation of camera	37
2.5.1	Camera settings	37
2.5.1.1	Exposure of light.....	38
2.5.1.2	White balance.....	38
2.5.2	Characterisation process	39
2.5.2.1	Characterisation methods.....	39
2.5.2.2	Colour charts	40
2.6	Colour characterisation of display	42
2.6.1	Calibration, characterisation, and gamma.....	42
2.6.2	Gain-Offset-Gamma (GOG) model	43
2.6.3	Channel independence and spatial independence	44
2.7	Colour measurement.....	45
2.7.1	Device-based measurement	45
2.7.1.1	Tele-spectroradiometer.....	45
2.7.1.2	Spectrophotometer	46
2.7.2	Image-based measurement	47
2.8	Psychophysical experiment methods.....	48
2.8.1	Scaling techniques	49
2.8.1.1	Categorical judgement.....	49
2.8.1.2	Pair comparison.....	51
2.8.1.3	Magnitude estimation and rank order	52
2.8.2	Threshold and matching techniques	52
2.8.3	Classification of psychophysical scales.....	53
2.9	Image processing techniques.....	54
2.9.1	Grey Level Co-occurrence Matrix (GLCM).....	54
2.9.2	2D Fast Fourier Transform (2D FFT)	57

2.9.2.1	Fourier Transform	57
2.9.2.2	Fast Fourier Transform	59
2.9.2.3	2D Fast Fourier Transform (2D FFT).....	59
2.9.2.4	Related studies.....	60
2.9.3	Wavelet Transform (WT)	60
2.9.4	A case of generating images from videos	62
2.10	Statistical analysis techniques.....	63
2.10.1	Central tendency and variability	64
2.10.2	z-standardisation.....	64
2.10.3	Normal distribution test.....	64
2.10.4	Pearson Correlation Coefficients.....	65
2.10.5	Mann-Whitney U test.....	66
2.10.6	Cumulative Link Mixed Model (CLMM)	67
2.10.7	Observer variability test.....	67
2.10.8	Regression techniques.....	68
2.10.8.1	Ordinal Least Square (OLS).....	68
2.10.8.2	Shrinkage techniques	69
2.10.9	Factors comparing model performance	70
2.10.9.1	Root Mean Square Error (RMSE).....	70
2.10.9.2	Coefficient of Determination (R^2).....	71
2.11	Summary	71
Chapter 3	Developing Leeds Fabric Tactile Database.....	73
3.1	Overview	74
3.2	Leeds Fabric Tactile Database preparation.....	74
3.2.1	Part I: colour-rendered fabric images and corresponding real fabrics.....	75
3.2.1.1	Real fabrics.....	75
3.2.1.2	Image capture.....	75
3.2.1.3	Colour rendering.....	76

3.2.2	Part II: real fabrics and their visual representations	77
3.2.2.1	Real fabrics.....	77
3.2.2.2	Fabric visual representation (images and videos).....	78
3.3	Experimental preparation	79
3.3.1	Camera characterisation	79
3.3.2	Display characterisation	80
3.3.3	Image processing	81
3.4	Experiment Phase I	83
3.4.1	Tactile properties	83
3.4.2	Tactile perception experiments.....	83
3.5	Experiment Phase II.....	86
3.5.1	Tactile properties	86
3.5.2	Tactile perception experiments.....	86
3.6	Summary	88
Chapter 4	Experiment Phase I: factors and correlations for visual-tactile and tactile perception	90
4.1	Overview	91
4.2	Statistical analysis.....	91
4.3	Observer variability.....	94
4.4	Normal distribution	95
4.5	The effect of fabric, colour, and experiment condition on visual-tactile perception.....	96
4.6	The correlations of tactile perceptual ratings among experiment conditions.	100
4.7	The correlations among the tactile perceptual ratings under each experiment condition	103
4.8	A further analysis of the effects of colour on the perceived warm-cool: CLMM model with three-way interactions.....	104
4.9	Discussion	105

4.9.1 The practical effects of colour for warm-cool.....	106
4.9.2 Individual fabrics largely affected the fitted tactile perceptual ratings based on CLMM models	108
4.10 Summary	109
Chapter 5 Experiment Phase II: correlations for visual-tactile and tactile perception	110
5.1 Overview	111
5.2 Statistical analysis	111
5.3 Observer variability.....	112
5.4 The differences of the visual-tactile perception between three viewing angles of draped fabric images	113
5.5 The correlations of the tactile perceptual ratings among the experiment conditions	114
5.5.1 Comparisons with Section 4.6: the consistency and discrepancy in using rendered and real fabric images.....	117
5.6 The correlations among tactile perceptual ratings under each experiment condition	117
5.6.1 Comparison with Section 4.7: the consistency and discrepancy in correlations among tactile properties	120
5.7 The differences of the tactile perceptual ratings between using visual representations and real fabrics	121
5.8 Discussions	124
5.8.1 The similar role of draped fabric images and fabric rotation videos in the tactile perception	124
5.8.2 Positively and negatively correlated tactile properties.....	125
5.8.3 Comparisons of the correlations between fabrics and images in Leeds Fabric Tactile Database Part I and Part II.....	127
5.9 Summary	129
Chapter 6 Experiment Phase II: factors for visual-tactile and tactile	

perception.....	131
6.1 Overview	132
6.2 Statistical analysis	132
6.3 Normal distribution test.....	134
6.4 The effects of fabric structures on visual-tactile perception and tactile perception.....	135
6.4.1 The distribution of tactile perceptual ratings for woven and knitted fabrics, respectively.....	135
6.4.2 The fixed effects and interaction of fabric structures and experiment conditions	137
6.4.3 The fitted perceptual ratings for woven and knitted fabrics.....	139
6.5 The effects of measured fabric colours on the tactile perception	142
6.6 The different correlations for woven and knitted fabrics.....	144
6.6.1 The correlations of the tactile perception among experiment conditions for woven and knitted fabrics, respectively	144
6.6.2 The correlations among tactile perceptions under each experiment condition for woven and knitted fabrics, respectively	146
6.7 Discussion	147
6.7.1 The different perception of fabric tactile properties in woven and knitted fabrics	147
6.7.2 The practical effect of colour based on CLMM models on the tactile perception	149
6.8 Summary	150
Chapter 7 Modelling the visual-tactile and tactile perception	152
7.1 Overview	153
7.2 Feature extraction	153
7.2.1 Fabric draped width extracted from fabric rotation videos	154
7.2.2 Fabric width for draped fabric images	155
7.2.3 Fabric 3D appearance	155

7.2.4	Grey-level Co-occurrence matrix (GLCM).....	156
7.2.5	2D Fast Fourier Transform (2D FFT)	158
7.2.6	Wavelet transform (WT)	159
7.3	Modelling procedure.....	162
7.3.1	Dependent variables and the corresponding predictors.....	162
7.3.2	Correlations between dependent variables and predictors and interrelationships of predictors	163
7.3.3	Regression techniques.....	166
7.3.3.1	Ridge Regression (RR)	166
7.3.3.2	Least Absolute Shrinkage and Selection Operator Regression (LASSO) technique.....	166
7.3.3.3	The Elastic Net Regression (EN).....	167
7.3.3.4	Ordinary Least Squares Regression (OLS).....	166
7.3.4	Training and testing datasets	166
7.4	Model performance and comparisons	167
7.4.1	Comparisons between regression techniques	167
7.4.2	Comparisons of predictive power among target conditions	169
7.4.3	Comparisons of the predictive power among tactile properties....	172
7.5	Ranking of predictors by EN and LASSO.....	175
7.6	Models excluding thickness as a predictor.....	178
7.7	Discussion	179
7.7.1	Flat fabric images in visual-tactile and tactile perception and prediction.....	179
7.7.2	Relatively lower RMSE and R^2 in the models of spongy-crisp	181
7.7.3	The role of fabric draped width in prediction	182
7.7.4	Limitations of the models and corresponding solutions applied ...	183
7.8	Summary	185
Chapter 8	Conclusions	187
8.1	Overview	188

8.2	The effect of individual fabrics and fabric structures	189
8.3	The effect of rendered colour and measured colour of fabrics.....	190
8.4	The correlations among experiment conditions and among tactile properties.....	190
8.5	The differences in the perception of tactile properties across different conditions	191
8.6	Model performance	192
8.7	Summary and contributions.....	192
8.8	Future work	194
Reference.....		196
List of Abbreviations		215
Appendix A: the fabric materials in Leeds Fabric Tactile Database		217
Appendix B: Ethical approval for the experiment Phase I and Phase II..		222

List of Tables

Table 2.1 Studies that evaluating visual-tactile perception and tactile perception under different conditions.....	10
Table 2.2 Summary of the tactile description/attributes in previous studies.	17
Table 2.3 Summary of fabric databases.	22
Table 2.4 Previous studies used categorical judgement to assess tactile properties.	50
Table 2.5 Four types of psychophysical scales, and their properties and examples (Fairchild, 2013; Stevens, 1946).	54
Table 3.1 CIE LAB values of the selected 16 colours.	76
Table 3.2 GOG model of the BenQ display.....	81
Table 4.1 Observer variability in the experiment Phase I.	95
Table 4.2 The results of Shapiro-Wilk test for the experiment Phase I....	95
Table 4.3 Comparisons between CLMM models with and without three-way interactions for the experiment Phase I.	97
Table 4.4 The fixed effects in all CLMM models and their significance for the experiment Phase I.....	98
Table 4.5 The Pearson Correlation Coefficients of the tactile perceptual ratings between vision and touch, and between using flat and draped fabric images.	100
Table 4.6 The fixed effects in warm-cool CLMM models with three-way interaction.	105
Table 4.7 Parameter estimates (β) of L^* , a^* , b^* in the full CLMM model for warm-cool.	105
Table 5.1 Observer variability in the experiment Phase II.	113
Table 5.2 RMS values for draped fabric images in three observing angles.	113
Table 5.3 Comparison of the Pearson Correlation Coefficients (r) between	

Section 4.6 (left) and Section 5.5 (right).	117
Table 6.1 The results of Shapiro-Wilk test for the experiment Phase II.	134
Table 6.2 The results of Mann-Whitney U test.	136
Table 6.3 Comparisons between CLMM models with and without interactions (fabric structures*experiment conditions) for the experiment Phase II.	137
Table 6.4 The fixed effects in all CLMM models and their significance for the experiment Phase II.	138
Table 6.5 Comparisons between CLMM models with and without three-way interactions for the experiment Phase II.	143
Table 6.6 CLMM models parameter estimates of the fixed effects L^* , a^* , and b^*	143
Table 7.1 Models predicting the tactile perception under the corresponding conditions, and the corresponding predictors.	162
Table 7.2 Comparisons of OLS, RR, LASSO, EN for predicting visual-tactile and tactile perception, based on the average RMSE and R^2 values.	168
Table 7.3 The best model trained by EN for all tactile properties, including predictors from the corresponding image category, assessed by RMSE and R^2	174
Table 7.4 Rank of top 10 predictors for visual-tactile perception models and the best models for tactile perception in Table 7.3.	175

List of Figures

Figure 1.1 The structure of the thesis.....	6
Figure 2.1 Left: plain weave. Middle: twill weave. Right: satin weave. Black represents the yarn underneath the interlacing structure. White represents the yarn above the interlacing structure. Figures are reproduced from Breen and House (2000, p.15).	19
Figure 2.2 The interloped knitted structure. The figure is from Breen and House (2000, p.126).	19
Figure 2.3 Examples of woven (top three) and knitted (bottom three) fabrics in the present study.....	20
Figure 2.4 Triangle of colour. The image of X-Rite ColorChecker® Classic chart was downloaded from X-Rite (2025a).	27
Figure 2.5 The spectral sensitivity of cones (solid lines) and rod (broken line). The figure is from Hunt and Pointer (2011, p.6).	28
Figure 2.6 The principle of trichromatic colour matching. The figure is from Hunt and Pointer (2011, p.25).	28
Figure 2.7 The initial colour-matching functions $r\lambda, g\lambda, b(\lambda)$. The figure is from Hunt and Pointer (2011, p.30).	29
Figure 2.8 The CIE colour-matching functions $x\lambda, y\lambda, z(\lambda)$. Solid line: CIE 2° observer. Broken lines: CIE 10° observer. The figure is from Hunt and Pointer (2011, p.34).	30
Figure 2.9 Four CIE standard geometries of illumination and viewing/measurement. Figure is from Hunt and Pointer (2011, p.104)	30
Figure 2.10 CIE xy chromaticity diagram. The figure is from Hunt and Pointer (2011, p.48)	33
Figure 2.11 The CIE u', v' chromaticity diagram. The figure is from Hunt and Pointer (2011, p.49).	34
Figure 2.12 Left: CIELAB uniform colour space. Right: CIELUV uniform	

colour space. The right figure is from Hunt and Pointer (2011, p.54).

.....	35
Figure 2.13 Colour charts. (a) X-Rite ColorChecker® Classic chart, (b) ColorChecker® Digital SG chart, (c) GretagMacbeth ColorChecker® DC, and (d) DigiEye calibration chart DigiTizer. All charts were captured by Digieye colour measurement system.....	41
Figure 2.14 Left: Pantone skin tone guide (Pantone, 2025a). Right: Pantone fashion, home + interiors colour guide (Pantone, 2025b)...	42
Figure 2.15 Digieye colour measurement system. Figure was downloaded from Verivide (2025).	48
Figure 2.16 Example of the procedures to generate GLCM. Figure was reproduced from Haralick et al. (1973).	55
Figure 2.17 Interpretation of Fourier Transform. The figure is from Brigham (1988, p.5)	58
Figure 2.18 Decomposition of an image by 2D WT. The figure is reproduced from Chang and Kuo (1993). LL: Low-Low, LH: Low-High, HL: High-Low, HH: High-High.	62
Figure 2.19 An example of the horizontal space*time slice from Bouman et al. (2013, p.1984 & 1985).	63
Figure 2.20 Visualisations of a normally distributed dataset. Left: distribution. Right: Q-Q plot.	65
Figure 2.21 Examples of perfectly positive correlation (left), perfectly negative correlation (middle), and nearly no correlation (right).	66
Figure 2.22 Minimising the residual sum of squares. The figure is from (Hastie et al., 2009, pp.45)	68
Figure 3.1 Experiments Overview.	74
Figure 3.2 The schematic diagram for capturing flat fabric images (left) and draped fabric images (right).....	76
Figure 3.3 The distribution of the selected 16 colours in CIE a^*b^* (left) and CIE C^*L^* (right) colour space.....	77

Figure 3.4 The distribution of fabric colours in CIE a^*b^* (left) and CIE C^*L^* (right) colour space.	78
Figure 3.5 The top view schematic representation of the rotating fabrics. Left: drape_0. Middle: drape_45. Right: drape_90.	79
Figure 3.6 Workflow of the image processing for the Leeds Fabric Tactile Database.	82
Figure 3.7 Experiment Phase I: interfaces and scene. First row: experiment 1 (flat fabric images). Middle row: experiment 2 (draped fabric images). Last row: experiment 3 (touch-only).	86
Figure 3.8 Experiment Phase II: scenes when vision was allowed only (first figure), and when both touch and vision was allowed (second figure).	88
Figure 4.1 The fitted perceptual ratings of each fabric for all visual-tactile perceptions perceived from flat fabric images and draped fabric images.	99
Figure 4.2 Individual fabrics in Leeds Fabric Tactile Database Part I....	100
Figure 4.3 The correlations of the average perceptual ratings between touch-only condition and using flat (blue) and draped fabric images (red). Error bar indicates the standard deviation (SD) of the tactile perceptual ratings across 16 colours for each fabric.	103
Figure 4.4 The correlations among tactile perceptual ratings under each experiment condition.....	104
Figure 5.1 The Pearson Correlation Coefficients between each experiment condition.	115
Figure 5.2 The Pearson Correlation Coefficients between each pair of tactile properties under the experiment conditions.	119
Figure 5.3 Comparisons of the correlations of the perception among tactile properties. Below diagonal: using rendered fabric images (Section 4.7). Above diagonal: using real fabric images (Section 5.6).....	121
Figure 5.4 Comparisons between the tactile perception perceived from	

visual representations (images and videos) and real fabrics.....	123
Figure 5.5 The correlation between fabric thickness and the perception of warm-cool, flexible-stiff, smooth-rough, soft-firm, and spongy-crisp under each experiment condition.....	127
Figure 5.6 Comparison of the fabric thickness between fabrics in Leeds Fabric Tactile Database Part I and Part II.	128
Figure 6.1 The distribution of the raw data for each pair of tactile properties under each experiment condition.....	136
Figure 6.2 The comparisons of the fitted tactile perception between fabric structures.	139
Figure 6.3 Quantified differences of the fitted perceptual ratings between woven and knitted fabrics for all tactile properties under each experiment condition.....	141
Figure 6.4 The correlations among experiment conditions for each pair of tactile properties. Above diagonal: woven fabrics. Below diagonal: knitted fabrics.....	145
Figure 6.5 The correlations among tactile properties under each experiment condition. Above diagonal: woven fabrics. Below diagonal: knitted fabrics.....	147
Figure 7.1 space*time slice with space on the horizontal axis and time on the vertical axis.	154
Figure 7.2 Computing the fabric draped width in fabric rotation videos.	155
Figure 7.3 time*space slice with time on the horizontal axis and space on the vertical axis.	156
Figure 7.4 Computing GLCM features for draped fabric images and time*space slices. 'X' in red means excluding the grey level 0 in GLCM.	158
Figure 7.5 An example of the draped fabric image after WT decomposition up to level 6.	160
Figure 7.6 The correlations between tactile perceptual ratings and	

corresponding predictors, and interrelationships among predictors.

..... 164

Figure 7.7 EN model performance assessed by RMSE (left) and R^2 (right).

Comparisons focused on differences among target conditions. Black lines indicate the median values from the 50 repeats. Boxes indicate IQR. 171

Figure 7.8 EN model performance assessed by RMSE (left) and R^2 (right).

Comparisons focused on the differences among tactile properties. Black horizontal lines indicate the median values from the 50 repeats. Boxes indicate IQR. 173

Figure 7.9 Comparison of tactile perception EN models between excluding

and including thickness, assessed by RMSE (left) and R^2 (right) from 50 repeats. Black lines indicate the median values. Boxes indicate IQR.

..... 179

Figure 7.10 The range of original tactile perceptual ratings averaged across

all observers. Black lines indicate the median values. Boxes indicate IQR. 181

Figure 7.11 Left: The test apparatus of fabric drape. Figure is from British

Standards Institution (1073, p.3). Right: the calculation of drape ratio: $(A-B)/(C-B)*100\%$, reproduced from Carrera-Gallissa et al. (2017).

..... 183

Chapter 1

Introduction

1.1 Background

The tactile properties of the fabric are of great importance in the textile industry and potentially contribute to the applications of textiles in computer virtual reality, 3D printing, remote surgery, and product design (Basdogan et al., 2004; Griffiths and Kulke, 2002; Rabin and Gordon, 2004). However, given the widespread use of smart electronic products, for example, for internet shopping, the judgement of the tactile properties of fabrics relies on images rather than actual products. Viewing the images of the fabrics may results in a different perception than viewing and touching the physical fabrics. When buying online, it is one thing to be able to see a fabric on a display, but the visual impression of the tactile response is an important influence on a customer's decision to make a purchase.

Conventional methods to define the tactile properties of fabrics rely on instruments or other devices, such as Kawabata Evaluation System for Fabric (KES-F system), Fabric Assurance by Simple Testing (FAST system), the Leeds University Fabric Handle Evaluation System (LUFHES), and tactile sensors. The measured data are calculated to give scores to represent the tactile properties. Devices such as tactile sensors give signals reproducing human movement when touching the surface, which enhances the understanding of the tactile properties and benefits the development of robots (Gao et al., 2016; Chu et al., 2013; Luo et al., 2018). However, the notable limitations of such instruments are that they are not consumer friendly. The general public normally had no access to professional devices, and the generated data are difficult for consumers to interpret. Furthermore, such objective measurement results cannot represent the subjective human perception of the tactile properties when either fabric images or real fabrics are available.

Apart from the above, psychophysical experiments have been conducted to study the subjective human perception of tactile properties. In virtually all

experiments, observers were presented either with the real fabric (Baumgartner et al., 2013; Wijntjes et al., 2019; Mirjalili et al., 2019) or fabric images and videos (Bouman et al., 2013; Winjintjes et al., 2019) or both (Xiao et al., 2016; Wijntjes et al., 2019) under the corresponding conditions (vision, touch, or both). With a few notable exceptions, these studies generally evaluated the perceived tactile properties using a single format of the fabric. The exceptions include a study that conducted three separate experiments to evaluate the tactile perception using fabric images and videos by means of rating scales; using real fabrics when one touched the fabric and the other observed the fabric and the process; using both by the means of a match-to-sample task (Wijntjes et al., 2019). In addition, a study that investigated the correspondence between the visual and haptic perception of roughness, and so on, used a rating scale method, which showed high correlations between visual and haptic modalities (Baumgartner et al., 2013). Drewing et al. (2009) evaluated the softness of rubber under haptic-only, vision-only, and visuo-haptic conditions separately by means of magnitude estimation and claimed that the perceived softness was significantly different. Overall, the methods and fabric formats used in the previous studies were mixed, and none considered all the fabric formats in real-life scenarios and used a consistent method. It remains unknown whether the perception of tactile properties is correlated between using images and videos, and actual touch and observation of real fabrics.

Moreover, different tactile properties were evaluated individually or collectively in the previous studies. There are similarities and overlap among them. For example, stiffness and smoothness were studied in (Pan 2006; Bacci et al., 2012; Bouman et al., 2013), and their antonyms flexibility and roughness were studied in (Baumgartner et al., 2013; Mahar et al., 2013; Mao, 2014). Even so, it is not known whether these tactile properties are correlated, particularly under the different evaluation conditions due to the various methods applied in previous studies.

There are also large effects of fabric itself on the perception of tactile properties. Almost infinite fabric appearances are available due to the variations of fabric structures and colours (Breen and House, 2000). Since consumers rely on the fabric appearance to judge the tactile properties when buying online, it is important to study the individual effect of fabric structure and colour by effectively isolating the two variables. Previous studies used either woven fabrics (Rombaldoni et al., 2010; Kawabata, 1984; Chae et al., 2011), knitted fabrics (Jeguirim et al., 2010; Mahar et al., 2013; Suzuki and Sukigara, 2013), or selected fabrics based on the materials. The differences between fabric structures in the perception of tactile properties remain unclear. Moreover, colour is less investigated and not satisfactorily evaluated in a scientific colour space.

1.2 Aim and objectives

The aim of the present study is to investigate the perception of fabric tactile properties through images, videos, and actual touch and observation, and model the perception for the purpose of benefitting the public consumers in practical insights. After conducting a comprehensive literature review, separate objectives were set:

- To investigate the effects of fabric structure, colour, and evaluated conditions on the visual-tactile and tactile perception (Chapter 4, Chapter 6).
- To investigate the correlations among different conditions and among tactile properties for all data (Chapter 4, Chapter 5) and for data collected for woven and knitted fabrics separately (Chapter 6).
- To investigate the differences in tactile perceptual ratings collected between images/videos and real fabrics (Chapter 5).
- To model the visual-tactile and tactile perception through fabric images and

videos (Chapter 7).

To achieve the specific objectives, the first task is to develop a database to be used in the experiment. The specific requirements of the database include:

- It is necessary to introduce variable control in the database, i.e., the same fabric in different colours and different fabrics in the same colour. This allows for independent investigations into the effects of fabric appearances.
- The images in the database are supposed to comprehensively represent the fabric's appearance, including flat-state appearance, draped-state appearance, and 360-degree appearance in the draped state.
- The database should allow for the continuous addition of new samples.

The approach taken in the present study is psychophysical experiment, collecting the participants' responses to evaluate the visual-tactile and tactile perception.

1.3 Outline of the thesis

The structure of the thesis follows the research process of the present study, as shown in Figure 1.1. An overview of the thesis is given below.

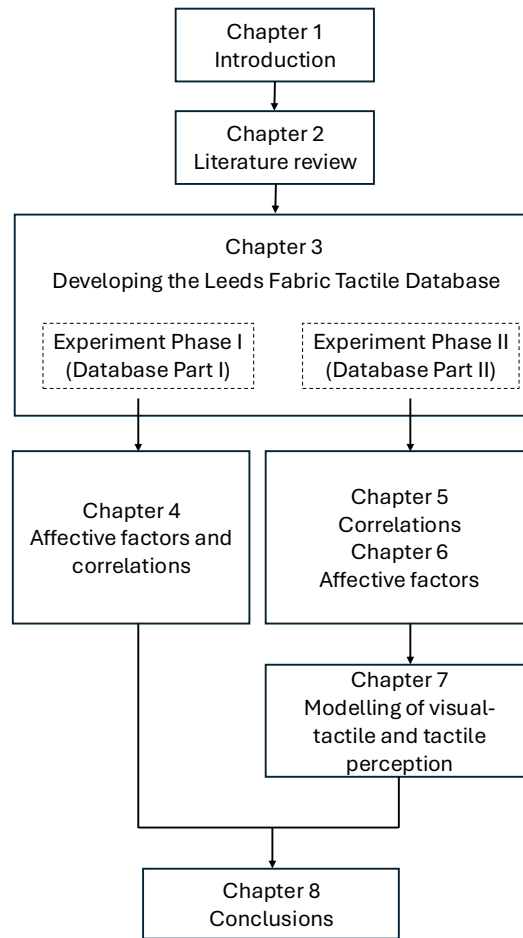


Figure 1.1 The structure of the thesis.

The current Chapter 1 describes the research background, aim and objectives, and the structure of the thesis.

Chapter 2 introduces the comprehensive literature review, including the perception of tactile properties, the existing fabric database, the fundamental of CIE colorimetry, the process of camera and display colour characterisation, psychophysical experiments, and data analysis techniques.

Chapter 3 describes the development of Leeds Fabric Tactile Database, and all aspects of experiment preparation. Experiment Phase I was firstly conducted using Leeds Fabric Tactile Database Part I, evaluating the perception of flexible-stiff, smooth-rough, soft-firm, spongy-crisp, and warm-cool using flat fabric images, draped fabric images, and under the condition of touch-only. Experiment Phase II used Leeds Fabric Tactile Database Part II. In addition to

the three experiment conditions in experiment Phase I, three more experiment conditions: fabric rotation video, vision-only (using real fabrics), vision+touch were added in the experiment Phase II.

Chapter 4 provides the analysis of data collected in the experiment Phase I. The effects of individual fabrics, colours, and experiment conditions were evaluated. The correlations of the tactile perceptual ratings were analysed among experiment conditions and among tactile properties.

Chapter 5 focuses on the tactile perceptual ratings averaged from all participants in the experiment Phase II. The correlations among experiment conditions and among tactile properties were evaluated, and comparisons were made between experiment Phase I and Phase II. In addition, the tactile perceptual ratings were compared between using images/videos and real fabrics.

Chapter 6 focuses on the effect of fabric structure, colour, and the interaction between fabric structures and experiment conditions, using data collected in the experiment Phase II. The fabric structures were categorised into woven and knitted fabrics. The correlations among experiment conditions and among tactile properties were analysed for woven and knitted fabrics separately to further compare the two fabrics structures.

Chapter 7 provides the modelling procedure and model performance for visual-tactile and tactile perception. Predictors were extracted from flat fabric images, draped fabric images, fabric rotation videos, respectively. The predictive performance was compared among regression techniques, among conditions, and among tactile properties.

Chapter 8 summarises the major findings in the present study. The contributions of the entire study are identified.

Chapter 2

Literature review

2.1 Overview

In this Chapter, the background information and related work was reviewed. Here is the outline:

Section 2.2 provides an overview of the perception of fabric tactile properties. The term ‘tactile perception’ and ‘visual-tactile perception’ is identified and differentiated for the present study. Previous studies evaluated tactile properties using a mix of tactile attributes under a mix of evaluation conditions. The effect of the fabric appearance including fabric structure and fabric colour remains unclear.

Section 2.3 reviews the existing fabric databases and demonstrates the necessity to develop a Leeds Fabric Tactile Database for a comprehensive evaluation of tactile and visual-tactile perception.

Section 2.4 introduces the CIE colorimetry which is the foundation of colour specification. It is the tool for correcting images and specify colours of fabrics in the present study.

Section 2.5 and **Section 2.6** introduce the principles and the pipelines to characterise the fabric images in the Leeds Fabric Tactile Database, including the camera colour characterisation and display colour characterisation.

Section 2.7 introduces the methods for colour measurement, which is a necessary step in colour characterisation and fabric colour specification to ensure an accurate reproduction.

Section 2.8 introduces the psychophysical techniques used in the tactile-related studies and in the present study.

Section 2.9 introduces the image processing techniques. In the present study, fabric images and videos are processed by these techniques to extract the features. Those features are used as predictors in Chapter 7 to model the tactile and visual-tactile perception.

Section 2.10 introduces the statistical methods and modelling techniques used in the present study.

2.2 The perception of fabric tactile properties

2.2.1 Tactile perception VS visual-tactile perception

The textile industry is possibly the largest market in the world, as all humans are consumers of garment. As an everyday product, the appearance and the tactile properties of fabrics attract consumers' attention during purchase decision. As online shopping continues to expand globally, purchasing decisions are made based on not only the real fabric products, but the fabric images present on the digital display. To distinguish between tactile perception derived from real fabrics and that inferred from visual stimuli such as images and videos in the present study, 'tactile perception' refers to the perception through direct interaction with real fabrics, and 'visual-tactile perception' describes the tactile impression formed through images and videos. Table 2.1 lists example studies that evaluated human visual-tactile and tactile perception using various modalities, including image only, video only, touch-only, vision-only (using real fabrics), vision+touch, and any combination of these.

Table 2.1 Studies that evaluating visual-tactile perception and tactile perception under different conditions.

Conditions		References
Visual-tactile perception	Images	Experiment II from Wijntjes et al. (2019) Takahashi and Tan (2019)
	Videos	Bouman et al. (2013) Experiment II from Wijntjes et al. (2019)
Tactile perception	Touch-only	Baumgartner et al. (2013) Drewing et al. (2009) Fenko et al. (2010)
	Vision-only (using real fabrics)	Baumgartner et al. (2013) Drewing et al. (2009) Experiment III from Wijntjes et al. (2019) Fenko et al. (2010)

Vision+touch	Mehta et al. (2024) Yenket et al. (2007) Drewing et al. (2009) Experiment III from Wijintjes et al. (2019) Soufflet et al. (2004) Rombaldoni et al. (2010)
A combination of images and real fabrics	Experiment I from Wijintjes et al. (2019) Xiao et al. (2016)

Wijintjes et al. (2019) designed three experiments to evaluate tactile perceptions. Experiment I involved a combination of fabric images, videos, and touch-only condition, using both real fabrics and visual stimuli to assess tactile matching accuracy. Experiment II focused only on fabric images and videos to assess the similarities between pairs of fabric samples, representing visual-tactile perception. In Experiment III, participants were asked to observe the touching interaction performed by another individual and judge the similarity between two fabric samples (vision-only using real fabrics). Xiao et al. (2016) adopted a similar way to Experiment I from Wijintjes et al. (2019), asking participants to match fabric images while touching real fabrics without visual access to the samples at the same time. Both of the experiments used fabric images and real fabrics at the same time, and thus it was hard to differentiate whether the perception originated from images or real fabrics.

In addition to the combination of experiment conditions, images and real fabrics were also used individually. Bouman et al. (2013) presented only fabric videos to participants and asked them to judge the fabric stiffness. Real fabrics were rated under the touch-only condition and vision-only condition (using real fabrics) separately. In the vision-only condition (using real fabrics), participants were asked to either observe the fabrics directly (Baumgartner et al., 2013) or observe the manipulation process by another participant (Drewing et al., 2009; Fenko et al., 2010). Besides, in the vision+touch condition, Yenket et al. (2007) focused on rating the tactile perception in which vision and touch were both

allowed. Soufflet et al. (2004) conducted three experiments in which participants freely sorted the fabrics, described the fabrics, and rated the tactile pleasantness, incorporating both touch and vision. Mehta et al. (2024) used fabric swatches mounted between two sheets of paper to ensure a fixed position, allowing participants to touch and rate the fabrics.

Overall, previous studies have primarily focused on assessing human tactile perception through real fabric samples, while only a limited number of studies have explored visual-tactile perception using images or videos. With a few notable exceptions, these studies generally evaluated the perceived tactile properties under limited conditions. The experiment conditions adopted in these studies were mixed, and none considered all possible scenarios in which fabric tactile perception occurs. Furthermore, the relationship between visual-tactile and tactile perception, and the overall correlations among all possible conditions have not been fully investigated. It is unclear whether the results obtained under one condition would remain consistent in another.

2.2.2 Description of fabric tactile properties

2.2.2.1 Instrument-based description

Over the years, instruments were developed to define the tactile properties of fabrics. Objective measurement serves as a powerful tool for the fabric quality control, and the corresponding standards have been widely adopted, enhancing communication between fabric manufactures and academics (Hu, 2004). For example, the Kawabata Evaluation System for Fabric (KES-F system) and Fabric Assurance by Simple Testing (FAST system) measures the low-stress mechanical properties of the fabrics (Hu, 2004; Kawabata, 1984; Minazio, 1995). Both systems mimic the real deformation process of fabric, while KES-F system measures the recovery process from deformation and FAST system measures the amount of deformation. Deformation including bending, compression and extension/tensile are tested in both systems. Surface friction is assessed from

KES-F system, while dimensional stability is only measured by FAST system.

When using KES-F system to evaluate fabric tactile properties, the results are debatable because it was developed to evaluate tactile properties based on the results from subjective tactile judgement from a panel of Japanese experts. FAST system was developed to measure similar deformation to KES-F, but no subjective judgement results were considered in the system. KES-F system is much expensive than FAST system, and both systems are time-consuming. Considering the above, instruments were further developed to evaluate the tactile properties. Comparisons were made between the measurement results from KES-F and FAST system, and between the newly developed instruments with KES-F and FAST (Yim and Kan, 2014; Strazdiene, 2011; Sun et al., 2018). Furthermore, studies have examined how the subjective tactile perception links with the objective measurement results (Strazdiene, 2011; Sun et al., 2018, Mazzuchetti et al., 2008; Bacci et al., 2012; Rombaldoni et al., 2010). Overall, good correlations were found between the subjectively perceived tactile attributes and objectively measured results. For example, the perception of stiffness was found to be closely correlated with the KES-F and FAST measurement results (Sun et al., 2018; Bacci et al., 2012), and the perception of softness closely correlated to the mechanical results measured by FAST system (Mazzuchetti et al., 2008; Bacci et al., 2012). In addition, stiffness, smoothness, and softness were found to be the first three most important components to describe the fabric hand assessed by extracting the fabric through a nozzle (Pan, 2006).

More recently, the Leeds University Fabric Handle Evaluation System (LUFHES) was developed by Mao (2014). In addition to measuring the displacement of deformation, LUFHES measures the energy consumed during fabric compression, twisting, and friction (Mao, 2014). The measured data are calculated to give scores to represent the tactile properties, including crispness, flexibility, sponginess, stiffness, stretchability, firmness, roughness, and

smoothness. In addition, devices such as tactile sensors give signals reproducing human movement when touching the surface, which enhances the understanding of the tactile properties and benefits the development of robots (Gao et al., 2016; Chu et al., 2013; Luo et al., 2018; Yuan et al., 2018; Xu et al., 2024).

However, the notable limitations of such instruments are that they are not available to the general public, and the generated data are difficult for consumers to interpret. Furthermore, such objective measurement results cannot represent the subjective human perception of the tactile properties when either fabric images or real fabrics are available. As the aim of the present study is not to explore the connection between objective measurement and subjective perception, the objective measurement will not be involved in the present study. The review of instruments and related studies in this section provides references for the tactile attributes, which are summarised in Table 2.2 in the next section (No.1 – 4 for instruments, No. 5 – 11 for studies evaluating specific tactile attributes).

2.2.2.2 Perceptual-based description

Different tactile attributes were evaluated individually or collectively in the previous studies. Guest et al (2011) developed a Touch Perception Task (TPT) that contained 26 adjectives by asking participants to rate how much the word related to the sense of touch, including warm, cool, soft, rough, smooth, firm, etc, together with 14 emotional descriptors. Experiments were conducted to identify and exclude descriptors in the sensory and emotional scales. After that, the TPT descriptors were adopted in other studies, most of which focused on the relationship between sensory and emotional descriptors on different materials and different skin sites (Ackerley et al., 2014; Bhatta et al., 2017). The results also showed that the TPT performed well in the discrimination of small differences in touch sensation (Ackerley et al., 2014). Ratings have also been used in studies focusing on different tactile attributes. For example, Fenko et al.

(2010) investigated the perception warmth of scarves, demonstrating that both scarf materials and colours affected the perceptual warmth. Bouman et al. (2013) examined the perception of stiffness and density of fabrics from videos, where good correlations were found between human perception and ground truth measurement. Additionally, another study rated 10 different attributes across 7 different materials (e.g., fabric, leather, fur, paper etc), revealing that hardness and roughness were the two dominant principal components under both touch-only and vision-only conditions (using real fabrics) (Baumgartner et al., 2013). Mehta et al. (2024) rated eight aspects of tactile properties and found that tactile sensitivity, including the frequency of working time with textiles and familiarity of textiles, significantly affected the tactile perception.

In addition to rating the tactile attributes, the methods of open-ended response and matching were also adopted in studies. Two tactile attributes, smoothness and softness, were recognised as two important factors on texture perception of fabrics (Mirjalili and Hardeberg, 2019). Wijintjes et al. (2019) designed a match-to sample task in which participants were asked to identify the correct fabric by touching in an unseen box, relying only on fabric videos and images. The experiment demonstrated the significant advantage of movies over images in fabric identification, while no differences were found in matching accuracy across different video styles. Similarly, Xiao et al. (2016) prepared flat and draped fabric images in RGB format and greyscale format. Participants were presented with a pair of images and were instructed to correctly position the two fabrics inside an unseen box. The results demonstrated that higher matching accuracy was achieved when using RGB images or draped fabric images.

Mahar et al. (2013) reviewed the tactile evaluation focused on knitted fabrics. Bipolar tactile descriptors were identified as important to next-to-skin knitted fabrics by five organisations. Even though no information about the organisations was provided in the review, the bipolar descriptors are useful references for comparisons with tactile attributes in other studies.

Considering all the above in Section 2.2.2, the tactile attributes are summarised and compared in Table 2.2. Notably, there are different tactile properties that were studied in previous work, but there is also similarity and overlap among them. For example, stiffness and smoothness were studied in Mao (2014), Yim and Kan, (2014), Sun et al. (2018), and Pan (2006), warmth was studied in Strazdiene (2011), Guest et al. (2011), Fenko et al. (2010), Baumgartner et al (2013), and Mahar et al. (2013), softness was studied in Yim and Kan (2014), Mazzuchetti et al. (2008), Bacci et al. (2012), Pan (2006), Guest et al. (2011), Mehta et al. (2024) and Mahar et al. (2013), and crispness was studied in Mao (2014) and Rombaldoni et al. (2010). The attributes used in different studies were mixed, and none of them made effective comparisons among different attributes and evaluate their interconnections. It is challenging for consumers to find comprehensive and explanatory information across studies investigating different tactile attributes that can help them understand the visual-tactile perception and tactile perception. Therefore, by reviewing the tactile attributes from previous studies, one of the objectives of this study is to choose representative tactile attributes and provide a clearer understanding for the public.

Table 2.2 Summary of the tactile description/attributes in previous studies.

No.	Tactile description/attributes	Methods
1	Tensile and shear, pure bending, compression, surface characteristics (fabric surface profile and coefficient of friction)	The Kawabata Evaluation System for Fabric (KES-F system) (Hu, 2004).
2	Compression, bending, extension, dimensional stability	Fabric Assurance by Simple Testing (FAST system) (Hu, 2004).
3	Crispness, flexibility, sponginess, stiffness, stretchability, firmness, roughness, smoothness	Leeds University Fabric Handle Evaluation System (LUFHES) (Mao, 2014).
4	Signals from tactile sensors	Reading data from tactile sensors (Gao et al., 2016; Chu et al., 2013; Luo et al., 2018; Yuan et al., 2018; Xu et al., 2024).
5	Smoothness, softness, stiffness	Correlation of the objective measurements between KES-F and PhabrOmeter system (Yim and Kan, 2014).
6	Falling, cold-warm, supple-rigid, responsive, crumple like	Correlation between sensory evaluation attributes and KEF-F results and Griff-Tester results (Strazdiene, 2011).
7	Stiffness, smoothness, fullness, formability, total hand	Correlation between the predicted tactile properties through Wool HandleMeter, KES-F results, and subjective evaluation on the listed attributes (Sun et al., 2018).
8	Softness	Correlation between the perceived softness and FAST measurement results (Mazzuchetti et al., 2008)
9	Stiffness, softness, force of compression, tensile stretch	Correlation between the perceived tactile properties and FAST results (Bacci et al., 2012).
10	"a feeling coming from a crisp fabric surface that gives a cool feeling"	Correlation between the perceived attributes and FAST measurement results (Rombaldoni et al., 2010)
11	Stiffness, smoothness, softness	The first three most important components to describe the fabric hand (Pan, 2006).
12	Warm, cool, soft, rough, smooth, firm, etc	Touch perception task (TPT) (Guest et al., 2011).
13	Warmth	Rate the warmth of materials including 10 difference scarves (Fenko et al., 2010).
14	Stiffness, density of fabrics	Measured how well observers could perceive the stiffness and density of fabrics from videos (Bouman et al., 2013).
15	Glossiness, colourfulness, roughness, orderliness, hardness, warmth, elasticity, friction, 3-dimensionality, texture.	Determine the first and second principal components for visual modality and haptic modality (Baumgartner et al., 2013).

16	Rough/smooth, hard/soft, bumpy/flat, sticky/slippy, scratch/slick, hairy/shorn, uniform/irregular, isotropic/anisotropic	To assess the tactile impact on tactile perception (Mehta et al., 2024)						
17	Smooth, soft, homogeneous, geometric variation, random, repeating, regular, colour variation, strong, complicated	Verbal description of the texture of the textiles (Mirjalili and Hardeberg, 2019).						
18	<table><tr><td><ul style="list-style-type: none">Slippy-stickySmooth-roughLimp-firm</td><td><ul style="list-style-type: none">Soft-harshClean-hairyCool-warm</td></tr><tr><td><ul style="list-style-type: none">Cool-warmStretchy-tightLofty-lean</td><td><ul style="list-style-type: none">Soft-harshSmooth/cleanStretch/resilienceFullness/bulk</td></tr><tr><td><ul style="list-style-type: none">Smooth-roughCool-warmTextured-cleanStretch-rigidDry-greasy</td><td><ul style="list-style-type: none">Soft-roughResilient-non-recoveryTexture-flatStretch-non-stretch</td></tr></table>	<ul style="list-style-type: none">Slippy-stickySmooth-roughLimp-firm	<ul style="list-style-type: none">Soft-harshClean-hairyCool-warm	<ul style="list-style-type: none">Cool-warmStretchy-tightLofty-lean	<ul style="list-style-type: none">Soft-harshSmooth/cleanStretch/resilienceFullness/bulk	<ul style="list-style-type: none">Smooth-roughCool-warmTextured-cleanStretch-rigidDry-greasy	<ul style="list-style-type: none">Soft-roughResilient-non-recoveryTexture-flatStretch-non-stretch	Reviewed important fabric handle descriptors for next-to-skin knitted fabrics from five organisations (Mahar et al., 2013).
	<ul style="list-style-type: none">Slippy-stickySmooth-roughLimp-firm	<ul style="list-style-type: none">Soft-harshClean-hairyCool-warm						
	<ul style="list-style-type: none">Cool-warmStretchy-tightLofty-lean	<ul style="list-style-type: none">Soft-harshSmooth/cleanStretch/resilienceFullness/bulk						
<ul style="list-style-type: none">Smooth-roughCool-warmTextured-cleanStretch-rigidDry-greasy	<ul style="list-style-type: none">Soft-roughResilient-non-recoveryTexture-flatStretch-non-stretch							
19	No attributes used	Match-to-sample task (Wijintjes et al., 2019; Xiao et al., 2016)						

2.2.3 Fabric appearance

When a fabric is present, it is usually judged from two aspects: what we see and what we feel. The former one is related to the appearance of the fabrics, and the latter one corresponds to the tactile properties. The last sections reviewed related studies evaluating different tactile properties under various conditions. This section reviews the appearance of the fabrics from the perspectives of structural differences and colour effects.

2.2.3.1 Structure difference

There are two major types of fabric structures: woven and knitted. The woven fabric has an interlaced structure with perpendicular warp and weft direction. The warp and weft intersect at the interlacing points, creating basic woven structures such as plain, twill, and satin weave (Breen and House, 2000). The weft yarn alternatively passes over and under each warp yarn to form the simple plain weave, passes over two warp yarns before going under the next to form

the twill weave, or floats over four or more warp yarns and then going under the next to form the satin weave. Figure 2.1 illustrates the three woven structures.

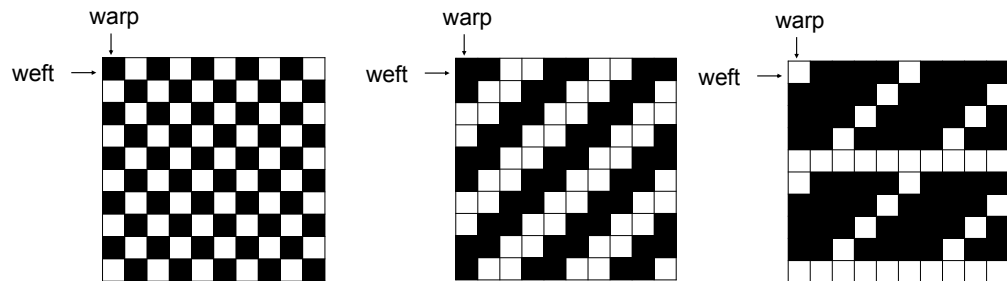


Figure 2.1 Left: plain weave. Middle: twill weave. Right: satin weave. Black represents the yarn underneath the interlacing structure. White represents the yarn above the interlacing structure. Figures are reproduced from Breen and House (2000, p.15).

Compared to the directly interlaced woven structure, knitted fabric has an interloop structure, where the loops interlock vertically and horizontally (Breen and House, 2000). The vertical direction is called the wale direction, and the horizontal direction is called the course direction. The interlooping describes how the yarns form interconnected loops and create the knitted structure. Figure 2.2 illustrates the wale and course directions, as well as the interloop structure.

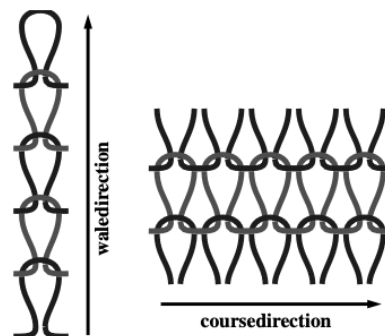


Figure 2.2 The interlooped knitted structure. The figure is from Breen and House (2000, p.126).



Figure 2.3 Examples of woven (top three) and knitted (bottom three) fabrics in the present study.

Figure 2.3 shows examples of the woven and knitted fabric from the Leeds Fabric Tactile Database in the present study (the database will be introduced in Chapter 3). It clearly illustrates the differences in appearance between woven and knitted fabrics, as well as the variations within each fabric structure. From the perspective of fabric structure, these differences result from the choice of fibre, the yarn weight, and the arrangement of interlacing and interlooping during the manufacturing process. There is an almost infinite variety fabric appearance designs, depending on the underlying fabric structure.

Previous studies used woven fabric only (Rombaldoni et al., 2010; Kawabata, 1984; Chae et al., 2011), knitted fabrics only (Jeguirim et al., 2010; Mahar et al., 2013; Suzuki and Sukigara, 2013), or a combination of different fabric structures (Mehta et al., 2024; Soufflet et al., 2004; Bertaux et al., 2007) to evaluate the tactile properties based on either instrument measurement or subjective judgement. With a few notable exceptions, these studies generally evaluate the tactile properties on the selected samples rather than making comparisons between woven and knitted fabrics. The exception includes the study by Bertaux et al. (2007), which evaluated the relationship between ground truth

measurement of friction and subjectively perceived roughness. It concluded that the correlation was found only for knitted fabrics but not for woven fabrics. However, it was not to compare the perception differences, and the differences in perceived tactile properties between woven and knitted fabrics remain unclear. In addition, studies also selected fabric samples based on fabric materials and made comparisons among individual fabrics (Jiao et al., 2019; Bouman et al., 2013; Wijntjes et al., 2019; Baumgartner et al., 2013). To prevent an overwhelming number of comparisons between individual fabrics, a limited number of fabrics was usually used in these studies.

2.2.3.2 The effects of colours

Observations in real life rely on the interplay between light, human eye, and the physical object. Colour plays a significant role in visual observation and perception. As the term tactile is more related to palm than eyes, the effect of colour on tactile perception has not been frequently investigated. Yenket et al. (2007) used dyed cotton fabrics to evaluate fabric handle properties including bright, soft, firm, warm, rough etc (in total of 24 attributes). Five colours, white (undyed), light blue, dark blue, pink, and yellow, were dyed on four cotton fabrics. The results showed that there was little difference on the perceptual ratings for both consumer panel and expert panel. However, limited colours were used in the study, and the number of samples was only 20. The evaluation was not perfectly sufficient to define the effect of different colours on tactile perception. In addition, Xiao et al. (2016) conducted a matching-to-sample task, matching the fabric in an unseen box with the corresponding images in RGB format and greyscale format. They found that using RGB images improved the matching accuracy between touch and vision. Colour was not well controlled as a variable in previous studies, and it remains unknown of the role, particularly the impact of different colours on tactile perception. Therefore, in the present study, colours were carefully selected to generate images of the same fabrics in different colours (see Chapter 3, Section 3.2.1). Additionally, real fabrics were selected


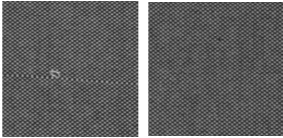
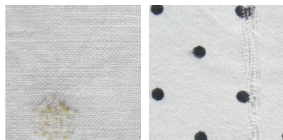

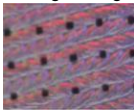
with evenly distributed colours (see Chapter 3, Section 3.2.2) to fully investigate the role of different colours.

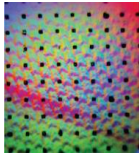
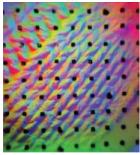







2.3 Fabric database

Through the review of previous studies of tactile and visual-tactile perception of fabrics, the next step is to select proper stimuli in the present study. This section reviews the existing fabric databases used in fabric-related research.

Fabric databases were developed for various purposes, including texture analysis, fabric defects detection and classification, texture perception, and also tactile-related purposes. Table 2.3 summarises the objectives for the corresponding fabric databases, including the type of images and their examples.

Table 2.3 Summary of fabric databases.

	References	Objectives	Database	Examples	
1	Kampouris et al. (2016)	Use micro-geometry and reflectance of fabric surface from images for material classification.	Over 2,000 fabric surface images with material classification labels (THE FABRICS DATABASE, 2016)		
2	Silverstre-Blanes et al. (2019)	Detection and classification of fabric defects by image processing methods.	140 detect-free fabric images, 105 images with detect (256*256 pixels).		
3	Zhang et al. (2020)	Detection of fabric defects by machine learning and deep learning.	ZJU-Leaper: 98,777 images of fabrics from 19 categories		
4	Luo et al. (2018)	Use images and tactile data collected through tactile sensor to recognize fabric texture	ViTac: 1,000 camera images and images recorded by tactile sensor	Camera image 	Corresponding GelSight image 

5	Yuan et al. (2018)	Use images recorded by tactile sensor to recognise the physical properties and semantic properties	153 pieces of cloths	<div>Cotton polo</div>  <div>Knit jacket</div> 
6	Xu et al. (2024)	To build a dataset that consists of images and corresponding tactile data for leather.	743 records, each record includes one camera image, two tactile images, and one defect segmentation image (620*410 pixels)	 
7	Takahashi and Tan, (2019)	Estimate tactile properties to enhance the robot understanding of environment.	Cropped fabric images	 
8	Bouman et al. (2013)	Predict the fabric stiffness and density from fabric videos and correlate the objective measurement results with human perception results.	30 fabric videos (859*851 pixels). Fabrics were hung and exposed to winds.	 
9	Mirjalili and Hardeberg, (2019)	Study the perceptual attributes that affects the human perception of texture of fabrics.	52 real fabrics, no images or videos were captured and used	
10	Sztandera et al. (2013)	Define the tactile comfort perception through mechanical measurement, tactile perception, and fabric construction analysis	48 real fabrics, no images or videos were captured and used	

All example images were derived from corresponding references.

Fabric images were frequently used to build the fabric database. Kampouris et al. (2016) built a large fabric database containing over 2,000 fabric images, each annotated with pre-defined labels specifying the material types. By analysing the micro-geometry and the reflectance properties of the fabric, they found that

the material classification accuracy outperformed the methods using only texture information. A database was developed to detect fabric defects and classify the defection types (Silverstre-Blanes et al., 2019). Moreover, Zhang et al. (2020) collected almost 10,000 fabric images to perform defects classification by advanced learning methods.

In addition to fabric images, Luo et al. (2018) collected both fabric images and images recorded by a tactile sensor GelSight. The sensor was pressed on the surface of the fabric, and the texture was then recorded and captured by GelSight. Incorporating both images and tactile data, the study developed a new algorithm to recognise fabric textures. Similar to Luo et al.'s study, Yuan et al. (2018) also used GelSight to record the cloth images when pressing the sensor against the fabrics, aiming to recognise fabric properties such as thickness, fuzziness, softness, durability, and so on. In addition, camera and a force sensor were used in Xu et al.'s study (2024) to build the relationship between images and tactile data for one specific fabric material, Crazy Horse Leather. Moreover, Takahashi and Tan (2019) trained a Convolutional Neural Network (CNN) model, using fabric images as inputs and signals from tactile sensors as outputs to estimate the slipperiness and roughness. All four studies extended human tactile perception to robotic systems equipped with tactile sensors, enabling the automated recognition of fabric images and interpretation of tactile data.

Bouman et al. (2013) collected a database of fabric videos where fabrics were hung and exposed to winds of three different strength. The stiffness and fabric density were predicted by analysing the fabric motion in the video. In addition, the ground truth of fabric stiffness and fabric density exhibited an exponential dependence on the human perceived stiffness and density.

Instead of images and videos, studies also developed fabric database using real fabrics. Mirjalili and Hardeberg (2019) collected 52 real fabrics and used them to find ten frequently used attributes to interpret the texture appearance of fabrics, including tactile-related properties (smooth and soft), and appearance-

related attributes (colour variation and repeating). Sztanderaz et al. (2013) built a model for tactile comfort perception predicted from the mechanical measurement of KEF-S, the tactile perception, and fabric construction. Three attributes, the rate at which sample sponges back to the original shape, fabric weight, and amount of small round particles in the surface of the fabrics were found to be the most influential attributes for tactile comfort.

Overall, the fabric databases can be generally divided into the following categories, and the limitations are also identified:

(1) only containing images or videos (e.g., reference 1, 2, 3, and 8 in Table 2.3). Such database normally requires a large number of images or videos, especially when advanced machine learning and deep learning techniques are used to make classification and recognition. However, there are few fabric image and video databases specifically developed for studying human visual-tactile perception of fabrics. The existing databases are insufficient to fulfil the aim of the present study.

(2) containing images and tactile data recorded by tactile sensor (e.g., reference 4, 5, 6, and 7 in Table 2.3). Tactile information was taken into consideration in previous studies, while such information was recorded by tactile sensors such as GelSight and force sensor. Using the tactile sensor can be helpful in research. However, in everyday life, a big limitation is that such devices are usually not accessible for the public. Reading and understanding the recorded data by tactile sensor will be the other big problem for most of consumers to understand the tactile properties of the fabric products.

(3) only containing real fabrics (e.g., reference 9 and 10 in Table 2.3). The first limitation of such fabric databases is that the number of real fabrics is usually less than the databases of images, due to the time consumed to evaluate fabric samples. In addition, using real fabrics cannot to result in good reproducibility. Although different studies normally select fabrics based on the fabric type and

material, cross-study comparisons remain difficult.

(4) involving ground truth data from objective measurements (e.g., reference 8 and 10 in Table 2.3). Similar to (2), devices measuring fabric properties are not accessible to the public, and reading and understanding such data requires professional training. Additional human perception experiments are required to link such results to human perceptual attributes.

Considering all above, it is necessary to develop a Leeds Fabric Tactile Database specifically designed for tactile and visual-tactile perception of fabrics. This database is supposed to incorporate both images/videos and real fabrics to establish a connection between what humans see and what they feel in terms of tactile properties. An important consideration of the database is that all the data will be easy to be interpreted to the public including not only researchers but the general consumers in the textile market.

2.4 CIE colorimetry

After setting the plan to collect a Leeds Fabric Tactile Database, the visual stimuli in the database need to be carefully captured and processed. It is essential to review the colorimetric information before handling colours in images and videos.

A simplified explanation of colorimetry is that colorimetry is the measurement of colour (Fairchild, 2013). The *Commission Internationale de l'Éclairage* (CIE) is responsible for providing standards and recommendations for the application of colorimetry. Colour is visually perceived because of three components: light source, an object, and an observer, as shown in Figure 2.4. Accordingly, CIE made recommendations on the standard illuminants, standard observer data, and standard geometric conditions for the triangle of colour, as well as colorimetric calculation including tristimulus values, uniform colour space, and colour difference formulae (CIE, 2018). This section reviews the CIE standards relevant to the present study. The book *Measuring colours* is used as the

general reference (Hunt and Pointer, 2011).

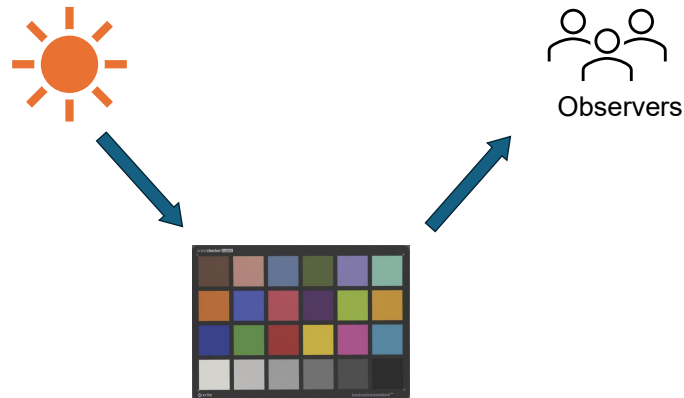


Figure 2.4 Triangle of colour. The image of X-Rite ColorChecker® Classic chart was downloaded from X-Rite (2025a).

2.4.1 CIE standard illuminants

Light source plays an essential role in observing colour, which is referred to as physical emitters of visible energy (Fairchild, 2013). Illuminant, however, is a standardised representation of spectral power distribution (SPD) of the light source. SPD represents the radiant power per unit area at each wavelength across the visible spectrum of a light source. For example, daylight is one of the light sources to which humans are exposed daily, and CIE illuminant D65 is a standardised representation of daylight. While the SPD of daylight varies, the SPD of CIE illuminant D65 has been set to represent the daylight with a correlated colour temperature (CCT) of 6504K (Hunt and Pointer, 2011). Other CIE standard illuminants include CIE illuminant A with a CCT of 2856K and CIE illuminant D50 with a CCT of 5003K. The SPD of CIE standard illuminants are available in Hunt and Pointer (2011).

2.4.2 CIE colour-matching functions and standard observers

Two types of photoreceptors, cones (ρ, γ, β) and rod, work together on the retina to give a colour vision of human (Hunt and Pointer, 2011). The three cones and the rod have different sensitivities across the visible spectrum as shown in

Figure 2.5. It is essential to use the cone spectral sensitivity data to determine how the human visual system perceives colours from a given spectral stimulus. However, the spectral sensitivity cannot be precisely measured due to the restriction of devices at the time of development. CIE colour-matching functions were then developed to replace the cone spectral sensitivities to quantify colour.

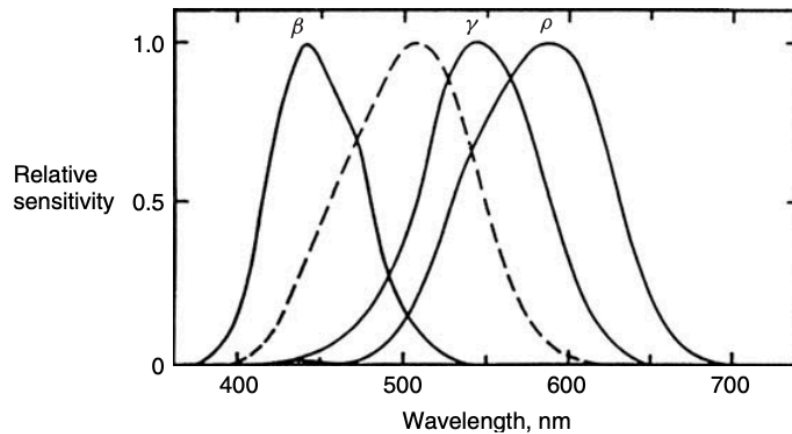


Figure 2.5 The spectral sensitivity of cones (solid lines) and rod (broken line). The figure is from Hunt and Pointer (2011, p.6).

Two independent trichromatic colour-matching experiments were conducted by John Guild and W. David Wright. The principle of the experiments is shown in Figure 2.6. Participants were asked to adjust the amount of R, G, B light source until the mixture matched the test colour. The CIE colour-matching functions were initially derived from the two experiments' results and represented as $\bar{r}(\lambda)$, $\bar{g}(\lambda)$, $\bar{b}(\lambda)$. They are the measures of amount of R, G, B needed to match a constant equi-energy stimulus, as shown in Figure 2.7.

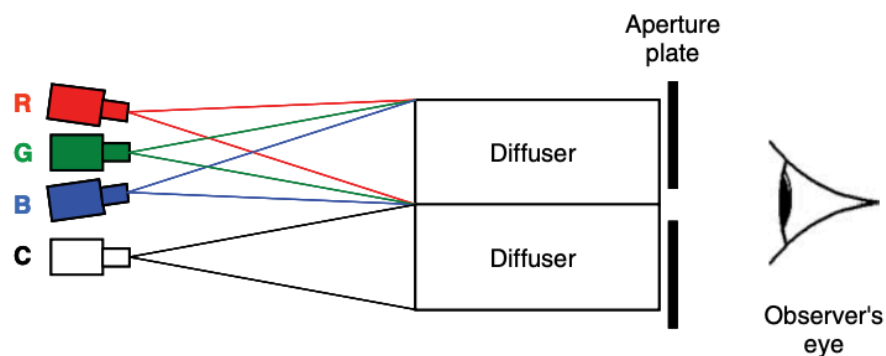


Figure 2.6 The principle of trichromatic colour matching. The figure is from

Hunt and Pointer (2011, p.25).

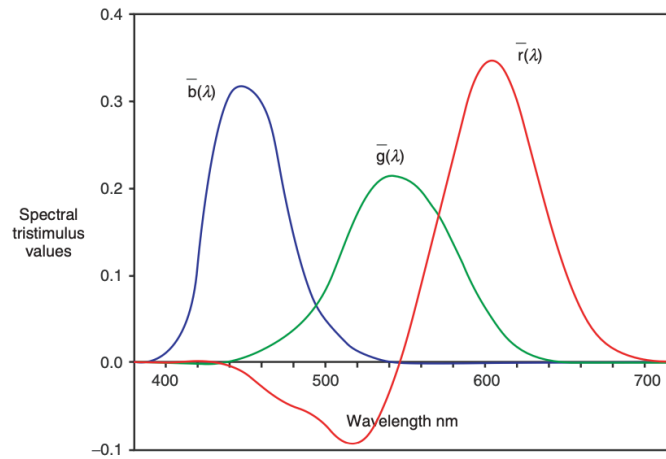


Figure 2.7 The initial colour-matching functions $\bar{r}(\lambda)$, $\bar{g}(\lambda)$, $\bar{b}(\lambda)$. The figure is from Hunt and Pointer (2011, p.30).

It is noted that each colour-matching function curve is negative in specific parts. To eliminate the negativity, CIE recommended new colour-matching functions $\bar{x}(\lambda)$, $\bar{y}(\lambda)$, $\bar{z}(\lambda)$ through linear transformation of $\bar{r}(\lambda)$, $\bar{g}(\lambda)$, $\bar{b}(\lambda)$ in Equation 2.1 (Hunt and Pointer, 2011). The 3*3 matrix in Equation 2.1 were carefully defined so that the new colour-matching function curves are always positive across the visible spectrum, shown as the solid curves in Figure 2.8.

$$\begin{bmatrix} \bar{x}(\lambda) \\ \bar{y}(\lambda) \\ \bar{z}(\lambda) \end{bmatrix} = \begin{bmatrix} 0.49 & 0.31 & 0.20 \\ 0.17697 & 0.81240 & 0.01063 \\ 0.00 & 0.01 & 0.99 \end{bmatrix} \begin{bmatrix} \bar{r}(\lambda) \\ \bar{g}(\lambda) \\ \bar{b}(\lambda) \end{bmatrix} \quad \text{Equation 2.1}$$

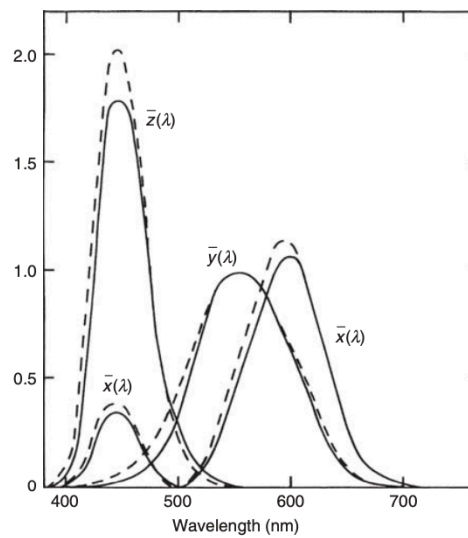


Figure 2.8 The CIE colour-matching functions $\bar{x}(\lambda)$, $\bar{y}(\lambda)$, $\bar{z}(\lambda)$. Solid line: CIE 2° observer. Broken lines: CIE 10° observer. The figure is from Hunt and

Pointer (2011, p.34).

In the trichromatic experiments, the matching was conducted within a 2° field. When a larger field is used, the matching may be no longer consistent. Therefore, CIE recommended another set of values of colour-matching functions for samples with a field size greater than 4° in 1964, as shown in the broken curves in Figure 2.8. The use of colour-matching functions depends on the sample size and is discriminated by subscripts. For a 2° field size, it is also referred to as the CIE 1931 Standard Observer. For a 10° field size, the colour-matching functions are represented as $\bar{x}(\lambda)_{10}$, $\bar{y}(\lambda)_{10}$, $\bar{z}(\lambda)_{10}$, and are referred to as the CIE 1964 Standard Observer. It is essential to specify which set of data is used when quantifying colours from colour-matching functions.

2.4.3 CIE standard geometric condition

In addition to standard illuminants and standard observer, the final component of the triangle of colour is the object being viewed or measured. The colour could be perceived differently when different illuminants, observers, and viewing angles are applied. CIE recommended four standard geometries of illumination and viewing, which are also applied to measurement as shown in Figure 2.9 (Hunt and Pointer, 2011).

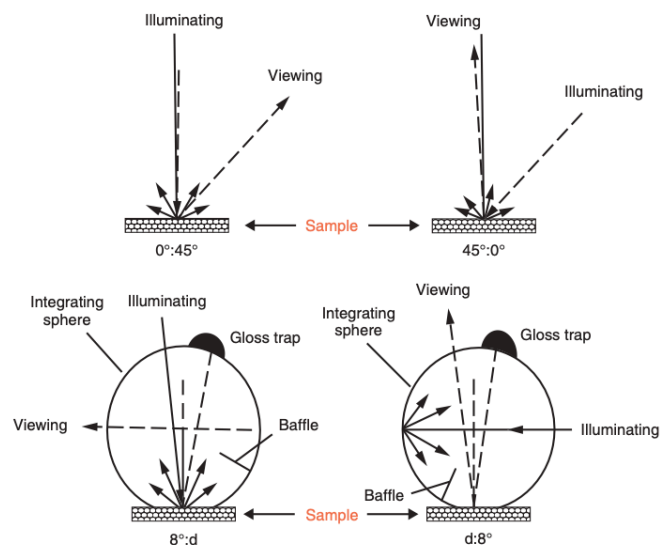


Figure 2.9 Four CIE standard geometries of illumination and viewing/measurement. Figure is from Hunt and Pointer (2011, p.104)

For 0°:45° geometry, the object is illuminated nearly at the normal incidence and the reflection of light is captured at an angle of approximately 45° from the normal to the object surface. The 45°:0° geometry is similar to 0°:45°, except that the illumination occurs at an angle of approximately 45° and the reflection of light is captured nearly at the normal incidence. A strict 0° is usually not recommended due to the inter-reflections between the object and the light source. 'd' represents diffuse, and 8° is the offset angle of light source in the CIE 8°:d and the offset angle of detecting the light in the CIE d:8° geometries. An integrating sphere is used to provide diffuse illumination, and a white-coated baffle is usually included in the integrating sphere to prevent the direct light between object and measurement spot. A gloss trap is fitted in the integrating sphere. If using the gloss trap, it will absorb the light reflected at the specular angle relative to the incident light or measurement beams, excluding the specularly reflected light (SCE mode). Without using the gloss trap, the specular reflection will be included (SCI mode). It is essential to identify which CIE geometry is used and whether the specular reflection is included when measuring colour.

2.4.4 CIE tristimulus values XYZ and chromaticity diagram

In the previous three sections, CIE standard illuminants, standard observers, and standard geometric conditions were reviewed. By these three components, the CIE tristimulus values CIE XYZ can be calculated and specify colours. Two colour stimuli with the same CIE XYZ values will match if they are viewed under the same lighting, by an observer whose colour vision is close to CIE Standard Observer, and under the same CIE geometry (Hunt and Pointer, 2011). The CIE XYZ values are computed from CIE colour-matching functions using Equation 2.2.

$$\begin{aligned} X &= k \sum_{\lambda} S(\lambda) R(\lambda) \bar{x}(\lambda) d\lambda \\ Y &= k \sum_{\lambda} S(\lambda) R(\lambda) \bar{y}(\lambda) d\lambda \end{aligned} \quad \text{Equation 2.2}$$

$$Z = k \sum_{\lambda} S(\lambda) R(\lambda) \bar{z}(\lambda) d\lambda$$

$$k = 100 / \sum_{\lambda} S(\lambda) \bar{y}(\lambda) d\lambda$$

where k is the constant when Y is set to 100 for the perfect diffuser, $S(\lambda)$ is the SPD of the light source, $R(\lambda)$ is the spectral reflectance of the measured object, λ is the wavelength across the visible spectrum with an interval of $d\lambda$.

For a perfect diffuser, the Y value is set to 100 as the reflectance factor $R(\lambda)$ of a perfect diffuser is equal to 1 across the visible spectrum, meaning it reflects 100% of the incident light in all directions (Hunt and Pointer, 2011). Y is therefore regarded as the percentage luminance factor and has an approximate correlation with the perceptual lightness.

The tristimulus values X and Z , however, has no correlation with any perceptual attributes. Chromaticity coordinates, denoted as x , y , z , were developed to correlate CIE XYZ tristimulus values as defined in Equation 2.3. The sum of x , y , z is equal to 1. Based on x and y , CIE xy chromaticity diagram can be plotted in Figure 2.10 and a colour can be usually specified by CIE xy together with the luminance factor Y .

$$x = \frac{X}{X + Y + Z}$$

$$y = \frac{Y}{X + Y + Z}$$

$$z = \frac{Z}{X + Y + Z}$$

Equation 2.3

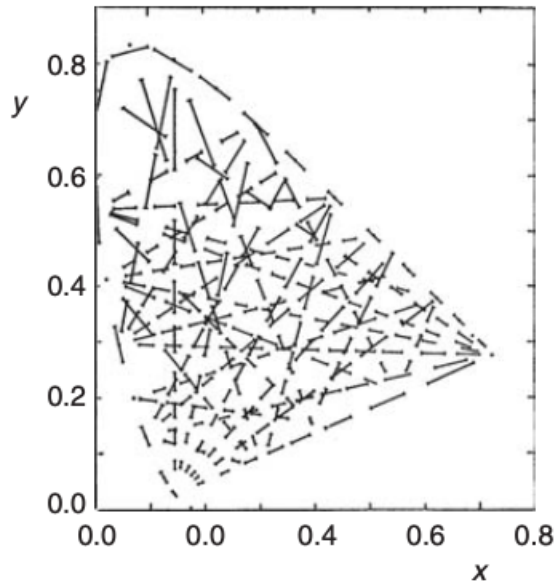


Figure 2.10 CIE xy chromaticity diagram. The figure is from Hunt and Pointer (2011, p.48)

2.4.5 CIE uniform colour space

2.4.5.1 CIE u',v' chromaticity diagram

A major limitation of the CIE xy chromaticity diagram is non-uniformity. The short lines in CIE xy chromaticity diagram (Figure 2.10) illustrate the perceived colour difference between two colours of the same luminance. If the perceived colour differences are of the same magnitude, the length of the short lines is supposed to be equal, but it is not the fact in Figure 2.10. To uniformly represent colour, *CIE 1976 uniform chromaticity scale diagram* (also known as u',v' chromaticity diagram) was developed by deriving u' and v' chromaticity coordinates from CIE XYZ values (Equation 2.4). Figure 2.11 illustrates the approximately uniform CIE u',v' chromaticity diagram. Compared to the non-uniform CIE xy chromaticity diagram in Figure 2.10, the colour difference of the equal magnitude can be uniformly plotted in the CIE u',v' chromaticity diagram.

$$u' = \frac{4X}{X + 15Y + 3Z}$$

Equation 2.4

$$v' = \frac{9Y}{X + 15Y + 3Z}$$

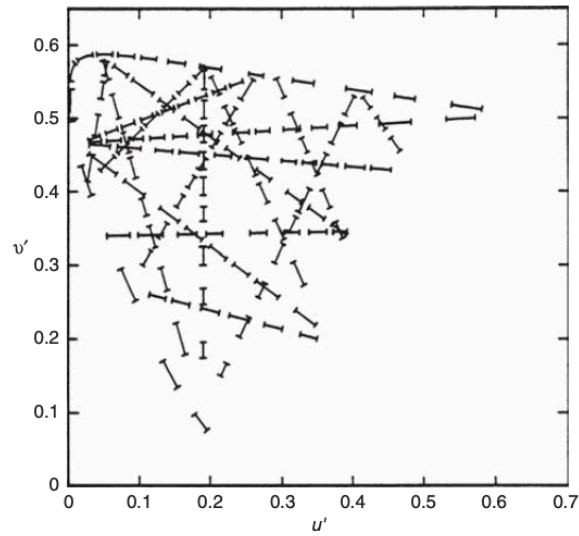


Figure 2.11 The CIE u', v' chromaticity diagram. The figure is from Hunt and Pointer (2011, p.49).

2.4.5.2 CIELAB and CIELUV colour space

Even though the CIE u', v' chromaticity diagram is nearly uniform, it only shows the ratio of CIE XYZ values but not the magnitude, and it is only applicable for colours of the same luminance (Hunt and Pointer, 2011). Two uniform colour spaces, CIELAB and CIELUV colour space, were then developed. CIELAB uniform colour space defines three axes, L^* (lightness), a^* (redness-greenness), and b^* (yellowness-blueness), defined in Equation 2.5 and illustrated in Figure 2.12-left.

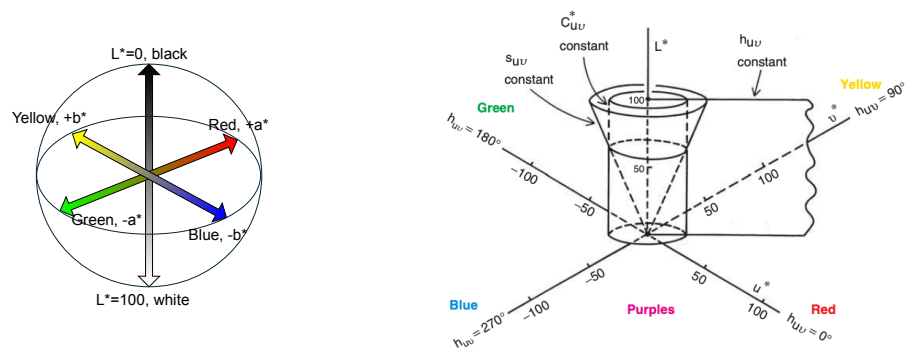


Figure 2.12 Left: CIELAB uniform colour space. Right: CIELUV uniform colour space. The right figure is from Hunt and Pointer (2011, p.54).

$$\begin{aligned}
L^* &= 116f\left(\frac{Y}{Y_n}\right) - 16 \\
a^* &= 500\left[f\left(\frac{X}{X_n}\right) - f\left(\frac{Y}{Y_n}\right)\right] \\
b^* &= 200\left[f\left(\frac{Y}{Y_n}\right) - f\left(\frac{Z}{Z_n}\right)\right] \\
f(I) &= \begin{cases} I^{1/3}, & \text{for } I \geq 0.008865 \\ 7.787(I) + 16/116, & \text{for } I < 0.008865 \end{cases}
\end{aligned}
\tag{Equation 2.5}$$

where X_n , Y_n , Z_n are the CIE XYZ tristimulus values for the chosen reference white. As the CIE tristimulus values are transformed using cube-roots functions to the CIE LAB values, the mixture of any two colours will not fall on a straight line in the CIELAB colour space, and thus no chromaticity diagram available. The saturation is not defined in the CIELAB colour space, but hue-angle (h_{ab}) and chroma (C_{ab}^*) are defined based on a^* and b^* in Equation 2.6 and Equation 2.7, respectively.

$$h_{ab} = \arctan\left(\frac{b^*}{a^*}\right) \tag{Equation 2.6}$$

$$C_{ab}^* = \sqrt{a^{*2} + b^{*2}} \tag{Equation 2.7}$$

CIELUV is another CIE uniform colour space. Similar to CIELAB colour space, it also has three orthogonal dimensions as shown in Figure 2.12-right, denoted as L^* (lightness), u^* (the values along red-green dimension), and v^* (the values along yellow-blue dimension):

$$\begin{aligned}
L^* &= 116f\left(\frac{Y}{Y_n}\right) - 16 \\
u^* &= 13L^*(u' - u'_n) \\
v^* &= 13L^*(v' - v'_n) \\
f(I) &= \begin{cases} I^{1/3}, & \text{for } I \geq 0.008865 \\ \left(\frac{841}{108}\right)I + \frac{4}{29}, & \text{for } I < 0.008865 \end{cases}
\end{aligned}
\tag{Equation 2.8}$$

where u'_n and v'_n are the chromaticity coordinates of the chosen reference white, transformed from CIE XYZ tristimulus values using Equation 2.4. Hue-

angle, chroma, and saturation are correlated to CIELUV colour space and defined as follows:

$$h_{uv} = \arctan\left(\frac{v^*}{u^*}\right) \quad \text{Equation 2.9}$$

$$C_{uv}^* = \sqrt{u^{*2} + v^{*2}} \quad \text{Equation 2.10}$$

$$s_{uv} = C_{uv}^*/L^* \quad \text{Equation 2.11}$$

The lightness L^* has the same definition in CIELAB and CIELUV uniform colour spaces, while multiplicative normalisation of tristimulus values was adopted for a^* and b^* and the subtractive shift in chromaticity coordinates was adopted for u^* and v^* (Fairchild, 2013).

2.4.6 Colour difference formulae

The difference between two colours in a colour space is quantified by using colour difference formulae. The calculation can be simply defined as the Euclidean distance between the three coordinates of two colours in either CIELUV colour space (Equation 2.12) or CIELAB colour space (Equation 2.13), generally based on the CIE XYZ tristimulus values. The difference in lightness L^* between two colours is denoted as ΔL^* , and the same regulation is applied to the differences in u^* , v^* , a^* , and b^* .

$$\Delta E_{uv}^* = \sqrt{(\Delta L^*)^2 + (\Delta u^*)^2 + (\Delta v^*)^2} \quad \text{Equation 2.12}$$

$$\Delta E_{ab}^* = \sqrt{(\Delta L^*)^2 + (\Delta a^*)^2 + (\Delta b^*)^2} \quad \text{Equation 2.13}$$

Since the development of CIE 1976 $L^*a^*b^*$ and CIE 1976 $L^*u^*v^*$ colour difference formulae, efforts were made on proposing new colour difference formulae to obtain a more accurate prediction. Examples include CMC(l:c) (Clarke et al., 1984), CIE94, and CIEDE2000 colour difference formulae (Luo et al., 2001). Currently CIE recommended CIEDE2000 colour difference formula in industry applications (CIE, 2018).

2.5 Colour characterisation of camera

To capture high-quality images, Digital Single-Lens Reflex (DSLR) cameras are commonly used in both everyday life and research. The light travels through the camera lens and reaches the image sensor embedded in the camera. The image sensor converts the incoming light into electronic signals, which are then processed by the camera's image signal processor (ISP) to generate image data. The different image sensors and algorithms embedded in the image signal processors result in device-dependent RGB images. The characterisation process is usually achieved by transforming RGB data to device-independent coordinates such as CIE XYZ (Hunt and Pointer, 2011).

2.5.1 Camera settings

The output RGB image from cameras are highly dependent on ISP. Since there is nearly no way to modify the embedded algorithm in ISP, adjusting the camera settings to reproduce the scene's colours as close to the scene as possible is a fundamental concept in photography. The camera is usually set to the manual model to adjust shutter speed, ISO speed, and aperture. White balance is normally customised based on the lightness of the scene to be captured. The book *Camera Image Quality Benchmarking* is used as the general reference in this section (Philips and Eliasson, 2018).

2.5.1.1 Exposure of light

Shutter speed is the time that the camera captures light, usually measured in seconds (Philips and Eliasson, 2018). The slower the shutter speed, the more light can be captured by the camera, making the image appear brighter. However, excessively long exposure times can also lead to motion blur. Common sets of shutter speed can be 1/2, 1/4, 1/8.

ISO speed represents the sensitivity of camera sensor to incoming light (Philips and Eliasson, 2018). A lower ISO speed corresponds to lower sensor sensitivity,

making it suitable for well-lit scene. For indoor or low-light scene, a relatively higher ISO speed is typically used. Common sets of ISO speed can be ISO 100, ISO 200, ISO 400, ISO 800, etc.

The aperture directly controls the amount of light entering the camera by adjusting the diameter of the lens opening, referred to as f-number (Philips and Eliasson, 2018). A smaller f-number represents larger diameter that the lens opens, and thus more light reaches the camera sensor and results in a brighter image. Common sets of f-number can be f2.0, f3.0, f4.0. The aperture also affects the depth of field (DOF), where a larger aperture results in a shallow DOF and a smaller aperture results in a deep DOF. A shallow DOF produces a blurred background, whereas a deep DOF keeps both foreground and background in focus.

Adjusting shutter speed, ISO speed, and aperture jointly affects the resulting image. Careful selection of each attribute is essential to avoid overexposure, motion blur and other problems.

2.5.1.2 White balance

Human adjusts the lightings in different colour temperatures automatically, but it is not the fact of camera. The white balance setting adjusts the overall colour appearance in a camera shot by compensating for the colour temperature of the scene being captured (Adobe, 2024). The adjustment ensures that white objects appear white in the image, preserving accurate colour representation across the image. Cameras can be set to auto white balance (AWB) mode to compensate for the colour temperature of the scene by the built-in light meter. For example, under tungsten lighting (around 3200K), AWB compensate for the warm tone by boosting the blue channel intensity. In contrast, with higher colour temperature lighting (e.g., 7000K), AWB increases the red channel ratio to neutralise the bluish tone. However, AWB is not always precise. Customising the white balance setting in the camera becomes essential, especially when shooting

under a well-controlled lighting. This process is usually achieved by measuring the colour temperature of the stable light source and setting it as the custom white balance in the camera.

2.5.2 Characterisation process

As mentioned at the beginning of Section 2.5, the fundamental principle of colour characterisation process is to transform the device-dependent data (e.g., RGB) to device-independent data (e.g., CIE XYZ) (Hunt and Pointer, 2013). Two methods of the transformation are introduced and compared firstly in this section. Practical considerations, including colour measurement and the use of colour charts, are introduced later in this section.

2.5.2.1 Characterisation methods

Two characterisation methods, spectral sensitivity method and colorimetric method, are often used by camera manufacturers, testing laboratories, and ordinary users (Hong et al., 2001). For the spectral sensitivity method, the camera spectral sensitivity is measured by professional devices, such as monochromator and radiance meter, and then mapped to CIE colour-matching functions (CMF). For the colorimetric method, RGB and CIE XYZ (or other device-independent coordinates) data of a suitable number of test colours are collected (Hunt and Pointer, 2013), and the relationship is then decided.

Compared to colorimetric method, spectral sensitivity method requires: (1) a monochromator to produce tuneable monochromatic light source that spans the spectrum; (2) the camera to capture RAW images under each single-wavelength illumination; (3) accurate processing to extract RGB values from RAW data. The process is cost and time consuming. On the other hand, colorimetric method only requires colour measurement device, a standard colour charts, and an image of the colour charts captured by the camera. Most studies used colorimetric method to characterise the camera due to its simplicity and practicality (Hong et al., 2001; Kikuchi et al., 2020; He et al., 2021).

To apply the colorimetric method, the standard colour chart is required to put at the same place as the objects to be shot. The stable and uniform lighting provided by a professional lighting cabinet is luminated on the colour chart. Any shadow or highlight is supposed to be avoided during imaging. The RGB data can then be extracted from the image for each colour patch in the chart. In addition, two methods can be used to obtain the CIE XYZ values of the colour chart: (1) directly measure the spectral power distribution (SPD) of all colour patches and compute them to CIE XYZ; and (2) measure the SPD of the lighting in the cabinet and measure the spectral reflectance of the physical colour chart (Hunt and Pointer, 2013). Methods including linear regression and polynomial regression were applied to build the relationship between RGB and CIE XYZ values and were compared in previous study (Hong et al., 2001). He et al.'s study expanded on this by incorporating lookup tables and neural networks and further compared the transformations (He et al., 2021).

2.5.2.2 Colour charts

To build a reliable colour characterisation process, a reference colour chart with neutral grey colour patches is used in colorimetric method for camera colour characterisation. Popular colour charts include X-Rite ColorChecker® Classic chart (X-Rite, 2025a), X-Rite ColorChecker® Digital SG chart (X-Rite, 2025b), GretagMacbeth ColorChecker® DC (Chromaxion, 2025), and DigiEye calibration chart DigiTizer (Verivide, 2025), as shown in Figure 2.13. Neutral colours including white, black, and a series of grey colours are included in all colour charts. For X-Rite ColorChecker® Classic chart, other 18 colours representing different hues are included. Together with 6 neutral colours, the X-Rite ColorChecker® Classic chart is also included in X-Rite ColorChecker® Digital SG chart (area from row 2 column E to row 5 column J). In addition, the X-Rite ColorChecker® Digital SG chart provides a wider colour gamut with an expanded range of colours beyond those in the classic charts (X-Rite, 2025b). The GretagMacbeth ColorChecker® DC chart (DC standing for digital camera)

consists of 237 colour patches, including 8 glossy-surfaced patches and 229 matt-surfaced patches. DigiEye calibration chart DigiTizer is designed for the DigiEye colour measurement system, involving a stable lighting cabinet and a top-mounted camera captures for consistent imaging conditions.

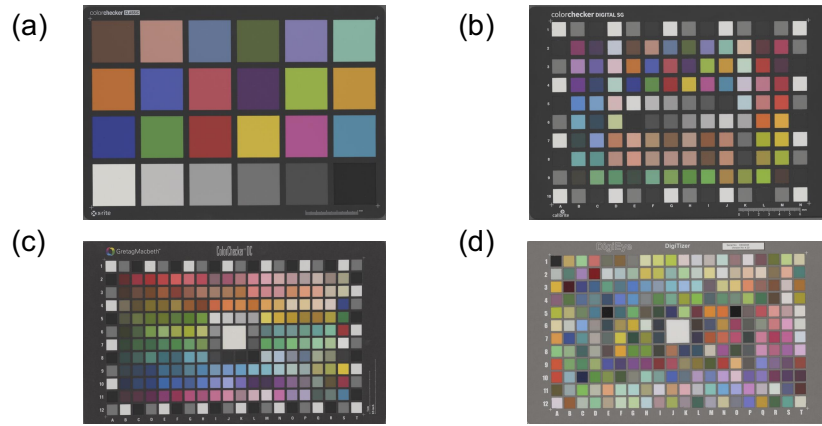


Figure 2.13 Colour charts. (a) X-Rite ColorChecker® Classic chart, (b) ColorChecker® Digital SG chart, (c) GretagMacbeth ColorChecker® DC, and (d) DigiEye calibration chart DigiTizer. All charts were captured by Digieye colour measurement system.

In addition to standard colour charts, charts are designed for specific applications, and efforts are also made on developing general guides for various practical applications. For example, Pantone collected 138 skin tones by measuring the full spectrum of real human skin types (Pantone, 2025a), as shown in Figure 2.14-left. It can serve as a guide in any skin-related market. Due to the characteristics of human skin, skin tone occupies a relatively narrow colour gamut. The colours of fabric, on the other hand, span a much wider colour gamut than skin tone. More than 2,000 colours were collected by Pantone to make the Fashion, Home+Interiors colour guide (Pantone, 2025b), as shown in Figure 2.14-right. These two colour guides are usually used in relevant industries rather than characterising camera colours.



Figure 2.14 Left: Pantone skin tone guide (Pantone, 2025a). Right: Pantone fashion, home + interiors colour guide (Pantone, 2025b).

2.6 Colour characterisation of display

After the process of colour characterisation of camera, images still will be present differently across various displays or one display that adopts different settings. In the present study, a liquid crystal display (LCD) backlit BenQ display was used to present images in the psychophysical studies (see Chapter 3). Truly reproduce the images is of vital importance in the visual assessments. The works proposed by Berns are used as the general reference in this section (Berns, 1996; Berns et al., 1993).

2.6.1 Calibration, characterisation, and gamma

Predefining the display setting, including the system gain, system offset, system gamma, brightness, contrast, sharpness, peak white with chromaticity equivalent to CIE D65, and peak white luminance, is referred as the calibration of display (Berns, 1996). Similar to the colour characterisation of camera, the characterisation of display is the process of transforming device-dependent RGB data to device-independent coordinates (usually CIE XYZ colour space) and vice versa. The predefined display settings remained unchanged for one characterisation, as the images have to be viewed under the same conditions in which the characterisation is performed. Calibration and characterisation are

two essential steps to ensure an accurate and consistent colour reproduction. Gamma describes the non-linear relationship between the input digital signal and the output luminance of each channel (Berns, 1996; Westland et al, 2012). Ignoring gain and offset but adjusting gamma will cause errors in dark colours (Berns, 1996).

2.6.2 Gain-Offset-Gamma (GOG) model

As indicated by its name, the role of GOG model is to optimise the values of gain, offset, and gamma to build the relationship between RGB and CIE XYZ. It was initially proposed by Berns (1996) for CRT displays. Although CRT displays are nearly replaced by new technologies such LCD, the nonlinear relationship between the input signal and output luminance was corrected to mimic the CRT display (Bala, 2003). The computation process of the GOG model is given in Equation 2.14 and Equation 2.15, where a_r , b_r , and γ_r are the gain, offset, and gamma values for R channel (the same for G and B channel but with different subscripts) where the sum of gain and offset is set to 1, d_r , d_g , d_b are the input RGB signals (Westland et al., 2012).

$$R = \left(\frac{a_r d_r}{255} + b_r \right)^{\gamma_r}$$

$$G = \left(\frac{a_g d_g}{255} + b_g \right)^{\gamma_g}$$
Equation 2.14

$$B = \left(\frac{a_b d_b}{255} + b_b \right)^{\gamma_b}$$

$$\begin{bmatrix} X \\ Y \\ Z \end{bmatrix} = \begin{bmatrix} X_{r,max} & X_{g,max} & X_{b,max} \\ Y_{r,max} & Y_{g,max} & Y_{b,max} \\ Z_{r,max} & Z_{g,max} & Z_{b,max} \end{bmatrix} \begin{bmatrix} R \\ G \\ B \end{bmatrix}$$
Equation 2.15

In practical, it is necessary to predefine the display settings and warm up the display prior to the measurement to ensure a consistent characterisation. Developing a GOG model requires measuring a series of neutral colours present on the display, as well as a pure red, a pure green, and a pure blue (Berns et al., 1993). The values of gain, offset, and gamma are optimised by

measuring neutral colours and minimising the colour differences between the measured data and the data computed using Equation 2.14, where R, G, B are substituted by neutral colours in the equations. Once the coefficients are determined, the linearised RGB values can be derived from Equation 2.14 using the measurement data of pure red, green, and blue. These linearised RGB values are subsequently mapped to CIE XYZ via Equation 2.15, where the 3*3 matrix is built based on the measured CIE XYZ values of pure red ($X_{r,max}$, $Y_{r,max}$, $Z_{r,max}$), pure green ($X_{g,max}$, $Y_{g,max}$, $Z_{g,max}$), and pure blue ($X_{b,max}$, $Y_{b,max}$, $Z_{b,max}$). The 3*3 matrix can be inverted, allowing the CIE XYZ values to be mapped back to RGB space. A tele-spectroradiometer is normally used for measuring display colours, and information will be given in Section 2.7.1.1.

2.6.3 Channel independence and spatial independence

Before performing the display characterisation, the channel independence and spatial independence of the display is essential to be tested (Berns et al., 1993). Channel independence is the assumption that in a display system, the output of each RGB channel is not affected by the others. The sum of CIE XYZ values of RGB channels is expected to be equivalent to the display luminance based on the Grassmann's law of additive colour mixing (Berns, 2019). In practical, the channel independence is tested by measuring a full screen pure red, a full screen pure green, a full screen pure blue, and a full screen peak white. The colour difference between the sum of CIE XYZ values of pure RGB and the CIE XYZ values of peak white is used to quantify the channel independence.

Spatial independence is the assumption that the luminance and chromaticity of one pixel is not affected by other pixels in the display system (Berns et al., 1993). In practical, it is tested by measuring two peak white colour patches: one is a 5-cm square in the middle of the display, the other is a full screen peak white. The colour difference between the peak white square and full screen white is calculated and represent the spatial independence.

2.7 Colour measurement

Measuring colour is an essential step in camera colour characterisation and display colour characterisation. The measurement of fabric colour is also critical in assessing fabric quality. In previous studies, device-based methods measured self-luminous colours using tele-spectroradiometer, and non-self-luminous colours using spectrophotometer with the built-in lighting (Chae, 2024; Luo et al., 2016; Cabral et al., 2023; Popa et al., 2021; Much et al., 2021). More recently, image-based methods have been developed to measure the colour over a larger area than spot measurements or areas with complex shape (Luo et al., 2015; Luo et al., 2016). The book *Measuring Colour* is used as the general reference in this section (Hunt and Pointer, 2011).

2.7.1 Device-based measurement

2.7.1.1 Tele-spectroradiometer

The measurement of self-luminous colours is usually conducted by tele-spectroradiometer, which measures the radiant power (*radiometer*) by analysing the light throughout the spectrum (*spectro*) in a non-contact way (*tele*) (Hunt and Pointer, 2011). As mentioned in Section 2.5 and Section 2.6, the measurements of self-luminous colours involve measuring light source in the lighting cabinet and colours present on the display. For measuring light source, a standard reflecting white surface is required to be illuminated by the light source. The measurement is then performed by aligning the tele-spectroradiometer with the reflecting surface to capture the reflected light. However, for measuring the colour present on the display, if the same procedure for measuring light source is adopted, the amount of light reflected by the white surface will not be sufficient. The measurement is thus performed by aligning the tele-spectroradiometer with the colours on the display directly and capturing the light. This procedure has to be performed in a dark environment to prevent the effect of external lighting.

Non-self-luminous colours can also be measured by tele-spectroradiometer if proper illumination is available. However, it is not common in measuring fabric colours due to the limited measurement area. An exception is that Chae and Lee (2021) measured 203 fabric samples using CS-2000A under 16 different light sources and evaluated the colour attributes variation. Moreover, the small measurement spot can further lead to inaccurate colour measurements due to the influence of fabric structure.

Common spectroradiometers in laboratories include CS-2000 spectroradiometer developed by Konica Minolta (Konica Minolta, 2025) and specbos 1211-2 spectroradiometer developed by JETI (JETI, 2025). Both devices cover a wide spectral range and are capable of measuring a broad luminance range.

2.7.1.2 Spectrophotometer

The measurement of non-self-luminous colours is usually conducted by spectrophotometer. The device must be calibrated prior to measurement to set the reference of 100% reflection (by white calibration) and 0% reflection (by black calibration). Comparisons are made between the radiant power of the light reflected by the objects and by the calibrated working standard throughout the spectrum, and thus the results of reflectance factor or transmittance factor are usually produced (Hunt and Pointer, 2011). Because of the built-in lighting source, the measurement must be performed by contacting the spectrophotometer and the object to capture all the reflected light. The colour of liquid and irregular shaped objects cannot be measured using spectrophotometer. Common spectrophotometer in laboratories includes the portable CM-700d developed by Konica Minolta (Konica Minolta, 2025b) and benchtop DataColor 200 spectrophotometer developed by DataColor (DataColor, 2025).

Using spectrophotometer to measure the colour of fabrics is popular in previous

studies. Chae (2024) measured the colour of 108 100% cotton plain woven fabrics using CM-26d spectrophotometer developed by Konica Minolta. Samples were also visually assessed under four illuminations (2856k, 6504k, 100lx, 2000lx) to study the colour tolerance threshold. Luo et al. (2016) measured 44 pair of solid-colour yarn-dyed fabrics by DataColor 650 and compared the measurement results with their imaging measurement system. In addition to colour measurement, studies also used spectrophotometers to define the colour fastness after light exposure, washing, and rubbing (Cabral et al., 2023; Popa et al., 2021; Much et al., 2021).

2.7.2 Image-based measurement

As the measurement area is fixed and small for both tele-spectroradiometer and spectrophotometer, measuring the colour of large area of fabrics or fabrics with multiple colours requires repeated measurement. The process would be complex and time-consuming. Imaging system is becoming popular in colour measurement, which normally involving a high-quality camera and a stable lighting environment. Digieye colour measurement system is one of the popular methods adopted in studies to define the fabric colour, as shown in Figure 2.15. Cui et al. (2001) firstly compared the colour measurement results of a large set of samples between using Digieye and spectrophotometer. The good agreement between device-based method and image-based method supported the further development of image-based colour measurement of fabrics. Kumah et al. (2019) used Digieye system to measure the digital printed fabrics colour by transforming RGB data to CIE LAB coordinated. Li et al. (2014) used both spectrophotometer and Digieye system to measure the dope-dyed fabrics and test the full-colour effects. Accurate camera characterisation is the key in image-based measurement system to collect CIE colorimetric information (Cui et al., 2001). In addition, the colour of fabrics in draped condition cannot be measured by image-based methods, as the fold causes highlight and shadow in the image. For a draped fabric image, the fabric colour cannot be precisely defined.

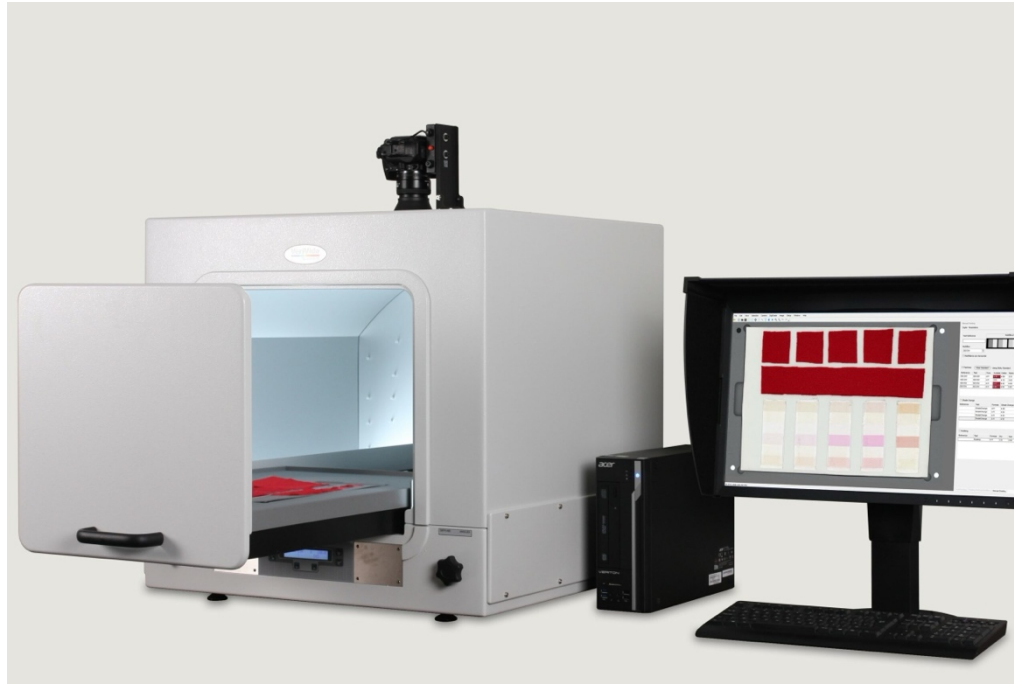


Figure 2.15 Digieye colour measurement system. Figure was downloaded from Verivide (2025).

2.8 Psychophysical experiment methods

The evaluation of the perception based on psychophysics, which is a tool to assess the relationship between the physical measurement of the stimulus intensity and the resulting sensation or perception (Morovic, 1998; Gescheider, 1997; Fairchild, 2013). Human perception is normally considered as being subjective, and a carefully designed and well-analysed perceptual experiment can provide an objective perspective to explain the subjective phenomenon. As the present study focused on tactile perception through images, videos, and actual touch, the experiments designed here are in the field of psychophysics.

Before conducting the psychophysical experiments, understanding the experimental techniques and the property of the resulting scale becomes essential. Even though the experiments in the present study included not only human visual but the tactile perception, the predictions were conducted for visual assessment and for tactile perception based on images and videos (see Chapter 7). Therefore, techniques in the application of visual assessment are introduced in this section and adopted in the experiment design. The book *Color*

Appearance Models (Fairchild, 2013) is used as a general reference in this section.

Two types of visual assessments are widely adopted: threshold and matching experiment which focus on small differences in perceptual magnitude, and scaling experiment which values the relationship between physical and perceptual magnitude of the stimuli (Fairchild, 2013). The present study adopted the latter one, and the former one is widely used in the field of colour science.

2.8.1 Scaling techniques

To ensure data interpretability and experiment validity, a careful selection of scaling techniques is essential before conducting the visual assessments. Four techniques are introduced in this section.

2.8.1.1 Categorical judgement

The law of categorical judgement on equal-interval scales, developed by Torgerson (1958), is the major scaling method used in the present study. It relates to the relative position of stimuli and the category boundaries of the cumulative proportions judged by participants (Morovic, 1998; Torgerson, 1958). There is no need to set a reference in the experiments, and particularly useful when the number of samples is massive. Table 2.4 lists the studies in tactile and fabric-related studies using categorical judgement.

Table 2.4 Previous studies used categorical judgement to assess tactile properties.

No.	Objectives and details	scale	reference
1	Exp1: To identify 262 sensory words describing tactile properties. 1: completely unrelated with touch 4: highly related to touch	4-point categorical judgement	Guest et al. (2011)
2	Exp2: To identify the dissimilarity of all possible combinations of 33 sensory descriptors derived from Exp1. 1: no difference in meaning	15-point scale	Guest et al. (2011)

	15: most different in meaning		
3	Exp3: To test the degree to which the descriptors derived from Exp2 were descriptive when touching fabrics. 1: completely not descriptive 5: very highly descriptive	5-point categorical judgement	Guest et al. (2011)
4	To study the effect of colour on 19 tactile attributes 1: none 9/15: extremely	9-point categorical judgement for consumer panel, and 15-point scale for expert panel	Yenket et al. (2007)
5	To rate the tactile perception by touch-only and vision-only (using real fabrics). 1: no reflection / monochromatic / smooth / irregular / soft / warm / not elastic / slippery / flat / uniform 7: shiny / colourful / rough / regular / hard / cold / elastic / friction / 3D structure / textured	7-point categorical judgement	Baumgartner et al. (2013)
6	To evaluate the perception of fabric stiffness and weight for a pair of fabric video. -3: fabric A is stiffer/lighter 0: fabric A and B is of the same stiffness/density 3: fabric B is stiffer/lighter	7-point categorical judgement (together with pair comparison)	Bouman et al. (2013)
7	To rate the similarity of tactile properties between vision and touch 1: completely dissimilar 9: completely similar	9-point categorical judgement	Fradin et al. (2023)
8	To rate the tactile perception of flooring materials. 1: more rough / hard / stiff 9: more smooth / soft / compliant	9-point categorical judgement	Topliss et al. (2023)
9	To evaluate the tactile properties in Virtual Reality. 1: extremely soft / smooth 9: extremely hard / rough	9-point categorical judgement	Feick et al. (2023)

To develop the Touch Perception Task (TPT) lexicon, Guest et al. (2011) designed three experiments (No.1 – 3 in Table 2.4) to refine the lexicon from 262 to 26 sensory descriptors, using a 4-point scale to determine how strongly

the word represented the touching experience, a 15-point scale to identify the dissimilarity of all pairs of combinations, and a 5-point scale to evaluate how accurately each sensory word described the actual touch sensation, respectively. The TPT lexicon consists of a comprehensive set of adjectives describing tactile properties. In other tactile-related studies, the investigated tactile attributes often overlapped with the descriptors in the TPT lexicon. When the tactile descriptors and their antonyms are used together for categorical judgement, researchers used to adopt a broader range of rating scales to enable better distinctions, such as 7-point scale and 9-point scale. In the present study, tactile attributes were evaluated in pairs, with each pair consisting of an adjective and its antonym. The 9-point scale was adopted in the experiments in the present study to enable a better understanding.

2.8.1.2 Pair comparison

A paired comparison method can be applied on a small number of stimuli (Fairchild, 2013). All possible pairwise combinations will be presented to observers one pair at a time. A third stimulus is sometimes used as a reference. Observers will be usually asked to choose one stimulus that outperforms the other, and the proportion of one stimulus is selected is normally recorded and calculated. The method is based on the law of comparative judgement developed by Thurstone (Thurstone, 1927). Compared to categorical judgement, pair comparison is not used frequently in the field of fabrics. One exception is that Bouman et al. (2013), combined pair comparison and categorical judgement, presenting a pair of fabric videos and asking participants to choose which one is stiffer/lighter and rate the perception. In the present study, the number of stimuli is relatively large (see Chapter 3), resulting in a massive number of pairwise assessment and thus a highly complex and time-consuming experiment. Therefore, pair comparison was not adopted in the present study.

2.8.1.3 Magnitude estimation and rank order

The methods of magnitude estimation and rank order are introduced in this

section; however, they were not used in the present study, as only limited literature applied them on fabric visual and tactile assessment. Similar to categorical judgement, the method of magnitude estimation asks observers to assign numbers to the stimuli to represent the relative intensity of the perception (Fairchild, 2013). The difference is that there are no assigned categories for each score adopted in magnitude estimation. Observers are free to assign any score within the designated range, and thus the variation between observers can be relatively larger compared to categorical judgement. Rank order, instead of assigning scores to the stimuli, asks observers to rank the stimuli in an increasing or decreasing magnitudes of perception. As reranking will be needed if new stimuli are added in the experiment, ranking is not appropriate for the present study, where fabric images and videos collection is an ongoing process.

2.8.2 Threshold and matching techniques

Threshold experiments are helpful to detect the sensitivity of the perception. Normally observers are asked to report when the stimulus is the just perceptible (absolute threshold) and just perceptibly different (difference threshold) (Fairchild, 2013). A broader threshold indicates lower sensitivity of the perception. There are rarely tactile-related studies applied this method.

Similar to threshold experiment, matching experiment is used to determine when two stimuli are perceived similarly. Participants can be asked to rate the similarity of a pair of samples regarding whether they gave a similar tactile feeling between vision and touch (Fradin et al., 2023; Xiao et al., 2016).

2.8.3 Classification of psychophysical scales

The previous sections introduced visual experimental techniques, and the resulting scales collected in those techniques are introduced in this section.

Nominal scale is unrestricted assignment of numerals, typically represented as a label or naming (Stevens, 1946). In Table 2.5, four classes of psychophysical

scales are listed, and the number “4” here is the numeral assigned to the number of classes.

Ordinal scale is usually used for rank order assessment. A group of fabrics can be ranked by thickness from the thickest to the thinnest (or vice versa), where the thickest fabric is assigned a rank of 1 (or the other way around). However, the differences between the rank do not correspond to the differences in thickness.

In contrast, equal interval is specified for interval scales, based on the assumption that the differences between any two neighbouring points are equal in the scale. An example is the Likert scale where each point is assigned to a specific meaning. However, the differences between points on a Likert scale can also be unequal when using lower number of points (e.g., 3-point Likert scale). Careful mathematical manipulations are required when dealing with Likert scale based on the number of scales and the underlying assumption. In addition, a score of 0 is sometimes set in the interval scales, but it does not imply the nonexistence of the perceived attributes.

Ratio scale is rarely used in visual assessment, as the perception typically lacks a true zero point. The fact that a ratio scale has an absolute zero does not mean that the attributes must necessarily reach that absolute zero (Stevens, 1946). Arithmetic operation such as addition, subtraction, multiplication, and division can be applied on ratio scale such as fabric thickness.

Table 2.5 Four types of psychophysical scales, and their properties and examples (Fairchild, 2013; Stevens, 1946).

Scale	Properties	Examples
Nominal	Naming, label	‘4’ classes of psychophysical scales in this table
Ordinal	Ordered, unequal interval	Ranking the thickness of fabrics
Interval	Equal interval, arbitrary zero	Likert scale (in cases of more scales)
Ratio	Equal interval, natural zero,	The thickness of fabrics

2.9 Image processing techniques

After collecting perceptual ratings through psychophysical experiment, images and videos in the Leeds Fabric Tactile Database are processed to obtain the predictors to predict the tactile and visual-tactile perception. This section reviews various image processing techniques and related studies that have adopted these techniques, including grey-level co-occurrence matrix, Fourier Transform, Wavelet transform. For each method, the principle is firstly introduced, followed by reviewing the related studies.

2.9.1 Grey Level Co-occurrence Matrix (GLCM)

GLCM was firstly proposed as a texture feature computation method by Haralick in 1973 (Haralick et al., 1973). It was initially developed for image classification by computing the spatial statistical distribution of grey levels within the images. Figure 2.16 illustrates the concept of generating a GLCM. The example starts from a 4*4 greyscale image with grey levels from 0 to 3 (step 1). For each pixel in the example image, a maximum of 8 neighbouring pixels, distributed across four orientations (0° , 45° , 90° , and 135°) can be defined (step 2). GLCM generated for four orientations separately, computing the times that any two grey levels have been neighbours (step 3 and 4). For example, for GLCM of 0° (step 3 in Figure 2.16), value at the first row and the first column represents the times that grey level 0 and grey level 0 have been neighbours in the horizontal direction, and values at the first row and the second column represents the times that grey level 0 and grey level 1 have been neighbours in the horizontal direction. The two neighbouring pixels can be replaced by a pair of pixels with a specified distance.

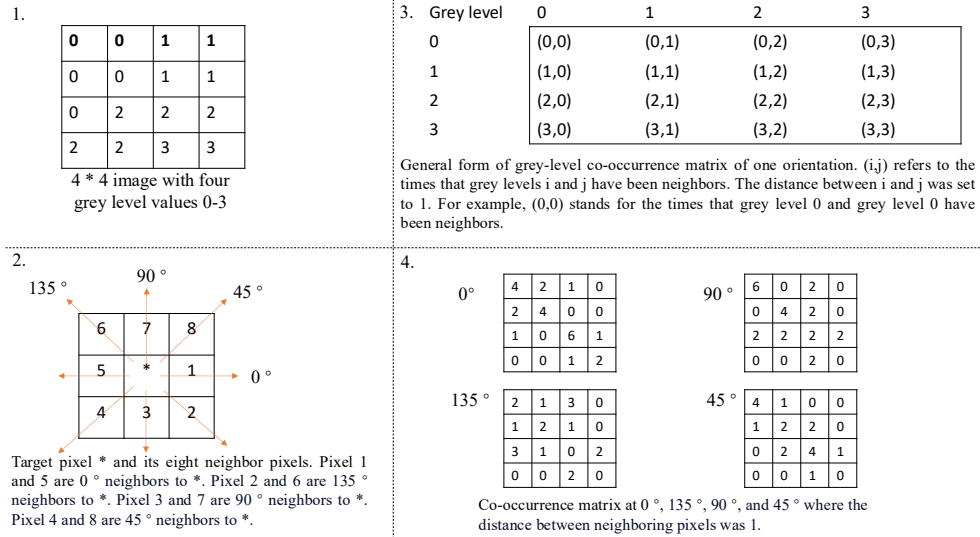


Figure 2.16 Example of the procedures to generate GLCM. Figure was reproduced from Haralick et al. (1973).

There were in total 14 GLCM-based features defined by Haralick et al. (1973). Five features, which are contrast, correlation, angular second moment (ASM, also known as energy), homogeneity, and entropy were widely selected due to their effectiveness in recognising fabrics nature (Kuo and Tsai, 2006) and evaluating the tactile properties (Wang and Georganas, 2009; Elkharraz et al., 2013; Hassan et al., 2023; Wang et al., 2023; Zhang et al., 2017). In these studies, real fabric samples were used to collect the human subjective ratings or structural information, while the corresponding images were analysed to extract the GLCM-based features.

Kuo and Tsai (2006) decomposed 180 fabric images using wavelet transform and extracted only the second-level sub-band images to compute GLCM-based features. GLCM contrast, correlation, ASM, and entropy features were calculated at 0° and 90° orientations with a pixel distance of 1. The feature set was used as the input to train a model classifying the fabric structures, distinguishing between plain, twill, satin, single knitted, double knitted, and non-woven. The model performed good with the accuracy of 95%.

Wang and Georganas (2009) calculated the five features along with dissimilarity, variance and mean for eight single-colour fabrics. The calculation of GLCM-

based features was performed at four orientations with a pixel distance of 1. They concluded that the GLCM features agreed well with human visually perceived fabric roughness. Elkharraz et al. (2013) used 3D printed textures in a rating experiment to evaluate tactile attributes such as warmth, roughness, hardness, and likeness, without allowing participants to see the printed textures. They found that the GLCM correlation feature exhibited good correlation with the perceived naturalness and simplicity. Hassan et al. (2023) developed a haptic texture space consisting of four directions which were rough-smooth, flat-bumpy, sticky-slippery, and hard-soft. A psychophysical experiment was conducted in which participants touched and rated 100 textured materials. A feature set containing GLCM features, Local Binary Patterns, and ResNet 50 was extracted from the images of materials, and used to train a model to predict the tactile perceptual ratings. The model achieved good performance with the RMSE values ranging from 7.91 to 13.39 points on a 100-point scale. Wang et al. (2023) proposed a visual-tactile model trained by GLCM-based features through Siamese Network. The model achieved 90.2% accuracy in classifying the subjectively perceived roughness and stickiness of fabrics. Zhang et al. (2017), analysed the relationship between GLCM-based features, including contrast, correlation, energy, and entropy and the friction coefficients of 100 materials including fabrics, carpet, metal, plastic and so on. Rather than collecting the human perceptual ratings of roughness, they calculated the friction coefficients from the signals that a pen sliding over the surface of materials. Good correlation was observed between the GLCM-based features and objective measurement of friction.

Considering all the above, GLCM exhibited strong effectiveness in correlating the image-based features and tactile perception. Real samples were used, and the GLCM-based features were computed from the corresponding images, which provides valuable references for predicting tactile perception in the present study. However, the role of GLCM in predicting visual-tactile perception

remains underexplored. Therefore, in this study, the GLCM-based features were computed from images and used to predict both visual-tactile and tactile perception.

2.9.2 2D Fast Fourier Transform (2D FFT)

To understand the 2D Fast Fourier Transform used in the present study, it is essential to first understand the concept of Fourier Transform, and then Fast Fourier Transform, and finally 2D FFT. This section follows this structure and uses the book *The Fast Fourier Transform and its application* as the general reference (Brigham, 1988).

2.9.2.1 Fourier Transform

A signal, such as electromagnetic wave, can be represented as a waveform with the x-axis indicating time and y-axis indicating amplitude. The nature of Fourier Transform is to decompose the waveform into a sum of sinusoids with different frequencies. Figure 2.17 illustrates the Fourier Transform in a simple way (Brigham, 1998, p.5). The left component in Figure 2.17 is a waveform to be decomposed. In the middle component, the waveform is decomposed to two sinusoids with different frequencies and different amplitudes. The right component illustrates how the Fourier Transform converts a time-domain waveform (left component) into a frequency-domain representation, showing the amplitude of each frequency component and the corresponding frequency values. The higher amplitude, the frequency contributes more to reconstructing the original waveform.

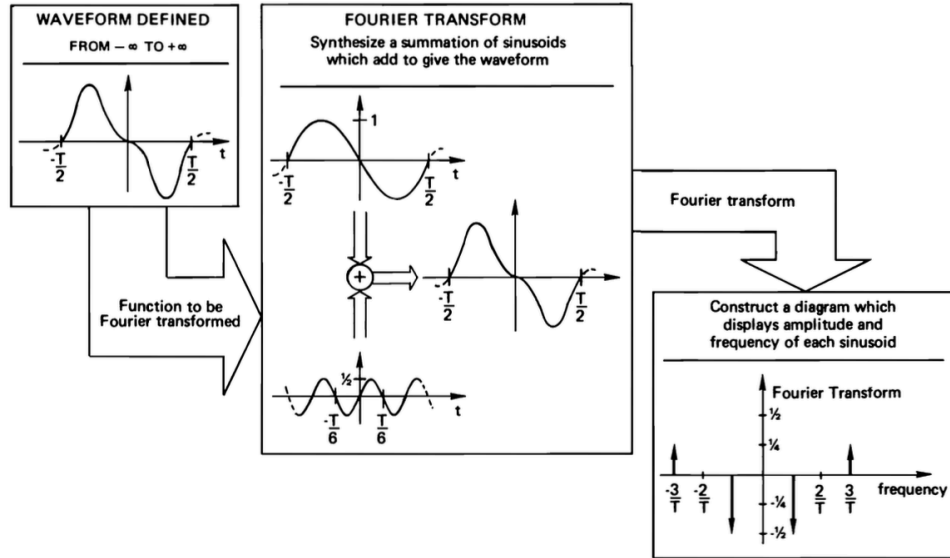


Figure 2.17 Interpretation of Fourier Transform. The figure is from Brigham (1988, p.5)

The Fourier Transform is typically applied to continuous signals over time, however, the pixels in an image represent discrete spatial data rather than a continuous signal. In addition, computational systems can only process discrete numerical data, so any practical implementation of the Fourier Transform on a computer depends on the discrete Fourier Transform (DFT). The difference between Fourier Transform (Equation 2.16) and DFT (Equation 2.17) can be simply reflected through their formulae. The Fourier Transform calculates an integral of a continuous signal over an infinite interval (from $-\infty$ to $+\infty$), while the DFT is a finite summation over N discrete samples of a signal.

$$F(w) = \int_{-\infty}^{+\infty} f(t)e^{-j\omega t} dt \quad \text{Equation 2.16}$$

where $F(w)$ is the frequency spectrum of the continuous signal $f(t)$, j is the imaginary unit where $j^2 = -1$, w is the angular frequency measured in radians per seconds.

$$F(k) = \sum_{n=0}^{N-1} f(n)e^{-j\frac{2\pi}{N}kn} \quad \text{Equation 2.17}$$

where $F(k)$ is the frequency spectrum of the discrete signal $f(n)$, N is the number of discrete samples in the signal representing the total number of time-

domain points available for transformation, k is the frequency index ranging from 0 to $N-1$.

2.9.2.2 Fast Fourier Transform

From Equation 2.17, it is clear that the computation of DFT is massive and requires a significant number of calculations. Specifically, DFT requires N^2 times complex multiplications and additions, making it computationally intensive and not effective for large datasets (Brigham, 1988). Fast Fourier Transform (FFT) is an optimised DFT computation method to solve the issue, reducing the computation to $N \cdot \log N$ times, and thus becomes effective and highly suitable for processing large datasets in practical applications.

2.9.2.3 2D Fast Fourier Transform (2D FFT)

Fourier Transform, Discrete Fourier Transform, and Fast Fourier Transform are all designed to process one-dimensional signal, such as audio signal and one row of pixel values in an image. Two-dimensional discrete signal, such as pixel values in an image, is processed by 2D FFT to obtain the frequency spectrum (Brigham, 1988). For an image with size $M \times N$, the formulae of 2D FFT is shown in Equation 2.18.

$$F(u, v) = \sum_{x=0}^M \sum_{y=0}^N f(x, y) e^{-j2\pi(\frac{ux}{M} + \frac{vy}{N})} \quad \text{Equation 2.18}$$

where $F(u, v)$ is the 2D frequency spectrum, describing the frequency characteristics of the 2D signal in the frequency domain, u is the horizontal frequency and v is the vertical frequency. Higher values of u and v represent higher frequencies, which corresponds to areas of rapid variation in the spatial domain. When $u = 0$ and $v = 0$, it represents the lowest frequency component in the frequency spectrum (also known as DC components), indicating the smoothest and most uniform component in the spatial domain. If an image contains large uniform or smoothly varying area, the low frequency component is typically stronger. Transform an image to the frequency domain contains two

sequential steps: apply the FFT to each row in the image and then apply the FFT to each column in the image. In this way, the 2D FFT can be regarded as the results of two successive one-dimensional FFT operation.

2.9.2.4 Related studies

Previous studies used the frequency spectrum to generate a set of features. For example, 2D FFT are widely used in fabric defects detection by scanning the fabric appearance and analysing the irregular change of frequency (Malek et al., 2013; Chan et al., 2000; Hu et al., 2015). Wang et al. (2020) applied band filters to the frequency spectrum and computed the total spectrum energy within each band respectively. The spectrum energy within each band across the full spectrum were grouped as the feature set and were used to train a classification model of fabric smoothness. Choi et al. (2009) developed a quantitative fabric wrinkle grading system based on 2D FFT. The basic idea was increased number and intensity of wrinkles is associated with rapid variation in greyscale intensity. They applied a set of band filters with different band width and calculated the total spectrum energy within each band. A good correlation was found between the sub-band total spectrum energy and wrinkle grades.

In addition to the frequency spectrum, studies also found that the fabric surface roughness can be evaluated by fractal dimension calculated by estimating the FFT power spectrum (Wang and Georganas, 2009). The FFT features selected in the present study are summarised in Chapter 7, Section 7.2.5.

2.9.3 Wavelet Transform (WT)

An image can be transformed into the frequency domain by 2D FFT, where the frequency and corresponding amplitudes of the image are analysed. However, the 2D FFT only provides a global frequency information, and the local spatial information of the frequency cannot be analysed. Therefore, wavelet transform was developed to analyse the signals in time and frequency domain simultaneously, and the formula is shown in Equation 2.19. The nature of

wavelet is the small wave with rapid oscillation that decays quickly (Sifuzzaman, 2009). Similar to Fourier Transform, wavelet transform decomposes a signal $f(t)$ to a sum of wavelet functions rather than sinusoids as in Fourier Transform. The wavelet functions are generated through a mother function $\psi(t)$ by dilation and translation, where a controls the scale of dilation and b controls the translation (time position). $CWT(a, b)$ are the wavelet coefficients, indicating the similarity or correlation between the signal $f(t)$ and the wavelet functions at different scales and positions. Higher wavelet coefficient means stronger similarity between the wavelet and the signal at the corresponding scale and position.

$$CWT(a, b) = \frac{1}{\sqrt{|a|}} \int_{-\infty}^{+\infty} f(t) \psi\left(\frac{t-b}{a}\right) dt \quad \text{Equation 2.19}$$

The above equation is for implementing wavelet transform on a continuous signal. Both a and b vary continuously to compute the wavelet coefficients, generating a large and redundant dataset. In practical application, parameters a and b can be discretised to simplify the continuous wavelet transform (CWT) to the discrete wavelet transform (DWT), reducing the computational complexity and achieving a more efficient transform.

For a two-dimensional signal $f(x, y)$, e.g., an image, the DWT contains two steps. The decomposition process is illustrated in Figure 2.18, using the image of size $M \times M$ as an example (Chang and Kuo, 1993). The first step is to decompose each row of pixels to obtain the low frequency component and high frequency components. In the second step, the resulting low and high frequency components from the first step are further decomposed column-wise. The two sequential steps decompose the $M \times M$ image into four sub-images: Low-Low (LL), Low-High (LH), High-Low (HL), and High-High (HH) components with the size of $\frac{M}{2} \times \frac{M}{2}$. LL sub-image represents the approximation information, LH sub-image represents the horizontal details, HL sub-image represents the vertical

details, and HH sub-image represents the diagonal details. Wavelet transform allows an image to be decomposed repeatedly by decomposing the LL sub-images. Each process reduces the image size to half of those before decomposition.

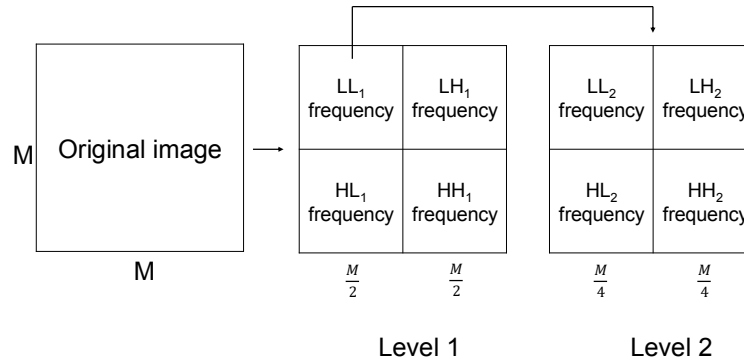


Figure 2.18 Decomposition of an image by 2D WT. The figure is reproduced from Chang and Kuo (1993). LL: Low-Low, LH: Low-High, HL: High-Low, HH: High-High.

Similar to Fourier Transform, the wavelet transform is also widely used in fabric defect analysis, such as locating the fabric defects (Li et al., 2015; Mahmood et al., 2023), classifying the fabric defects (Talu et al., 2022), and detecting fabric defects (Kang et al., 2013). Sun (2012) used wavelet transform to decompose fabric images five times. The wavelet coefficients at level 4 and level 5 were used to compute five features: total energy, wrinkle hardness, wrinkle density, wrinkle directionality, and contrast, to classify the fabric wrinkle ratings. The results showed that the features were effective in indicating the orientation and softness of the wrinkles and agreed with the wrinkle ratings. Similarly, Wang et al. (2020) used the same five features, together with features from GLCM and 2D FFT, to classify the fabric smoothness. The features total energy and contrast were adopted in the present study, with the details given in Chapter 7 Section 7.2.6.

2.9.4 A case of generating images from videos

The above subsections introduced three image processing techniques. In the present study, visual-tactile perception was evaluated using both fabric images

and videos. One way to apply image processing techniques to videos is to process each frame individually and then average the results. However, the process requires significant computational resources and is highly time-consuming. In Bouman et al.'s study (2013), they used horizontal space*time slice of the video to evaluate the fabric stiffness and density. To generate the horizontal space*time slice, one row of each frame in the video was extracted and stacked over time, and the non-fabric area was masked out. An example from Bouman et al. (2013), is shown in Figure 2.19. A fabric (the left figure in Figure 2.19) was hung, and a video was recorded when the fabric was exposed to three different strengths of wind. The horizontal space*time slices (the right three figures in Figure 2.19) can be generated from the video, and thus further process can be performed on the space*time slices, saving the computational resources and time.

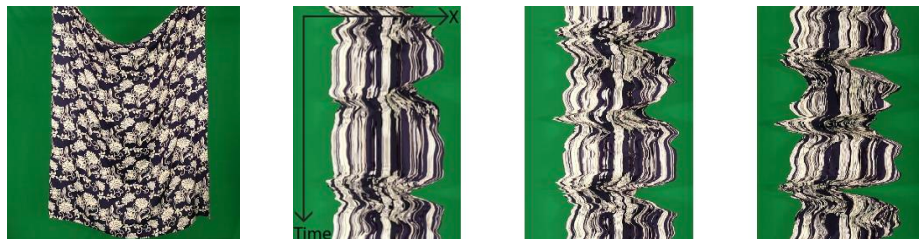


Figure 2.19 An example of the horizontal space*time slice from Bouman et al. (2013, p.1984 & 1985).

Inspired by the horizontal space*time slice from Bouman et al. (2013), the fabric rotation videos in the present study were processed in a similar way first, and then processed by different image processing techniques. The details are given in Chapter 7, Section 7.2.1, 7.2.2, and 7.2.3.

2.10 Statistical analysis techniques

In this section, the statistical analysis techniques used were introduced. All the analyses in the present study were conducted using Microsoft Excel, Rstudio, and MATLAB.

2.10.1 Central tendency and variability

The measure of central tendency gives a single data to describe a set of data, and the measure of variability describes the distribution of a set of data (Aron et al., 2013). Mean (or average) and median are two frequently used measures of central tendency. The mean of a set of data is usually represented by \bar{X} , calculated by dividing the sum of all data points by the total number of observations (N), as given in Equation 2.20. Median is the middle data point when sorting the data from lowest to highest.

$$\bar{X} = \frac{\sum X}{N} \quad \text{Equation 2.20}$$

Variability of a set of data describes the spread of the data around the mean, typically represented by *variance* or *standard deviation* (SD), where SD equals to the square root of the variance. The formula is given in Equation 2.21.

$$SD^2 = \frac{\sum (X - \bar{X})^2}{N} \quad \text{Equation 2.21}$$

2.10.2 z-standardisation

Using mean or median to describe a set of data can be misleading in the presence of outliers. Comparisons between multiple sets of data can also be distorted because of different ranges and variance of data sets. A z-score is normally computed for each data point in the dataset, by subtracting the mean and dividing by the SD, as given in Equation 2.22 (Aron et al., 2013). The data pre-processing step is referred to as z-standardisation. In this way, the dataset will have a mean value of 0 and a SD of 1, allowing for effective comparisons between multiple datasets.

$$z = \frac{X - \bar{X}}{SD} \quad \text{Equation 2.22}$$

2.10.3 Normal distribution test

A normally distributed dataset exhibits a bell-shaped curve, which is roughly symmetric to the mean (Aron, et al., 2013). Statistical analysis methods usually

follow an assumption that the dataset needs to be normally distributed. The bell-shaped curve is one of the methods to directly to be compared whether the distribution of the data follows the shape. Q-Q plot is an alternative to visualise the distribution of the data. Figure 2.20 shows examples of a normally distributed dataset, illustrated by a histogram and a Q-Q plot. Comparisons can be made on whether the data follows the bell-shaped curve in the histogram and whether the data follows the diagonal in Q-Q plot. Hypothesis tests are also available to test the normality, such as Shapiro-Wilk test and Kolmogorov-Smirnov test. The null hypothesis states that the data is normally distributed, and a rejection of null hypothesis ($p < 0.05$) indicates not normal distribution.

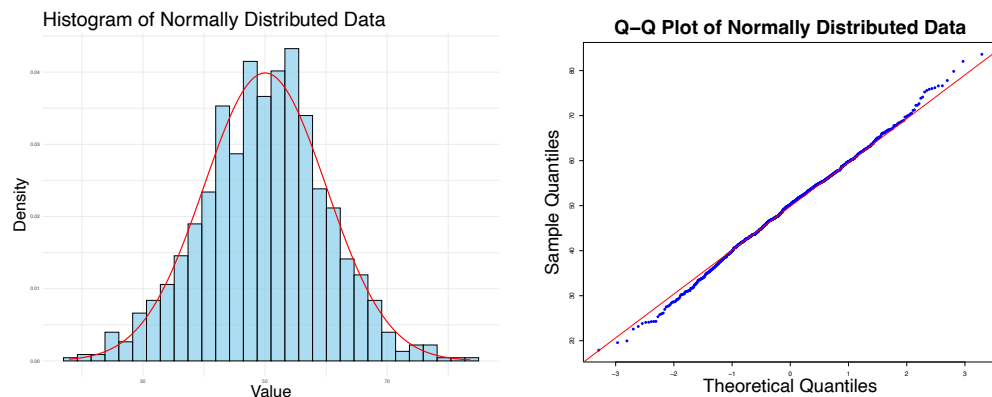


Figure 2.20 Visualisations of a normally distributed dataset. Left: distribution. Right: Q-Q plot.

2.10.4 Pearson Correlation Coefficients

The relationship between two or more datasets is normally referred to as correlation. A scatter diagram directly reveals the correlation between two datasets (z-standardisation can be pre-processed if the ranges and variations differ significantly), while the interpretation of correlation coefficients can be more effective. Pearson Correlation Coefficients, r , can be used on continuous data, defined in Equation 2.23 (Howitt and Cramer, 2011). The coefficients range from -1 to 1, where -1 represents a perfectly negative correlation, 1 represents a perfectly positive correlation, and 0 represents nearly no correlation. Examples are illustrated in Figure 2.21.

$$r = \frac{\sum(X - \bar{X})(Y - \bar{Y})}{\sqrt{\sum(X - \bar{X})^2} \sqrt{\sum(Y - \bar{Y})^2}}$$

Equation 2.23

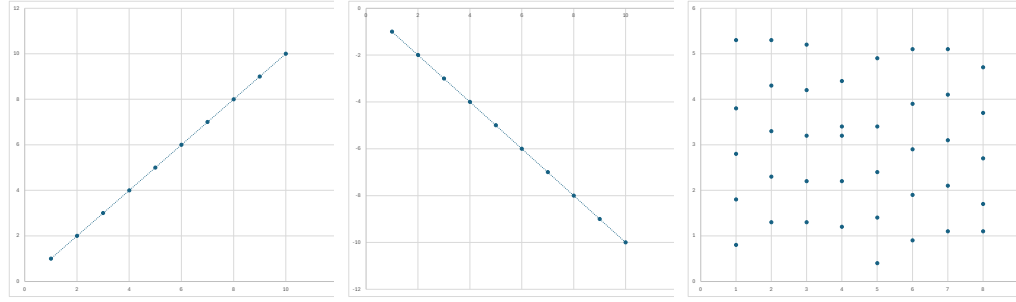


Figure 2.21 Examples of perfectly positive correlation (left), perfectly negative correlation (middle), and nearly no correlation (right).

In addition, the significance of the correlation coefficients become important along with the coefficients, indicated by p as defined in Equation 2.24 (Aron, et al., 2013). $P(T > |t|)$ represents the two-tailed probability of the t -value under a t -distribution with $N-2$ degree of freedom. Normally, the significance level is set at $p < 0.05$. Pearson Correlation Coefficients were used in the present study to interpret the data.

$$t = \frac{r}{\sqrt{(1 - r^2)/(N - 2)}}$$

$$p = 2 * P(T > |t|)$$

Equation 2.24

2.10.5 Mann-Whitney U test

Mann-Whitney U test is a nonparametric test to compare the distribution of two independent sets of data (Siegel and Castellan, 1988). The word “nonparametric” here means that no assumption is specified for parameters (e.g., mean or variance). For parametric test, e.g., t -test, a strong assumption has to be ensured that the data is normally distributed, otherwise the result can be less effective. Since the raw data collected in the present study do not follow normal distribution (see Section 6.3 for experiment Phase II), Mann-Whitney U test was selected to compare the distribution of the tactile perceptual ratings between woven and knitted fabrics.

2.10.6 Cumulative Link Mixed Model (CLMM)

Cumulative Link Model (CLM) is a regression model for categorical data. Cumulative Link Mixed Model (CLMM) is an extension of CLM that allows for both fixed effects and random effects to be assessed in one model (Agresti, 2010). Rather than predicting categories directly, CLMM models the response variable through cumulative probability and thresholds using a logit link function, defined as Equation 2.25, where α_j is the intercept for each category j , β is a column of vectors of parameters describing the effects of fixed effects X_i , and Zb is the random effects.

$$\begin{aligned} \text{logit}(P(Y \leq j)) &= \log \frac{P(Y \leq j)}{1 - P(Y \leq j)} & \text{Equation 2.25} \\ &= \alpha_j + \beta X_i + Zb \end{aligned}$$

2.10.7 Observer variability test

In all psychophysical studies, observer variability is essential to be tested prior to the data analysis to ensure a consistent understanding of the experiments and thus prevent a misleading result and conclusion due to confusion. It includes two parts: the variability between observers (inter-observer variability, also known as observer accuracy) and within individual observer (intra-observer variability, as known as observer repeatability). Root Mean Square (RMS) defined in Equation 2.26 was used in the present study to assess the observer variability. For each sample, an RMS value can be calculated, indicating the difference between two sets of ratings in the original rating scale. Observer variability can also be tested in various methods, for example, the mean colour difference of the mean (MCDM) has been widely used in studies where colour data were obtained from human participants. In the present study, RMS values were calculated as a measure of observer variability to directly reveal the differences in the 9-point Likert scale.

$$RMS = \sqrt{\frac{\sum_i (x_i - \bar{x})^2}{N}} \quad \text{Equation 2.26}$$

2.10.8 Regression techniques

Integrating the image processing techniques in Section 2.9 and statistical methods in Section 2.10, one of the objectives of the present study is to model the visual-tactile and tactile perception using explanatory information extracted from fabric images. Different linear regression techniques were used and compared, and the following subsections introduced the principle, advantages and limitations.

2.10.8.1 Ordinal Least Square (OLS)

Ordinal Least Square (OLS) is one of the least square methods applied to linear regression (Hastie et al., 2009). Equation 2.27 gives the basic form of a linear regression model. The effects of the explanatory variables X_i are interpreted through the parameter β_i by minimising the residual sum of squares (RSS). Figure 2.22 visualises the minimisation principle, where β_i is adjusted for each X_i to minimise the sum of the differences between the original data and the fitted data.

$$\hat{y}_i = \beta_0 + \sum_{i=1}^N \beta_i X_i \quad \text{Equation 2.27}$$

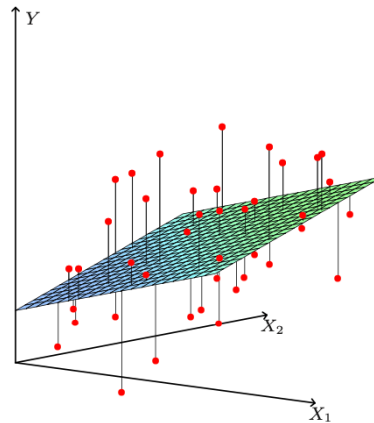


Figure 2.22 Minimising the residual sum of squares. The figure is from Hastie et al. (2009, pp.45).

There is no limitation of the number of explanatory variables fitted into an OLS model. However, including too many irrelevant variables in an OLS model could increase complexity and lead to overfitting. Methods such as forward- and backward-stepwise selection can be implemented to reduce the dimension of explanatory variables, by either adding or excluding an irrelevant predictor one by one from the input (Hastie et al., 2009). A notable limitation is that the selection of a subset of data is a discrete process. A predictor can be retained in one dataset but excluded in the other, leading to high variance between models. Therefore, stepwise selection was not implemented in the present study, and more effective shrinkage methods were adopted instead.

2.10.8.2 Shrinkage techniques

The regression coefficients β are regularised by incorporating L1, L2 or a combination of both penalties into the regression models (Hastie et al., 2009). Ridge Regression (RR) shrinks coefficients toward but not equal to zero by incorporating L2 penalty (Equation 2.28). Least Absolute Shrinkage and Selection Operator Regression (LASSO) forces coefficients of irrelevant variables towards zero by incorporating L1 penalty to only fit relevant variables in the model (Equation 2.29). The Elastic Net (EN) regression incorporates both L1 and L2 penalties to balance the shrinkage and selection of variables (Equation 2.30). Tuning parameter λ controls the strength of shrinkage applied to parameter. A larger λ means greater penalty, shrinking the parameter more strongly towards zero. Tuning parameter α balances the L1 and L2 penalty. The three linear regression methods with penalty continuously control the parameters and prevent high variance from the model. They are also effective for high-dimensional data and dataset with multicollinearity.

$$\hat{\beta}_{RR} = \underset{\beta}{\operatorname{argmin}} \left\{ \sum_{i=1}^N (\hat{y}_i - y_i)^2 + \lambda \sum_{j=1}^p \beta_j^2 \right\} \quad \text{Equation 2.28}$$

$$\hat{\beta}_{LASSO} = \underset{\beta}{\operatorname{argmin}} \left\{ \sum_{i=1}^N (\hat{y}_i - y_i)^2 + \lambda \sum_{j=1}^p |\beta_j| \right\} \quad \text{Equation 2.29}$$

$$\begin{aligned} \hat{\beta}_{EN} = \underset{\beta}{\operatorname{argmin}} \{ & \sum_{i=1}^N (\hat{y}_i - y_i)^2 + \lambda [(1 - \alpha) \sum_{j=1}^p \beta_j^2 + \\ & \alpha \sum_{j=1}^p |\beta_j|] \} \end{aligned} \quad \text{Equation 2.30}$$

The tuning process of λ and α is usually achieved by repeated k-fold cross-validation. The data is randomly split into k folds, where k-1 folds are used to fit the model. For RR and LASSO, models with a predefined set of λ values are fitted respectively, and the optimal λ is decided based on the one that minimise the RMSE (or maximise R^2) evaluated on the remaining k fold. For EN model, the parameter α is predefined within the range of 0 and 1, and for each α , the optimal λ is defined as described above. The final optimal α is thus defined when the RMSE value is minimized evaluated by the remaining k fold. The implementation of RR, LASSO, and EN was carried out using *glmnet()* R package (Friedman et al., 2010) in the present study, where k was set to 10 as the default setting of the package.

2.10.9 Factors comparing model performance

Multiple models were developed in the present study (See Chapter 7). The model performance was compared using Root Mean Square Error (RMSE) and Coefficient of Determination (R^2).

2.10.9.1 Root Mean Square Error (RMSE)

RMSE, defined as Equation 2.31, measures the difference between original data (y_i) and predicted data (\hat{y}_i) in the original rating scale. Smaller RMSE indicates better predictive performance and more effective model.

$$RMSE = \sqrt{\frac{1}{N} \sum_{i=1}^N (y_i - \hat{y}_i)^2} \quad \text{Equation 2.31}$$

2.10.9.2 Coefficient of Determination (R^2)

The coefficient of determination is usually equals to the square of correlation coefficients (Howitt and Cramer, 2011), while the equation is individually shown below. It explains to what extent the variance of dependent variable can be explained by independent variable. The R^2 value ranges from 0 to 1, where 1 indicates a perfect fitted model.

$$R^2 = 1 - \frac{\sum_{i=1}^N (y_i - \hat{y}_i)^2}{\sum_{i=1}^N (y_i - \bar{y})^2} \quad \text{Equation 2.32}$$

2.11 Summary

This Chapter reviews the relevant studies, following the structure of the present study.

- The relevant research on tactile and visual-tactile perception were firstly reviewed. The following limitations were found: (1) the tactile properties of fabrics were evaluated mainly using real fabrics, leading to the concept of tactile perception. Images and videos were less used but attracted attention to evaluate the what humans see and what humans touch, leading to the concept of visual-tactile perception; (2) the tactile properties were evaluated under different conditions, such as images only, video only, touch-only, vision-only (using real fabrics), and a combination of vision and touch. It is unknown whether there is correlation and difference among them; (3) studies evaluated various tactile attributes from the perspectives of objective measurement and subjective perception. For consumers, readings from instruments are hard to interpret, and the results from subjective perception are mixed. It remains unclear whether the various tactile attributes correlate with each other; (4) the fabric structure and fabric colour give infinite appearances of fabrics. The effects of fabric structure and colour have not been fully investigated.
- Given the above limitations, it is necessary to evaluate the tactile properties

thoroughly, and the results are supposed to be simple and interpretable for consumers. The existing fabric databases were reviewed, and the reasons why a new Leeds Fabric Tactile Database was developed by the present studies were identified.

- The CIE colorimetry was reviewed to provide basic concepts in camera colour characterisation and display colour characterisation, which are two necessary steps to process the images and videos in the Leeds Fabric Tactile Database. CIE XYZ values were calculated in the characterisation processes, and CIE uniform LAB colour space was adopted in specifying fabric colours.
- To precisely reproduce the fabric appearance, all fabric images and videos in the Leeds Fabric Tactile Database were processed by the camera characterisation model and display characterisation model. The processes were reviewed.
- Colour measurement methods were reviewed, which was adopted in camera and display characterisation and measuring fabric colours.
- The techniques in psychophysical experiment were reviewed. In the present study, categorical judgement was used in all psychophysical experiments to rate the tactile and visual-tactile perception.
- To model the tactile and visual-tactile perception, predictors were extracted from fabric images and videos. Image processing techniques were reviewed and applied to the present study.
- The statistical analysis techniques were reviewed at the end of this chapter, providing the basic concepts for the analyses in the present study.

Chapter 3

Developing Leeds Fabric Tactile Database

3.1 Overview

In this Chapter, the development of Leeds Fabric Tactile Database was described (Section 3.2), and the psychophysical experiments for assessing fabric visual-tactile perception and tactile perception were conducted using categorical judgement methods (Section 3.4 and 3.5). The experiments have been carefully prepared by conducting colour characterisation and image processing (Section 3.3). The database includes two parts: colour-rendered fabric images and real fabric images, together with the corresponding tactile ratings. Figure 3.1 describes the use of two parts and the overall experiment design. Leeds Fabric Tactile Database Part I was used in experiment Phase I, and the experiment Phase II used Leeds Fabric Tactile Database Part II. Through the two series of experiments, a comprehensive investigation of fabric visual-tactile and tactile perception was provided in the following chapters.

Experiments	Stimulus	Conditions	Task	Data analysis
Part I (experiment Phase I)	<ul style="list-style-type: none"> • 240 flat fabric images • 240 draped fabric images (15 fabric images*16 colours) 	<ul style="list-style-type: none"> • Flat fabric images • Draped fabric images • Touch-only 	<ul style="list-style-type: none"> • Flexible-stiff • Smooth-rough • Soft-firm • Spongy-crisp • Warm-cool 	Chapter 4
Part II (experiment Phase II)	<ul style="list-style-type: none"> • 118 flat fabric images • 354 draped fabric images • 118 fabric rotation videos • 118 real fabrics 	<ul style="list-style-type: none"> • Flat fabrics images • Draped fabric images • Fabric rotation videos • Touch-only • Vision-only • Vision+touch 	<ul style="list-style-type: none"> • Flexible-stiff • Smooth-rough • Soft-firm • Spongy-crisp • Warm-cool 	Chapter 5, Chapter 6, Chapter 7

Figure 3.1 Experiments Overview.

3.2 Leeds Fabric Tactile Database preparation

Fabric products are the must-buy commodities that humans are exposed to. Current fabric image databases were developed mainly for pattern recognition and classification. Despite the large number of fabric images available in other databases, the inaccessible of the real fabrics make them less suitable for

studying the differences in the perception between images and real fabrics. One of the objectives of this work is to build a ready-to-use Leeds Fabric Tactile Database, including both fabric visual representations, real fabrics, and the corresponding tactile perceptual ratings.

3.2.1 Part I: colour-rendered fabric images and corresponding real fabrics

3.2.1.1 Real fabrics

Fifteen fabrics were selected in Part I, twelve of which were purchased due to their various appearances and textures from the Whaleys-Bradford online store, and three of which were selected in the testing lab in the School of Design, University of Leeds. The fabric thickness was measured in millimetres (mm), ranging between 0.10 mm and 1.15 mm. Fabrics and their images were used in the experiment Phase I in Section 3.4. The information of the fifteen fabrics is given in Appendix A.

3.2.1.2 Image capture

The fabrics were cut into 20*20 cm pieces. The image capture was conducted under the simulated CIE D65 illuminant within the X-Rite Virtual Lighting Booth (VLB) without any external lighting. The setup of the capturing environment is shown in Figure 3.2. For flat fabric images capturing, the fabric was placed on the equilateral triangle stand with the degree of 60°, and the angle of the camera was set to 30°, thus the camera can capture fabrics in the vertical direction. For draped fabric images capturing, the centre of the fabric was put onto a cylindrical stand with a diameter of 6 cm and height of 20 cm, making the fabric drapes in a natural condition. A SONY DLSR ILCE-7RM4A camera with a shutter speed of 1/200 second, focus of 5.0, ISO 500, and white balance of 6200K was used to capture the images. The distance between the lens and the fabric was set to approximately 45 cm.

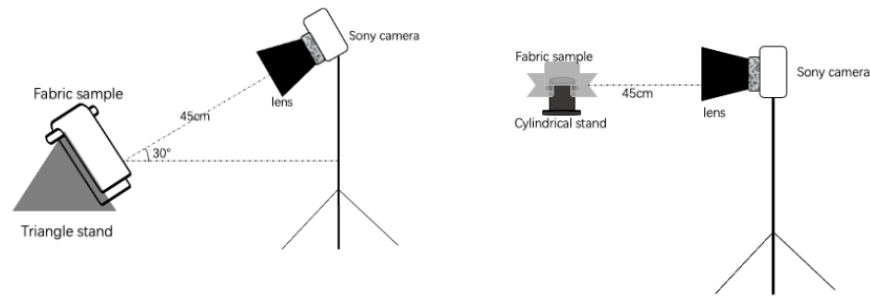


















Figure 3.2 The schematic diagram for capturing flat fabric images (left) and draped fabric images (right).

3.2.1.3 Colour rendering

To generate fabric images in different colours while preserving the same texture, four neutral colours that are close to the CIE reference grey, and three levels of those four colours that are close to the CIE reference colours (red, yellow, green, blue) were selected (Robertson, 1978). The CIE LAB values of the 16 colours are listed in Table 3.1.

Table 3.1 CIE LAB values of the selected 16 colours.

Colour		L*	a*	b*
1		25.7	0.3	-1.5
2		88.0	-2.1	0.4
3		43.2	0.3	0.2
4		72.1	0.4	0.6
5		65.1	10.5	43.5
6		82.2	3.7	90.0
7		53.6	21.6	64.5
8		61.4	-26.4	-1.8
9		38.9	-8.4	-34.2
10		48.8	14.6	-21.8
11		53.6	32.3	14.3
12		54.7	64.7	51.3
13		32.9	48.5	25.4
14		71.4	-37.6	35.7
15		43.1	-13.8	43.7
16		55.5	-52.6	25.3

The colours gave an average distribution in the CIE LAB colour space, as shown in Figure 3.3. 16 images in selected colours were thus generated for each fabric and each condition by a colour rendering process in MATLAB. There were

15*16=240 images generated for flat and draped fabrics separately. Details of image processing was described in Section 3.3.3.

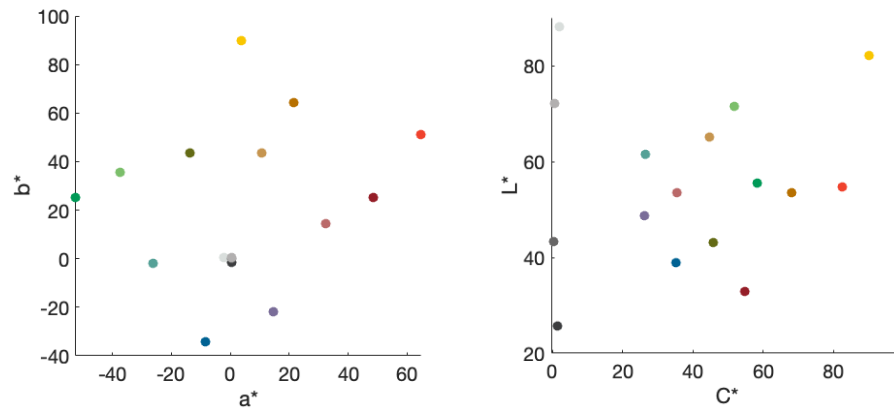


Figure 3.3 The distribution of the selected 16 colours in CIE a^*b^* (left) and CIE C^*L^* (right) colour space.

3.2.2 Part II: real fabrics and their visual representations

3.2.2.1 Real fabrics

A set of 118 fabrics purchased online were prepared in Part II, including but not limited to merino-woollen wool, melton wool, viscose, linen, polyester, silk, and cotton. The information of the fabrics is given in Appendix A. The fabrics were cut into 30*30 cm pieces. The fabric thickness was measured in millimetres (mm), ranging between 0.06 mm and 4.56 mm. The colours were measured using Konica Minolta CM-700d spectrophotometer, set to SCI, MAV (diameter=8 mm), CIE D65 illuminant. Figure 3.4 shows the reasonable distribution of fabric colours in the CIELAB colour space. A total of 48 fabrics were semi-transparent, meaning that objects, e.g., a palm, placed behind them can still be observed. Fabrics and their images and videos were used in the experiment Phase II described in Section 3.5.

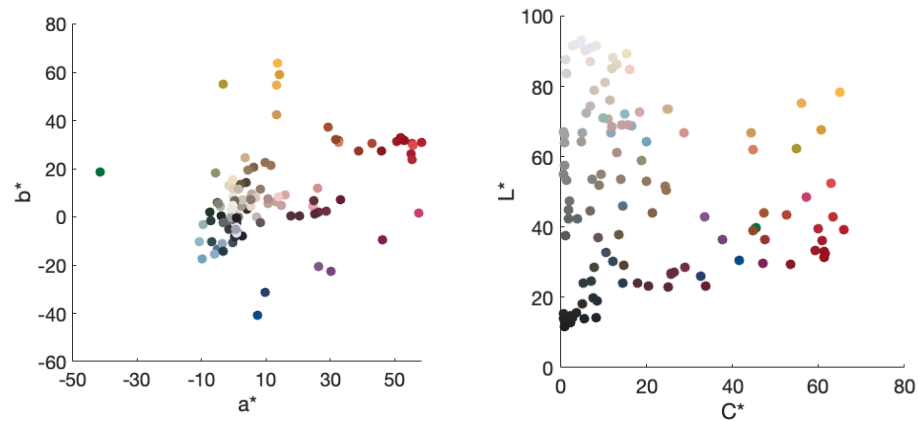


Figure 3.4 The distribution of fabric colours in CIE a^*b^* (left) and CIE C^*L^* (right) colour space.

3.2.2.2 Fabric visual representation (images and videos)

As the same as in Part I, the flat fabric images in Part II were taken under the simulated CIE D65 illuminant within the VLB. There was no other lighting in the room where the photography took place. The SONY DSLR ILCE-7RM4A camera with a speed of 1/8 second, ISO 2000, focus of 5.0 and white balance of 6200K was used to capture the flat fabric images. 118 flat fabric images were captured and used in the experiments.

In addition, the VLB provided a rotation stage with adjustable rotational speed, where the fabric was draped freely over a cylindrical stand with a diameter of 6 cm and a height of 30 cm. The rotation stage was adjusted to rotate clockwise at approximately 270 degree per minute, and the same Sony camera was used to capture the video in manual mode. The fabric completed a 360-degree rotation in each video, with a duration of approximately 80 seconds and a frame rate of 25 per second. It is noted that the shadows and highlights caused by folds can be different when observed from different angles, leading to different fabric appearances. Additionally, it is not feasible to maintain the fabric's drape condition completely consistently through repeated draping. Therefore, three frames were extracted from each video at specific frames: (1) at the start of the video (drape_0); (2) when the fabric had rotated clockwise by 45 degrees (drape_45); (3) and when the fabric had rotated clockwise by 90 degrees

(drape_90). Figure 3.5 shows the fabric rotation process during video capture, along with representations of three extracted frames. The warp direction of the fabric was always at the left side at the beginning of the video (drape_0). 118 fabric rotation videos were captured, and 354 draped fabric images were prepared in the experiments. Details of the image processing were described in Section 3.3.3.

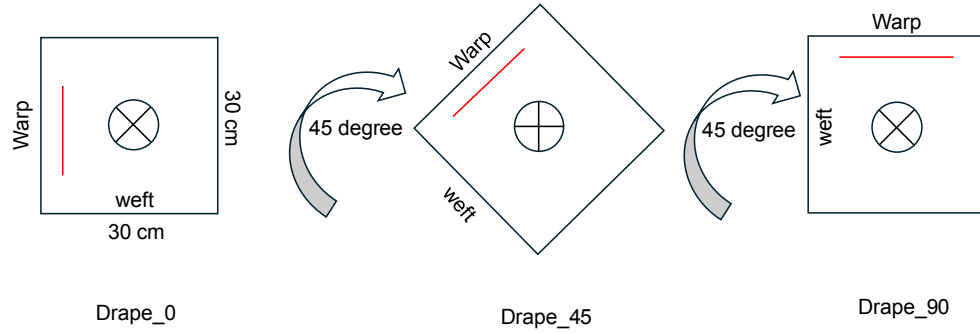


Figure 3.5 The top view schematic representation of the rotating fabrics. Left: drape_0. Middle: drape_45. Right: drape_90.

3.3 Experimental preparation

3.3.1 Camera characterisation

An image of the GretagMacbeth ColorChecker® DC chart was captured at the same position as the fabrics in the VLB, using the same SONY camera with the same camera settings. The RGB values of each colour patch were derived from the captured DC chart image. The spectral reflectance of each colour patch in the DC chart was measured by the Konica Minolta CM-700d spectrophotometer (MAV, CIE D65 illuminant), and the CIE XYZ tristimulus values were calculated with the CIE 1931 colour matching functions (CMFs) and the measured spectral power distribution (SPD) of the CIE D65 illumination in the VLB. Technique of third-order polynomial regression was used as the mapping method to train an optimized characterisation model between the input (camera RGB) and the output (the calculated CIE XYZ tristimulus values) (He et al., 2021). The model achieved good prediction of less than $3.0 \Delta E^*_{00}$ unit averaged from 240 DC

colour chart patches as test colours.

3.3.2 Display characterisation

The experiment Phase I and Phase II were both conducted on a 24.1-inch BenQ colour professional display (LCD backlit, adobe RGB colour space, brightness 24, contrast 50, sharpness 5). To truly reproduce the appearance of the fabrics, the colour characteristics of the display were measured, and a characterisation process was conducted. The following colour patches were prepared in Microsoft PowerPoint software:

1. To evaluate the display spatial independence, a white patch (RGB=255, 5*5 cm) displayed in the centre of the screen with a black surrounding, and an identical full-screen white patch were prepared.
2. To evaluate the display channel independence, a full-screen pure red (R=255, G=0, B=0), a full-screen pure green (R=0, G=255, B=0), and a full-screen pure blue (R=0, G=0, B=255) were prepared.
3. To conduct the display characterisation, 18 grey patches with RGB values ranging from (0, 0, 0) to (255, 255, 255), increasing by 15 at each step were prepared in the centre of the screen with a grey background.
4. To test the display characterisation performance, 30 randomly selected colour patches were prepared in the centre of the screen with a grey background.

The BenQ display was placed where the experiments would be conducted and warmed up for 30 minutes before the colour characteristics measurements. The colour patches were displayed in full-screen mode of Microsoft PowerPoint and measured in the dark room. The Konica Minolta CS-2000 spectroradiometer was used to measure the CIE XYZ tristimulus values of each colour patch in unit of cd/m^2 . The spectroradiometer was set to 1° field of view and CIE 2 degree observer, and the distance between the spectroradiometer and the display was set to approximately 0.6 m.

The CIEDE2000 colour difference between the white patch with black surrounding and the full-screen white patch was calculated as the spatial independence. Good spatial independence was achieved for the BenQ display with the result of $0.19 \Delta E^*_{00}$ unit. In addition, a prediction of full-screen white was calculated by adding the CIE XYZ tristimulus values of the pure full-screen red, pure full-screen green, and pure full-screen blue. The CIEDE2000 colour difference between the measured full-screen white and the predicted full-screen white was then calculated as the channel independence. Good channel independence was achieved for the BenQ display with the result of $1.61 \Delta E^*_{00}$ unit.

The display characterisation was implemented using the gain-offset-gamma (GOG) model (Berns, 1996), trained by conducting transformation between the pre-defined RGB values of the 18 grey patches and the measured CIE XYZ tristimulus values. The developed GOG model achieved a prediction of less than $0.2 \Delta E^*_{00}$ unit averaged from the 18 grey patches as test colours, and less than $0.8 \Delta E^*_{00}$ unit averaged from 30 randomly selected colour patches as test colours. The results showed that the BenQ display has been well characterised. Details of the GOG model was listed in Table 3.2 in terms of the gain, offset, gamma values for RGB channels.

Table 3.2 GOG model of the BenQ display.

	Gain	Offset	Gamma
R	0.9970	-0.0017	2.2507
G	1.0152	-0.0081	2.2270
B	1.0159	-0.0126	2.2234

3.3.3 Image processing

Figure 3.6 shows the details of the image processing. For fabric images in Part I, the selected 16 colours were transformed from CIELAB values to the CIE XYZ tristimulus values using the measured BenQ display white point, and then converted to the RGB values based on the BenQ display characterisation GOG

model. The fabric RGB images were transformed to greyscale images using the *rgb2gray* function in MATLAB. The greyscale value of each pixel was multiplied by the newly converted RGB values respectively to reconstruct the RGB channels of the images. Each channel was then adjusted using the corresponding mean value. For draped fabric images, the colour rendering process was only implemented on the fabric areas.

For fabric images in Part II, images were processed through the camera characterisation model first. The RGB values of each pixel were converted into the CIE XYZ tristimulus values, and then transformed back to RGB values through the BenQ display characterisation GOG model to generate the final images. For fabric videos in Part II, each frame was processed in the same way as the images. The image process was implemented using MATLAB. Examples of the flat fabric images and draped fabric images in Part I and Part II were shown in Figure 3.6. The display was an AdobeRGB-calibrated monitor. While sufficient for most colours within the AdobeRGB gamut, it may not fully reproduce colours especially those near the boundary.

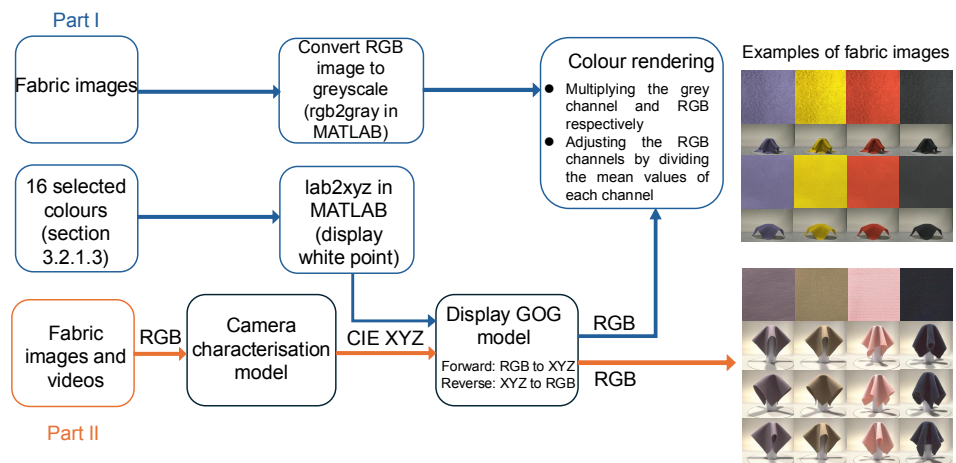


Figure 3.6 Workflow of the image processing for the Leeds Fabric Tactile Database.

3.4 Experiment Phase I

3.4.1 Tactile properties

Both instrumental and psychophysical aspects were considered in the determination of the tactile properties in the experiment Phase I. Table 2.2 in Chapter 2 lists the tactile properties used in previous studies. Ten descriptors of the tactile properties, soft, smooth, rough, firm, warm, cool, spongy, crisp, flexible, and stiff, can be directly or potentially derived from Table 2.2. Based on their definition in the widely used Oxford online dictionary (Oxford University Press, 2025a), for example, the explanation of “stiff” is “rigid; not flexible or pliant” (Oxford University Press, 2025b), the ten descriptors were divided into five pairs of scales that had opposite meanings: flexible-stiff, smooth-rough, soft-firm, and spongy-crisp, and warm-cool.

3.4.2 Tactile perception experiments

Three separate sets of perceived evaluation data for fabric tactile and visual-tactile properties were collected through the experiment Phase I as follows:

1. Flat: the 240 flat fabric images were presented on the calibrated BenQ display in random order.
2. Draped: the 240 draped fabric images were presented on the calibrated BenQ display in random order.
3. Touch-only: observers could touch the 15 fabrics without observing them. The fabrics were passed to the observers under a desk.

Experiment 1 and 2 were conducted in a dark room, and the distance between the observer and the display was approximately 40 cm. A self-complied MATLAB program was used to control the random image presentation. Experiment 3 was conducted under room lighting. 20 observers (11 females, 9 males, average age=28.5±5.4) who passed the Ishihara test participated in the

experiment Phase I. In each experiment, observers made categorical judgement of flexible-stiff, smooth-rough, soft-firm, spongy-crisp, and warm-cool separately with no time restrictions. The judgements were made using a 9-point Likert type scale, and each point represents the following meaning:

- 1: completely flexible/smooth/soft/spongy/warm
- 2: very much flexible/smooth/soft/spongy/warm
- 3: moderately flexible/smooth/soft/spongy/warm
- 4: slightly flexible/smooth/soft/spongy/warm
- 5: neither flexible/smooth/soft/spongy/warm nor stiff/rough/firm/crisp/cool
- 6: slightly stiff/rough/firm/crisp/cool
- 7: moderately stiff/rough/firm/crisp/cool
- 8: very much stiff/rough/firm/crisp/cool
- 9: completely stiff/rough/firm/crisp/cool

For the tactile description, observers were trained prior to the experiment to have a unified understanding:

- Flexible-stiff: (imagine) the fabric is draping over your hand. If you can clearly see the contour of your hand due to the draping fabrics rather than the translucency of the fabric, then the fabric is more flexible, otherwise is stiffer.
- Smooth-rough: (imagine) you are touching the surface of the fabric. If you feel no hairy and there is limited force stopping your movement, then the fabric is smoother, otherwise is rougher.
- Soft-firm: (imagine) you are crushing the fabric into a ball in your hand. If you think it is very easy to crush it into a ball, the fabric is softer, otherwise is firmer.

- Spongy-crisp: (imagine) you are crushing the fabric into a ball in your hand and then opening the palm and check if the fabric bounces back. If it bounces back quickly, then the fabric is spongier; if not and crease are shown on the surface, then the fabric is crisper.
- Warm-cool: (imagine) you are putting the fabric over your hand. If you feel warmer, then the fabric is warmer; if you feel cooler, then the fabric is cooler.

For experiment 1 and 2, 20 images were randomly selected to be repeated at the end of experiment to test the variability of observers. For experiment 3, the 15 fabrics were repeated at the end of experiment to test the variability of observers. Figure 3.7 shows the experimental interfaces and scene. The fabric images were set to an appropriate size so that the fabrics in the images were seen at a similar size as seen physically. Images were put in the centre of the BenQ display with the grey background (RGB=128).

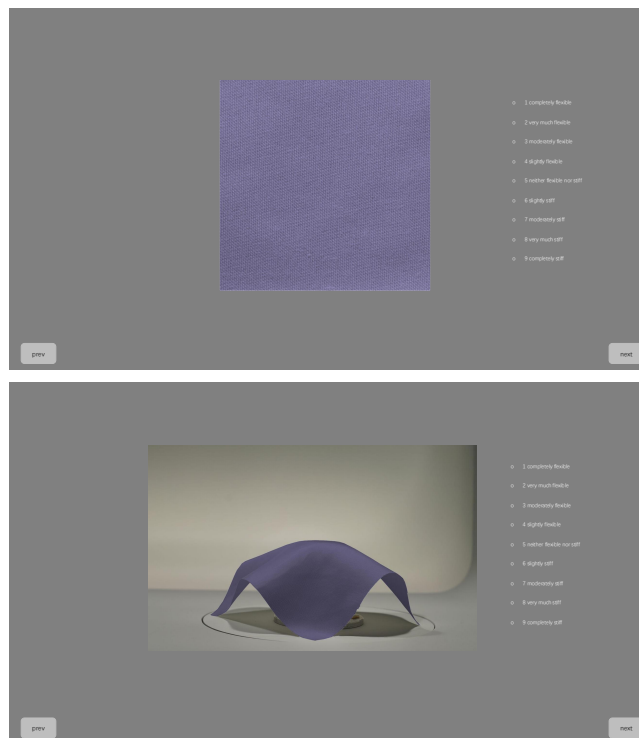




Figure 3.7 Experiment Phase I: interfaces and scene. First row: experiment 1 (flat fabric images). Middle row: experiment 2 (draped fabric images). Last row: experiment 3 (touch-only).

3.5 Experiment Phase II

3.5.1 Tactile properties

In the experiment Phase I, five pairs of tactile properties were evaluated using colour-rendered fabric images: flexible-stiff, smooth-rough, soft-firm, spongy-crisp, warm-cool. They were also evaluated in the experiment Phase II using real fabrics and the corresponding visual representations in the Leeds Fabric Tactile Database Part II.

3.5.2 Tactile perception experiments

Compared to the experiment Phase I, experiment Phase II was improved to cover almost all conditions of fabric tactile properties perception. Six separate sets of perceived evaluation data for fabric tactile and visual-tactile properties were collected under the following experiment conditions:

1. Flat: The flat fabric images characterised through camera and display characterisation models were presented on the calibrated BenQ display in random order.
2. Draped: The draped fabric images characterised through camera and display characterisation models were presented on the calibrated BenQ display in random order.
3. Video: The fabric rotating videos characterised through camera and display

characterisation models were presented on the calibrated BenQ display in random order. Observers were asked to watch the videos for at least 50 seconds before providing the tactile response.

4. Touch-only: Observers could touch the fabric samples without observing them. The fabrics were passed to observers under a desk.
5. Vision-only (using real fabrics): Observers could see the draped fabric samples rotating on the rotation stage in the VLB illuminated by the CIE D65 lighting, but not touch them.
6. Vision+touch: Observers could see and touch the fabric samples in the VLB illuminated by the CIE D65 lighting.

The experiments 1, 2, 3, 4, and 6 were conducted in the dark room, and the experiment 5 for tactile perception was conducted under room lighting. Eleven observers (4 males and 7 females, mean age \pm SD=31.18 \pm 4.98) who passed the Ishihara test participated in the experiments. Nine observers completed all the experiments using 118 fabrics, and two completed all the experiments using 29 fabrics and 89 fabrics, respectively. The distance between the observer and the fabric sample (visual representation and real fabrics) was set to approximately 40 cm. In each experiment, observers were required to make categorical judgement of flexible-stiff, smooth-rough, soft-firm, spongy-crisp, and warm-cool using a 9-point Likert scale. Each point represents the same meaning as described in the experiment Phase I, and observers were trained prior to the experiment Phase II to have the same understanding as in the Phase I (see Section 3.4.2). To avoid the memory effect, observers were required to follow the experiment order as above. To evaluate the observer variability, observers were asked to repeat 2 experiments using random 29 fabrics, one from either experiment 1, 2, or 3, and one from either experiment 4, 5, or 6. The experimental interfaces for experiment 1, 2, and 3 are the same as in the experiment Phase I, except for the images used. Examples of the scene of experiment 4, 5, 6 are shown in Figure 3.8.

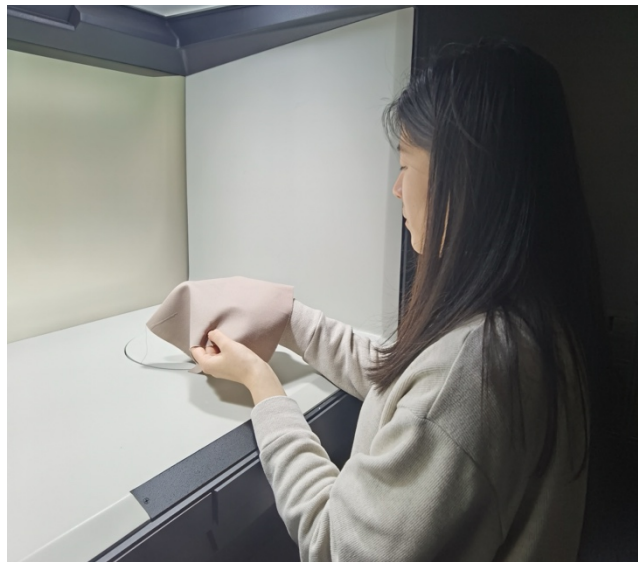
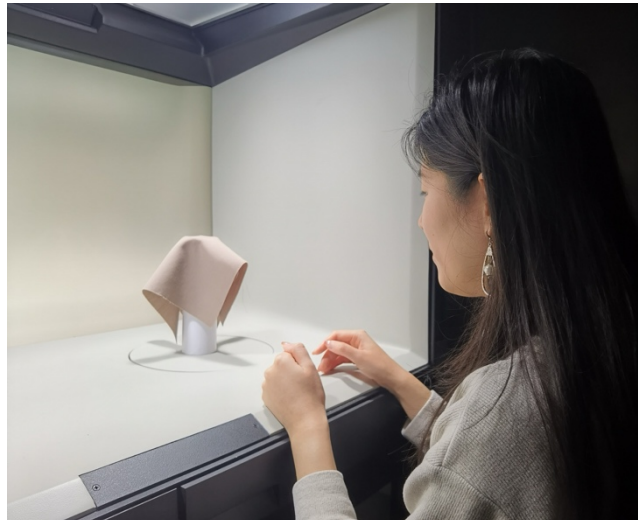


Figure 3.8 Experiment Phase II: scenes when vision was allowed only (first figure), and when both touch and vision was allowed (second figure).

3.6 Summary

In this chapter, a Leeds Fabric Tactile Database was developed. Experiment Phase I and Phase II were conducted using the database. Details of the database and the experiments were summarised as following:

1. Two parts were developed in the Leeds Fabric Tactile Database. Part I: 15 real fabrics and colour-rendered images (240 flat fabric images, 240 draped fabric images). Part II: 118 real fabrics, 118 flat fabric images, 354 draped

fabric images, and 118 fabric rotation videos. In addition to the images and real fabrics, comprehensive tactile perceptual ratings were included in the database.

2. The colours in images and videos were carefully characterised through camera characterisation model and the display GOG model.
3. Experiments Phase I were conducted using Part I, and experiments Phase II were conducted using Part II. The perception of fabric tactile and visual-tactile properties was evaluated in both experiments.

Chapter 4

Experiment Phase I: factors and correlations for visual-tactile and tactile perception

4.1 Overview

In this Chapter, the data collected using Leeds Fabric Tactile Database Part I were analysed. The experiments Phase I were introduced in Section 3.4. For psychophysical experiments, the observer variability was tested within observer (intra-observer variability) and between observers (inter-observer variability) to ensure a consistent understanding of the experiment among participants (Section 4.3). Whether the collected raw data were normally distributed was tested, so that analytical methods with appropriate assumption can be selected (Section 4.4). Two main analyses were conducted in this Chapter: one focused on initially evaluating the factors affected the visual-tactile perceptual ratings (Section 4.5), and the other focused on the associations between flat fabric images, draped fabric images, and touch-only experiment conditions (Section 4.6) and the associations among five pairs of tactile properties (Section 4.7). An interesting bias was found on the effects of colour on the perceived warm-cool between Section 4.5 and Section 4.6. Therefore, a full CLMM model was fitted to further understand the effects of colour (Section 4.8). The statistical analysis was introduced in Section 4.2. The practical effect of colour was taken into account, and the effect of fabric structure was further discussed to support the analysis of real fabrics in the following chapters.

4.2 Statistical analysis

In Section 4.3, the inter-observer variability and intra-observer variability was computed using the Root Mean Square (RMS) values, following studies that used the method of categorical judgement (Ou et al., 2006; Lee et al., 2000; Ou et al., 2012). RMS indicates how well individuals agreed with the mean scale value, where 0 means perfect agreement. The formulae are given in Equation 4.1 and Equation 4.2.

$$RMS_{inter} = \sqrt{\frac{\sum_i (x_i - \bar{x})^2}{N}}$$

Equation 4.1

Equation 4.2

$$RMS_{intra} = \sqrt{\frac{\sum_i (x_i - y_i)^2}{N}}$$

where N is the number of observations, x_i is one observer's tactile perceptual ratings in one set, \bar{x} is the mean tactile perceptual ratings from all observers for assessing inter-observer variability, y_i is the same observer's tactile perceptual ratings in the repeat set for assessing intra-observer variability, i is the stimulus.

The raw data were integer values that indicated the tactile perceptual ratings evaluated in the experiment Phase I. Whether the raw data of all observers was normally distributed was assessed for each pair of tactile properties under all experiment conditions by Shapiro-Wilk test in Section 4.4.

In Section 4.5, Cumulative Link Mixed Models (CLMM) with (full) and without (simple) three-way interactions were fitted for each pair of tactile properties, setting the fabrics, experiment conditions (flat and draped), and colours that were selected to render the fabrics (L^* , a^* , b^*) as the fixed effects, and images and observers as the random effects. Full models allow all interactions between fabrics, experiment conditions, and colours, while simple models exclude the three-way interactions between fabrics, experiment conditions, and colours, but remain the two-way interactions of fabrics and experiment conditions. Contrast coding was used in all CLMM models to convert fabrics and experiment conditions to coded categorical factors. CIELAB values were z-standardised before fitting the CLMM models to ensure an evenly distribution. Comparisons between simple and full model were made using *anova()* function from *stats* R package. P values of the fixed effects in CLMM models were computed using Likelihood Ratio Test (LRT) with Type III sums of squares, using *Anova()* function from *car* R package.

The fitted perceptual ratings of the visual-tactile perception were computed for the two-way interaction (fabric:experiment condition). The default CLMM

models were fitted on the scale of linear predictor scale using logit link function in CLMM models, rather than the original category scales (1-9) (Agresti, 2010). Higher linear predictor scales represent higher probabilities of selecting higher categories in the original scale. The probability of selecting each scale is defined in Equation 4.3, by using the threshold estimates and the results of linear predictors from the CLMM models. Threshold estimates define the boundaries between the original categories on the linear predictor scale. Linear predictor scale reflects the overall influence of the fixed effects and random effects. The fitted tactile perceptual ratings for each interaction were computed on the original scales using Equation 4.4.

$$P(Y \leq j) = \frac{\exp(\tau_j - \eta)}{1 + \exp(\tau_j - \eta)}$$

$$\eta = \beta X + Zb$$

$$P(Y = j) = P(Y \leq j) - P(Y \leq j - 1) \quad \text{Equation 4.3}$$

The fitted tactile perception

$$= \sum_{j=1}^9 j \times P(Y = j) \quad \text{Equation 4.4}$$

where j represents the category scale (1-9), τ_j represents the threshold estimates of each category scale fitted in the CLMMs, η is the linear predictor, βX reflects the fixed effects, Zb reflects the random effects. Pairwise contrasts analyses were conducted with Bonferroni correction to evaluate the significant differences between using flat and draped fabric images by *contrast()* function in *emmeans* R package.

In Section 4.6 and Section 4.7, the observed scores were averaged across all observers to create a score for each image sample and fabric sample under all experiment conditions. Overall, a higher score means the fabric was judged as stiffer/rougher/firmer/crisper/cooler, and a lower score means the fabric was judged as more flexible/smoothier/softer/spongier/warmer. Pearson Correlation Coefficients (two-tailed) was used to evaluate the correlations of the tactile perceptual ratings between vision and touch and between flat and draped fabric

images. Since each of the 15 fabrics was rendered in 16 different colours, a number of 240 averaged data was obtained from experiment using flat and draped fabric images, respectively. In contrast, a number of 15 averaged data was obtained from experiment touching the fabrics. The correlation of the tactile perceptual ratings between using flat and draped fabric images was computed directly from the averaged data. Since the effect of colour was not significant in CLMM models (reported in Section 4.5), data from the image-only experiment were averaged across 16 colours for each fabric. The correlation of the tactile perceptual ratings between viewing images and touching fabrics was thus computed. In addition, the correlations among the tactile perceptual ratings were computed for flat fabric images, draped fabric images, and touch-only, respectively in Section 4.7.

In Section 4.8, the effects of colours were further analysed for the perceived warm-cool by fitting a CLMM model with three-way interaction between fabrics, experiment conditions (flat and draped fabric images), and colours (L^* , a^* , b^*). The fixed effects were derived from CLMM model using *Anova()* function from *car* R package. The parameter estimates for L^* , a^* , and b^* were computed within each interaction.

The significant level was fixed to 0.05 in all analyses in this Chapter. In all figures and tables, asterisks *** indicate $p < 0.001$, ** indicate $p < 0.01$, * indicate $p < 0.05$.

4.3 Observer variability

Table 4.1 lists the inter-observer and intra-observer variability in the experiment Phase I, indicated by RMS values. RMS values range from 0.83 to 1.93 points within the 9-point Likert scale for inter-observer variability, with averages of 1.74 points, 1.42 points, and 1.29 points achieved under the experiment conditions of flat fabric images, draped fabric images, and touch-only, respectively. For intra-observer variability, RMS values range from 0.55 to 1.35 points, with averages decreased to 1.03 points, 1.10 points, and 1.21 points compared to

inter-observer variability. Compared to the studies using categorical judgement (Ou et al., 2006; Lee et al., 2000; Ou et al., 2012), the RMS values shown here are reasonable, indicating a consistent understanding from all observers.

Table 4.1 Observer variability in the experiment Phase I.

		Conditions	Flexible -stiff	Smooth -rough	Soft- firm	Spongy- crisp	Warm- cool	Mean
Inter- observer variability	Flat		1.93	1.76	1.86	1.80	1.39	1.74
	Draped		1.22	1.63	1.29	1.54	1.44	1.42
	Touch-only		1.27	1.46	1.24	1.67	0.83	1.29
Intra- observer variability	Flat		1.35	1.15	1.09	1.00	0.55	1.03
	Draped		1.30	1.29	1.09	1.17	0.67	1.10
	Touch-only		0.99	1.25	1.31	1.56	0.93	1.21

4.4 Normal distribution

Whether the raw perceptual ratings of all observers were normally distributed was evaluated by Shapiro-Wilk test first. Table 4.2 lists the results of the normality for each pair of tactile properties, where a value of w closer to 1 means a better match to the normal distribution, and p -value means the rejection or not to the null hypothesis. The w values were not very close to 1, and the significant p -values indicated the rejection of null hypothesis. The raw perceptual ratings for all tactile properties were not normally distributed, and thus the analysis methods used in this Chapter were chosen without relying on the assumption of normality.

Table 4.2 The results of Shapiro-Wilk test for the experiment Phase I.

	Flexible- stiff	Smooth- rough	Soft-firm	Spongy- crisp	Warm-cool
Flat	$w=0.93$, $p<0.001^{***}$	$w=0.94$, $p<0.001^{***}$	$w=0.95$, $p<0.001^{***}$	$w=0.95$, $p<0.001^{***}$	$w=0.96$, $p<0.001^{***}$
Draped	$w=0.93$, $p<0.001^{***}$	$w=0.95$, $p<0.001^{***}$	$w=0.94$, $p<0.001^{***}$	$w=0.95$, $p<0.001^{***}$	$w=0.96$, $p<0.001^{***}$
Touch-only	$w=0.87$, $p<0.001^{***}$	$w=0.92$, $p<0.001^{***}$	$w=0.91$, $p<0.001^{***}$	$w=0.94$, $p<0.001^{***}$	$w=0.95$, $p<0.001^{***}$

4.5 The effect of fabric, colour, and experiment condition on visual-tactile perception

CLMM models with and without interactions were fitted and compared firstly to define the models to be evaluated. Equation 4.5 and Equation 4.6 are the fitted models with and without three-way interaction, respectively.

With interactions: Tactile perceptual ratings= Equation 4.5

$$fabrics * conditions * L +$$

$$fabrics * conditions * a +$$

$$fabrics * conditions * b +$$

$$(1|image) + (1|observer)$$

Equation 4.6

Without interaction: Tactile perceptual ratings=

$$fabrics * conditions + L + a + b$$

$$(1|image) + (1|observer)$$

Table 4.3 lists the comparisons of models with and without three-way interactions. For models of flexible-stiff, smooth-rough, soft-firm, and spongy-crisp, model without three-way interactions outperformed model with interactions, as indicated by the lower AIC and BIC values and the non-significant p-values. For models of warm-cool, even though the AIC value and p-value preferred the model with three-way interaction, the BIC value strongly supported the model without three-way interaction. To ensure the comparability and consistency across the five pair of tactile properties, models without interactions were reported in the following analyses in this section.

Table 4.3 Comparisons between CLMM models with and without three-way interactions for the experiment Phase I.

	no. par	AIC	BIC	logLik	χ^2	p-values
Flexible-stiff						
With interactions	129	33129	34054	-16436	59.739	p=0.99
Without interactions	42	33015	33316	-16466		
Smooth-rough						
With interactions	129	34747	35671	-17245	65.549	p=0.96
Without interactions	42	34639	34969	-17277		
Soft-firm						
With interactions	129	34038	34962	-16890	30.17	p=0.99
Without interactions	42	33894	34195	-16905		
Spongy-crisp						
With interactions	129	34865	35789	-17303	26.538	p=0.99
Without interactions	42	34718	35018	-17317		
Warm-cool						
With interactions	129	34002	34926	-16872	201.71	p<0.001***
Without interactions	42	34030	34330	-16973		

Table 4.4 lists the fixed effects of the CLMM models for each pair of tactile properties. The fabrics, the experiment conditions, and the interaction between fabrics and experiment conditions were significant for all fitted tactile perceptual ratings. Among all fixed effects, fabrics had the greatest impact on all tactile perceptual ratings, indicated by χ^2 . χ^2 is the statistical value obtained by comparing the full model and simple model without the corresponding fixed effect. A larger χ^2 , along with a significant p-value, indicates that the fixed effect significantly improves the model fit. The interaction between fabrics and experiment conditions also significantly affected visual-tactile perception, indicating that the effect of experiment conditions was different among fabrics when perceiving visual-tactile properties. Lightness (L^*) significantly affected all visual-tactile perceptions except for smooth-rough. However, the χ^2 are relatively small, indicating that the effect was statistically significant while the practical impact was weak. Similarly, a^* and b^* are significant in visually perceiving warm-cool, but the effect is limited due to the smaller χ^2 . Colour played no role in flexible-stiff, smooth-rough, soft-firm, and spongy-crisp

perception.

Table 4.4 The fixed effects in all CLMM models and their significance for the experiment Phase I.

Fixed effects		χ^2	df	p
Flexible-stiff	Fabrics	4485.96	14	p<0.001***
	Experiment conditions	170.01	1	p<0.001***
	L*	24.24	1	p<0.001***
	a*	0.33	1	p=0.56
	b*	2.73	1	p=0.10
	Fabrics:experiment conditions	1943.08	14	p<0.001***
Smooth-rough	Fabrics	2698.88	14	p<0.001***
	Experiment conditions	8.88	1	p=0.003**
	L*	0.35	1	p=0.55
	a*	2.00	1	p=0.16
	b*	0.37	1	p=0.54
	Fabrics:experiment conditions	347.60	14	p<0.001***
Soft-firm	Fabrics	4059.45	14	P<0.001***
	Experiment conditions	162.40	1	P<0.001***
	L*	5.94	1	P=0.01*
	a*	0.27	1	P=0.61
	b*	1.55	1	P=0.21
	Fabrics:experiment conditions	975.71	14	P<0.001***
Spongy-crisp	Fabrics	3175.78	14	p<0.001***
	Experiment conditions	398.19	1	p<0.001***
	L*	6.38	1	p=0.01*
	a*	0.00	1	p=0.99
	b*	0.59	1	p=0.44
	Fabrics:experiment conditions	682.890	14	p<0.001***
Warm-cool	Fabrics	996.87	14	p<0.001***
	Experiment conditions	16.62	1	p<0.001***
	L*	31.06	1	p<0.001***
	a*	135.15	1	p<0.001***
	b*	119.4	1	p<0.001***
	Fabrics:experiment conditions	294.87	14	p<0.001***

To further understand the interaction between fabrics and experiment conditions, the fitted perceptual ratings of all interactions were computed using Equation 4.4. Figure 4.1 compares the fitted perceptual ratings of visual-tactile perception perceived between using flat fabric images and draped fabric images for each fabric. Overall, experiment conditions played different roles across 15 fabrics in the Leeds Fabric Tactile Database Part I. For the fitted flexible-stiff and soft-firm

models, the effect of experiment conditions was significant on most of the fabrics. No significant difference was observed between using flat and draped fabric images in perceiving flexible-stiff for fabric 13 and in perceiving soft-firm for fabric 4. Among the 15 fabrics, eight, two and five fabrics exhibited similar perceptual ratings between flat and draped fabric images for the fitted smooth-rough, spongy-crisp, and warm-cool, respectively.

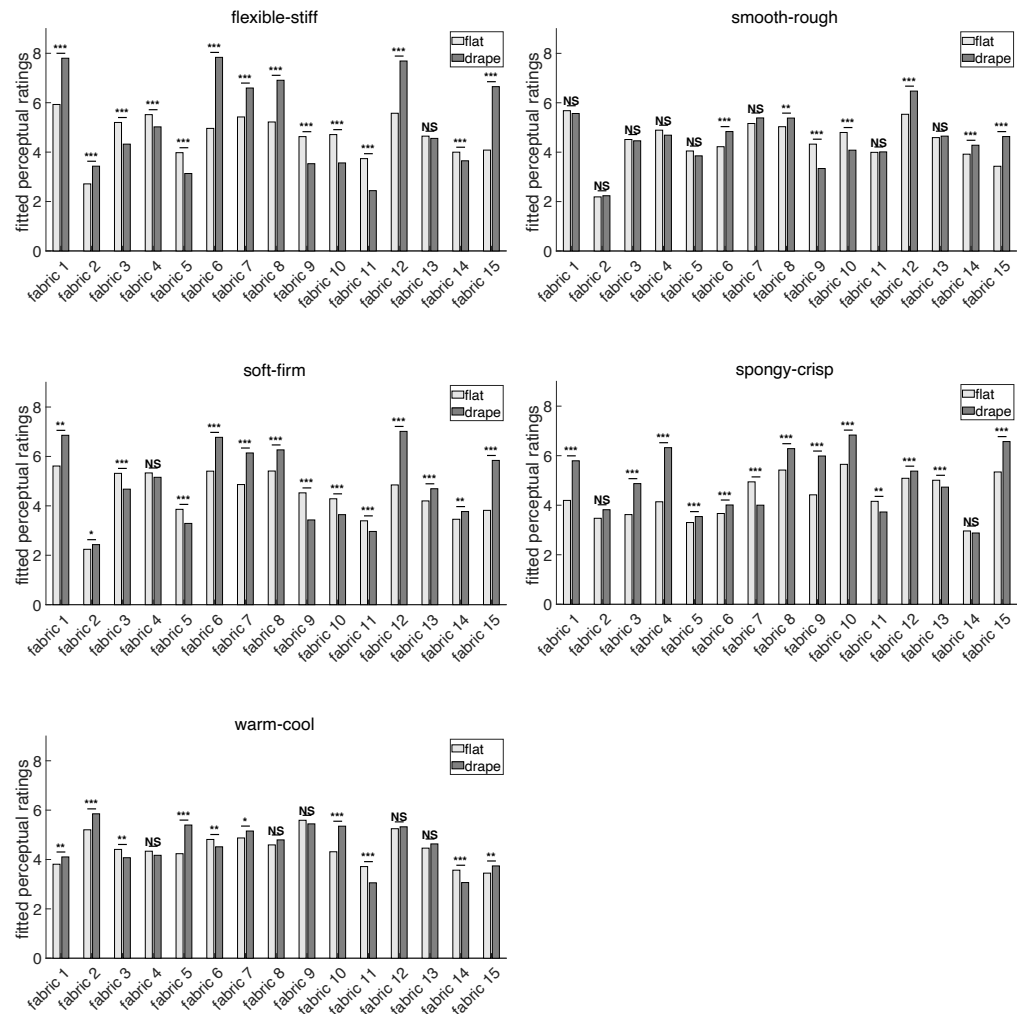


Figure 4.1 The fitted perceptual ratings of each fabric for all visual-tactile perceptions perceived from flat fabric images and draped fabric images.

Apart from the significance, the relative magnitude of fitted tactile perceptual ratings between flat and draped fabric images was not consistent. Higher perceptual ratings represent stiffer, rougher, firmer, crisper, and cooler, and lower perceptual ratings represent more flexible, smoother, softer, spongier, and warmer. The fitted tactile perceptual ratings perceived from flat and draped

fabric images showed mixed results across all fabrics, with no consistent tendency in which fabric image type had higher or lower perceptual ratings. For example, in Figure 4.1, fabric 1, 2, 6, 7, 8, 12, and 15 were rated with higher scores, i.e., stiffer, when perceived from draped fabric images, while the rest were perceived as stiffer when perceived from flat fabric images. In addition, whether there were significant differences between using flat and draped fabric images was independent of the relative magnitude of tactile perceptual ratings. A significant difference does not indicate higher or lower tactile perceptual ratings using either flat or draped fabric images. Figure 4.2 shows the examples of flat and draped fabric images for fabric 1-15, illustrating the individual appearance differences.



Figure 4.2 Individual fabrics in Leeds Fabric Tactile Database Part I.

4.6 The correlations of tactile perceptual ratings among experiment conditions.

The correlations of the average tactile perceptual ratings among experiment conditions were listed and compared in Table 4.5.

Table 4.5 The Pearson Correlation Coefficients of the tactile perceptual ratings between vision and touch, and between using flat and draped fabric images.

	Touch-only vs flat	Touch-only vs draped	Flat vs draped
Flexible-stiff	0.51	0.89***	0.66***
Smooth-rough	0.42	0.63*	0.75***

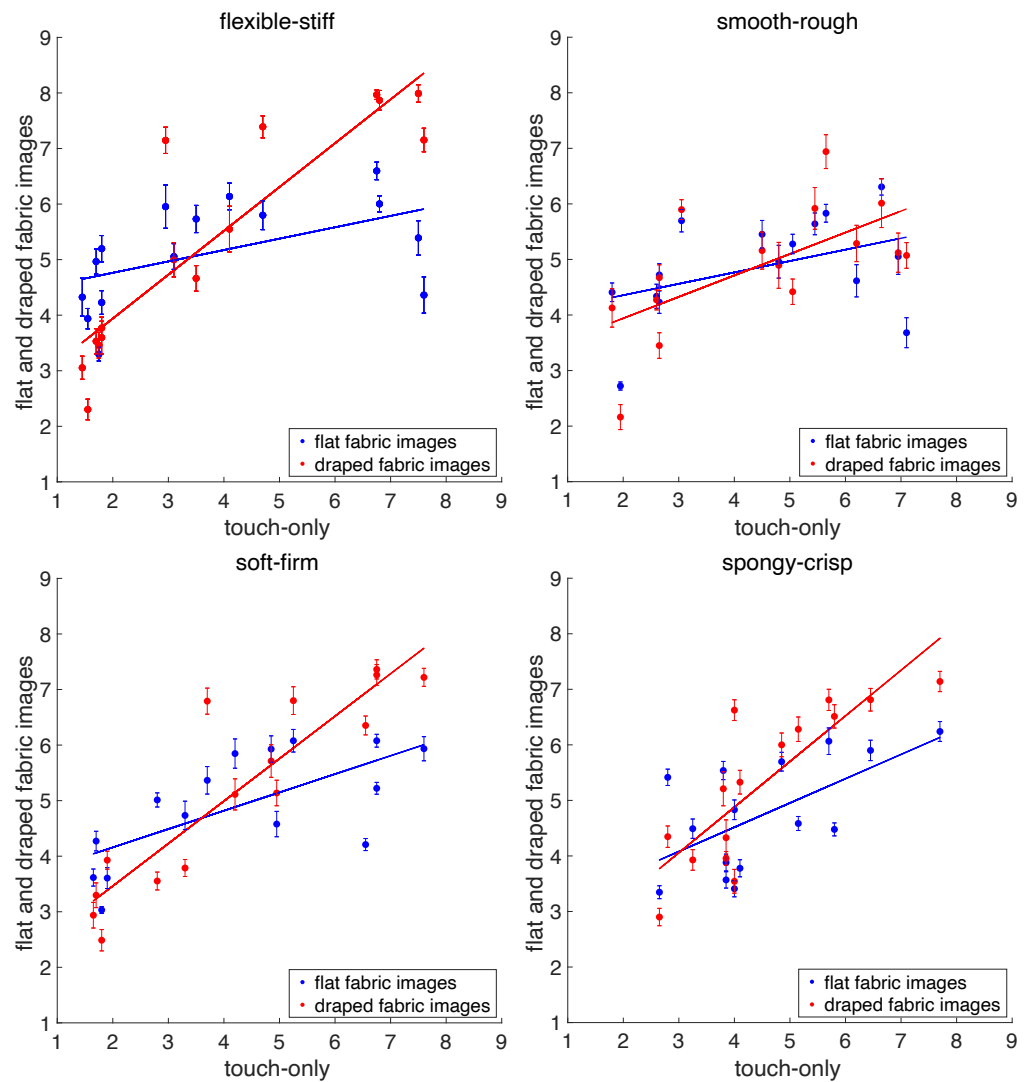
Soft-firm	0.68**	0.90***	0.74***
Spongy-crisp	0.61*	0.83***	0.72***
Warm-cool	0.81***	0.88***	0.66***

In Table 4.5, overall, tactile perceptual ratings of flexible-stiff and smooth-rough obtained by touching the fabrics showed no significant correlation with those obtained by viewing flat fabric images ($r=0.51$, $p>0.05$ for flexible-stiff; $r=0.42$, $p>0.05$ for smooth-rough). In contrast, all other correlations were all significant and relatively high ($r>0.61$).

For each pair of tactile properties, the correlations between draped fabric images and touching the fabrics were consistently higher than that between flat fabric images and touching the fabrics. Draped fabric images accurately conveyed all visual-tactile perception similar to those from actually touching the fabrics. However, the perceived warm-cool from flat fabric images also showed high and positive correlations with those from touching the fabrics ($r=0.81$, $p<0.001$ ***). In addition, tactile perceptual ratings from using flat fabric images and draped fabric images showed positive and significant correlations, with r ranging from 0.66 to 0.75.

It is noted that the Pearson Correlation Coefficients for the perceived flexible-stiff and warm-cool were both equal to 0.66. For the perceived warm-cool, correlations between vision and touch were both significant and highly positive, however, the correlation between using flat fabric images and touching the fabrics for flexible-stiff was not significant. Possible reason can be the data used to compute the Pearson Correlation Coefficients. As described in Section 4.2, r between vision and touch were computed by the averaged data across 16 colours for each fabric, resulting in 15 data for each condition. For perceived warm-cool, the SD within each fabric across 16 colours was larger than that for flexible-stiff, as well as other tactile perception, indicating a wider range of variation in perceived warm-cool across different colours (see Figure 4.3). As analysed in Section 4.5, the effect of colour was statistically significant but weak

on the perceived warm-cool. The larger SD observed here possibly can be the evidence that the effect of colour was underestimated before. It also possibly explained why the correlation between touch-only and flat fabric images was higher than other tactile perceptions. As only CLMM model without interactions were reported for the perceived warm-cool, a separate CLMM model with three-way interactions between colour and fabrics and experiment conditions was individually fitted and analysed in Section 4.8.



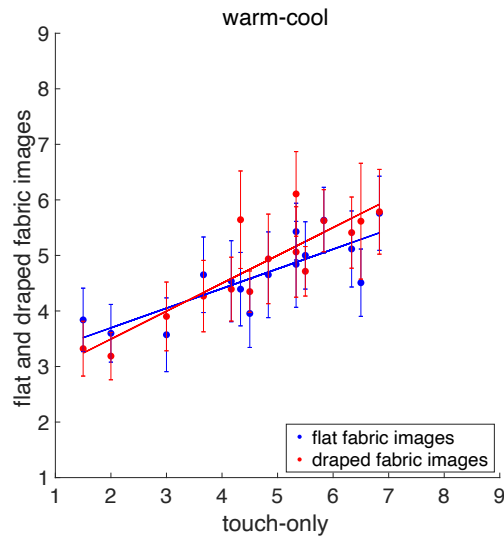


Figure 4.3 The correlations of the average perceptual ratings between touch-only condition and using flat (blue) and draped fabric images (red). Error bar indicates the standard deviation (SD) of the tactile perceptual ratings across 16 colours for each fabric.

4.7 The correlations among the tactile perceptual ratings under each experiment condition

The correlations among the tactile perceptual ratings were shown in Figure 4.4. Consistent correlations were observed across three experiment conditions. Firstly, the perceived flexible-stiff, smooth-rough, soft-firm, and spongy-crisp were highly correlated to each other ($r > 0.51$ when using flat fabric images, $r > 0.76$ when using draped fabric images, $r > 0.72$ when only touch allowed). A fabric perceived as more flexible was often associated with increased roughness, firmness, and crispness. In contrast, the perceived warm-cool has no correlation with other tactile properties.

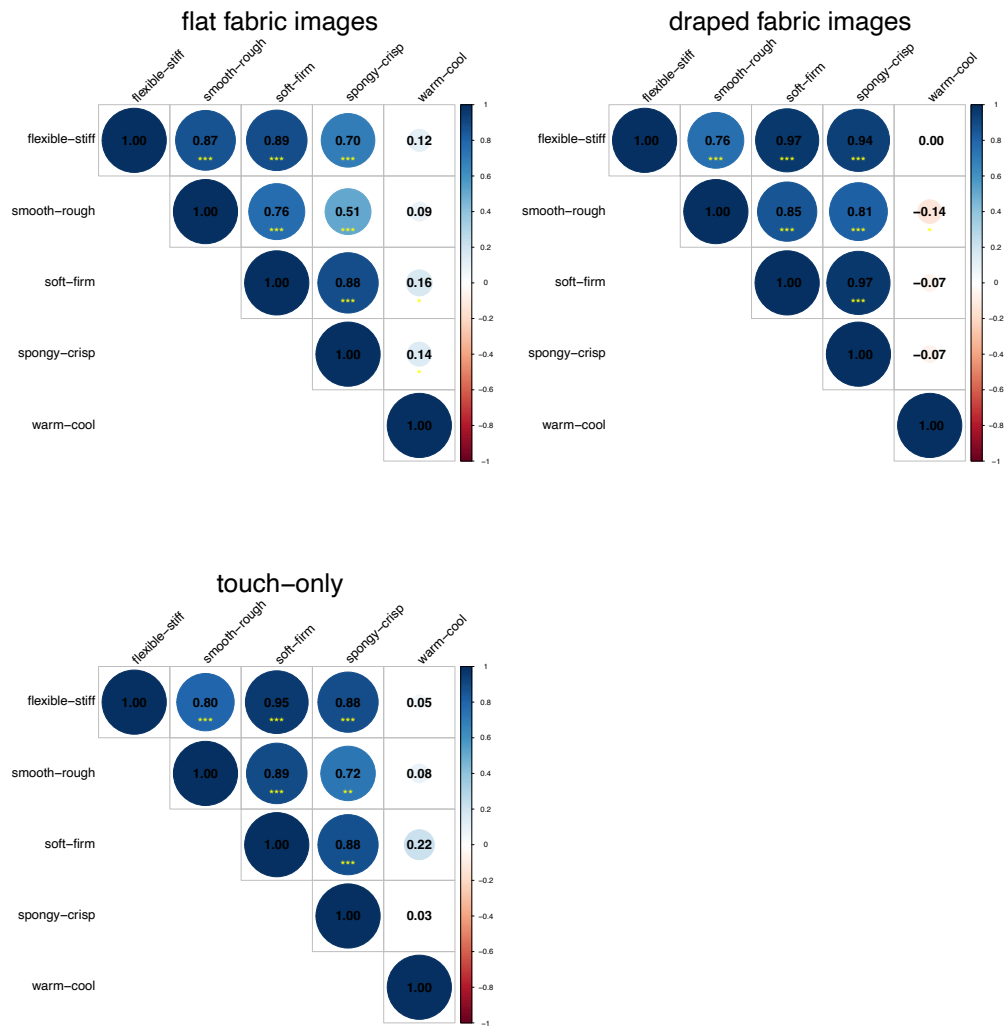


Figure 4.4 The correlations among tactile perceptual ratings under each experiment condition.

4.8 A further analysis of the effects of colour on the perceived warm-cool: CLMM model with three-way interactions

A separate full CLMM model with the three-way interaction between fabrics, experiment conditions, and colours (L^* , a^* , b^*) was fitted. The formula of the CLMM model was given in Equation 4.5. Table 4.6 lists all the fixed effects in the full CLMM model for warm-cool. There were significant effects of two-way and three-way interactions of colour. Significant two-way interactions included condition:colour, fabric: L^* ($p=0.02^*$), and fabric: a^* ($p=0.04^*$), and only the three-way interaction of fabric:condition: b^* was not significant ($p=0.70$). Based on the

CLMM model, colour had different effects on the perceived warm-cool when using different fabric images.

Table 4.6 The fixed effects in warm-cool CLMM models with three-way interaction.

Fixed effects	χ^2	η^2	df	p
Fabric	1149.20	0.11	14	$p < 0.001^{***}$
Condition	14.53	0.00	1	$p < 0.001^{***}$
L*	38.70	0.00	1	$p < 0.001^{***}$
a*	173.42	0.02	1	$p < 0.001^{***}$
b*	153.24	0.02	1	$p < 0.001^{***}$
Fabric:condition	297.23	0.03	14	$p < 0.001^{***}$
Fabric:L*	27.25	0.00	14	$p = 0.02^*$
Condition:L*	14.05	0.00	1	$p < 0.001^{***}$
Fabric:a*	16.14	0.00	14	$p = 0.30$
Condition:a*	4.16	0.00	1	$p = 0.04^*$
Fabric:b*	22.82	0.00	14	$p = 0.06$
Condition:b*	8.11	0.00	1	$p = 0.004^{**}$
Fabric:condition:L*	64.51	0.01	14	$p < 0.001^{***}$
Fabric:condition:a*	27.08	0.00	14	$p = 0.02^*$
Fabric:condition:b*	10.81	0.00	14	$p = 0.70$

To further reveal the roles of colour in each subgroup of fabric and experiment condition, parameter estimates (β) on the original scales and significant levels of L*, a*, and b* were computed from the CLMM model. Since there are in total 30 subgroups of fabrics (15) and experiment conditions (2), reporting all results will be redundant. Only significant parameter estimates were listed in Table 4.7.

Table 4.7 Parameter estimates (β) of L*, a*, b* in the full CLMM model for warm-cool.

	fabric	flat	draped	fabric	flat	drape
L*	3	NS	$\beta = 0.024^{***}$	7	NS	$\beta = 0.026^{***}$
	4	NS	$\beta = 0.016^{**}$	9	NS	$\beta = 0.030^{***}$
	5	NS	$\beta = -0.014^*$	10	NS	$\beta = 0.049^{***}$
a*	1	$\beta = -0.011^{***}$	NS	9	$\beta = -0.013^{***}$	$\beta = -0.012^{**}$
	2	NS	$\beta = -0.015^{***}$	10	$\beta = -0.012^{***}$	$\beta = -0.010^{**}$
	3	$\beta = -0.008^{**}$	NS	11	$\beta = -0.008^{**}$	$\beta = -0.011^{***}$
	4	$\beta = -0.008^*$	NS	12	$\beta = -0.010^*$	$\beta = -0.008^*$
	5	$\beta = -0.011^{***}$	$\beta = -0.019^{***}$	13	$\beta = -0.010^{**}$	$\beta = -0.015^{***}$
	6	$\beta = -0.012^{***}$	NS	14	$\beta = -0.008^*$	NS
	7	$\beta = -0.014^{***}$	NS	15	$\beta = -0.008^{**}$	$\beta = -0.006^*$
	8	$\beta = -0.011^{***}$	$\beta = -0.014^{***}$			

b*	1	$\beta=-0.007^*$	NS	8	$\beta=-0.008^{**}$	$\beta=-0.012^{***}$
	2	$\beta=-0.008^*$	NS	10	$\beta=-0.009^{**}$	$\beta=-0.007^*$
	3	$\beta=-0.013^{***}$	$\beta=-0.012^{***}$	11	$\beta=-0.008^{**}$	NS
	4	$\beta=-0.016^{***}$	$\beta=-0.010^{***}$	12	$\beta=-0.010^{**}$	NS
	5	$\beta=-0.010^{***}$	$\beta=-0.008^*$	13	$\beta=-0.016^{***}$	$\beta=-0.010^{**}$
	6	NS	$\beta=-0.006^*$	14	$\beta=-0.006^*$	NS
	7	$\beta=-0.010^{**}$	$\beta=-0.009^{**}$	15	$\beta=-0.009^{**}$	$\beta=-0.006^*$

NS: Non-significant.

The effects of colour on the perceived warm-cool were independent between using flat and draped fabric images. Significant effects of colours when using flat fabric images can be no longer significant when using draped fabric images (e.g., fabric 1 β_{a^*} and β_{b^*}), and vice versa (e.g., fabric 3 β_{L^*} , fabric 2 β_{a^*}). In addition, the effects of colour were statistically significant but still weak in the CLMM model with three-way interaction. For example, an increase of one unit in L^* resulted in a 0.024 unit increase in the perceived warm-cool for fabric 3 when using draped fabrics; an increase of one unit in a^* resulted in a 0.011 unit decrease for fabric 1, and an increase of one unit in b^* resulted in a 0.007 unit decrease for fabric 1 when using flat fabric images. All units of the perceptual ratings were based on the 9-point Likert scale. Based on the CLMM model, an increase of L^* was associated with cooler perception, while an increase of a^* and b^* was associated with warmer perception.

4.9 Discussion

4.9.1 The practical effects of colour for warm-cool.

The effect of colour was statistically significant on the fitted warm-cool perception in both simple and full CLMM models. The simple CLMM model excluded the three-way interaction between fabrics, experiment conditions, and colours, while the full CLMM models included the three-way interaction. It is found that the decrease of L^* and increase of a^* and b^* was associated with warmer perception. A Higher a^* value represents reddish colour and a higher b^* value represents yellowish colour. This result is consistent with the findings of

Atav and Keskin (2024), where red, yellow, and orange cotton fabrics were perceived as warmer, and blue, green, and purple cotton fabrics were perceived as cooler. Similarly, Fenko et al. (2010) also found that orange and red scarves were perceived as warmer, and cyan, green, and blue scarves were perceived as cooler, using materials such as silk, wool, and cotton. In both studies (Atav and Keskin, 2024; Fenko et al., 2010), the fabric colours were described in terms of hue and not quantified within a uniform colour space. In contrast, in the present study, the 16 colours were selected because of their average distribution in the CIELAB colour space and then rendered on 15 different fabric images in a digital way. This approach enabled better control over colour and fabric as variables. It also eliminated inconsistencies in colour appearance caused by different dyeing performance across fabric materials. Instead of dyeing real fabrics, Ou et al. (2004) used pure colour patches from NCS Color Atlas to evaluate warm-cool perception as one of the colour emotion scales. The colours of colour patches gave a uniform distribution in the CIELAB colour space. They found that reddish colour patches were rated as warmer and bluish colour patches were rated as cooler. Overall, a consistent tendency of the role of colour in warm-cool perception has been found, observed both in fabric tactile perception and in pure colour patches.

The effects of colour on the perceived warm-cool have been quantified in the full CLMM models, indicated by the parameter estimates in Table 4.8. However, the effects of colour were limited. For each unit increase in L^* , a^* , or b^* , the change in the fitted perceptual warm-cool was small on a 9-point Likert scale, with variations less than 0.05 points for L^* and less than 0.02 points for a^* and b^* . Nevertheless, it is important to note that this result only reflected a change of 1 unit in L^* , a^* , or b^* . In practical, the colour variation between fabrics can be larger. L^* of the selected colours used to render the fabric images ranged from 25.7 to 88.0, a^* ranged from -52.6 to 64.7, and b^* ranged from -34.2 to 90.0 (see Chapter 3, Table 3.1). For fabrics with small differences in L^* , a^* , or b^* , the

effect of colour is expected to be negligible when differentiating warm-cool perception. In contrast, for fabrics with significantly larger colour differences, one cannot ignore the effect of colour.

4.9.2 Individual fabrics largely affected the fitted tactile perceptual ratings based on CLMM models

In the simple CLMM models, fabric had the greatest impact on all fitted visual-tactile perceptual ratings. The variation in visual-tactile perception largely depended on the inherent differences among individual fabrics. During observing the fabric images, the individual differences were primarily reflected in the fabric's appearance, which is large determined by its structure and colour.

From a structural perspective, the fabrics can generally be divided into woven and knitted fabrics. Woven fabrics have the interlace structure while knitted fabrics have the interloop structure, which is the primary difference between woven and knitted fabrics. In addition, within each category, the fabric appearance also varies largely. In woven fabrics, factors such as the type of weave (plain, twill, satin) and yarn count play significant roles. In knitted fabrics, factors such as loop length, knitted structure, and yarn thickness contribute to the overall appearance. In this chapter, as only 15 fabrics were analysed, comparisons were made among individual fabrics and between using flat and draped fabric images. Although the differences of visual-tactile perception among individual fabrics and between flat and draped fabric images were significant, the magnitude of the differences was not consistent. One primary reason is of the fabric appearance variation. As the colour had no role in visual-tactile perception (possibly except for warm-cool), the differences of visual-tactile perception largely resulted from the structural differences. However, given that only 15 fabrics were investigated in this Chapter, the comparisons did not effectively reveal the role of fabric structures. A larger set of fabrics were investigated in Chapter 6 using real fabric images, and comparisons were made

between two broader categories: woven and knitted, to avoid a redundant comparison.

4.10 Summary

This Chapter, together with the Leeds Fabric Tactile Database Part I, provides an initial exploration of visual-tactile and tactile perception by ensuring the control over colours and fabrics. A summary of the major findings is listed below:

- Observers had consistent perception of tactile properties perceived through both images and real fabrics.
- The differences in visual-tactile perception of fabric images were predominantly driven by the inherent variations among individual fabrics.
- Colour had a limited role in the fitted flexible-stiff, smooth-rough, soft-firm, and spongy-crisp perception, but it impacted the fitted warm-cool perception.
- Significant differences of the visual-tactile perception were found between flat and draped fabric images for most of fabrics. However, there was no consistent tendency that whether flat or draped fabric images led to higher or lower fitted perceptual ratings. It varied across individual fabrics.
- For the perception of all tactile properties, the correlations between draped fabric images and touching the fabrics were consistently higher than that between flat fabric images and touching the fabrics. The perceived flexible-stiff, smooth-rough, soft-firm, and spongy-crisp were positively correlated to each other, while the perceived warm-cool had no association with them.

Chapter 5

Experiment Phase II: correlations for visual-tactile and tactile perception

5.1 Overview

In the last Chapter, data collected using colour rendered fabric images were initially analysed. In this Chapter, data collected from experiment Phase II were investigated, covering comprehensive real-life scenarios involving contact with fabrics. Fabrics were presented and evaluated in the form of images (flat and draped) and videos (rotation), and real fabrics under the conditions of touch-only, vision-only, and the combination of both. Observer variability was tested firstly to ensure a consistent understanding of the experiments among participants (Section 5.3). Whether the tactile perceptual ratings differed among different viewing angles from draped fabric images was tested (Section 5.4). Separate analyses were conducted to fully investigate the tactile perception of real fabric samples, achieved by detailed correlation analyses (Section 5.5 and 5.6) and comparisons (Section 5.7). In addition, the correlations in this Chapter were compared with the correlations in the last Chapter that using rendered fabric images and real fabrics. Consistency and differences between using real fabric images and rendered fabric images were reported.

5.2 Statistical analysis

The data collected in the experiment Phase II was used in this Chapter to conduct the following analyses.

Inter-observer variability and intra-observer variability were assessed using RMS values as defined in Equation 4.1 and Equation 4.2, averaged across all experiment conditions for each pair of tactile properties. The calculation was the same as described in Section 4.2.

The raw data were integer values that indicated the tactile perceptual ratings evaluated in the experiment Phase II. The observed scores were averaged across all observers to create a score for each fabric sample under each experiment condition. Overall, a higher score means the fabric was judged as

stiffer/rougher/firmer/crisper/cooler, and a lower score means the fabric was judged as more flexible/smoothier/softer/spongier/warmer.

Three draped fabric images in different viewing angles were prepared for each fabric sample in the experiment Phase II. The effects of the viewing angles were evaluated by RMS values (Equation 4.1), where x_i represents the average score across all observers for three viewing angles respectively, \bar{x} represents the average scores across the three viewing angles (Section 5.4). The Pearson Correlation Coefficient (two-tailed) was computed to assess the relationships of the perception of tactile properties among different experiment conditions (Section 5.5), and the relationships among the perception of tactile properties under each experiment condition (Section 5.6). The significant level was set to 0.05. Asterisks *** indicate $p < 0.001$, ** indicate $p < 0.01$, * indicate $p < 0.05$ in all analyses. To further investigate the difference of the tactile perception between using visual representation and real fabrics (Section 5.7), the tactile responses were averaged from flat fabric images, draped fabric images, and fabric rotation video to represent the visual representation data. Similarly, the tactile responses from vision-only (using real fabrics), touch-only, and vision+touch were averaged to represent the real fabric data.

5.3 Observer variability

The RMS values were calculated as a measure of both inter-observer variability and intra-observer variability for tactile perceptual ratings across observers in the experiment Phase II. As shown in Table 5.1, the RMS values range from 1.17 to 1.63 with a mean value of 1.38 for inter-observer variability, and from 0.94 to 1.34 with a mean value of 1.25 for intra-observer variability. The observer variability for warm-cool was found to be the lowest, with the RMS of 1.17 and 0.94, and the highest for spongy-crisp with the RMS of 1.63 and 1.34 for inter- and intra-observer variability, respectively. Compared to the studies using categorical judgement (Ou et al., 2006; Lee et al., 2000; Ou et al., 2012), the

RMS values shown here are reasonable, indicating it can achieve observer variability within 1.38 points on a 9-point scale within the group, and 1.25 points on a 9-point scale within the observer.

Table 5.1 Observer variability in the experiment Phase II.

	Flexible- stiff	Smooth- rough	Soft-firm	Spongy- crisp	Warm- cool	Mean
Inter-observer variability	1.24	1.44	1.39	1.63	1.17	1.38
Intra-observer variability	1.26	1.34	1.34	1.34	0.94	1.25

5.4 The differences of the visual-tactile perception between three viewing angles of draped fabric images

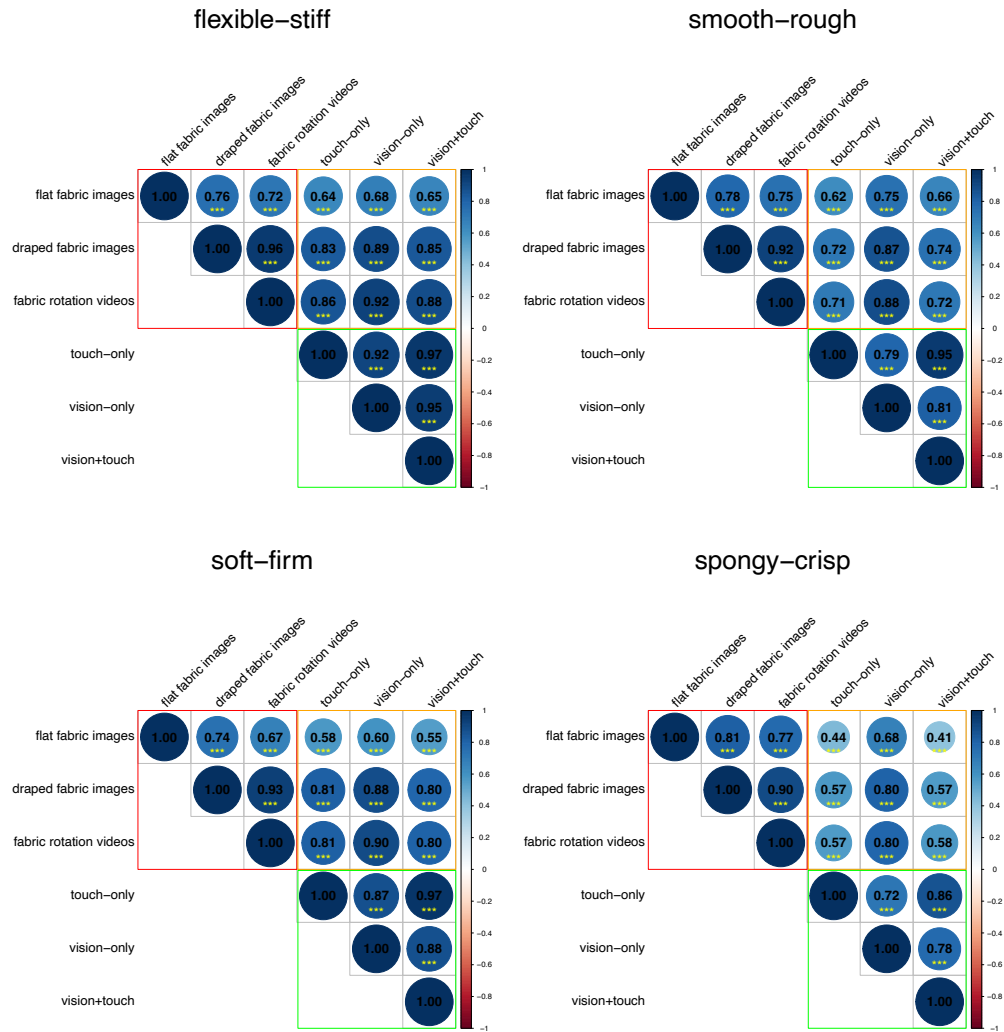
The differences of the visual-tactile perception between the three observing angles (drape_0, drape_45, drape_90) from the draped fabric images was tested by RMS values defined in Equation 4.1. The RMS values indicated the differences between the perceptual ratings at each observing angle and the average across the three angles. Overall, there were small differences of the tactile perceptual ratings in each pair of tactile properties. The RMS values were all lower than 0.33, indicating that a difference between one observing angle and the average was within 0.33 points on a 9-point Likert scale. A possible reason is that, when observers viewed one draped fabric image, it is likely they can imagine what the fabric would look like from different angles. To simplify, the tactile perceptual ratings averaged across the three observing angles were used in subsequent analyses to represent the tactile perceptual ratings obtained from the draped images.

Table 5.2 RMS values for draped fabric images in three observing angles.

	Flexible- stiff	Smooth- rough	Soft-firm	Spongy- crisp	Warm-cool
Drape_0	0.32	0.29	0.31	0.30	0.23
Drape_45	0.29	0.25	0.33	0.33	0.23
Drape_90	0.33	0.30	0.33	0.27	0.23

5.5 The correlations of the tactile perceptual ratings among the experiment conditions

Figure 5.1 shows the Pearson Correlation Coefficients of the perception of tactile properties among the six experiment conditions, along with the corresponding significance levels.



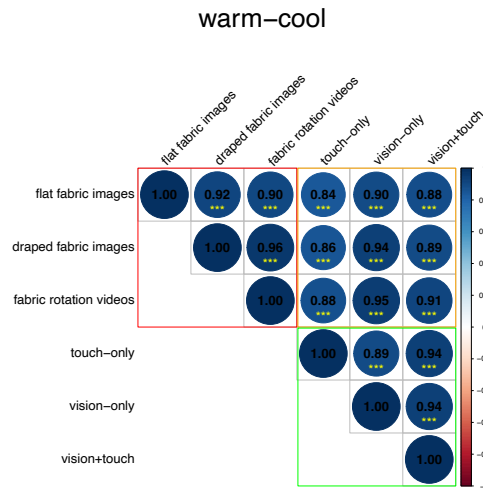


Figure 5.1 The Pearson Correlation Coefficients between each experiment condition.

When comparing the correlations of the visual-tactile perception observed through displaying images and videos (red rectangles in Figure 5.1), it is found that the correlations between the draped images and fabric rotation videos are always very high and significant for the five pairs of tactile properties ($0.9 < r < 0.96$, $p < 0.001^{***}$). On the other hand, the perception of flexible-stiff, smooth-rough, soft-firm, and spongy-crisp observed from flat images were positively correlated with those observed from draped fabric images and videos ($0.67 < r < 0.81$, $p < 0.001^{***}$). However, these correlations were not as high as the correlations between draped fabric images and fabric rotation videos as described above. It is noted that for warm-cool, the visual-tactile perception from flat fabric images, draped fabric images, and fabric rotation videos were highly consistent ($r > 0.9$, $p < 0.001^{***}$). What's more, the visual-tactile perception from flat fabric images showed a slightly stronger correlation with those perceived from draped fabric images than with those perceived from fabric rotation videos. A possible reason is that observers viewed the fabric rotation videos for at least 50 seconds before providing tactile responses, which is longer than the time spent observing static fabric images.

The correlation coefficients shown in the yellow rectangles in Figure 5.1 show how the different tactile properties perceived from fabric images and videos

correlate with those from the actual touch and observation (touch-only, vision-only using real fabrics, vision+touch) of fabrics. Firstly, the visual-tactile perception from draped fabric images and rotating videos had similar correlations with the tactile perception from actual touch and observation. Secondly, the visual-tactile perception from flat fabric images had a lower correlation with the actual touch and observation compared to draped fabric images and videos, but for warm-cool, the correlations were very similar and strongly positive. A previous study found that draped fabric images had better matching accuracy than flat images in the match-to-sample task (Xiao et al., 2016). A possible explanation of this discrepancy about warm-cool is that the perception of the tactile properties is a multiscale task (Pan, 2006; Bacci et al., 2012; Baumgartner et al., 2013; Bouman et al., 2013; Mahar et al., 2013). Compared to draped fabric images and videos, flat fabric images lack information such as drape, shape, shade, and folds. The presence of such information enhanced the understanding of tactile properties in the absence of actual touch and observation, but they were less important for perceiving warm-cool.

The green rectangles in Figure 5.1 show the correlations of the tactile perception obtained through the actual touch (touch-only), the observation (vision-only using real fabrics) and the combination of both (vision+touch). Condition of vision+touch provided observers with the most comprehensive perception of the real fabrics. Among them, the correlations between the touch-only and vision+touch were the highest for flexible-stiff ($r=0.97$, $p<0.001^{***}$), smooth-rough ($r=0.95$, $p<0.001^{***}$), soft-firm ($r=0.97$, $p<0.001^{***}$), spongy-crisp ($r=0.86$, $p<0.001^{***}$). For the perception of warm-cool, the correlations were the same and the highest between touch-only and vision+touch ($r=0.94$, $p<0.001^{***}$) and between vision-only (using real fabrics) and vision+touch ($r=0.94$, $p<0.001^{***}$). In addition, high and significant correlations of tactile perception between vision-only (using real fabrics) and vision+touch (minimum $r=0.78$, $p<0.001^{***}$ for

spongy-crisp) were observed. In the absence of either vision or touch, consistent tactile perception can be obtained using real fabrics.

5.5.1 Comparisons with Section 4.6: the consistency and discrepancy in using rendered and real fabric images

In the last Chapter, the correlations of tactile perceptual ratings collected using rendered fabric images and the corresponding real fabrics were reported. In this Chapter, the correlations of tactile perceptual ratings collected using real fabric images and real fabrics were analysed. Comparisons of the Pearson Correlation Coefficients (r) of these two correlations revealed the consistencies and differences between rendered and real fabric images regarding the visual-tactile and tactile perception. As listed in Table 5.3, r values obtained from rendered and real fabric images were generally consistent for all tactile properties. The exception includes spongy-crisp perceived from draped fabric images and touch-only ($r=0.83$ when using rendered fabric images, $r=0.57$ when using real fabric images), and warm-cool perceived from flat and draped fabric images ($r=0.66$ when using rendered fabric images, $r=0.92$ when using real fabric images). In addition, perception through draped fabric images always correlated more closely to the actual touching than that through flat fabric images.

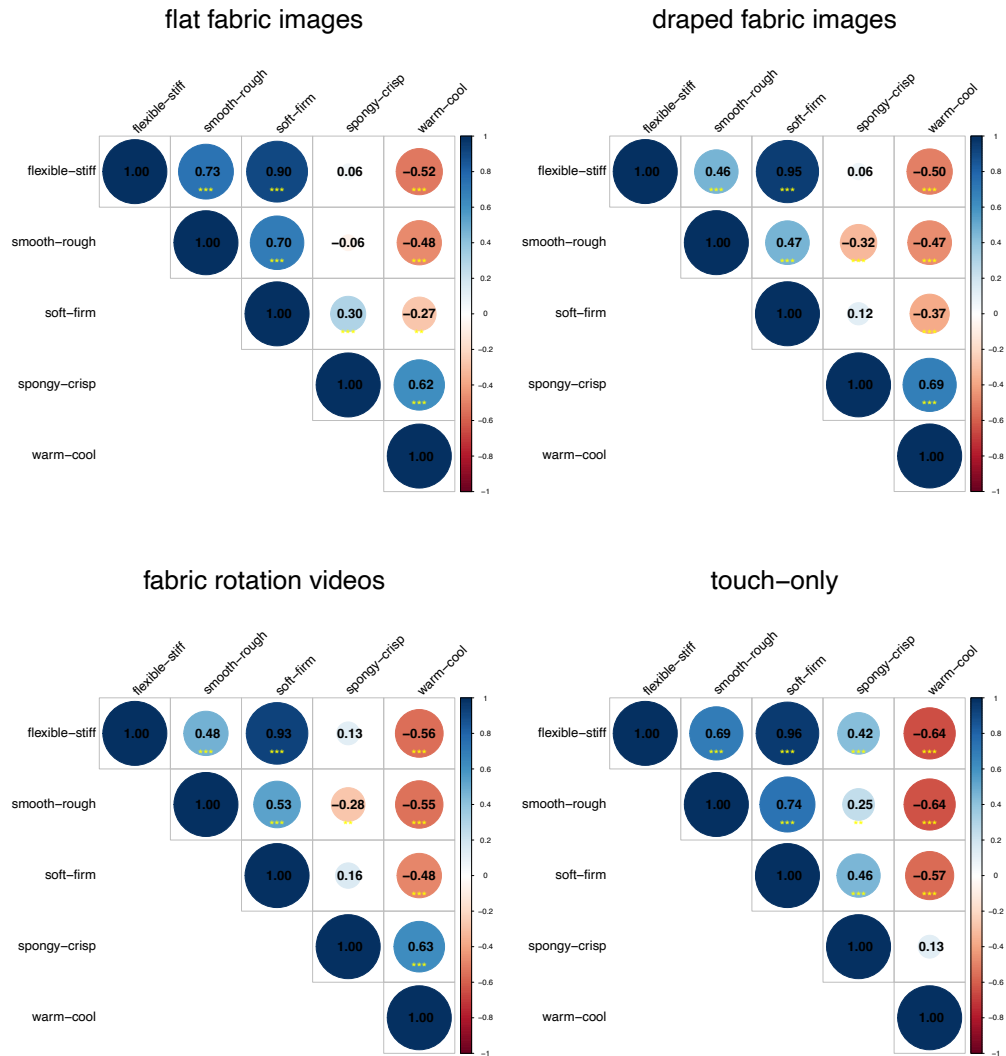
Table 5.3 Comparison of the Pearson Correlation Coefficients (r) between Section 4.6 (left) and Section 5.5 (right).

	Touch-only vs flat	Touch-only vs draped	Flat vs draped
Flexible-stiff	0.51 / 0.64	0.66 / 0.83	0.89 / 0.76
Smooth-rough	0.42 / 0.62	0.63 / 0.72	0.75 / 0.78
Soft-firm	0.68 / 0.58	0.90 / 0.81	0.74 / 0.74
Spongy-crisp	0.61 / 0.44	0.83 / 0.57	0.72 / 0.81
Warm-cool	0.81 / 0.84	0.88 / 0.86	0.66 / 0.92

5.6 The correlations among tactile perceptual ratings under each experiment condition

Overall, the tactile perceptual ratings perceived from the experiment conditions are positively and significantly correlated. To further understand the perception

of tactile properties, the correlations between tactile perceptual ratings under each experiment condition were assessed, and the correlation coefficients and the corresponding significance levels are shown in Figure 5.2.



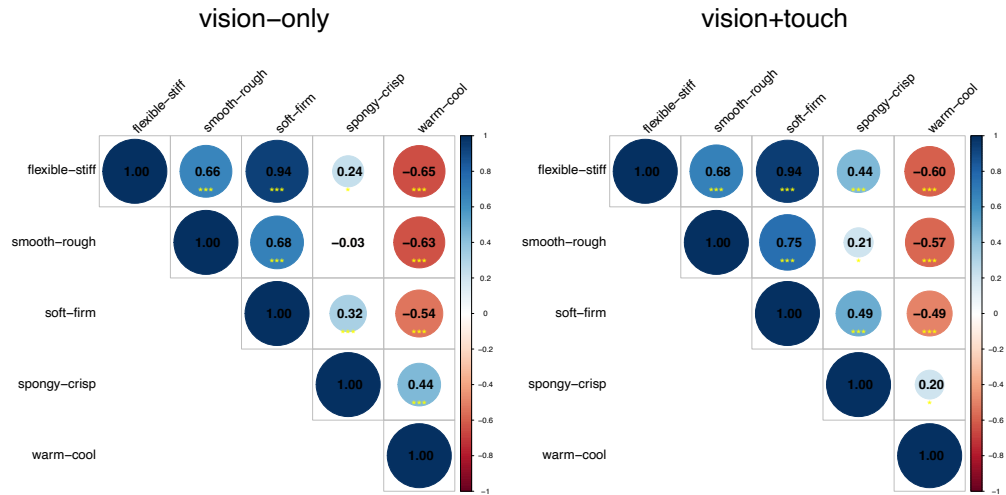


Figure 5.2 The Pearson Correlation Coefficients between each pair of tactile properties under the experiment conditions.

The correlations between the tactile perceptual ratings demonstrated consistency under all conditions, however, notable differences specific to each condition were also observed. For the consistency, firstly, the perceived flexible-stiff had very strong and significant correlations with the perceived soft-firm under all conditions ($r > 0.9$, $p < 0.001^{***}$). It is also found that the perceived smooth-rough positively correlated with flexible-stiff and soft-firm under all conditions, yet the correlations were not as high as 0.9. Basically, a fabric perceived as more flexible is highly possible to be perceived as smoother and softer, regardless of the experiment conditions under which it was presented. Secondly, negative correlations were found between the perceived warm-cool and other tactile perceptions except for spongy-crisp under all conditions. A fabric perceived as warmer tends to be perceived as stiffer, rougher, and firmer. However, when using fabric images and videos, the negative correlations were generally weaker than using real fabrics. Besides, it is also noted that the negative correlations between warm-cool and flexible-stiff were slightly stronger than the correlation between warm-cool and smooth-rough, and also slightly stronger than that between warm-cool and soft-firm under all conditions.

The correlation between spongy-crisp and other tactile perceptions showed different patterns across all the experiment conditions. Firstly, when using fabric

images and videos, there were no significant correlations between spongy-crisp and flexible-stiff. However, with real fabrics, the correlations became significant, and increased when touch was allowed ($r=0.42$, $p<0.001^{***}$ when only touch was allowed, $r=0.44$, $p<0.001^{***}$ when both vision and touch were allowed). A similar regularity was observed for the correlation between spongy-crisp and soft-firm, except that when using flat images, the perception of spongy-crisp and soft-firm was slightly positively correlated. Generally, a fabric perceived as spongier tends to be more flexible and softer, but it was not the fact when the perception came from images or videos. Secondly, the perception of spongy-crisp weakly negatively correlated to smooth-rough when using draped fabric images and fabric rotation videos, while weak but positive correlations between them were found when touching the real fabrics was allowed. A fabric perceived as spongier through images and videos tends to be rougher, but when observed and touched in real life, it tends to be smoother. Thirdly, no significant correlations were found between spongy-crisp and warm-cool when touching the fabrics was allowed. However, notable positive correlations were observed when touching the fabrics was not allowed, whenever through observing the fabric images and videos or observing the real fabrics without touching. A fabric perceived as spongier tends to be warmer under specific experiment conditions.

5.6.1 Comparison with Section 4.7: the consistency and discrepancy in correlations among tactile properties

In the last Chapter, the correlations among the perception of all tactile properties were reported using data from rendered fabric images and corresponding real fabrics in Leeds Fabric Tactile Database Part I (see Figure 4.3, page 102). In Section 5.6, the correlations were reported using data from real fabric images and corresponding fabrics in Leeds Fabric Tactile Database Part II. Comparisons were made between these two correlations and were illustrated in Figure 5.3. Firstly, the perceived flexible-stiff, smooth-rough, soft-firm were highly and positively correlated, regardless of whether rendered or real fabric

images were used. However, the correlations between spongy-crisp and flexible-stiff, smooth-rough, soft-firm were significant only when rendered fabric images were used. While these correlations remained significant when actually touching the fabrics, the correlation coefficients computed for Part II fabrics were lower than those for Part I fabrics. The other differences are the correlations between warm-cool and other tactile properties. The perceived warm-cool has no correlation with other tactile properties for fabrics and images in Part I, but had negative correlations with flexible-stiff, smooth-rough, soft-firm and positive correlations with spongy-crisp for fabrics and images in Part II.

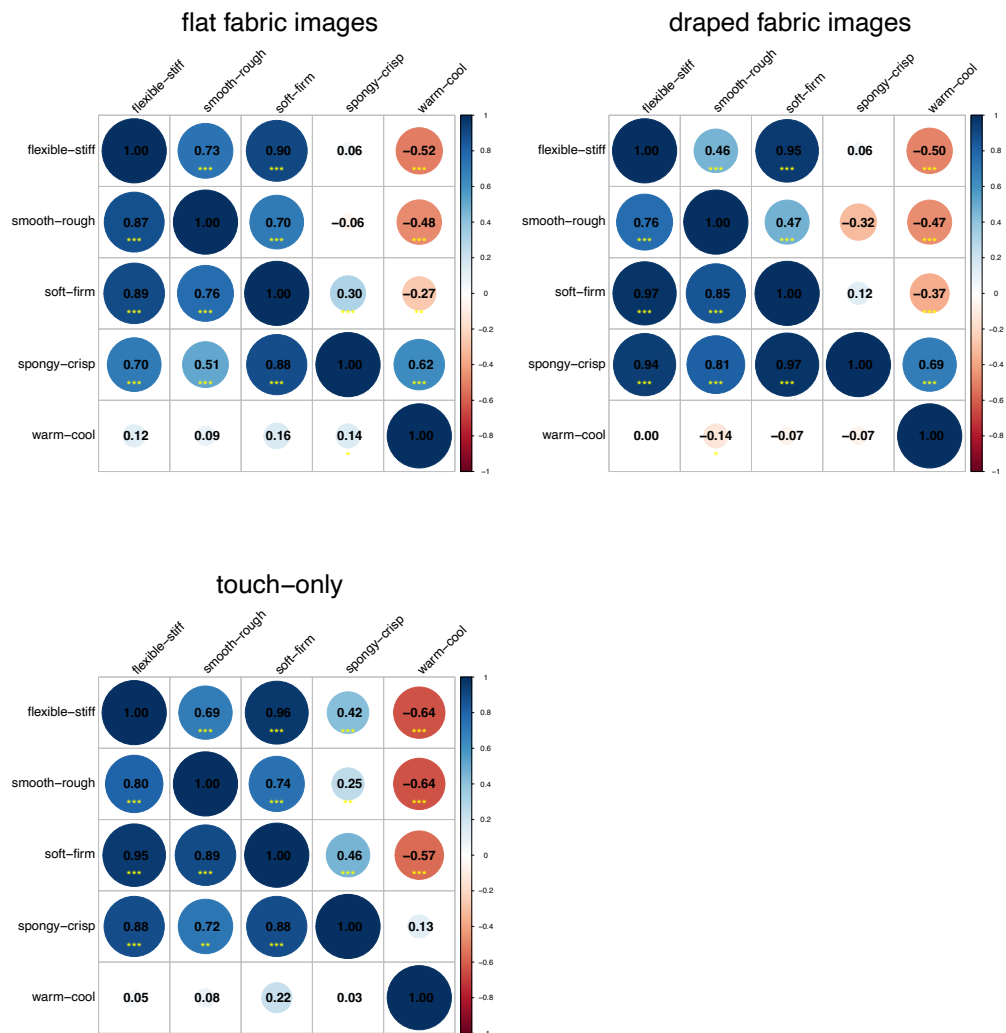
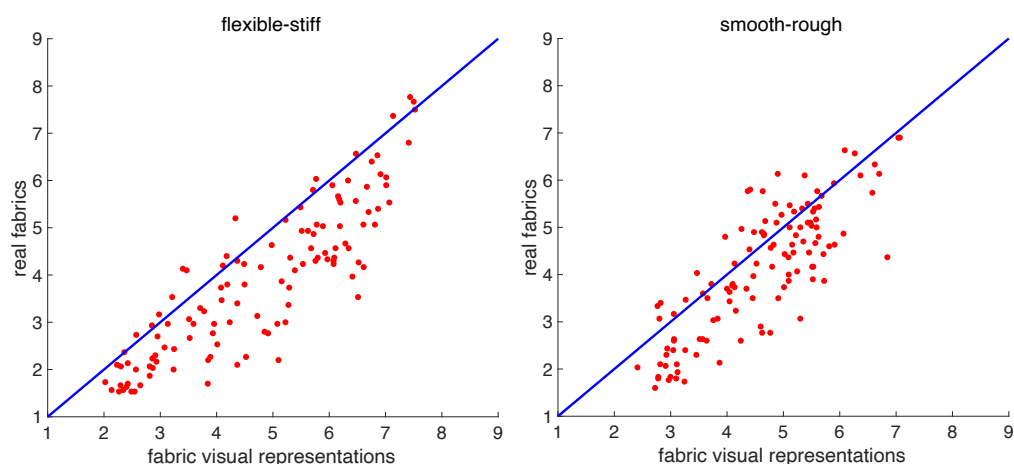


Figure 5.3 Comparisons of the correlations of the perception among tactile properties. Below diagonal: using rendered fabric images (Section 4.7). Above diagonal: using real fabric images (Section 5.6).

5.7 The differences of the tactile perceptual ratings between using visual representations and real fabrics

In Section 5.5 and Section 5.6, detailed correlation analyses were provided to investigate the correlations of tactile properties between experiment conditions, and the correlations between the tactile properties under each experiment condition. In Figure 5.1, high and positive correlations were observed between the tactile perceptual ratings perceived through flat fabric images, draped fabric images, and fabric rotation videos (red rectangles, $0.67 < r < 0.96$, $p < 0.001^{***}$), as well as those through vision only, touch only, and vision +touch (green rectangles, $0.72 < r < 0.97$, $p < 0.001^{***}$). This section further investigates the differences of the tactile perceptual ratings between using visual representation and real fabrics. Figure 5.4 compares the differences of the tactile perceptual ratings perceived between visual representations and real fabrics. Each red point represents a fabric. Blue lines are diagonal lines at a 45-degree angle to both x and y axes. Points above blue lines indicate stiffer/rougher/firmer/crisper/cooler perception perceived through real fabrics. Points below blue lines indicate stiffer/rougher/firmer/crisper/cooler perception perceived through visual representations. The x axes represent the tactile perceptual ratings from visual representation, and the y axes represent the tactile perceptual ratings from real fabrics.



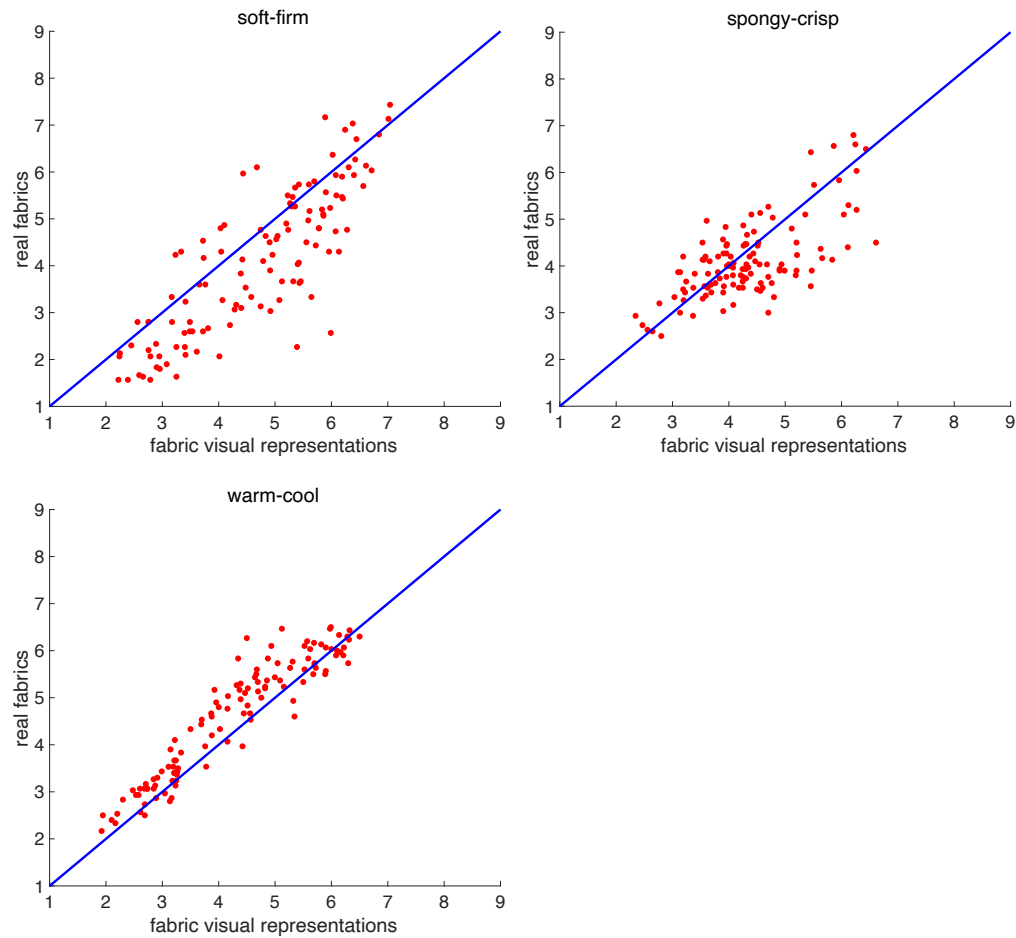


Figure 5.4 Comparisons between the tactile perception perceived from visual representations (images and videos) and real fabrics.

Most fabrics, when observed through visual representation, tended to be perceived as stiffer compared to when observed through real fabrics. Similar trends have also been observed in the perception of smooth-rough and soft-firm, where fabrics tend to appear rougher and firmer when perceived through visual representation compared to real fabrics. This is reasonable as strong and positive correlations were found among the perception of flexible-stiff, smooth-rough, and soft-firm, regardless of whether the fabrics were perceived through visual representation or real fabrics (see Figure 5.1). On the other hand, fabrics perceived through real fabrics tended to be perceived as cooler compared to those perceived through visual representation. The fabrics were conditioned in a standard environment of $20\text{ }^{\circ}\text{C} \pm 2^{\circ}\text{C}$ and $65\% \pm 4\%$ relative humidity for 48 hours prior to the experiment Phase II according to ISO 139:2005 (International Organization for Standardization, 2005). The conditioning temperature was

lower than the human palm temperature. When perceiving warm-cool through direct touch, the lower conditioning temperature may reduce the perception of warmth. Besides, it is noticed that approximately half of the fabrics in this study were perceived as spongier through real fabrics, while the other half were perceived as spongier through visual representation. There was no clear trend indicating a consistent difference between real fabrics and visual representation regarding the spongy-crisp perception.

5.8 Discussions

5.8.1 The similar role of draped fabric images and fabric rotation videos in the tactile perception

In Figure 5.1, it is found that the tactile properties perceived through draped fabric images were strongly and positively correlated with those perceived through fabric rotation videos ($0.90 < r < 0.96$, $p < 0.001^{***}$). This is reasonable because the draped fabric images were extracted from the videos. The observers, when observing the fabric rotation videos, certainly also observed the draped fabric images.

The tactile properties perceived through draped fabric images were highly correlated with those perceived through actual touch and observation (touch-only, vision-only using real fabrics and vision+touch). Similarly, the tactile properties perceived through fabric rotation videos showed similar correlation coefficients to those of draped fabric images. There is no clear trend indicating that the correlation between either draped fabric images or fabric rotation videos and actual touch and observation was stronger. A previous study compared the tactile perception obtained from jean fabric images and videos (Wijntjes et al., 2019). Unlike findings here, they concluded that videos have a better identification performance over images in the match-to-sample task. It is noted that these videos included the process of manipulating the fabrics by human hand, whereas only fabric itself was featured in the experiment Phase II. In the

absence of the experience of hands touching the fabrics in the video, fabric images and videos played similar roles in conveying tactile properties.

5.8.2 Positively and negatively correlated tactile properties

In the study of Pan (2006), stiffness, smoothness, and softness were evaluated as the first three orthogonal features of fabric hand by the fabric extraction method. A fabric was pulled out through a designed metal nozzle, and the fabric displacement and force figures were recorded. According to their objective methods and data analysis strategies, the stiffness, smoothness, and softness contributed differently yet complementarily to the fabric hand. However, in the present study, the perceptions of flexible-stiff, smooth-rough, soft-firm were highly correlated to each other under the conditions of flat images, draped images, videos, touch-only, vision-only (using real fabrics), and vision+touch (see Figure 5.2). A fabric subjectively perceived as stiffer is highly possible to be perceived as rougher and firmer, regardless of the experiment conditions under which it is presented. Discrepancies have been found here between the objective measurement and subjective judgement. The perceived flexible-stiff, smooth-rough, soft-firm were strongly correlated to each other in this study, while stiffness, smoothness, and firmness were orthogonal in the objective measurement. On the other hand, efforts were made to evaluate the correlation between objective measurements and subjective judgement (Bergmann Tiest et al., 2006; Bacci et al., 2012; Bouman et al., 2013). Good correlations have been found between the perceived fabric stiffness and fabric density with the ground truth measurement using fabric videos (Bouman et al., 2013); between the perceived softness, stiffness, force of compression, and tensile stretch with FAST measurement (Bacci et al., 2012); and between the perceived compressibility and roughness with the objective measurement (Bergmann Tiest et al., 2006). The inconsistency in stiffness, smoothness, and firmness between Pan (2006) and this study, despite other studies reporting good correlations of tactile properties between objective measurements and

subjective evaluation, suggests that the tactile properties are not fully understood by either measurement devices or human perception. Choosing measurement methods or subjective judgment approaches based on the aim and objectives is the best way to benefit the target audience.

In Figure 5.1, strong and positive correlations were found for the perception of warm-cool among the experiment conditions ($r > 0.84$, $p < 0.001^{***}$). Touch and vision, whether using the images/videos or real fabrics, made no difference in the perception of warm-cool. Consistent results were observed from Fenco et al. (2010), where touch and vision were found to be equally important for the perception of warmth in scarf and breakfast tray. Another finding from Fenco et al. (2010), is that materials had a significant impact on the perception of warmth for scarf, with fleece and wool being rated as the warmest, and viscose and silk as the coolest. In this study, it is found that the findings from Fenco et al. (2010), applied not only to scarf but also to fabrics with unspecified uses. Fur and fleece fabrics were rated the top seven warmest fabrics and viscose fabrics were rated the top six coolest fabrics under the condition of vision+touch.

In Figure 5.2, significant correlations were observed between the perception of warm-cool and other tactile properties under each experiment condition. Fabrics perceived as warmer were also perceived as stiffer, rougher, and firmer under all experiment conditions, and spongier except when touching the fabrics. As mentioned above, fabric material significantly affected the perception of warm-cool, but it cannot explain the correlation between warm-cool and other tactile properties. However, it is found that the fabric thickness effectively explained the correlations by analysing the correlation between fabric thickness and the tactile perception. As shown in Figure 5.5, thicker fabrics were perceived as warmer, spongier (negative bars), stiffer, rougher, and firmer (positive bars). Fabric material, together with fabric thickness, were considered to affect the insulating properties (Havenith, 1999) and thus affect the thermal comfort of the clothing (McCullough et al., 2009) which possibly reveals the role of thickness

in the perception of warm-cool, flexible-stiff, smooth-rough, soft-firm, and spongy-crisp.

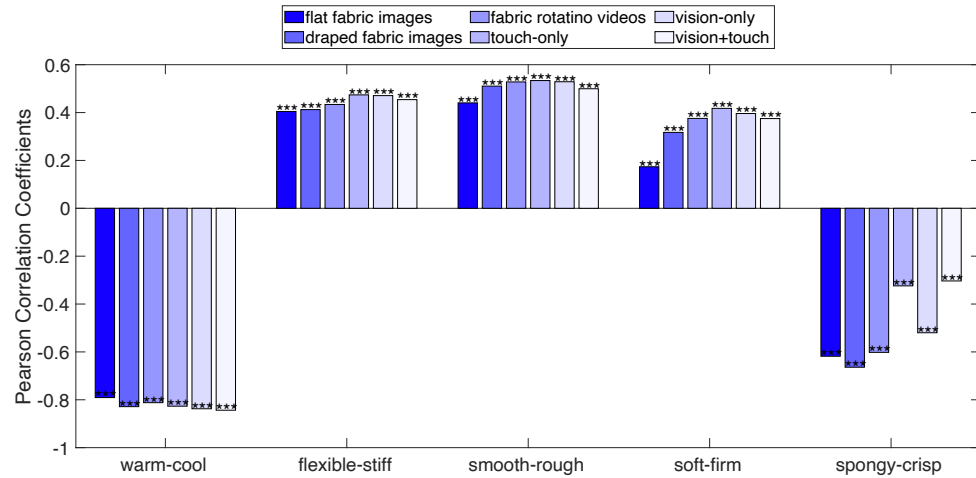


Figure 5.5 The correlation between fabric thickness and the perception of warm-cool, flexible-stiff, smooth-rough, soft-firm, and spongy-crisp under each experiment condition.

5.8.3 Comparisons of the correlations between fabrics and images in Leeds Fabric Tactile Database Part I and Part II

In Section 5.5 and Section 5.6, the correlations of the tactile properties among experiment conditions, and the correlations among tactile properties under each experiment condition were reported. Fabrics and images in Leeds Fabric Tactile Database Part II were utilised. In addition to that, the correlations were compared with those in the last Chapter where rendered fabric images and corresponding fabrics in Leeds Fabric Tactile Database Part I were analysed (Section 5.5.1 and 5.6.1). Both consistencies and discrepancies were observed between samples in Leeds Fabric Tactile Database Part I and Part II. Consistencies were mainly observed for the perception of flexible-stiff, smooth-rough, and soft-firm, while discrepancies were mainly observed for the perception of spongy-crisp and warm-cool. Few studies have conducted similar comparisons before. The observed consistencies and discrepancies are further investigated by taking the differences in the fabrics in Part I and Part II into account.

As discussed in previous section, fabric thickness affected the perception of tactile properties. In Figure 5.6, the fabric thickness was compared for fabrics in Part I and Part II. Compared to fabrics in Part I, thicker fabrics were available in Part II.

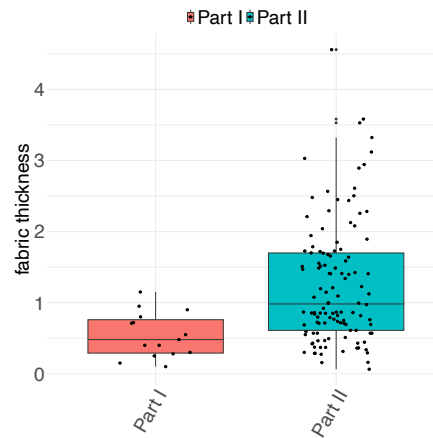


Figure 5.6 Comparison of the fabric thickness between fabrics in Leeds Fabric Tactile Database Part I and Part II.

There were two major consistencies observed in fabrics between Part I and Part II: (1) the similar correlations of the perception of tactile properties between experiment conditions, and (2) the similar correlations between the perceived flexible-stiff, smooth-rough, and soft-firm. Although thicker fabrics were available in Part II, the fabric thickness generally did not affect these correlations. Instead, these correlations demonstrated a robust consistency, supporting the reliability and generalisability of the findings.

Moreover, fabric thickness can be the possible reason to explain the discrepancies of the perceived spongy-crisp and warm-cool. As discussed in Section 5.8.2, thicker fabrics were perceived as warmer, stiffer, rougher, and firmer, and spongier (except when touching the fabrics). The lack of thicker fabrics in Part I may have underestimated the relationship between the perceived warm-cool and other tactile properties. It further supports the reliability of the correlations observed in fabrics in Part II.

5.9 Summary

In this Chapter, the relationship of the perception of tactile properties was investigated. Comparisons were made on the results obtained using Leeds Fabric Tactile Database Part I (Chapter 4) and Part II (this Chapter). A summary of major findings is listed below:

- There were no significant differences in visual-tactile perception across three viewing angles of the draped fabric images.
- The visual-tactile perception from draped fabric images were strongly correlated to that from fabric rotation videos. Both draped fabric images and fabric rotation videos demonstrated similar levels of correlations with the tactile perception from actual touch and observation. In the absence of either vision or touch, consistent tactile perception can be obtained using real fabrics.
- The perceived flexible-stiff, smooth-rough, and soft-firm had positively correlations, regardless of the experiment conditions under which it was present. The perceived warm-cool, however, had negative correlations with them. A fabric perceived as more flexible is highly possible to be perceived as smoother, softer, and cooler. The correlations between spongy-crisp and other tactile properties were mixed and specific for experiment conditions.
- For each sample, two scores were created to represent the tactile perceptual ratings obtained from visual representation and real fabric, respectively. Most fabrics, when observed through visual representation, tended to be perceived as stiffer, rougher, firmer, and warmer compared to those observed through real fabrics. No consistent difference between real fabrics and visual representation was observed for spongy-crisp perception.
- Comparisons were made on the tactile perceptual ratings between from Leeds Fabric Tactile Database Part I (Chapter 4) and Part II, regarding the

correlation analyses. The perceived flexible-stiff, smooth-rough, and soft-firm had consistent correlations, while discrepancies were observed for spongy-crisp and warm-cool.

Chapter 6

Experiment Phase II: factors for visual-tactile and tactile perception

6.1 Overview

In this Chapter, the visual-tactile and tactile perceptual ratings collected using Leeds Fabric Tactile Database Part II were analysed. Significant effects of fabric appearance were found on the visual-tactile perception in Chapter 4, which was based on an analysis conducted for each individual fabric. Given the countless fabric appearance available due to fabric structure and colour, it is not feasible to conduct similar analyses when a larger dataset was used. The fabrics in Leeds Fabric Tactile Database Part II were categorised into two groups based on the fabric structures: woven and knitted. Normal distribution tests were conducted firstly for the tactile perceptual raw data of all observers (Section 6.3). Cumulative Link Mixed Models (CLMMs) were fitted for each pair of tactile properties to conduct the analyses. Whether the tactile and visual-tactile perception differs between woven and knitted fabrics, and the interactive effects of fabric structures and experiment conditions were analysed (Section 6.4). The effect of fabric colour on the tactile perception was further evaluated (Section 6.5). Correlation analyses were conducted among experiment conditions and tactile perceptual ratings for woven and knitted fabric separately (Section 6.6). The analytical methods were introduced in Section 6.2.

6.2 Statistical analysis

The raw data collected in the experiment Phase II was used in this Chapter, and the following analyses were conducted:

Before conducting the analysis, whether the collected observations are normally distributed was assessed firstly by Shapiro-Wilk test (Section 6.3). To assess the effects of fabric structures, the distribution of the tactile perceptual ratings for woven and knitted fabrics was visualised firstly using box plot (Section 6.4). Mann-Whitney U tests were conducted to compare the distributions of the tactile perceptual ratings of woven and knitted fabrics (Section 6.4.1). CLMM models with (full models) and without (simple models) interactions were fitted for each

pair of tactile properties, setting the fabric structures and experiment conditions as the fixed effects, and fabric samples and observers as the random effects (Section 6.4.2). Comparisons between simple and full model were made using *anova()* function from *stats* R package. P values of the fixed effects in CLMM models were computed using Likelihood Ratio Test (LRT) with Type III sums of squares, using *Anova()* function from *car* R package. The fitted perceptual ratings of were computed for all interactions using Equation 4.4 (see page 92). Pairwise contrasts analyses were conducted with Bonferroni correction across experiment conditions to evaluate the significant differences between woven and knitted fabrics using *contrast()* function in *emmeans* R package (Section 6.4.3). Whether the tactile and visual-tactile perception differed with fabric structures was assessed in a practical sense considering the meaning assigned to each point.

In Chapter 4 the effect of colour on the visual-tactile perception was evaluated using rendered fabric images. Here the effect of colour was assessed on the tactile perception (Section 6.5). CLMM models were fitted for each pair of tactile properties, setting the following fixed effects: the measured lightness (L^*), redness (a^*), and yellowness (b^*) as continuous predictors, fabric structures and experiment conditions (touch-only, vision-only using real fabrics, vision+touch) as categorical predictors. Experiments using fabric visual representations (flat fabric images, draped fabric images, fabric rotation videos) were excluded in this section, as the colours were measured using real fabrics. Even though colours were characterised to reproduce the fabric images and videos, the folds and shadows of the draped fabrics cause discrepancies between the visual representations and the measured results. Simple models without interactions and full models with interactions between fabric colours (measured CIELAB values), fabric structures, and experiment conditions were compared. Fabrics and observers were set as the random effect. CIELAB values were z-standardised before fitting the CLMM models to ensure an evenly distribution.

The parameter estimates were computed for CIELAB separately for each pair of tactile properties.

To further reveal the difference in the perception of tactile properties between woven and knitted fabrics, the observed scores were averaged across all observers to create a score for each fabric samples under each experiment condition. Detailed correlation analyses were conducted by Pearson Correlation Coefficients (two-tailed) for woven fabrics and knitted fabrics, respectively. The correlations among experiment conditions for each pair of tactile properties, and among tactile perceptual ratings under each experiment condition were evaluated.

The CLMM models were implemented in *ordinal* R package. The significant level was fixed to 0.05 in all analyses. Contrast coding was used in all CLMM models to convert fabric structure and experiment conditions to coded categorical factors. Asterisks *** indicate $p < 0.001$, ** indicate $p < 0.01$, * indicate $p < 0.05$ in all analyses.

6.3 Normal distribution test

Shapiro-Wilk tests were conducted first for each experiment condition and each pair of tactile properties. The results are listed in Table 6.1. A value of w closer to 1 indicates a better match to the normal distribution, and the p -values indicate the rejection or not to the null hypothesis. The p -values are all at the significant level and reject the null hypothesis. The raw data of the tactile perceptual ratings were not normally distributed, and thus the analysis methods in this Chapter do not require the assumption of normality.

Table 6.1 The results of Shapiro-Wilk test for the experiment Phase II.

	Flexible- stiff	Smooth- rough	Soft-firm	Spongy- crisp	Warm-cool
Flat	$w=0.91$, $p < 0.001^{***}$	$w=0.93$, $p < 0.001$	$w=0.92$, $p < 0.001^{***}$	$w=0.93$, $p < 0.001^{***}$	$w=0.95$, $p < 0.001^{***}$
Draped	$w=0.90$, $p < 0.001^{***}$	$w=0.93$, $p < 0.001^{***}$	$w=0.91$, $p < 0.001^{***}$	$w=0.91$, $p < 0.001^{***}$	$w=0.94$, $p < 0.001^{***}$

Video	w=0.93, p<0.001***	w=0.94, p<0.001***	w=0.93, p<0.001***	w=0.94, p<0.001***	w=0.95, p<0.001***
Touch-only	w=0.91, p<0.001***	w=0.93, p<0.001***	w=0.92, p<0.001***	w=0.93, p<0.001***	w=0.94, p<0.001***
Vision-only (using real fabrics)	w=0.93, p<0.001***	w=0.93, p<0.001***	w=0.93, p<0.001***	w=0.94, p<0.001***	w=0.94, p<0.001***
Vision+touch	w=0.92, p<0.001***	w=0.94, p<0.001***	w=0.93, p<0.001***	w=0.94, p<0.001***	w=0.95, p<0.001***

6.4 The effects of fabric structures on visual-tactile perception and tactile perception

6.4.1 The distribution of tactile perceptual ratings for woven and knitted fabrics, respectively

Considering the different appearances between woven and knitted fabrics (Breen and House, 2000), the distribution of the tactile perceptual ratings collected using woven and knitted fabrics was compared and shown in Figure 6.1. In each figure, the boxes indicate the interquartile ranges (IQR), white points in the horizontal lines indicate the medians, whiskers indicate the maximum and minimum observation (within 1.5*IQR), and individual points outside the whiskers indicate outliers. Different median values and IQR can be observed for most of the tactile perceptual ratings between woven and knitted fabrics in Figure 6.1. As the tactile perceptual ratings are not normally distributed, a non-parametric test, Mann-Whitney U test was conducted to statistically compare the distribution of the tactile perceptual ratings between woven and knitted fabrics. The results of each pair of tactile properties and each experiment condition are listed in Table 6.2. For the perception of flexible-stiff, smooth-rough, soft-firm, and spongy-crisp, there were significant perceptual differences between using woven and knitted fabrics under all experiment conditions. For the perception of warm-cool, significant differences were only observed when touching the real fabrics were allowed (touch-only and vision+touch).

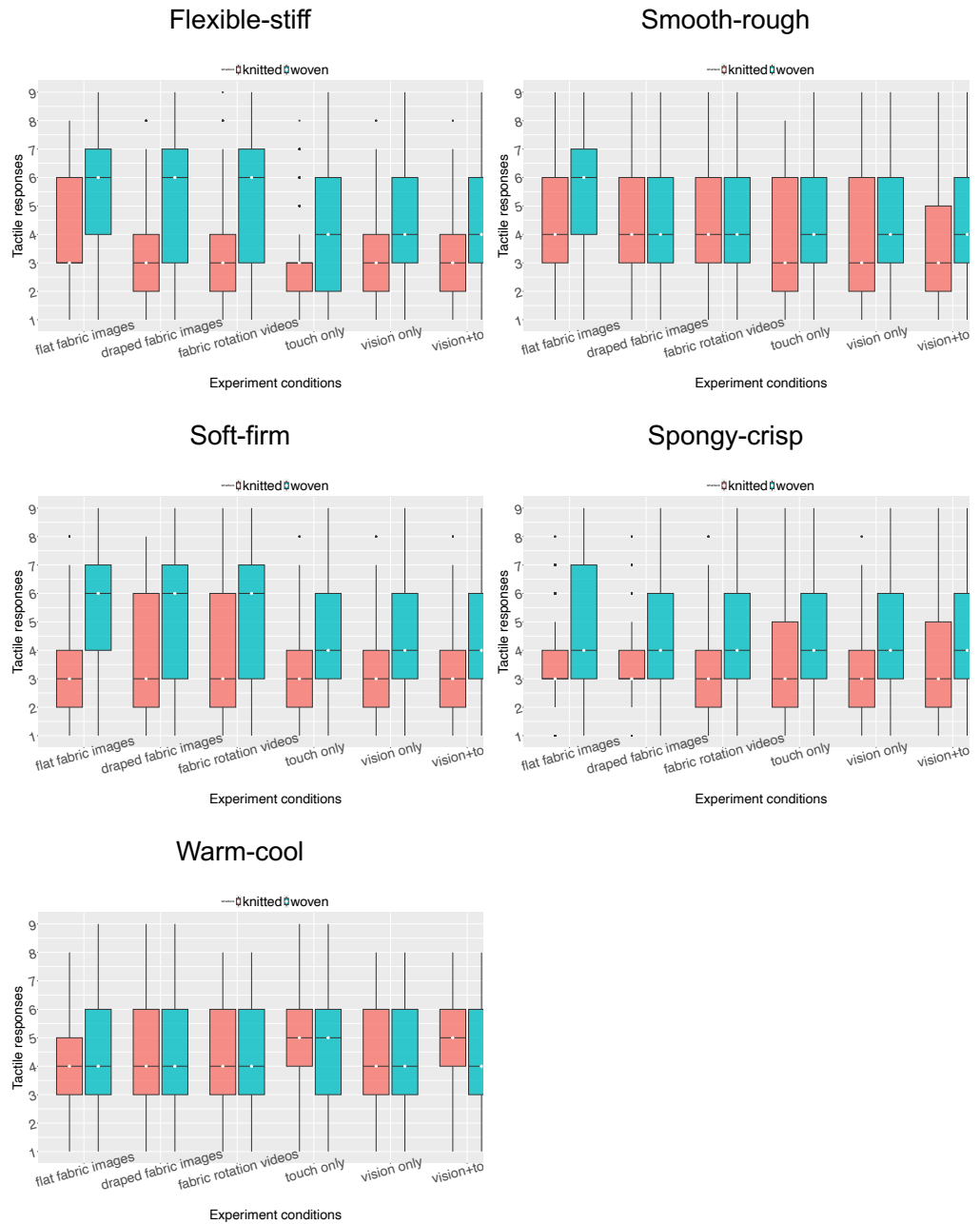


Figure 6.1 The distribution of the raw data for each pair of tactile properties under each experiment condition.

Table 6.2 The results of Mann-Whitney U test.

	Flexible- stiff	Smooth- rough	Soft-firm	Spongy- crisp	Warm-cool
Flat	$p < 0.001^{***}$	$p < 0.001^{***}$	$p < 0.001^{***}$	$p < 0.001^{***}$	p=0.19
Draped	$p < 0.001^{***}$	$p = 0.0029^{**}$	$p < 0.001^{***}$	$p < 0.001^{***}$	p=0.28
Video	$p < 0.001^{***}$	$p = 0.048^{*}$	$p < 0.001^{***}$	$p < 0.001^{***}$	p=0.43
Touch-only	$p < 0.001^{***}$	$p < 0.001^{***}$	$p < 0.001^{***}$	$p < 0.001^{***}$	$p = 0.0048^{**}$
Vision-only (using real	$p < 0.001^{***}$	$p < 0.001^{***}$	$p < 0.001^{***}$	$p < 0.001^{***}$	p=0.63

fabrics)					
Vision+touch	p<0.001***	p<0.001***	p<0.001***	p<0.001***	p=0.017*

6.4.2 The fixed effects and interaction of fabric structures and experiment conditions

CLMM models with and without interactions were compared. Equation 6.1 and Equation 6.2 list the fitting CLMM models with and without interactions. The comparison results of models between with and without interactions are shown in Table 6.3. For all tactile properties, the CLMM models with interactions outperformed the models without interactions. Smaller AIC values were observed in all models with interactions. The effect of interactions was significant for all tactile properties ($p<0.001^{***}$), indicating that the effects of fabric structures on the tactile perceptual ratings varied with the level of experiment conditions, and vice versa. Therefore, only CLMM models with interactions were fitted and analysed in Section 6.4.

With interactions: Tactile perceptual ratings= Equation 6.1

*structure * condition +*

(1|fabrics) + (1|observer)

Equation 6.2

Without interaction: Tactile perceptual ratings=

structure + condition +

(1|fabrics) + (1|observer)

Table 6.3 Comparisons between CLMM models with and without interactions (fabric structures*experiment conditions) for the experiment Phase II.

	no.par	AIC	logLik	LR.stat	p-values
Flexible-stiff					
With interactions	21	22255	-11106	52.436	p<0.001***
Without interactions	16	22297	-11133		
Smooth-rough					
With interactions	21	23434	-11696	43.078	p<0.001***
Without interactions	16	23467	-11718		
Soft-firm					

With interactions	21	23885	-11922	21.286	p<0.001***
Without interactions	16	23897	-11932		
Spongy-crisp					
With interactions	21	26233	-13095	24.813	p<0.001***
Without interactions	16	26247	-13108		
Warm-cool					
With interactions	21	22622	-11290	41.098	p<0.001***
Without interactions	16	22653	-11310		

Table 6.4 lists the fixed effects in the full CLMM models for all tactile properties. Rather than simply comparing the distribution of the tactile perceptual ratings in Section 6.4.1, the fixed effects reflected the overall effects of fabric structures, experiment conditions, and the interaction between structures and experiment conditions. For all fitted tactile perceptual ratings, both experiment conditions and the interaction had significant effects. The interaction indicated that the effect of structures on fitted tactile perceptual ratings was different when evaluated under different conditions, while the difference was limited due to the relatively lower χ^2 . In addition, the fitted flexible-stiff, smooth-rough, soft-firm, and spongy-crisp were significantly different between woven and knitted fabrics. For warm-cool, fabric structure had no significant effects. Detailed analyses of the interactions and the quantification of the difference between fabric structures and between experiment conditions were described in the next section.

Table 6.4 The fixed effects in all CLMM models and their significance for the experiment Phase II.

Fixed effects	χ^2	df	p
Flexible-stiff			
Structures	27.604	1	p<0.001***
Experiment conditions	544.259	5	p<0.001***
structures:experiment conditions	52.353	5	p<0.001***
Smooth-rough			
Structures	5.735	1	p=0.017*
Experiment conditions	354.002	5	p<0.001***
structures:experiment conditions	42.992	5	p<0.001***
Soft-firm			
Structures	36.191	1	p<0.001***
Experiment conditions	247.798	5	p<0.001***
structures:experiment conditions	21.311	5	p<0.001***

Spongy-crisp			
Structures	24.703	1	$p < 0.001^{***}$
Experiment conditions	24.828	5	$p < 0.001^{***}$
structures:experiment conditions	24.809	5	$p < 0.001^{***}$
Warm-cool			
Structures	0.003	1	$p = 0.956$
Experiment conditions	233.839	5	$p < 0.001^{***}$
structures:experiment conditions	41.011	5	$p < 0.001^{***}$

6.4.3 The fitted perceptual ratings for woven and knitted fabrics

The CLMM models were computed on the linear predictor scale initially and converted to original scale using Equation 4.4. Figure 6.2 shows the fitted perceptual ratings on the original scale.

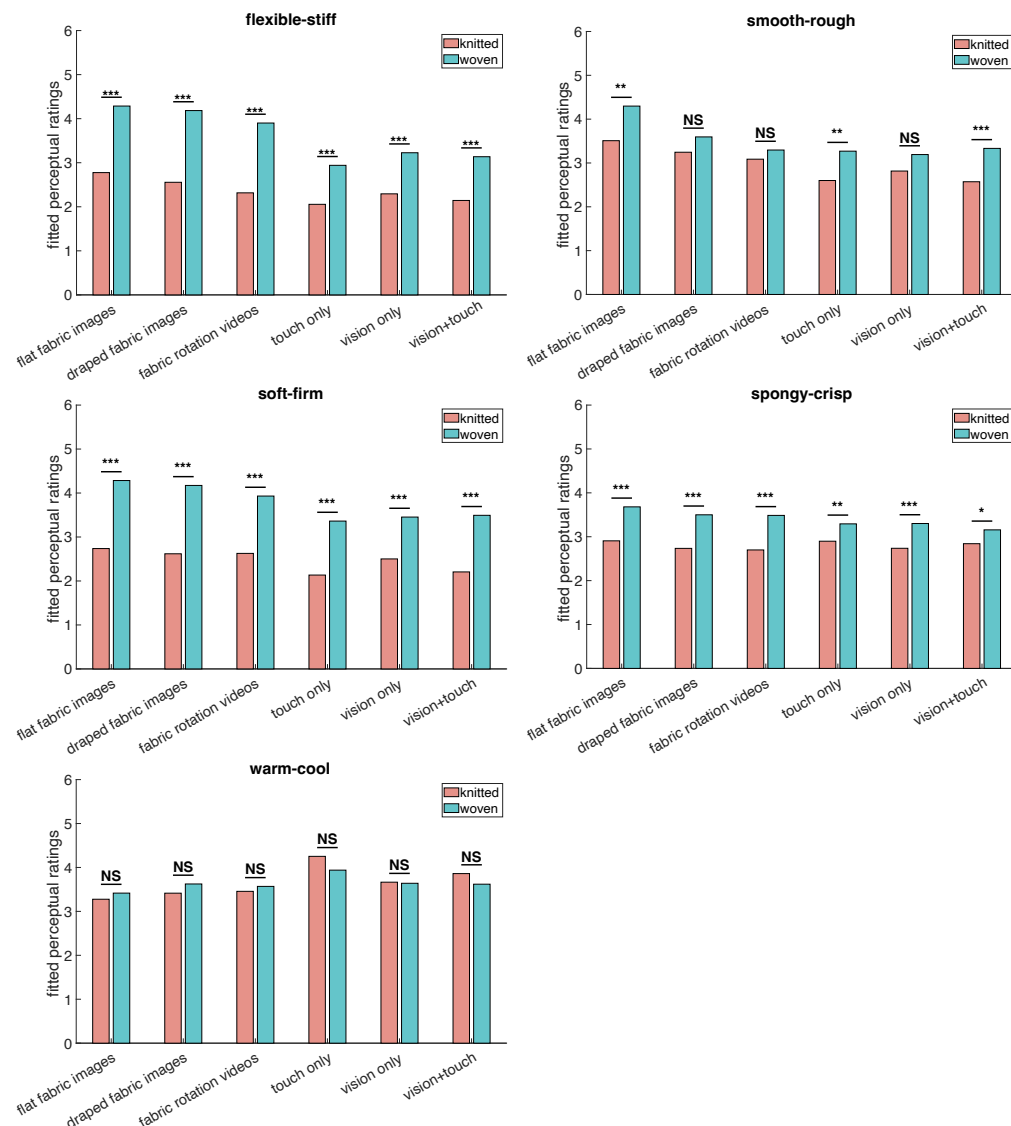


Figure 6.2 The comparisons of the fitted tactile perception between fabric structures.

Fabric structures showed statistically significant effects on the perceptual flexible-stiff, soft-firm, and spongy-crisp regarding experiment conditions ($p < 0.001^{***}$), which is almost consistent with the non-parametric tests comparing the distribution of woven and knitted fabrics in Table 6.2. The only differences are the significance levels, which were reduced when assessing spongy-crisp under touch-only and vision+touch conditions. In addition, after setting the fixed effects and random effects in the CLMM models, the differences of the perceptual smooth-rough between using woven and knitted fabrics were no longer significant when viewing the draped fabrics (experiment conditions: draped fabric images, fabric rotation videos, vision-only using real fabrics). The non-significances between using woven and knitted fabrics were observed for the perception of warm-cool under all experiment conditions.

Apart from the significances, Figure 6.2 illustrates the magnitude comparisons between fabric structures across experiment conditions. NS means non-significant. The fitted perceptual ratings of flexible-stiff, smooth-rough, soft-firm, and spongy-crisp are always higher when woven fabrics were used. Woven fabrics were perceived as stiffer, rougher, firmer, and crisper than knitted fabrics, regardless of the experiment conditions. On the other hands, the fitted perceptual warm-cool are slightly lower when real woven fabrics were used, but slightly higher when visual representations of woven fabrics were used. Real woven fabrics were generally perceived as warmer, whereas woven fabric images and videos were perceived as cooler.

Moreover, the fitted perceptual ratings of flexible-stiff, smooth-rough, and soft-firm were relatively higher under the conditions of images and videos, whereas the warm-cool showed comparatively lower ratings under the same conditions. Fabrics were fitted as stiffer, rougher, firmer, and warmer under the conditions of fabric images and videos, whereas they were more flexible, smoother, softer, and cooler when observing and touching the real fabrics. These findings agreed with the observers' perception as described in the last Chapter, Section 5.7.

As described above, woven fabrics were fitted to higher scores than knitted fabrics under all experiment conditions, except for the perception of warm-cool. The differences of the perceptual ratings between woven and knitted fabrics were computed and illustrated in Figure 6.3. Positive values indicate higher perceptual ratings of woven fabrics, and negative values indicate higher perceptual ratings of knitted fabrics.

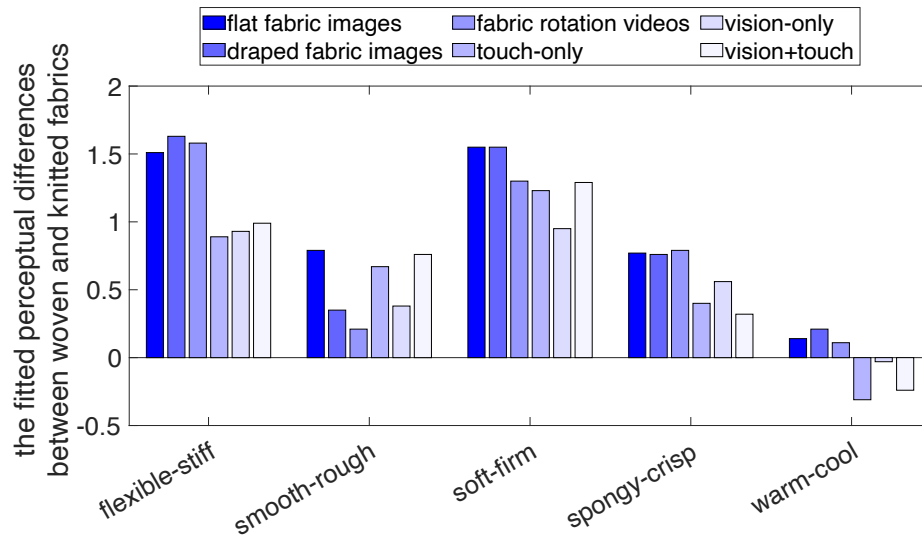


Figure 6.3 Quantified differences of the fitted perceptual ratings between woven and knitted fabrics for all tactile properties under each experiment condition.

When using fabric visual representations to judge flexible-stiff, soft-firm, and spongy-crisp, the fitted perceptual differences between woven and knitted fabrics were greater compared to that using real fabrics. Woven and knitted fabrics exhibited bigger tactile perception differences when presented digitally. For the fitted perceptual smooth-rough, when the fabrics were draped (experiment conditions: draped fabric images, fabric rotation videos, vision only), the differences between woven and knitted fabrics were smaller than that when fabrics were in flat condition or in palm (touch-only, vision+touch). For warm-cool, the fitted perceptual differences between woven and knitted fabrics were the smallest among the five pairs of tactile properties, within 0.5 units in the original scale.

The maximum difference was to assess flexible-stiff using draped fabric images,

with woven fabrics being fitted 1.63 units higher than knitted fabrics on the original scales. Woven fabrics were fitted to 4.29 units, and knitted fabrics were fitted to 2.78 units (see Figure 6.2). Given the meaning assigned to each point in the 9-points Likert scale (Section 3.4.2), 2 is *very much flexible*, 3 is *moderately flexible*, and 4 is *slightly flexible*. Even though significant perceptual differences were statistically observed by the pairwise comparison in Figure 6.2, whether the significant would remain in a practical sense depends on individuals.

6.5 The effects of measured fabric colours on the tactile perception

CLMM models with and without interactions were fitted and compared firstly for each pair of tactile properties assessed under the conditions of touch-only, vision-only (using real fabrics), vision+touch. Equation 6.3 and Equation 6.4 provide the formulas for the CLMM models, and the comparison results were listed in Table 6.5. Models with interactions allow all interactions between fabric structures, experiment conditions, and the measured colours, and models without interactions excluded the three-way interactions but remain the two-way interactions of fabric structures and experiment conditions. For all tactile properties, models without interaction outperformed the models with three-way interaction, indicated by the lower AIC values and non-significant p-values. The non-significant three-way interaction of *fabric structures:experiment conditions:measured colours* (L^* , a^* , b^*) indicated that the effect of fabric colours on the fitted perceptual tactile ratings is independent of the subgroups of fabric structures and experiment conditions. Therefore, only CLMM models without interactions were analysed in this section.

With interaction	Tactile perceptual ratings=	Equation
	$structures * conditions * L +$	6.3
	$structures * conditions * a +$	

$$structures * conditions * b +$$

$$(1|fabrics) + (1|observers)$$

Without interaction Tactile perceptual ratings=

Equation
6.4

$$structures * conditions + L * + a * + b * +$$

$$(1|fabrics) + (1|observers)$$

Table 6.5 Comparisons between CLMM models with and without three-way interactions for the experiment Phase II.

	no.par	AIC	logLik	LR.stat	p-values
Flexible-stiff					
With interactions	33	10460	-5197.2	18.69	p=0.228
Without interactions	18	10449	-5206.5		
Smooth-rough					
With interactions	33	11428	-5681.2	21.04	p=0.136
Without interactions	18	11419	-5691.7		
Soft-firm					
With interactions	33	11576	-5755.1	24.021	p=0.065
Without interactions	18	11570	-5767.2		
Spongy-crisp-6589					
With interactions	33	13262	-6589.1	7.829	p=0.931
Without interactions	18	13240	-6602.1		
Warm-cool					
With interactions	33	11137	-5535.6	20.21	p=0.164
Without interactions	18	11127	-5545.7		

Table 6.6 lists the models' parameter estimates on the original scales and significant levels of L^* , a^* , and b^* for all tactile properties. Only a few showed statistically significant effects, for example, for every 1 unit increase in L^* , the fitted perceptual flexible-stiff decreased by 0.02 units in the 9-point Likert scale. However, for all tactile properties, parameter estimates were very close to 0, indicating a limited role of colour in tactile perception.

Table 6.6 CLMM models parameter estimates of the fixed effects L^* , a^* , and b^* .

	L^*	a^*	b^*
Flexible-stiff	$\beta_L = -0.02, p=0.008^{**}$	$\beta_a = -0.00, p=0.74$	$\beta_b = 0.02, p=0.07$
Smooth-rough	$\beta_L = -0.01, p=0.07$	$\beta_a = -0.02, p=0.02^*$	$\beta_b = 0.02, p=0.03^*$

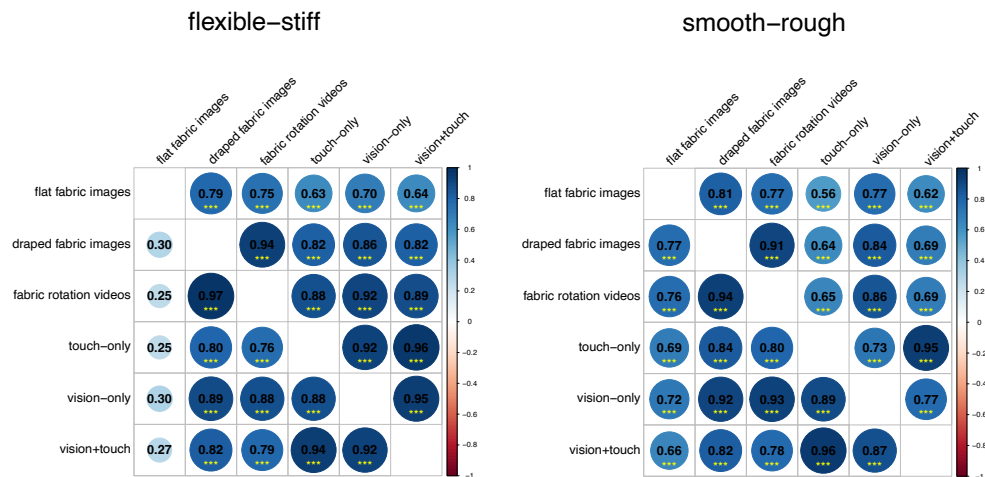
Soft-firm	$\beta_L = -0.02$, $p = 0.02^*$	$\beta_a = -0.01$, $p = 0.61$	$\beta_b = 0.02$, $p = 0.05$
Spongy-crisp	$\beta_L = -0.00$, $p = 0.71$	$\beta_a = 0.01$, $p = 0.21$	$\beta_b = 0.00$, $p = 0.68$
Warm-cool	$\beta_L = 0.02$, $p = 0.04^*$	$\beta_a = 0.01$, $p = 0.23$	$\beta_b = -0.01$, $p = 0.23$

6.6 The different correlations for woven and knitted fabrics

In previous sections, tactile properties, except for warm-cool, were perceived differently between woven and knitted fabrics, and the fitted differences between woven and knitted fabrics were provided. Whether the correlations among experiment conditions differ between woven and knitted fabrics, and whether the correlations among tactile properties differ between woven and knitted fabrics are evaluated in this section.

6.6.1 The correlations of the tactile perception among experiment conditions for woven and knitted fabrics, respectively

Figure 6.4 compares the correlations among experiment conditions between woven fabrics (above diagonal) and knitted fabrics (below diagonal). Differences were observed for flexible-stiff, soft-firm, and spongy-crisp.



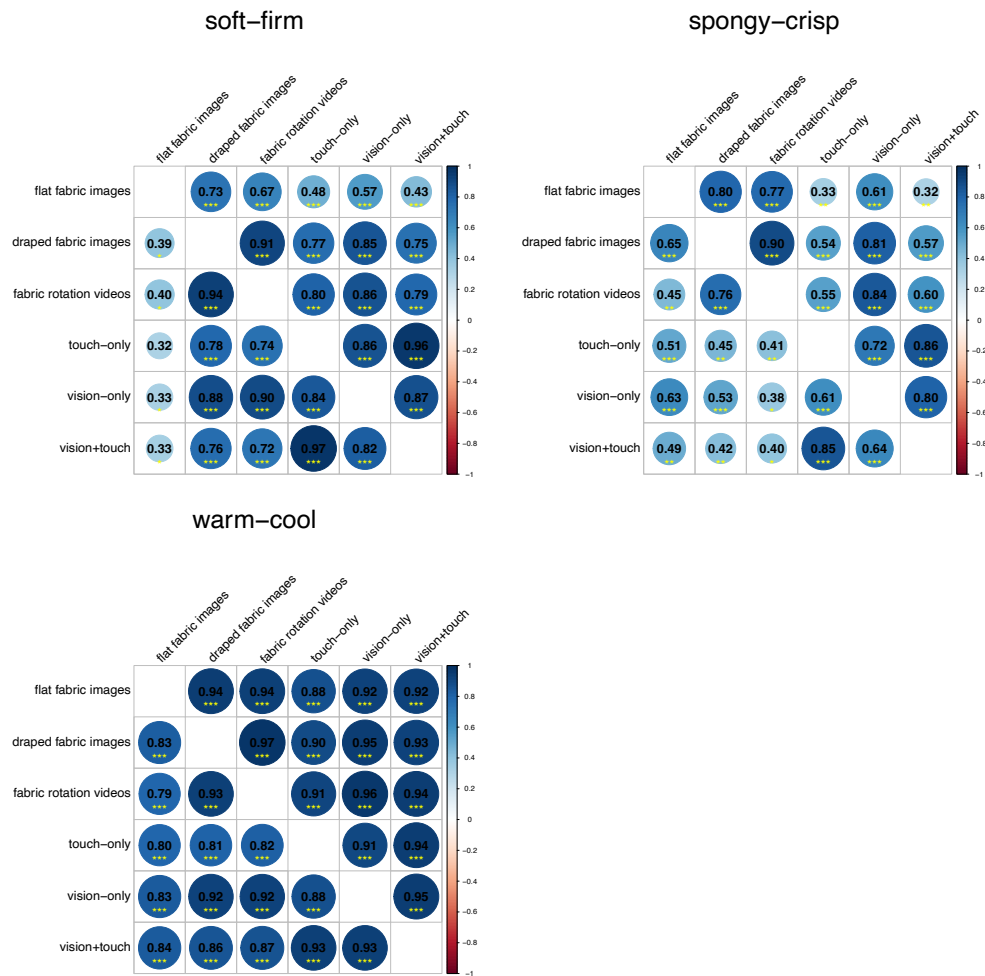


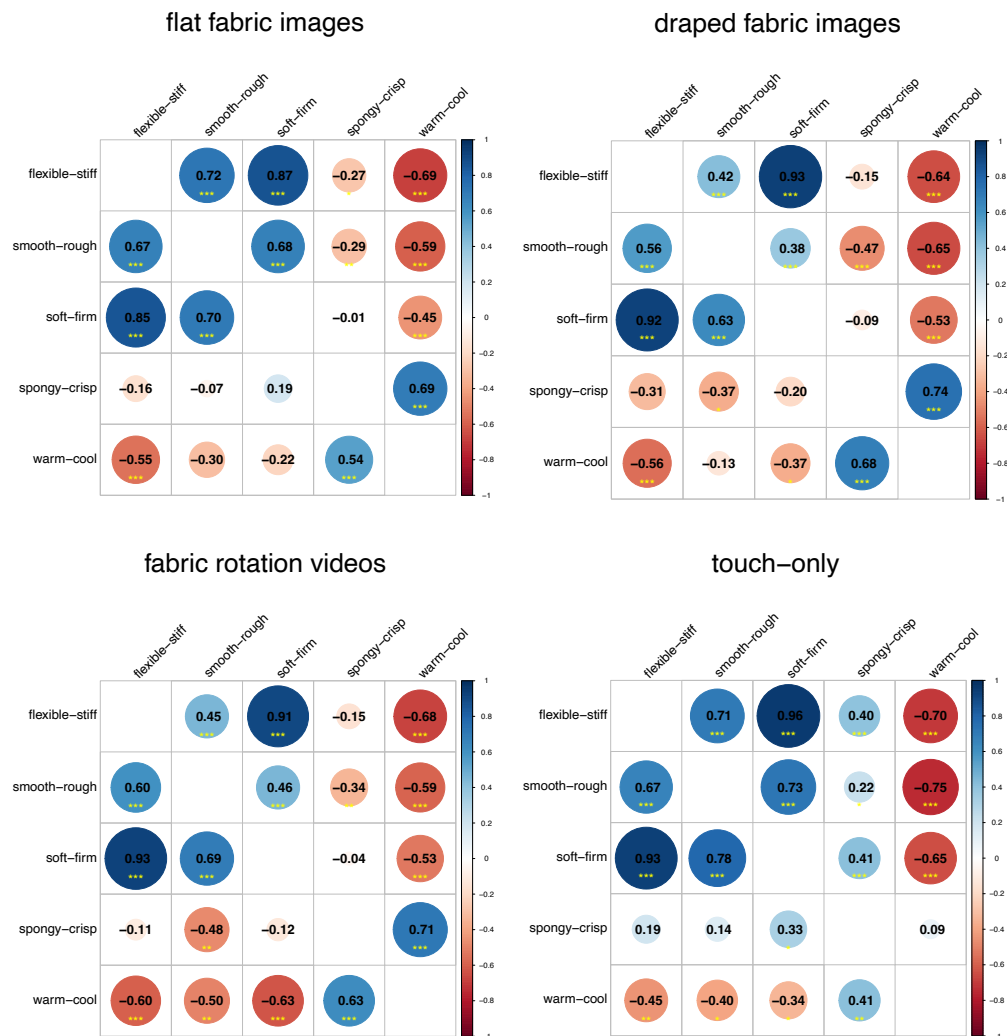
Figure 6.4 The correlations among experiment conditions for each pair of tactile properties. Above diagonal: woven fabrics. Below diagonal: knitted fabrics.

For the perception of flexible-stiff, positive and significant correlations were observed between using flat fabric images and other conditions for woven fabrics ($r > 0.63$, $p < 0.001^{***}$), while the correlations were no longer significant for knitted fabrics ($r < 0.30$, $p > 0.05$). Similar regularity was observed for the perception of soft-firm, where both the Pearson correlation coefficients and significance levels between flat fabric images and other experiment conditions were notably higher for woven fabrics but showed a clear decrease for knitted fabrics. For the perception of spongy-crisp, the correlation of tactile perception between using fabric rotation video and using vision-only condition (using real fabrics) was highly positive and significant for woven fabrics ($r = 0.84$, $p < 0.001^{***}$). The r value was decreased to 0.38 for knitted fabrics and the significance level

decreased as well. In addition to the differences, the perceived smooth-rough and warm-cool showed similar correlations among experiment conditions between woven and knitted fabrics.

6.6.2 The correlations among tactile perceptions under each experiment condition for woven and knitted fabrics, respectively

Figure 6.5 compares the correlations among tactile perceptions for each experiment conditions between woven (above diagonal) and knitted fabrics (below diagonal). The correlations were generally consistent between woven and knitted fabrics, while discrepancies were also observed under specific condition.



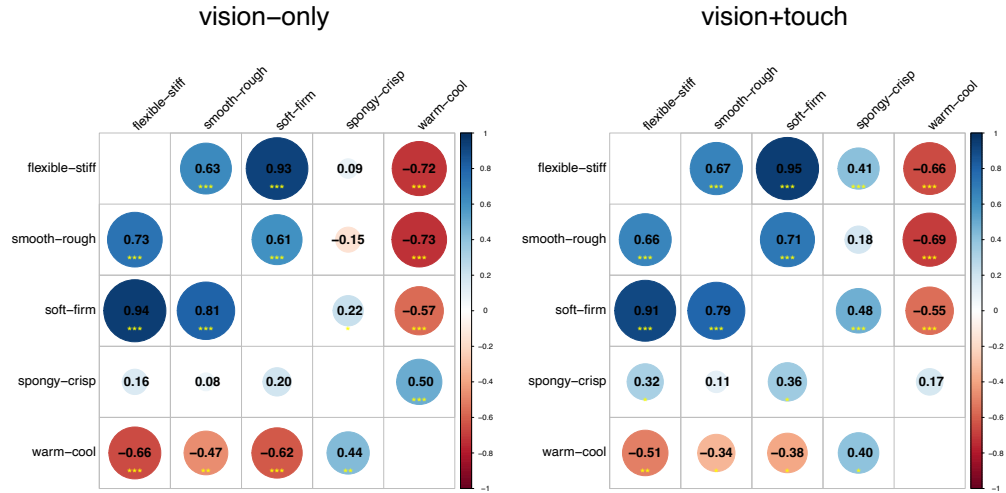


Figure 6.5 The correlations among tactile properties under each experiment condition. Above diagonal: woven fabrics. Below diagonal: knitted fabrics.

Discrepancies included the correlations between specific tactile properties under the condition of flat fabric images, draped fabric images, touch-only, and vision+touch. When perceiving through flat fabric images, the correlation between spongy-crisp and smooth-rough was weak but significant for woven fabrics ($r=-0.29^{**}$). For knitted flat fabric images, the two pairs of tactile properties were nearly uncorrelated ($r=-0.07$, $p>0.05$). When perceiving through draped fabric images, significant correlation was observed between smooth-rough and warm-cool for woven fabrics ($r=-0.65$, $p<0.001^{***}$), while no such correlation was observed for knitted fabrics ($r=-0.13$, $p>0.05$). In contrast, the correlations between warm-cool and spongy-crisp when only touch ($r=0.41^{**}$) or both vision and touch were allowed ($r=0.40^{*}$) were significant for knitted fabrics, while not for woven fabrics. In addition to the discrepancies, the other correlations among tactile properties were consistent between woven and knitted fabrics.

6.7 Discussion

6.7.1 The different perception of fabric tactile properties in woven and knitted fabrics

In the full CLMM models, significant differences were observed in the fitted

perceptual ratings between woven and knitted fabrics. Generally, woven fabrics were fitted as stiffer, rougher, firmer, and crisper than knitted fabrics under all experiment conditions. By analysing the correlations among experiment conditions and among tactile properties, both consistencies and discrepancies were observed between woven and knitted fabrics. Possible explanations of the discrepancies are the structure differences and the mechanical properties between woven and knitted fabrics. The woven fabrics normally exhibited higher Young's Modulus, as well as higher bending and shear moduli than knitted fabrics (Ji et al, 2006). Young's Modulus describes the linear relationship between stress and strain, indicating the stiffness of the fabric when exposed to stretching or compression. A higher Young's Modulus means that the fabric is resistant to being stretched or compressed. Bending Modulus reflects the fabric's capacity to retain its shape when bent, with higher values reflecting greater rigidity. Shear Modulus measures the resistance to deformation when exposed to shear force. With a higher value of shear modulus, fabric is more resistant to stretching and distortion under shear forces.

These mechanical properties explain the findings that woven fabrics were fitted as stiffer, firmer, and crisper in the present study. As trained prior to the experiment, flexible-stiff was rated based on the drapability and soft-firm was rated based on squeezing. If the fabric freely draped over the hand and the contour of the hand cannot be clearly seen, the fabric was considered as stiffer. If the fabric resisted to the force from palm, it was considered as firmer. Woven fabrics exhibited Young's Modulus and higher bending modulus, making them more resistant to draping and compression than knitted fabrics. Therefore, it is reasonable that woven fabrics were fitted as stiffer and firmer in the CLMM model. In addition, a criterion for rating spongy-crisp was that if creases were shown after squeezing the fabric, then it was considered as crisper. Knitted fabrics, due to their flexibility and lower resistance to compression and bending, adapted to external forces by smoothly reshaping without forming creases. In

contrast, woven fabrics, which were stiffer, tend to form creases to against the external force.

Moreover, a possible explanation of smooth-rough can be the interlaced structure of woven fabrics and interloped structure of knitted fabrics (Breen and House, 2000). The criterion for smooth-rough was to touch the fabric surface and evaluate the resistance felt during hand movement. In woven fabrics, the warp and weft yarns were crimped and perpendicularly interlaced together, forming textured elements at the surface. As the palm touching the surface of the fabrics, the distinct bumps may enhance the perception of roughness. In contrast, knitted fabrics consist of interloped yarns with fewer distinct bumps and a rich network of loops. When touching the surface of the fabrics, the hand tends to move along the curved loop, contributing to a smoother tactile perception.

6.7.2 The practical effect of colour based on CLMM models on the tactile perception

In Chapter 4, the effect of colour on visual-tactile perception through flat and draped fabric images was analysed. Colour played no role in the visually perceived flexible-stiff, smooth-rough, soft-firm, and spongy-crisp, but affected the perception of warm-cool. In this Chapter, the effect of colour was further analysed on the tactile perception through vision-only (using real fabrics), touch-only, and vision+touch. As discussed in previous chapters, the effect of colour on the perception of tactile properties was evaluated using either real fabrics (Atav and Keskin, 2024; Fenko et al., 2010; Yenket et al., 2007), or by matching fabric images and real fabrics (Xiao et al., 2016). Compared to these studies, the present study provided a comprehensive understanding of the effect of colour on the perception of tactile properties through both images and real fabrics. The effect of colour was firstly quantified in the uniform CIE LAB colour space and reflected into the categorical scale. In this way, for two fabric images

or two real fabrics, whether colour leads to a difference in tactile perception can be simply compared in the 9-point scale.

6.8 Summary

In this Chapter, a further exploration of visual-tactile and tactile perception was provided by fitting CLMM models. As significant differences were observed in the fitted tactile perceptual ratings between woven and knitted fabrics, the correlations of tactile perceptual ratings were analysed for woven and knitted fabrics, respectively. A summary of the major findings is listed below:

- The distributions of the tactile perceptual ratings were compared between woven and knitted fabrics under all experiment conditions. Significant differences were observed for all tactile properties except for warm-cool.
- Full CLMM models with interaction between fabric structures and experiment conditions were fitted. In addition to the differences between woven and knitted fabrics, it is found that woven fabrics were generally fitted as stiffer, rougher, firmer, and crisper than knitted fabrics under all experiment conditions, and as cooler than knitted fabrics only when images and videos were used.
- The effect of fabric colour on tactile perception was quantified in the CLMM models. Despite the statistical significance, colour played a very limited role in perceiving tactile properties through actual touching and observing.
- Both consistencies and discrepancies were observed between woven and knitted fabrics regarding the correlation analyses. For woven fabrics, flexible-stiff and soft-firm perceived from flat fabric images correlated well with those from other conditions, while no significant correlations were observed for knitted fabrics. The correlations among specific tactile perceptual ratings under the condition of flat fabric images, draped fabric images, touch-only, and vision+touch were different for woven and knitted

fabrics as well.

Chapter 7

Modelling the visual-tactile and tactile perception

7.1 Overview

In this Chapter, efforts were made on modelling the visual-tactile and tactile perception through fabric images and videos. Different categories of predictors were directly extracted from flat fabric images, draped fabric images, and images generated from fabric rotation videos (Section 7.2). The model development processes, including the input and output selection, regression methods, and training and testing procedures were introduced in Section 7.3. Comparisons of the model performance were conducted in Section 7.4, focusing on the performance between regression techniques, predictive accuracy between target conditions and tactile properties. As both EN and LASSO regression techniques involve variable selection during modelling, predictors were ranked based on the absolute standardised coefficients to evaluate the importance of predictors in Section 7.5. In addition to predictors from fabric images and videos, fabric thickness, which was found to be associated with tactile properties in previous chapters, was one of the predictors to model tactile perception. Comparisons were made between models with and without thickness in variables, reported in Section 7.6.

7.2 Feature extraction

Four categories of features were extracted from fabric images and videos: fabric draped width (Section 7.2.1 and 7.2.2), spatial distribution of grey levels (Section 7.2.4), features in frequency domain (Section 7.2.5), and features in frequency and time domain (Section 7.2.6). For fabric rotation videos, extracting features from all video frames will be time and energy consuming. Horizontal space-time slices, inspired by Bouman et al. (2013), were generated for all fabric rotation videos and used to extract fabric draped width and (Section 7.2.1). Additionally, similar to horizontal space-time slices, time-space slices were also generated and used to represent the 3D appearance of the rotating draped fabrics to extract other features (Section 7.2.3).

7.2.1 Fabric draped width extracted from fabric rotation videos

When fabrics were draped freely over the stand, different shapes can be observed from the camera's position when recording the fabric rotation videos, induced by the fabric folds. Fabrics that draped closely to the stand are typically more flexible and softer. Horizontal space*time slices were generated for all the fabric rotation videos. The process is shown in Figure 7.1.

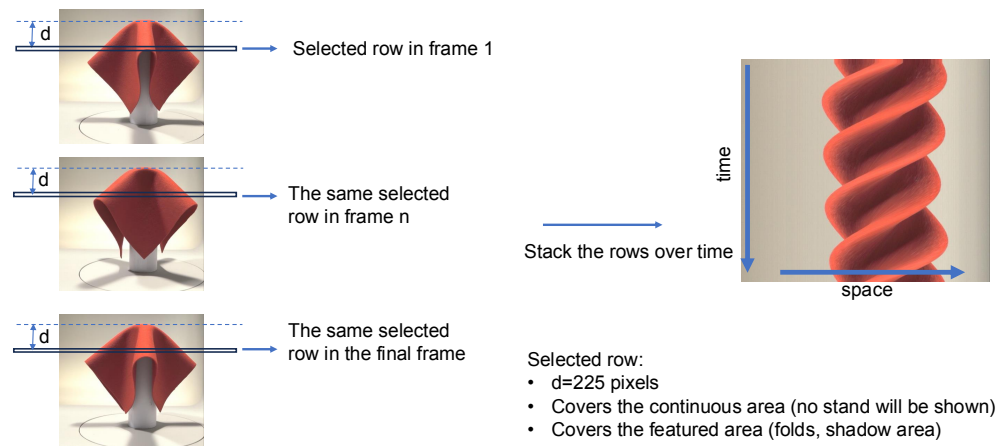


Figure 7.1 space*time slice with space on the horizontal axis and time on the vertical axis.

For each frame in the video, a row of pixels located 225 pixels from the top of the fabric was extracted. For all the fabric rotation videos in Leeds Fabric Tactile Database Part II, to prevent the stand portion being extracted and cover the features of folds and shadows, d was set to 225 pixels. The rows of pixels were then stacked over time, and thus the number of pixels in the vertical axis of the space*time slice are equal to the total number of frames in the videos. The space*time slice was generated for each fabric rotation video, representing the varying fabric draped width at the specific location over time.

The fabric area in the space*time slice was masked out using colour thresholds. The boundary of the fabric area was shown in green in Figure 7.2. For each row in the space*time slices, the number of pixels of the fabric area within the boundary were computed, denoted as n_1 . A separate video was recorded for the stand, and the width of the stand was computed by calculating the number

of pixels at the specific location where space*time slices were generated, denoted as n_2 . The ratio between n_1 and n_2 was computed for all rows in the space*time slices. The durations of fabric rotation videos were not perfectly equal, so the heights of the space*time slices were not exactly equal. The fabric draped width in fabric rotation videos was defined by the average ratio across the total number of frames.

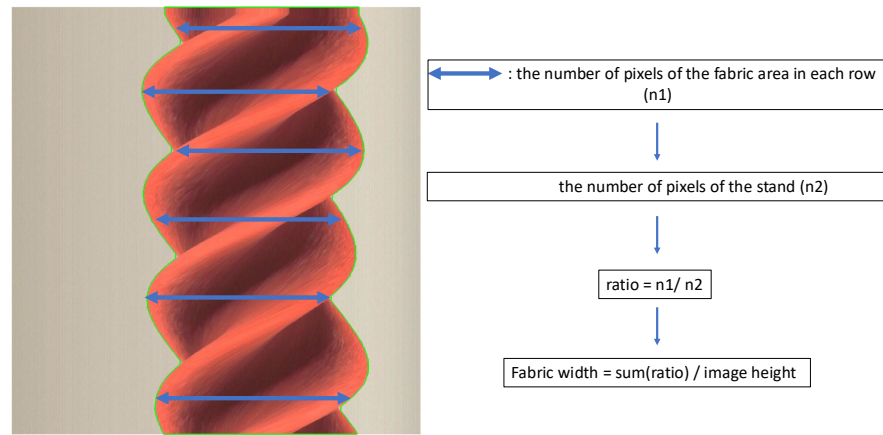


Figure 7.2 Computing the fabric draped width in fabric rotation videos.

7.2.2 Fabric width for draped fabric images

In Figure 7.2, the fabric width varies in each frame in the fabric rotation videos. Draped fabric images (drape_0) were the first frame extracted from fabric rotation videos. Therefore, the ratio of n_1/n_2 of the first row was taken as the fabric draped width for draped fabric images. Higher values of fabric width mean that the fabric draped farther away from the stand, while lower values mean that the fabrics draped closer to the stand.

7.2.3 Fabric 3D appearance

In Section 7.2.1, the space*time slices captured limited area of the fabric in the videos. Inspired by that, time*space slices were generated where x-axis represents time and y-axis represents space, and the process is shown in Figure 7.3. One column in the middle of the stand, located 1260 pixels from the

left, was extracted from all frames of the fabric rotation videos. The columns were stacked over time, and thus time was set on the horizontal axis, and space was set on the vertical axis. The number of pixels in the horizontal axis of the time*space slice was equal to the total number of frames of the fabric rotation videos. The draped fabric 3D appearances were thus displayed in the time*space slices, which were used to extract features to predict the visual-tactile and tactile perception through fabric rotation videos.

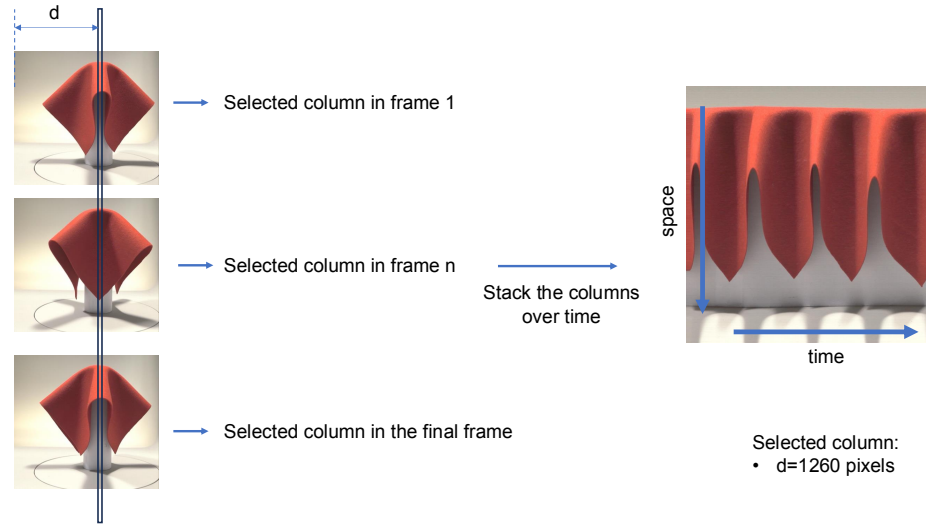


Figure 7.3 time*space slice with time on the horizontal axis and space on the vertical axis.

7.2.4 Grey-level Co-occurrence matrix (GLCM)

The concept of GLCM has been introduced in Chapter 2, Section 2.9.1. For each image, GLCMs were computed in four orientations and set the distance of 1, and five GLCM-based features (contrast, correlation, energy, homogeneity, entropy) were computed from each GLCM. The final values of the five GLCM-based features were then obtained by averaging the values across four orientations, forming the GLCM-based feature set as in Equation 7.1. GLCM is computed using *graycomatrix* function in MATLAB.

$$GLCM - based\ feature\ set = \{$$

$$GLCM_{contrast},$$

Equation 7.1

$$GLCM_{correlation},$$

$$GLCM_{energy},$$

$$GLCM_{homogeneity},$$

$$GLCM_{entropy}\}$$

For flat fabric images in Leeds Fabric Tactile Database, the GLCM-based features were directly computed by converting the RGB images to greyscale images. For fabric rotation videos, it will be time and energy consuming if the calculation was carried out for each frame. Time*space slices generated in Section 7.2.3, showing the fabric 360-degree draped appearance, were used to generate GLCM for each fabric rotation video. Figure 7.4 shows the processes to generate GLCM for draped fabric images and time*space slides. To reduce the effects of background area on computing GLCM features, masks were developed firstly for all draped fabric images and time*space slices by colour thresholds, remaining fabric areas while excluding the background (RGB set to 0). RGB images were then converted to greyscale images with the greyscale range set between 0 and 255. The background areas with RGB values of 0 were thus had a greyscale value of 0. Before generating GLCM, the fabric areas were checked to ensure that no pixel had a greyscale value of 0. The GLCM were then generated by computing the spatial distribution of greyscale values from 1 to 255, excluding the background area and the edge between the background and fabric area.

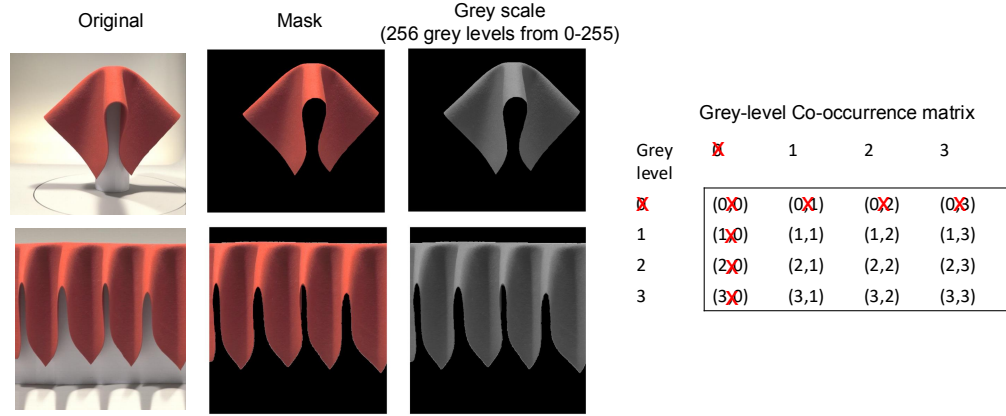


Figure 7.4 Computing GLCM features for draped fabric images and time*space slices. 'X' in red means excluding the grey level 0 in GLCM.

7.2.5 2D Fast Fourier Transform (2D FFT)

The image can be transformed from the spatial domain to frequency domain by applying 2D FFT. The basic concepts of 2D FFT has been provided in Chapter 2, Section 2.9.2. The transformation was conducted by *fft2* function in MATLAB firstly and by *fftshift* function to move the lowest frequency to the centre of the matrix. Two sets of features were computed directly from the frequency spectrum: the total spectrum energy across the whole spectrum defined in Equation 7.2, and the total spectrum energy of sub-bands by applying band filters defined in Equation 7.3 (Wang et al., 2020).

$$2D\ FFT_{totalEn} = \sum_{u=0}^{M-1} \sum_{v=0}^{N-1} F^2(u, v) \quad \text{Equation 7.2}$$

$$2D\ FFT_{bandwidth} = \sum_{u=0}^{M-1} \sum_{v=0}^{N-1} F^2(u, v) * h_n(u, v), \quad \text{Equation 7.3}$$

$$h_n(u, v) = \begin{cases} 0, & \text{when } D_n - \frac{w}{2} \leq D(u, v) \leq D_n + \frac{w}{2} \\ 1, & n = 1, 2, \dots, N \end{cases}$$

where $F^2(u, v)$ calculates the frequency spectrum energy, $h_n(u, v)$ is the band filter, w is the band width, N is the number of band filters, and D_n is the diameter of the n^{th} band filter. Given the image size, the width of band filter was decided as 150 in the present study.

In addition, another two sets of features were estimated from the frequency spectrum: the fractal dimension and the slope. The fractal dimension is a parameter to quantify the complexity of irregular textures. The method of power spectrum estimation is an accurate method to compute the fractal dimension, as defined in Equation 7.4 (Wang and Georganas, 2009).

$$p(\omega) \propto \omega^{-\beta}$$

$$FD = \frac{8 - \beta}{2}$$

Equation 7.4

where $p(\omega)$ is the power spectrum of radial frequency ω , indicating a power-law relationship between the power spectrum and the radial frequency. Inspired by that, the slope of the frequency spectrum was calculated to indicate the rate at which the spectrum energy declines with the increasing frequency. A higher slope means smoother and fewer details in an image, and a lower slope means more detailed textures.

Overall, the 2D FFT feature set is defined Equation 7.5. For flat fabric images in the Leeds Fabric Tactile Database, the 2D FFT feature set was computed directly, by converting the RGB images to greyscale images. For draped fabric images and time*space slices, the background areas were firstly cropped by identifying the top, bottom, right, and left boundaries of the fabric area, ensuring a maximum removal of background. The 2D FFT was then applied to the cropped draped fabric images and time*space slices to compute the feature set.

$$\begin{aligned} & \text{2D FFT feature set} \\ &= \{2D\ FFT_{totalEn}, 2D\ FFT_{bandwidth}, 2D\ FFT_{FD}, 2D\ FFT_{slope}\} \end{aligned}$$

Equation 7.5

7.2.6 Wavelet transform (WT)

Wavelet transform captures the frequency and time information of an image. In Chapter 2, 2.9.3, the principle of image WT decomposition was described. Figure 7.5 visualised one draped fabric image in the Leeds Fabric Tactile Database Part II during WT decomposition using the *haar* mother wavelet,

which was processed by *wavedec2* function in MATLAB. Wavelet coefficients of each direction and each level were computed using *detcoef2* function in MATLAB. The correlations between wavelet coefficients and the tactile perceptual ratings were significant from level 1 to level 6, which are described in Section 7.3.2 and shown in Figure 7.6. Therefore, all images were decomposed to level 6, and no further decomposition was performed.

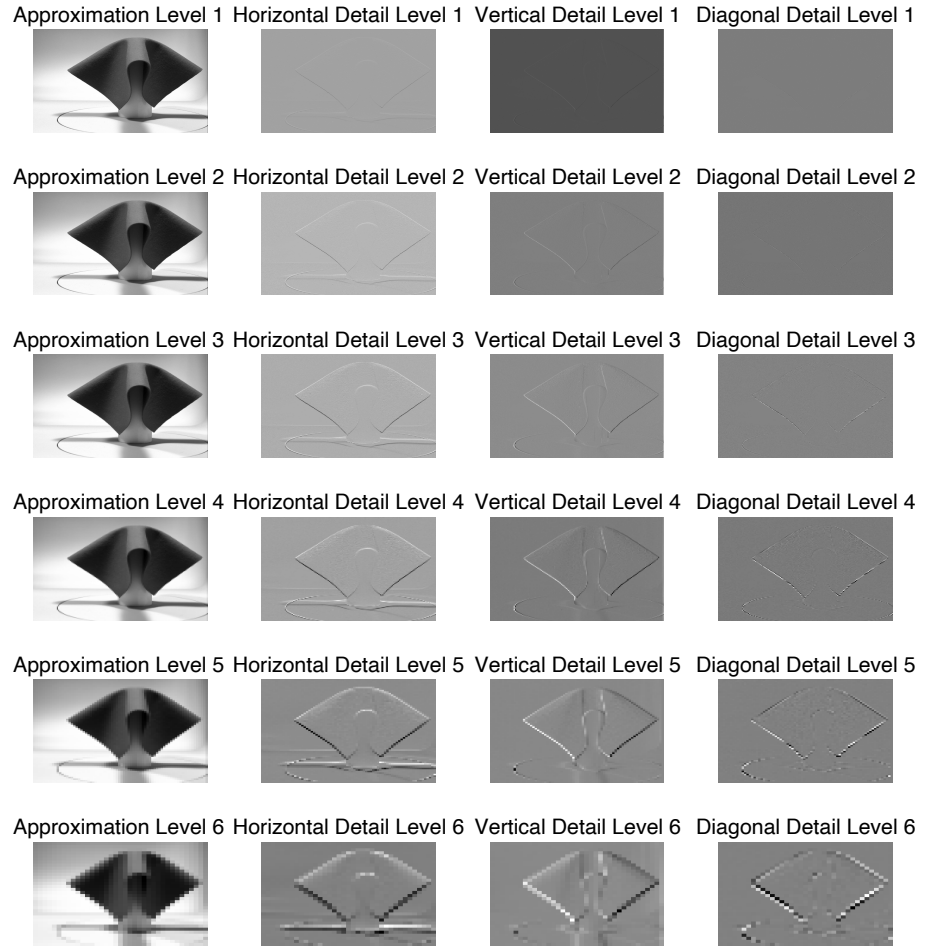


Figure 7.5 An example of the draped fabric image after WT decomposition up to level 6.

Inspired by Sun (2012), two features were computed as the WT based predictors: energy (E_n) and contrast (C_n). For each direction, the energy and contrast were computed as defined in Equation 7.6 and Equation 7.7. The energy and contrast for each level were the sum of values in each direction, generating the wavelet transform based feature set as defined in Equation 7.8. The computations were conducted in MATLAB.

$$E_n(d) = \frac{1}{M \times N} \sum_{i=1}^M \sum_{j=1}^N C_{ld}(i, j)^2$$

$$L_l E_n = E_n(H_l) + E_n(V_l) + E_n(C_l) \quad \text{Equation 7.6}$$

$$C_n(d) = \frac{1}{M \times N} \sum_{i=1}^M \sum_{j=1}^N |C_{ld}(i, j) - \text{Mean}(ld)|$$

$$L_l C_n = C_n(H_l) + C_n(V_l) + C_n(C_l) \quad \text{Equation 7.7}$$

where $M \times N$ is the size of greyscale image to be decomposed, l represents level, d represents the direction (H: horizontal, V: vertical, or C: diagonal), $C_{ld}(i, j)$ are the wavelet coefficients of decomposed images, $\text{Mean}(ld)$ is the average coefficients at level l and direction d .

$$\text{WT based feature set} = \{WT_{L_1-E_n}, WT_{L_1-C_n}, \dots, WT_{L_6-E_n}, WT_{L_6-C_n}\} \quad \text{Equation 7.8}$$

For flat fabric images in the database, the WT based features can be directly computed by converting the RGB images to greyscale images. For draped fabric images and time*space slices, the background areas were firstly cropped by identifying the top, bottom, right, and left boundaries of the fabric area, ensuring a maximum removal of background. The cropped draped fabric images and time*space slices were then decomposed, and the corresponding WT based features were computed.

7.3 Modelling procedure

7.3.1 Dependent variables and the corresponding predictors

Table 7.1 lists the models developed for predicting the visual-tactile and tactile perception under several conditions and the corresponding predictors. Models were built for flexible-stiff, smooth-rough, soft-firm, spongy-crisp, and warm-cool perceived under the conditions of flat fabric images (model 1), draped fabric images (model 2), fabric rotation videos (model 3), and vision+touch (model 4, 5, and 6), respectively. Image features from flat fabric images were used as predictors predicting visual-tactile perception under flat fabric images condition, and the same applied to draped fabric images and fabric rotation videos. For

predicting the tactile perception perceived through both vision and touch, predictors from flat fabric images, draped fabric images, and fabric rotation videos were used separately (model 4, 5, 6). The tactile perceptual ratings collected in the experiment Phase II were averaged across all observers and used as the dependent variables. Despite the GLCM feature set, 2D FFT feature set, and WT feature set, fabric draped width extracted from draped fabric images was used as one of the predictors of model 2 and 5, fabric draped width extracted from fabric rotation videos was used as one of the predictors of model 3 and 6, and fabric thickness was used as one of the predictors of model 4, 5, and 6. All predictors were z-standardised before training the model.

Table 7.1 Models predicting the tactile perception under the corresponding conditions, and the corresponding predictors.

	Target condition	Predictors	No. Predictors
Visual-tactile perception prediction	1. Flat fabric images	<ul style="list-style-type: none"> • GLCM based features • 2D FFT features • WT features 	31
	2. Draped fabric images	<ul style="list-style-type: none"> • Fabric width extracted from draped fabric images • GLCM based features • 2D FFT features • WT features 	27
	3. Fabric rotation videos	<ul style="list-style-type: none"> • Fabric width extracted from videos • GLCM based features • 2D FFT features • WT features 	29
Tactile perception prediction	4. Vision+touch (predicted by flat fabric images)	<ul style="list-style-type: none"> • Fabric thickness • Predictors of model 1 	32
	5. Vision+touch (predicted by draped fabric images)	<ul style="list-style-type: none"> • Fabric thickness • Predictors of model 2 	28

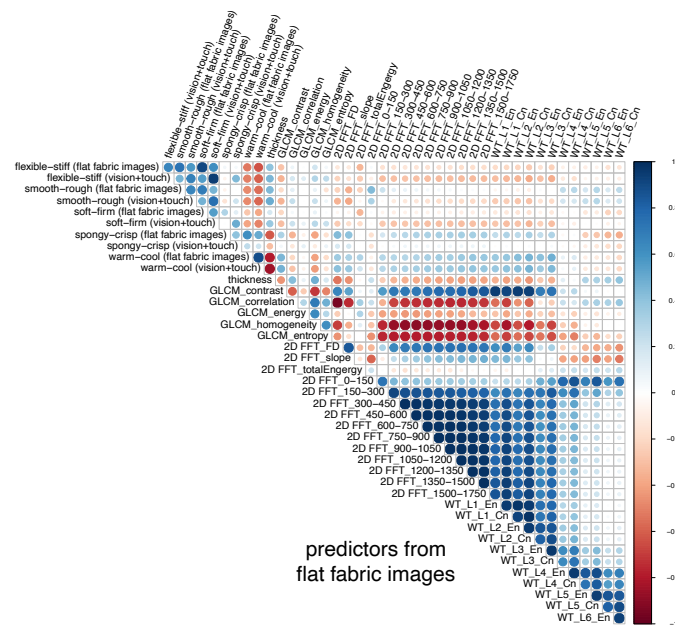
6. Vision+touch
(predicted by
fabric rotation
videos)
- Fabric thickness
 - Predictors of model 3

30

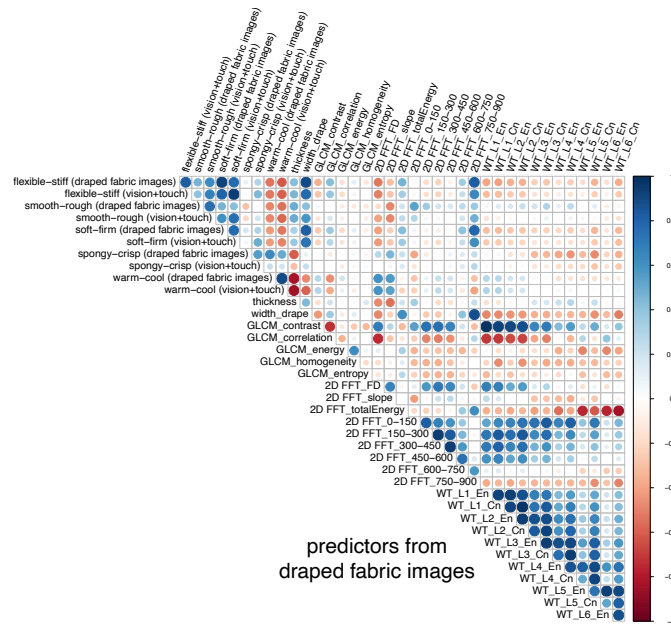
7.3.2 Correlations between dependent variables and predictors and interrelationships of predictors

The correlations between dependent variables and predictors, as well as the correlations between all predictors were shown in Figure 7.6. The predictors were extracted from flat fabric images (Figure 7.6-A), draped fabric images together with fabric width (Figure 7.6-B), and fabric rotation videos together with fabric width (Figure 7.6-C). The relationships between thickness and dependent variables were also included in each figure. All dependent variables were followed by the conditions under which the data were collected.

(A)



(B)



(C)

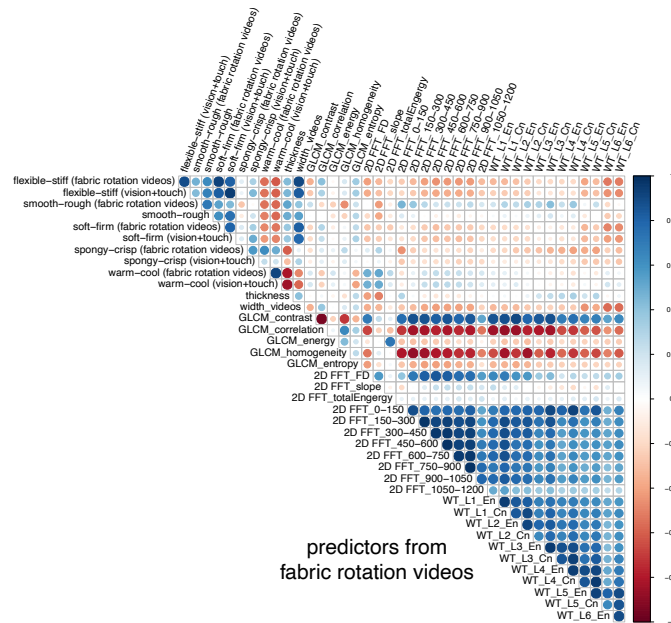


Figure 7.6 The correlations between tactile perceptual ratings and corresponding predictors, and interrelationships among predictors.

The correlations between dependent variables and predictors were mixed. Predictors which were significantly correlated with one dependent variable may be insignificantly correlated with another. For example, fabric draped width extracted from draped fabric images significantly correlated to most of the tactile perception, except for spongy-crisp (Figure 7.6-B). For each model, it is possible to remove irrelevant predictors based on the significant levels of the correlations

between dependent variables and predictors. However, inconsistencies in the predictors used for modelling could result from removal. Inconsistencies include the number of predictors used for modelling, and differences in the specific predictors selected. Either of the inconsistencies would compromise the comparability of the models. Therefore, all predictors were included initially to train the models.

The numbers of predictors ranged from 27 to 32, which lead to high-dimensional datasets. In Figure 7.6, multicollinearities were observed among some of predictors, which may affect the models' interpretability. Given that no predictors would be initially removed, regularisation regression techniques which remove or shrink less affected predictors were implemented, with details described in Section 7.3.3.1, 7.3.3.2, and 7.3.3.3.

7.3.3 Regression techniques

7.3.3.1 Ridge Regression (RR)

RR models implemented L2 penalty to shrink the coefficients of less affected predictors approaching but not to zero. The implementation was conducted using *cv.glmnet()* function under *glmnet* package in R. Parameter α was set to 0, and parameter λ was optimised by ten-fold cross-validation. A set of 100 λ was generated and tested during the training process, and the optimal λ was defined as the value giving minimum mean cross-validated error. Greater value of λ would strongly shrink the coefficients towards but not to zero.

7.3.3.2 Least Absolute Shrinkage and Selection Operator Regression (LASSO) technique

LASSO models implemented L1 penalty to shrink the coefficients of less affected predictors to zero, and thus the predictor selection can be achieved. The implementation process and the determination of optimal λ was the same as RR, while parameter α was set to 1. Greater value of λ would force the coefficients of irrelevant predictors to zero.

7.3.3.3 The Elastic Net Regression (EN)

EN models implemented both L1 and L2 penalty, and thus both optimal λ and α were defined during the training process. Parameter α was pre-defined as a sequence from 0 to 1 with 0.1 intervals. For each α , a ten-fold cross-validation was implemented, and the optimal α was defined as the value giving minimum cross-validated error. For the optimal α , a set of 100 λ values were generated and tested, and the optimal λ value was determined when cross-validated error was minimised. The combination of optimal α and λ was then used in the EN training process, where optimal α controls the balance of L1 and L2 penalties and optimal λ controls the degree of regularisation.

7.3.3.4 Ordinary Least Squares Regression (OLS)

All predictors were initially fitted into models to predict visual-tactile perception and tactile perception. Regularisation regression techniques were implemented to shrink and remove irrelevant predictors during the training processes by tuning α and λ as needed. Ordinary Least Square Regression (OLS) technique which includes all predictors was implemented for all models as comparisons. The implementation was conducted using *lm()* function under the *olsrr* package in R, without parameters tuning and predictors selection.

7.3.4 Training and testing datasets

Even though woven fabrics differed with knitted fabrics in terms of tactile perception (in Section 6.4), the statistically fitted differences between woven and knitted fabrics were small, being less than 1.63 unit on a 9-point Likert scale. Here, for all tactile properties, models were built using both groups. Tactile perceptual ratings collected using real fabric samples from Leeds Fabric Tactile Database Part II, were used to model the visual-tactile and tactile perception. A technique 4-fold cross-validation (repeated 50 times) from machine learning was implemented. The dataset was randomly split into two groups, with 75% used as training dataset and 25% used as testing dataset. The model would

always be tested by a new testing dataset to prevent the overfitting. The random splitting process was repeated 50 times, with a different training dataset generated each time, and the model was evaluated by a different testing dataset.

Predictors listed in Table 7.1 were fitted to the corresponding dependent variables by different regression techniques given in Section 7.3.3. Root Mean Square Error (RMSE) and R^2 were used to assess the model performance. RMSE reflects the average differences between the observed data and predicted data on the original scale. R^2 reflects the goodness of fitting of the model. Lower value of RMSE and higher value of R^2 are preferred for a good prediction model. For each model, the average RMSE and R^2 from the 50 times random data splits were adopted, reducing the negative effects of unbalanced data split.

7.4 Model performance and comparisons

In Section 7.4.1, comparisons were made between the regression techniques. Models trained by EN were further analysed in the following subsections. In Section 7.4.2, comparisons of the visual-tactile perception model performance were made between flat fabric images, draped fabric images, and fabric rotation videos. Through the three different fabric visual representations, tactile perception predicted by predictors extracted from corresponding visual representations are compared. In Section 7.4.3, the predictive power was compared among five pairs of tactile properties.

7.4.1 Comparisons between regression techniques

Table 7.2 lists RMSE and R^2 values averaged from 50 repeats for all models predicting tactile properties. Models trained by OLS technique had higher RMSE values and lower R^2 values, despite the dependent variables and target conditions. Compared to that, regularisation regression techniques performed better than OLS, with lower RMSE values and high R^2 values.

The results of comparisons between RR, LASSO, and EN were mixed. Overall, models trained by the three regularisation techniques were performed similarly. For example, for the flexible-stiff attributes, the RMSE values of the visual-tactile perception model using flat fabric images were 1.28 points across RR, LASSO, and EN methods. Similarly, the tactile perception model using flat fabric images showed RMSE values of 1.41, 1.44, 1.49 points for RR, LASSO, and EN, respectively. The comparison among RR, LASSO, and EN methods did not consistently indicate which method provided better predictive performance. The EN models were further analysed in Section 7.4.2 and 7.4.3 to compare the model performance between target conditions, due to its ability to shrink and select predictors simultaneously to achieve more efficient models.

Table 7.2 Comparisons of OLS, RR, LASSO, EN for predicting visual-tactile and tactile perception, based on the average RMSE and R^2 values.

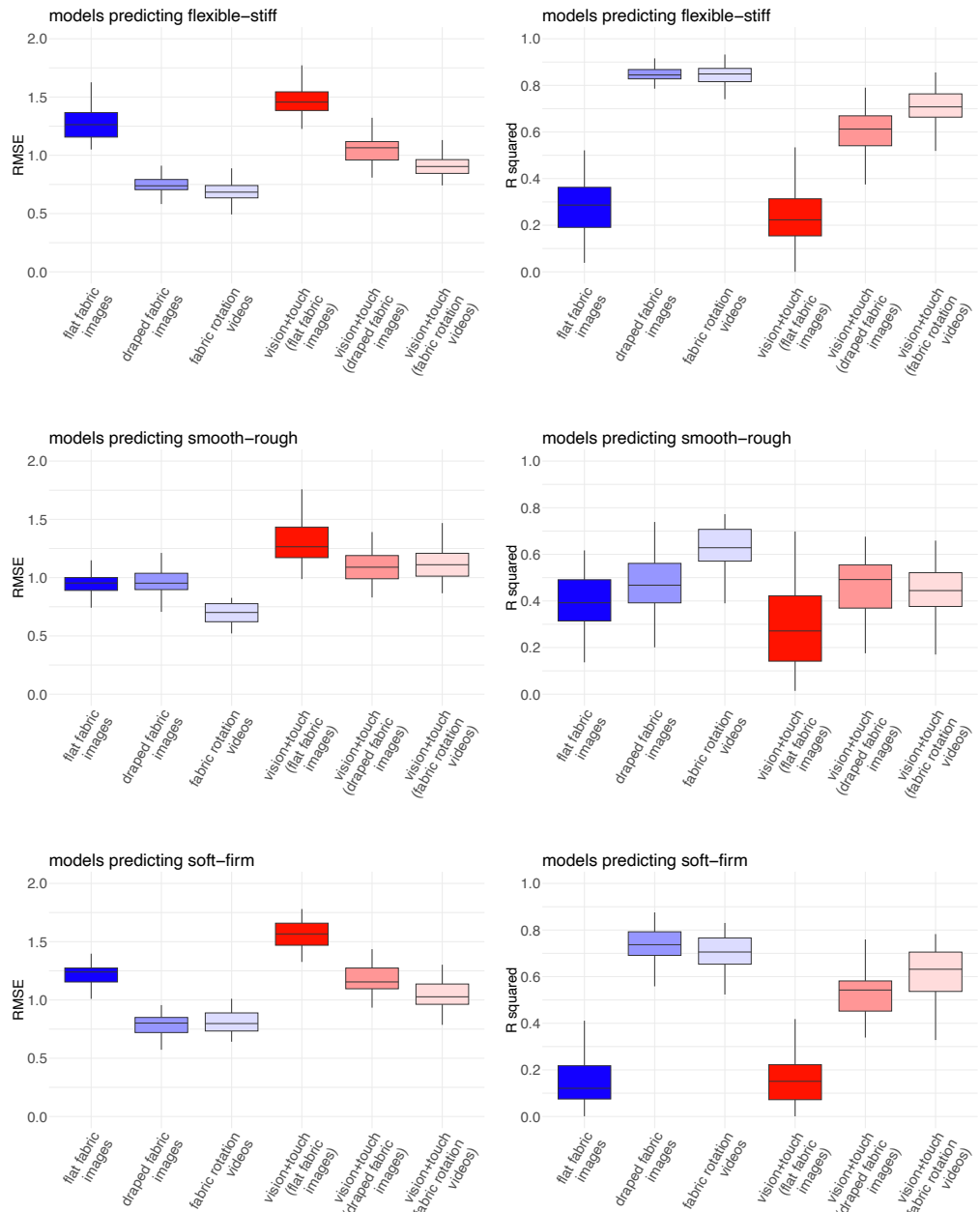
Flexible-stiff		OSL	RR	LASSO	EN
Flat fabric images	RMSE	1.55±0.38	1.28±0.26	1.28±0.29	1.28±0.28
	R^2	0.26±0.14	0.30±0.12	0.29±0.11	0.28±0.12
Draped fabric images	RMSE	1.00±0.22	0.78±0.08	0.75±0.08	0.75±0.08
	R^2	0.74±0.10	0.83±0.03	0.84±0.04	0.84±0.04
Fabric rotation videos	RMSE	0.92±0.15	0.74±0.08	0.69±0.08	0.69±0.10
	R^2	0.74±0.07	0.82±0.04	0.85±0.04	0.85±0.04
Vision+touch (flat)	RMSE	2.05±0.49	1.41±0.13	1.44±0.11	1.49±0.19
	R^2	0.16±0.11	0.27±0.14	0.27±0.12	0.23±0.12
Vision+touch (drape)	RMSE	1.25±0.15	1.05±0.12	1.04±0.11	1.04±0.12
	R^2	0.49±0.10	0.59±0.09	0.61±0.09	0.61±0.10
Vision+touch (video)	RMSE	1.23±0.27	0.90±0.08	0.82±0.08	0.92±0.11
	R^2	0.55±0.12	0.71±0.06	0.72±0.06	0.70±0.08
Smooth-rough		OSL	RR	LASSO	EN
Flat fabric images	RMSE	1.30±0.30	0.93±0.10	0.94±0.11	0.95±0.10
	R^2	0.24±0.15	0.40±0.12	0.40±0.11	0.39±0.12
Draped fabric images	RMSE	1.09±0.17	0.93±0.11	0.89±0.10	0.96±0.11
	R^2	0.40±0.13	0.50±0.11	0.54±0.11	0.47±0.12
Fabric rotation videos	RMSE	0.82±0.13	0.68±0.10	0.71±0.09	0.70±0.10
	R^2	0.53±0.13	0.66±0.09	0.63±0.09	0.63±0.09
Vision+touch (flat)	RMSE	1.79±0.45	1.27±0.13	1.25±0.12	1.30±0.18
	R^2	0.16±0.12	0.30±0.15	0.32±0.15	0.29±0.16
Vision+touch (drape)	RMSE	1.29±0.18	1.05±0.14	1.12±0.15	1.09±0.13
	R^2	0.38±0.12	0.50±0.15	0.44±0.15	0.46±0.16
Vision+touch (video)	RMSE	1.46±0.32	1.06±0.12	1.14±0.15	1.12±0.14

	R^2	0.29±0.15	0.50±0.14	0.43±0.14	0.44±0.13
Soft-firm		OSL	RR	LASSO	EN
Flat fabric images	RMSE	1.57±0.41	1.17±0.10	1.20±0.09	1.22±0.10
	R^2	0.14±0.11	0.18±0.10	0.17±0.09	0.15±0.11
Draped fabric images	RMSE	1.05±0.16	0.78±0.11	0.85±0.11	0.79±0.10
	R^2	0.57±0.11	0.74±0.08	0.69±0.08	0.73±0.08
Fabric rotation videos	RMSE	1.00±0.17	0.83±0.09	0.82±0.08	0.81±0.11
	R^2	0.61±0.10	0.71±0.08	0.71±0.06	0.70±0.08
Vision+touch (flat)	RMSE	2.07±0.45	1.57±0.12	1.59±0.12	1.57±0.14
	R^2	0.09±0.08	0.17±0.12	0.16±0.12	0.16±0.10
Vision+touch (drape)	RMSE	1.41±0.27	1.18±0.12	1.18±0.13	1.18±0.14
	R^2	0.42±0.13	0.51±0.11	0.51±0.10	0.52±0.11
Vision+touch (video)	RMSE	1.47±0.34	1.06±0.13	1.04±0.12	1.04±0.12
	R^2	0.43±0.12	0.60±0.10	0.62±0.10	0.62±0.11
Spongy-crisp		OSL	RR	LASSO	EN
Flat fabric images	RMSE	1.07±0.22	0.83±0.10	0.84±0.11	0.86±0.10
	R^2	0.24±0.16	0.30±0.12	0.32±0.16	0.30±0.14
Draped fabric images	RMSE	0.99±0.14	0.82±0.14	0.84±0.11	0.85±0.14
	R^2	0.24±0.14	0.38±0.13	0.35±0.11	0.32±0.13
Fabric rotation videos	RMSE	1.09±0.18	0.86±0.09	0.82±0.08	0.81±0.07
	R^2	0.13±0.10	0.20±0.11	0.31±0.10	0.26±0.09
Vision+touch (flat)	RMSE	1.26±0.24	0.96±0.12	0.96±0.12	0.93±0.10
	R^2	0.05±0.04	0.04±0.03	0.04±0.03	0.05±0.03
Vision+touch (drape)	RMSE	1.02±0.17	0.88±0.10	0.89±0.09	0.85±0.09
	R^2	0.18±0.10	0.18±0.13	0.21±0.13	0.20±0.11
Vision+touch (video)	RMSE	1.07±0.19	0.85±0.10	0.84±0.09	0.83±0.10
	R^2	0.15±0.10	0.23±0.11	0.28±0.13	0.24±0.11
Warm-cool		OSL	RR	LASSO	EN
Flat fabric images	RMSE	1.12±0.30	0.83±0.10	0.85±0.12	0.86±0.13
	R^2	0.40±0.16	0.51±0.11	0.48±0.13	0.48±0.14
Draped fabric images	RMSE	1.28±0.25	0.95±0.10	0.99±0.10	0.99±0.20
	R^2	0.36±0.15	0.56±0.08	0.51±0.09	0.52±0.13
Fabric rotation videos	RMSE	1.16±0.20	0.92±0.10	0.91±0.11	0.93±0.12
	R^2	0.43±0.12	0.54±0.09	0.56±0.10	0.54±0.11
Vision+touch (flat)	RMSE	0.80±0.16	0.61±0.07	0.60±0.09	0.62±0.08
	R^2	0.66±0.11	0.76±0.06	0.77±0.07	0.75±0.06
Vision+touch (drape)	RMSE	0.66±0.12	0.58±0.07	0.54±0.07	0.56±0.07
	R^2	0.72±0.09	0.78±0.07	0.81±0.07	0.79±0.07
Vision+touch (video)	RMSE	0.68±0.11	0.57±0.07	0.53±0.06	0.56±0.06
	R^2	0.71±0.07	0.78±0.06	0.82±0.04	0.79±0.05

7.4.2 Comparisons of predictive power among target conditions

Figure 7.7 compares the model performance on predicting the visual-tactile

perception (left three boxes in blue in each figure) and tactile perception (right three boxes in red in each figure), trained by EN. Each box indicates the distribution of the RMSE or R^2 values over the 50 repeated cross-validation during model training.



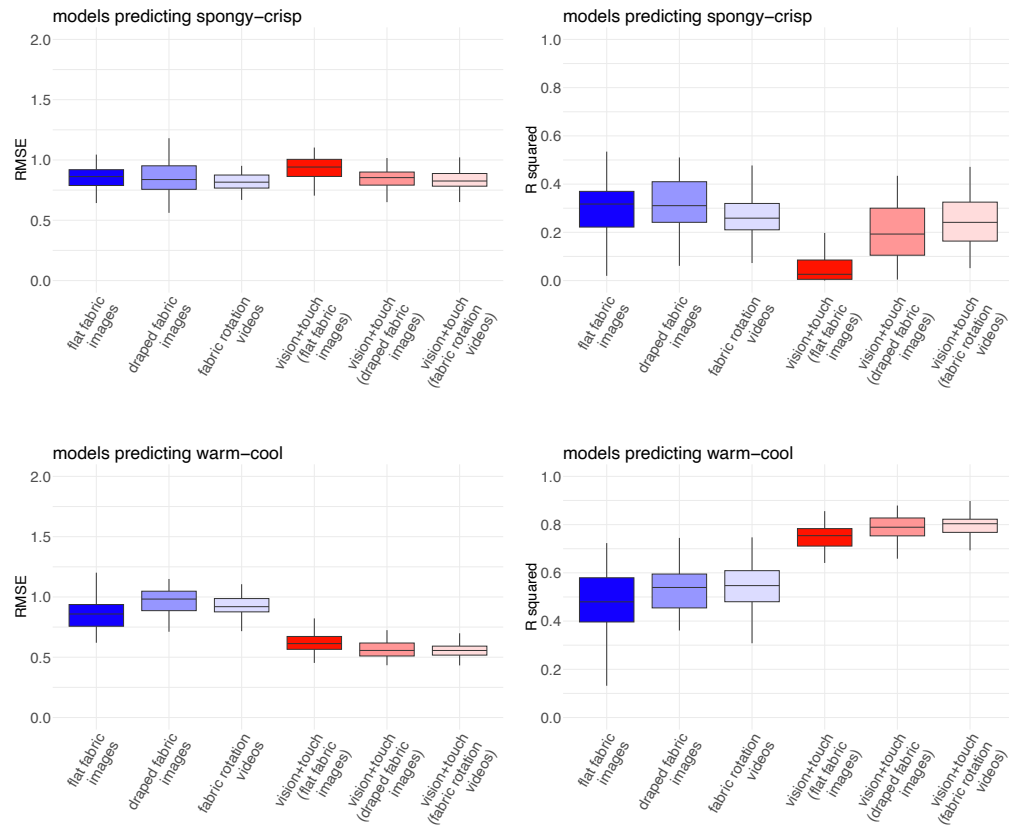


Figure 7.7 EN model performance assessed by RMSE (left) and R^2 (right). Comparisons focused on differences among target conditions. Black lines indicate the median values from the 50 repeats. Boxes indicate IQR.

For visual-tactile perception prediction, higher RMSE and lower R^2 values were observed when predictors extracted from flat fabric images were used to predict flexible-stiff and soft-firm perceived from these images. The average differences between predicted scores and rated scores were 1.28 and 1.22 units in the 9-points Likert scale for flexible-stiff and soft-firm, respectively. The models only explained 28% of the variance for flexible-stiff and 15% for soft-firm. Compared to models using draped fabric images predictors and time*space slices predictors, predictors from flat fabric images demonstrated relatively lower predictive power in visual-tactile perception. However, for spongy-crisp and warm-cool, predictors from flat fabric images, draped fabric images, and time*space slices had similar predictive power. The average RMSE ranges were from 0.81 to 0.86 for spongy-crisp, and 0.86 to 0.99 for warm-cool, with each range reflected results from three models using different image categories. The

best model for predicting spongy-crisp was based on draped fabric images, explaining 32% of the variance. The best model for predicting warm-cool was based on flat fabric images, with average RMSE values of 0.86. In addition, for smooth-rough, models using predictors from space*time slices performed better, with average RMSE value of 0.70 and R^2 value of 63%. Higher RMSE and lower R^2 values were obtained for models predicting smooth-rough perceived from flat fabric images and draped fabric images.

For tactile perception prediction, models using predictors from flat fabric images achieved poor performance for all tactile properties, compared to that using predictors from draped fabric images and time*space slices. It is reasonable since better correlations were observed between draped fabric images/fabric rotation videos and vision+touch, described in Section 5.5. For predicting flexible-stiff, soft-firm, spongy-crisp, and warm-cool perceived through vision and touch, model including predictors from time*space slices achieved the best performance. The average differences between predicted perception and rated perception from observers were 0.92, 1.04, 0.83, and 0.56 units for flexible-stiff, soft-firm, spongy-crisp, and warm-cool respectively. 70%, 62%, 24%, and 79% of the variance were explained in the corresponding models. On the other hand, models including predictors from draped fabric images achieved the best performance to predict smooth-rough perceived through vision and touch. The average RMSE values were of 1.09 units. Models explained 46% of the variance.

7.4.3 Comparisons of the predictive power among tactile properties

In Figure 7.7, the predictive power was compared among target conditions for each pair of tactile properties. Figure 7.8 was revised from Figure 7.7, clearly showing the comparisons among tactile properties. Top two figures in Figure 7.8 show models performance predicting visual-tactile perception and bottom two figures show models performance predicting tactile perception. Overall, models

predicting flexible-stiff and warm-cool outperformed those predicting other pairs of tactile properties under specific target condition.

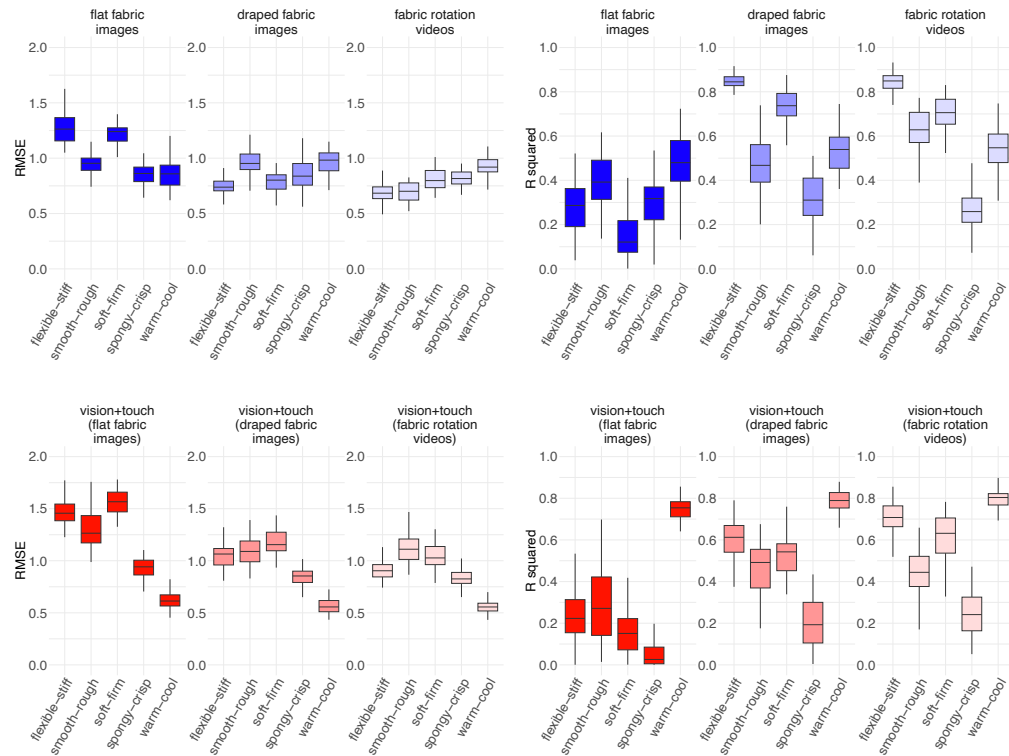


Figure 7.8 EN model performance assessed by RMSE (left) and R^2 (right). Comparisons focused on the differences among tactile properties. Black horizontal lines indicate the median values from the 50 repeats. Boxes indicate IQR.

When using predictors from draped fabric images to predict flexible-stiff perceived under this condition, the model achieved good accuracy of average $RMSE=0.75$ and average $R^2=84\%$. For other tactile properties prediction under the same target condition, models demonstrated slightly lower accuracy. The average $RMSE$ ranged from 0.79 (soft-firm) to 0.99 (warm-cool), and the average R^2 ranged from 32% (spongy-crisp) to 73% (soft-firm). Similarly, when using predictors from fabric rotation videos to predict flexible-stiff perceived under this condition, the difference between predicted scores and rated scores was 0.69, and up to 85% of the variance can be explained. Model predicting soft-firm performed nearly identical to that predicting flexible-stiff, with $RMSE$ value of 0.70 and R^2 value of 85%.

Notable irregularities have been found on models using predictors from draped

fabric images and fabric rotation videos to predict spongy-crisp perceived using corresponding images and videos. For a good prediction model, both lower RMSE and higher R^2 values are normally expected. While models achieved RMSE values of 0.85 and 0.81 points on a 9-point Likert scale, they explained only 32% and 26% of the variance for perception using draped fabric images and fabric rotation videos, respectively.

Models predicting warm-cool achieved better accuracies than those predicting other pairs of tactile properties under four target conditions: (1) using flat fabric images predictors for perception from flat fabric images (RMSE=0.86, R^2 =48%); (2) using flat fabric images predictors for perception from vision+touch (RMSE=0.62, R^2 =75%); (3) using draped fabric images predictor for perception from vision+touch (RMSE=0.56, R^2 =79%); (4) using fabric rotation videos predictors for perception from vision+touch (RMSE=0.56, R^2 =79%). A possible reason for the strong predictive power in cases (2)-(4) could be the inclusion of thickness as one of the predictors in the models. The role of thickness is further analysed in Section 7.6.

Table 7.3 summarised models that achieved the best performance for each pair of tactile properties. Overall, using predictors from draped fabric images and fabric rotation videos contributed to the prediction of all visual-tactile and tactile perception. One exception is that predictors from flat fabric images performed better on predicting warm-cool. In addition, all models predicting spongy-crisp performed ineffectively. Using predictors from fabric draped width, GLCM, 2D FFT, and WT extracted from images cannot effectively predict the perception of spongy-crisp.

Table 7.3 The best model trained by EN for all tactile properties, including predictors from the corresponding image category, assessed by RMSE and R^2 .

	Visual-tactile perception prediction	Tactile perception prediction
--	--------------------------------------	-------------------------------

Flexible-stiff	Fabric rotation video RMSE=0.69±0.10 R ² =0.85±0.04	Fabric rotation video RMSE=0.92±0.11 R ² =0.70±0.08
Smooth-rough	Fabric rotation video RMSE=0.70±0.10 R ² =0.63±0.09	Draped fabric images RMSE=1.09±0.13 R ² =0.46±0.12
Soft-firm	Draped fabric images RMSE=0.79±0.10 R ² =0.73±0.08	Fabric rotation video RMSE=1.04±0.12 R ² =0.62±0.11
Spongy-crisp	Draped fabric images RMSE=0.85±0.14 R ² =0.32±0.13	Fabric rotation video RMSE=0.83±0.10 R ² =0.24±0.11
Warm-cool	Flat fabric images RMSE=0.86±0.13 R ² =0.48±0.14	Fabric rotation videos RMSE=0.56±0.07 R ² =0.79±0.07

7.5 Ranking of predictors by EN and LASSO

The coefficients of the irrelevant predictors were shrunk to zero during the EN and LASSO training processes. As the predictors were z-standardised prior to the model training, the considerable variations in the scale of initial predictors no longer affected the models. Ranking the absolute standardised coefficients would reveal the relative importance of predictors. Table 7.4 listed the top 10 important predictors in each visual-tactile perception prediction model and in the best models predicting tactile perception through EN, followed by the ranking of predictors by LASSO lists in brackets.

Table 7.4 Rank of top 10 predictors for visual-tactile perception models and the best models for tactile perception in Table 7.3.

Flexible-stiff				
	Flat fabric images	Draped fabric images	Fabric rotation videos	Vision+touch (by fabric rotation videos)
1	WT_L3_Cn (2)	width_drape (1)	width_video (1)	width_video (1)
2	WT_L3_En (4)	FFT_750-900 (2)	GLCM_entropy (2)	GLCM_entropy (3)
3	FFT_0-150 (1)	GLCM_correlation (6)	FFT_1050-1200 (3)	thickness (2)
4	FFT_150-300 (5)	GLCM_entropy (4)	FFT_totalEnergy (4)	WT_L6_Cn (7)

5	WT_L4_Cn (17)	FFT_FD (3)	WT_L4_En (7)	GLCM_contrast (7)
6	FFT_1350-1500 (12)	WT_L1_En (7)	GLCM_correlation (8)	FFT_1050-1200 (5)
7	FFT_FD (15)	GLCM_contrast (12)	WT_L6_Cn (10)	FFT_totalEnergy (4)
8	FFT_totalEnergy (3)	FFT_slope (5)	WT_L6_En (9)	WT_L2_Cn (9)
9	WT_L6_Cn (6)	FFT_300-450 (8)	WT_L4_Cn (11)	WT_L3_Cn (9)
10	WT_L2_Cn (9)	WT_L6_Cn (12)	FFT_600-750 (14)	WT_L1_En (9)
Smooth-rough				
	Flat fabric images	Draped fabric images	Fabric rotation videos	Vision+touch (by draped fabric images)
1	FFT_0-150 (1)	FFT_0-150 (1)	FFT_0-150 (1)	width_drape (1)
2	WT_L3_Cn (4)	WT_L4_En (4)	WT_L6_En (4)	FFT_FD (9)
3	FFT_totalEnergy (2)	width_drape (2)	GLCM_entropy (5)	GLCM_entropy (5)
4	WT_L5_En (5)	FFT_450-600 (8)	GLCM_homo (2)	FFT_0-150 (4)
5	GLCM_homo (3)	FFT_150-300 (7)	width_video (3)	FFT_slope (2)
6	WT_L3_En (11)	FFT_slope (3)	FFT_150-300 (9)	thickness (3)
7	FFT_1500-1750 (7)	WT_L6_Cn (13)	WT_L6_Cn (11)	WT_L4_En (9)
8	FFT_1350-1500 (16)	GLCM_homo (6)	FFT_750-900 (12)	WT_L3_Cn (5)
9	WT_L2_Cn (10)	FFT_FD (17)	WT_L4_En (12)	WT_L6_Cn (9)
10	WT_L4_Cn (13)	GLCM_entropy (5)	FFT_slope (6)	WT_L1_Cn (9)
Soft-firm				
	Flat fabric images	Draped fabric images	Fabric rotation videos	Vision+touch (by fabric rotation videos)
1	FFT_0-150 (4)	width_drape (1)	width_video (1)	width_video (1)
2	FFT_totalEnergy (1)	FFT_750-900 (2)	GLCM_correlation (8)	GLCM_entropy (2)
3	WT_L6_Cn (6)	GLCM_correlation (3)	WT_L6_Cn (4)	GLCM_contrast (4)
4	WT_L3_En (13)	WT_L1_En (6)	FFT_600-750 (11)	WT_L3_Cn (5)
5	WT_L3_Cn (13)	FFT_FD (10)	WT_L3_Cn (3)	WT_L6_Cn (7)
6	FFT_300-450 (10)	WT_L5_Cn (13)	GLCM_entropy (5)	FFT_1050-1200 (7)
7	WT_L4_Cn (5)	GLCM_homo (9)	FFT_1050-1200 (9)	WT_L2_Cn (7)
8	GLCM_contrast (3)	WT_L4_En (13)	FFT_slope (12)	WT_L1_Cn (7)
9	WT_L6_En (2)	FFT_slope (5)	FFT_totalEnergy (2)	FFT_0-150 (7)
10	FFT_150-300 (13)	FFT_150-300 (13)	FFT_450-600 (14)	thickness (7)
Spongy-crisp				
	Flat fabric images	Draped fabric images	Fabric rotation videos	Vision+touch (by fabric rotation videos)
1	WT_L3_Cn (3)	FFT_0-150 (5)	FFT_0-150 (1)	thickness (1)
2	GLCM_homo (2)	FFT_FD (3)	FFT_FD (2)	Width_video (2)
3	FFT_slope (4)	WT_L5_Cn (1)	FFT_totalEnergy (10)	GLCM_contrast (17)
4	WT_L5_Cn (12)	GLCM_energy (6)	GLCM_energy (10)	GLCM_correlation (17)
5	FFT_300-450 (12)	FFT_750-900 (4)	WT_L5_En (5)	GLCM_energy (5)

6	WT_L1_En (8)	WT_L6_Cn (9)	WT_L4_En (7)	GLCM_homo (14)
7	WT_L4_Cn (7)	WT_L2_Cn (13)	FFT_slope (3)	GLCM_entropy (7)
8	WT_L6_Cn (1)	WT_L1_Cn (9)	WT_L6_Cn (9)	FFT_FD (17)
9	FFT_150-300 (12)	GLCM_homo (13)	GLCM_contrast (10)	FFT_slope (9)
10	GLCM_energy (8)	FFT_slope (2)	WT_L6_En (7)	FFT_totalEnergy (7)
Warm-cool				
	Flat fabric images	Draped fabric images	Fabric rotation videos	Vision+touch (by fabric rotation videos)
1	FFT_150-300 (5)	width_drape (2)	width_video (1)	thickness (1)
2	WT_L2_Cn (12)	WT_L5_Cn (6)	FFT_0-150 (3)	width_video (2)
3	FFT_0-150 (2)	FFT_0-150 (3)	FFT_FD (2)	GLCM_entropy (3)
4	FFT_1500-1750 (15)	FFT_FD (1)	FFT_totalEnergy (4)	FFT_totalEnergy (4)
5	WT_L6_Cn (4)	GLCM_correlation (5)	WT_L5_Cn (7)	FFT_slope (6)
6	FFT_300-450 (6)	WT_L2_Cn (15)	WT_L4_En (13)	FFT_FD (5)
7	WT_L3_En (10)	WT_L4_En (8)	GLCM_entropy (5)	WT_L5_En (10)
8	FFT_1200-1350 (18)	WT_L6_Cn (7)	WT_L1_En (12)	WT_L4_En (10)
9	FFT_600-750 (21)	GLCM_contrast (10)	GLCM_energy (8)	WT_L1_En (10)
10	WT_L3_Cn (1)	FFT_450-600 (12)	FFT_slope (6)	GLCM_homo (10)

Homo: homogeneity

In Table 7.4, a clear observation is that fabric draped width was ranked as the most affected predictor in several models. Models including: (1) predicting flexible-stiff and soft-firm perceived from draped fabric images, fabric rotation videos, and vision+touch; (2) predicting smooth-rough perceived from vision+touch; (3) predicting warm-cool perceived from draped fabric images and fabric rotation videos. However, fabric draped width was less important in predicting spongy-crisp. Given the relative higher predictive accuracy described in previous sections, the contribution of fabric draped width in predicting visual-tactile perception and tactile perception has been confirmed by ranking the predictors in models, except for the perception using flat fabric images.

Another clear observation is that both fabric draped width and thickness of fabrics were ranked as very important predictors in all tactile perception models (the right column in Table 7.4). Fabric draped width, GLCM based features, 2D FFT based features, and WT based features were the predictors computed from corresponding images, while thickness was the physical property of real fabrics. Despite the importance of thickness, in practical applications, the absence or

inaccessibility of physical property may cause challenges in remaining the good performance of tactile perception prediction models. Therefore, new models predicting tactile perception without thickness as one of the predictors were fitted to assess the model performance using only image-based predictors, which is described in Section 7.6.

The importance of predictors computed from GLCM, 2D FFT, and WT were mixed in all models, and thus the role of each predictor category cannot be clearly defined and compared. Certain predictors were found to be important across models for each pair of tactile properties. For flexible-stiff, GLCM_entropy and WT_L6_Cn were found to have relatively higher absolute coefficients in models of draped fabric images, fabric rotation videos, and vision+touch. These two predictors, together with WT_L4_En, FFT_0-150, played important roles in predicting smooth-rough perceived from draped fabric images, fabric rotation videos and vision+touch. GLCM_homogeneity exhibited relatively higher absolute standardised coefficients in visual-tactile models of smooth-rough. For soft-firm, WT_L6_Cn was an important predictor across all models except for draped fabric images. For spongy-crisp, only GLCM_energy was found important for all models, but it was excluded in the models for flat fabric images. For warm-cool, FFT_FD and WT_L4_En were found important for all models except for flat fabric images.

7.6 Models excluding thickness as a predictor

Same modelling procedures were conducted on models without thickness as the predictor. Predictors from fabric rotation videos were used for flexible-stiff, soft-firm, spongy-crisp, and warm-cool, and predictors from draped fabric images were used for smooth-rough, as provided in Table 7.3. Figure 7.9 compares the models predicting tactile perception through vision and touch between excluding thickness and including thickness. Models excluding thickness as the predictor indicated that the prediction was carried out based

on images only. Overall, excluding thickness slightly reduced the models' accuracies, which was indicated by the increased RMSE values and decreased R^2 values as shown in Figure 7.9. The prediction of flexible-stiff, smooth-rough, soft-firm, and warm-cool perceived through vision and touch remained reasonably good, while spongy-crisp cannot be accurately predicted by image-based predictors only.

Among all models, the exclusion of thickness had the largest effect on the prediction of warm-cool. The average RMSE increased from 0.56 (± 0.07) to 0.82 (± 0.09), and the average R^2 decreased from 0.79 (± 0.07) to 0.54 (± 0.09) by excluding thickness in the predictors. On the other hand, model of smooth-rough was almost not affected by thickness. The average RMSE (1.09 ± 0.13) and R^2 (0.46) were identical before and after excluding thickness, while the SD varied in R^2 .

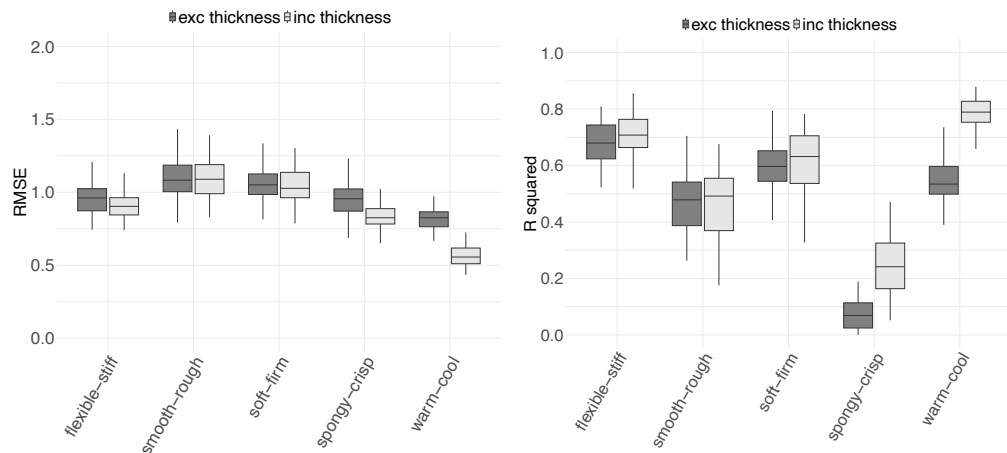


Figure 7.9 Comparison of tactile perception EN models between excluding and including thickness, assessed by RMSE (left) and R^2 (right) from 50 repeats. Black lines indicate the median values. Boxes indicate IQR.

7.7 Discussion

7.7.1 Flat fabric images in visual-tactile and tactile perception and prediction

In Chapter 5 Section 5.5, the tactile perceptual ratings obtained using flat fabric

images were compared with those under the condition of actual touch and observation. The results found that the perception from flat fabric images had lower correlations with the actual touch and observation compared to draped fabric images and fabric rotation videos. An exception included the perception of warm-cool, where the tactile perceptual ratings were highly correlated across all experiment conditions. In this Chapter, these findings were extended to predictive modelling, demonstrating that models trained with predictors from flat fabric images performed poorly in predicting visual-tactile perception and tactile perception. Both Chapters revealed the ineffectiveness of flat fabric images in perceiving and predicting visual-tactile and tactile perception.

From the perspective of perception, a previous study compared the flat and draped fabric images in tactile perception. Observers were asked to view the fabric images and match the fabric position by touching the corresponding fabrics without seeing them (Xiao et al., 2016). The results showed that a better matching accuracy was achieved when draped fabric images were used. Beyond the study of Xiao et al. (2016), few studies have utilised flat fabric images in evaluating the visual-tactile perception. One possible reason is that the flat fabric images lack critical 3D characteristics of fabrics, such as drape and surface contour. This limitation is also reflected in real-world online shopping practices. When purchasing fabric products online, the products are typically displayed in a natural 3D form to provide a better sense of tactile properties.

From the perspective of prediction, predictors extracted from flat fabric images were less effective in predicting the visual-tactile and tactile perception. The features from GLCM, 2D FFT, and WT were used to model the perception of tactile properties perceived from flat fabric images. GLCM focused on the spatial distribution of grey levels, while 2D FFT and WT focused on variations between grey levels in the frequency and time-frequency domain. In the flat fabric images, the distribution and variation of grey levels reflected the micro-structure of the

fabrics, referring to the yarn and fibre arrangement (Haleem et al., 2019), the tiny bumps or grooves on the fabric surface (Leung and Malik, 1999), and the fabric density and porosity due to the tight or loose weave and knit structure (Zhang et al., 2013). Such micro-structure information present in the flat fabric images made little contribution to the prediction of visual-tactile and tactile perception.

7.7.2 Relatively lower RMSE and R^2 in the models of spongy-crisp

An effective prediction model is expected to demonstrate a lower RMSE, representing smaller prediction errors, and a higher R^2 values, indicating a well-fitted model. However, in Section 7.4, the models of spongy-crisp exhibited lower RMSE and lower R^2 values at the same time, suggesting the good accurate predictions yet a poor model fit. To explore the reason of the discrepancy and further evaluate the effectiveness of models predicting spongy-crisp, the range of original tactile perceptual ratings were compared among five pairs of tactile properties, as shown in Figure 7.10.

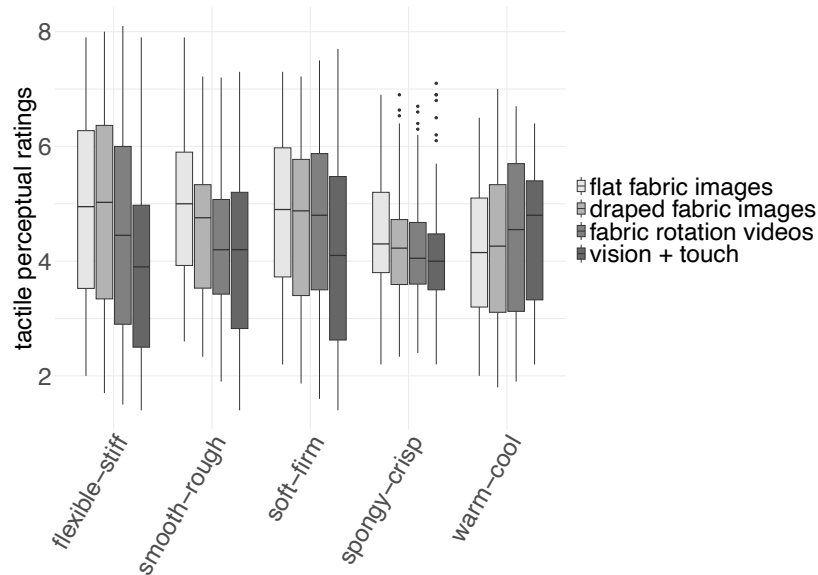


Figure 7.10 The range of original tactile perceptual ratings averaged across all observers. Black lines indicate the median values. Boxes indicate IQR.

As shown in Figure 7.10, the tactile perceptual ratings of spongy-crisp exhibited a narrower range compared to flexible-stiff, smooth-rough, soft-firm, and warm-cool. Across the 118 fabrics in Leeds Fabric Tactile Database Part II, few

participants provided ratings above 7 or below 2 on the 9-point Likert scale for spongy-crisp. During training the predictive model for spongy-crisp, the predicted scores were also constrained within the narrower range of 2-7 point. Consequently, the RMSE, which reflects the difference between predicted scores and original scores, may underestimate the actual prediction error, misleading the assessment of the model's performance. The use of R^2 provided a more reliable measure of the model's fitness and predictive accuracy. For models of spongy-crisp, R^2 were smaller than 30% in predicting visual-tactile and tactile perception, indicating that the models predicting spongy-crisp are less effective. Neither the spongy-crisp perceived from images and videos nor that from actual vision and touch could be accurately predicted.

7.7.3 The role of fabric draped width in prediction

From Table 7.4, it was found that fabric draped width was ranked as the most important predictor in models for predicting flexible-stiff and soft-firm perception through draped fabric images, fabric rotation videos, and actual touch and observation. The characteristics of fabric drape is normally measured using the drape meter shown in Figure 7.11 (left). Basically, the fabric was cut into circular shape and placed between two circular plates (Cusick, 1968; Chu et al., 1950; Sanad and Cassidy, 2015). The fabric drapes naturally over the plate, with a light source placed below to cast a shadow of the draped fabrics. The fabric drape is then measured by the drape ratio which related to the shadow area and fabric area.

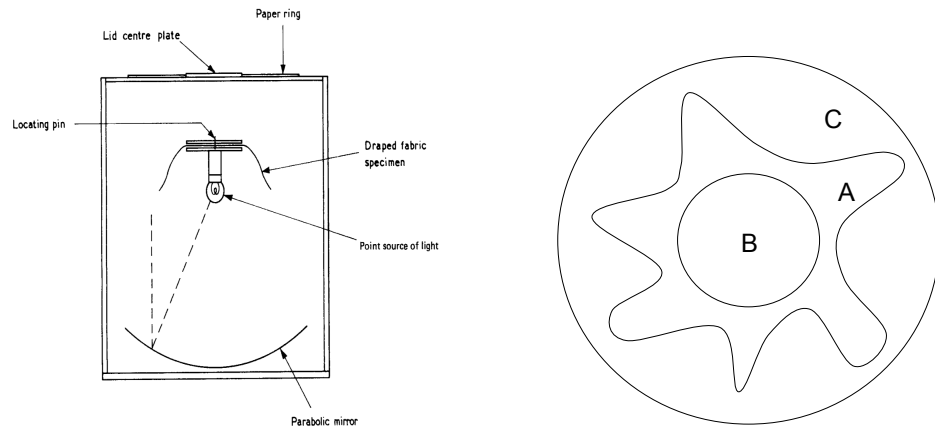


Figure 7.11 Left: The test apparatus of fabric drape. Figure is from British Standards Institution (1973, p.3). Right: the calculation of drape ratio: $(A-B)/(C-B)*100\%$, reproduced from Carrera-Gallissa et al. (2017).

During preparing the Leeds Fabric Tactile Database, the fabrics draped on a cylindrical stand, and images and videos were recorded. The fabrics exhibited a draping behaviour similar to that in the drape tester. However, the drape ratio calculated based on the shadow area was not robust. Two fabrics with the same value of drape ratio could drape significantly different. A variety of drape indicator was developed by Carrera-Gallissa et al. (2017) based on the top-view and side-view images of draped fabrics, and efforts were made on analysing the 3D structure of fabric shape to provide better measurement (Kenkare et al., 2008; Glombikova and Kus, 2014; Mei et al., 2015). The fabric draped width used in the present study was extracted from the side-view of draped fabric images and fabric rotation videos. Although fabric drape was not rated in the experiment, the ratings of flexible-stiff were based on how the fabric draped over hand. The use of fabric draped width significantly contributed to modelling the visual-tactile and tactile perception, highlighting its potential as a parameter for fabric drape assessment.

7.7.4 Limitations of the models and corresponding solutions applied

A good model should meet two key criteria: good predictive performance and

interpretability. Three limitations were taken into consideration before training models: (1) high-dimensional data and multicollinearities, (2) lack of an independent test data, and (3) small sample size. This section will discuss the limitations, and the approaches adopted to minimise their impact.

In the modelling process, the number of predictors varied from 27 to 32, leading to a high-dimensional dataset compared to the 118 samples available under each condition. Multicollinearities were also observed among predictors. Under such circumstances, the model faced the risks of overfitting and reducing coefficient interpretability. Overfitting represents a good performance on training dataset but a poor prediction on testing dataset, as the model may capture noise rather than the informative pattern in the predictors. Multicollinearity occurs when two or more predictors are highly correlated. During the training process, the effect of correlated predictors may be mixed, leading to unstable coefficient estimates where a key predictor may have a smaller coefficient than expected. Given these issues, three regularisation regression techniques were applied: RR, LASSO, and EN. RR reduces the effect of multicollinearity by shrinking the coefficient toward but not to zero, thereby preventing extreme variations of predictor coefficients. However, all predictors are included in the model, and thus the issue of high-dimensional data still remained, leading to the limited interpretation of predictors. LASSO applies strong selection by identifying a subset of predictors in the model, eliminating the irrelevant predictors and simplifying the model structure. However, for correlated predictors, LASSO selects one predictor randomly and shrinks the others to zero. The informative predictors may be eliminated, reducing the interpretability of the model. In contrast, EN achieves a balance between coefficient shrinkage of RR and predictor elimination of LASSO by adding a tuning parameter. The impact of both high-dimensional data and multicollinearities was reduced, which is the key reason that the results of EN were mainly reported in Section 7.4.2, 7.4.3, and 7.6.

To test the model performance, an independent testing dataset is required. Compared to the training dataset, the testing dataset can differ in several ways in the present study, such as being evaluated on entirely different samples and using different displays. As both images and real fabrics were included in the Leeds Fabric Tactile Database, the total number of samples was not extremely large. Even so, participants spent a very long time to complete the entire experiments, and no additional displays were used for visual-tactile evaluation. Therefore, 4-fold cross-validation was used to randomly split the dataset into a training dataset (75% of the entire data) and a testing dataset (25% of the entire data). The cross-validation ensured that the testing dataset was distinct from the training dataset, allowing for independent model validation. This process was repeated 50 times with different random split of the data, enhancing the robustness of the model performance evaluation.

As mentioned above, the total number of samples in the Leeds Fabric Tactile Database was not extremely large as real fabrics were required not only to evaluate tactile perception but also to compare it with the visual-tactile perception obtained from images and videos. This necessity limits the current database size, and thus advanced modelling techniques such as deep learning, neural network, and AI are not applicable in the present study. Therefore, the psychophysical experiments were designed to let participants rate the perception of tactile properties. This approach allows the database to be continuously expanded, with newly added images and real fabrics evaluated individually and seamlessly integrated into the existing database.

7.8 Summary

In this Chapter, predictors were extracted from flat fabric images, draped fabric images, and fabric rotation videos. Models were developed to predict the visual-tactile and tactile perception using the corresponding predictors. A summary of the major findings is listed below:

- By applying different regularisation techniques, including L1 penalty (LASSO), L2 penalty (RR), and a combination of L1 and L2 penalty (EN) in the modelling process, the predictive performance was improved compared to using traditional OLS regression technique. In addition, models trained by the three regularisation techniques were performed similarly.
- Models trained through EN regression technique were reported and compared. Comparisons were made among the target conditions and among tactile properties.
- Fabric draped width and thickness played important roles in predicting visual-tactile and tactile perception. Compared to other predictors, thickness is the predictor related to the real fabrics rather than fabric images and videos. Separate models were trained excluding thickness as the predictor. The results showed that tactile perception models of flexible-stiff, soft-firm, spongy-crisp, and warm-cool were affected by the exclusion of fabric thickness.

Chapter 8

Conclusions

8.1 Overview

This research aims to better understand the perception of tactile properties of fabrics through images, videos, and actual touch and observations. A Leeds Fabric Tactile Database was developed in the present study to provide a useful tool to fully evaluate the perception of tactile properties.

Two parts were separately prepared in the Leeds Fabric Tactile Database. Part I consisted of flat fabric images, draped fabric images, and the corresponding real fabrics. Images were rendered with different colour to achieve controlled variables, allowing for comparisons of the same fabric in different colours and different fabrics in the same colour. The perception flexible-stiff, smooth-rough, soft-firm, spongy-crisp, and warm-cool was rated using Part I in the experiment Phase I. The tactile properties were evaluated under three experiment conditions: observing flat fabric images, observing draped fabric images, and touching the real fabrics without seeing them.

Based on the experiment Phase I, the experiment Phase II was improved from two perspectives using Leeds Fabric Tactile Database Part II. The first improvement is that more fabrics were involved in the experiment Phase II, up to 118 real fabrics were prepared and captured using a digital camera. The second improvement is that the tactile properties were rated under six different experiment conditions, covering almost all real-life scenarios where tactile properties evaluation might be required. The six experiment conditions included flat fabric images, draped fabric images, fabric rotation videos, using real fabrics but only allowing vision (vision-only using real fabrics), using real fabrics but only allowing touch (touch-only), using real fabrics and allowing both vision and touch (vision+touch).

Both experiment Phase I and Phase II were well prepared. The colours in fabric images and videos were carefully characterised to ensure an accurate reproduction. Based on the experiments, the research work was achieved by

the following analyses. Chapter 4 analysed the data collected in the experiment Phase I, evaluating the effect of individual fabric, colour, and experiment condition on the visual-tactile perception. The correlations of the tactile perceptual ratings were achieved among experiment conditions and among different tactile properties. Based on that, Chapter 5 and Chapter 6 analysed the data collected in the experiment Phase II. Chapter 5 focused on the averaged tactile perceptual ratings across all observers, including the correlations among experiment conditions and among tactile properties, and the differences in the tactile perceptual ratings between using images/videos and real fabrics. Chapter 6 focused on the effect of fabric structure on the visual-tactile and tactile perception, the effect of fabric colour on the tactile perception, and the different correlations between woven and knitted fabrics. In Chapter 7, efforts were made on modelling the visual-tactile and tactile perception using flat fabric images, draped fabric images, and fabric rotation videos. A summary of the major findings and the contribution of the work is given in the following sections.

8.2 The effect of individual fabrics and fabric structures

The effect of individual fabrics was evaluated in the experiment Phase I, Chapter 4 Section 4.5. By fitting CLMM models, the results showed that fabrics were the strongest factor affecting the visual-tactile perception. The individual differences were primarily reflected in the fabric's appearance, which is large determined by its structure and colour. Despite having the same fabric structure, the appearance of fabrics can differ significantly due to variations in yarn, fibre types, finishing techniques, and additional surface treatment. When a larger number of fabrics are involved, comparing individual fabrics becomes impractical. Therefore, the effect of fabric structures was categorised into woven and knitted structures, and further evaluated in the experiment Phase II, Chapter 6, Section 6.4. The differences in the perception of tactile properties between woven and knitted were evaluated not only by comparing the distribution of participant

ratings, but also through fitted CLMM models, where structures were included as one of the fixed effects. The results showed that woven fabrics were typically perceived as stiffer, rougher, firmer, crisper than knitted fabrics under all experiment conditions, and as warmer than knitted fabrics when touching or observing the real fabrics.

8.3 The effect of rendered colour and measured colour of fabrics

Colour was a controlled variable in the experiment Phase I. By rendering the fabric images, the effect of rendered colour was evaluated on visual-tactile perception in the experiment Phase I. Meanwhile, the colours of fabrics in the experiment Phase II were measured, and the effect of fabric colour was evaluated on the tactile perception. Both analyses quantified the effect of colour in the CIELAB colour space. The results showed that colour played a limited role in visual-tactile and tactile perception. While a change of one unit in L^* , a^* , and b^* led to the variations in the tactile perceptual ratings, these variations were relatively minor on the 9-point Likert scale.

8.4 The correlations among experiment conditions and among tactile properties

The correlations were assessed from three perspectives: (1) data collected in the experiment Phase I (Chapter 4, Section 4.6 and 4.7), (2) data collected in the experiment Phase II (Chapter 5, Section 5.5 and 5.6), and (3) data from the experiment Phase II categorised by woven and knitted fabric structures (Chapter 6, Section 6.6).

As for the correlations among experiment conditions, several consistencies were observed across the three perspectives. Notably, draped fabric images and fabric rotation videos showed stronger correlations with actual touch and observation compared to flat fabric images. Strong and positive correlations

were observed between draped fabric images and fabric rotation videos, as well as among touch-only, vision-only (using real fabrics), and vision+touch.

Regarding the correlations among tactile properties, the perception of flexible-stiff, smooth-rough, and soft-firm remained consistently positively correlated. However, discrepancies were observed in the perceived spongy-crisp and warm-cool. In the experiment Phase I, the perception of spongy-crisp positively correlated with the perception of flexible-stiff, smooth-rough, and soft-firm, and the perception of warm-cool showed no significant correlation with other tactile properties. In contrast, data in the experiment Phase II revealed mixed correlations for the perception of spongy-crisp across different experiment conditions. The correlation between warm-cool and other tactile properties became significant.

8.5 The differences in the perception of tactile properties across different conditions

The differences in the perception of tactile properties were assessed from three perspectives: (1) between flat and draped fabric images in the experiment Phase I in Chapter 4 Section 4.5, (2) between visual representations (averaged from flat, draped fabric images and videos) and real fabrics (averaged from touch-only, vision-only using real fabrics, vision+touch) in the experiment Phase II in Chapter 5, Section 5.7, and (3) among the six experiment conditions evaluated using CLMM models in the experiment Phase II in Chapter 6, Section 6.4.3.

In the experiment Phase I, comparisons between flat and draped fabric images were made on individual fabrics, revealing mixed results across different fabrics. In contrast, most of fabrics were perceived as stiffer, rougher, firmer, and warmer through visual representations in the experiment Phase II. This trend was observed not only in the tactile perceptual ratings collected from participants, but also in the fitted tactile perceptual ratings from the CLMM models, indicating

robust consistency between the direct ratings and model predictions.

8.6 Model performance

In Chapter 7, models were developed to predict the visual-tactile perception and tactile perception through predictors from three categories: flat fabric images, draped fabric images, and fabric rotation videos. In addition to simple linear regression, three regularisation techniques (RR, LASSO, EN) were adopted to simplify the models by shrinking or eliminating irrelevant predictors. The results showed that the regularisation regressions outperformed the classical OLS linear regression, but the comparisons among RR, LASSO, and EN were mixed across tactile properties. For the models of flexible-stiff, smooth-rough, and soft-firm, predictors from draped fabric images or fabric rotation videos consistently outperformed those from flat fabric images in visual-tactile and tactile perception prediction. In contrast, models for warm-cool showed comparable performance across predictors from the three categories. However, despite the overall success of regularisation regression, the prediction of spongy-crisp remained a challenge, demonstrating poor performance across predictors from the three categories. By ranking the predictors based on the absolute standardised coefficients, fabric draped width emerged as a key predictor in visual-tactile perception and tactile-perception models, while fabric thickness was consistently identified as important in all tactile perception models. To further evaluate the image-irrelevant predictor, fabric thickness, additional models were developed for tactile perception by excluding thickness. The results showed that excluding thickness led to a slight reduction in model performance, except for smooth-rough. In addition, predictors extracted by GLCM, 2D FFT, and WT played different but important roles in all models.

8.7 Summary and contributions

The present study demonstrated a comprehensive evaluation of the perception of tactile properties of fabrics and developed predictive models to quantify

human tactile responses. The main contributions of the research were summarised below:

- A new Leeds Fabric Tactile Database was developed, and works were conducted using the database to evaluate the visual-tactile perception and tactile perception. Fabric images, fabric videos, real fabrics, and a set of tactile perceptual rating data were involved in the database.
- Compared to other fabric databases, the Leeds Fabric Tactile Database provided not only images and videos of real fabrics, but also digitally rendered images with controlled fabric material and colour variables. This approach allows for systematic investigation of different colours within the same fabric and different fabrics in the same colour. The use of digital rendering eliminates issues related to uneven dyeing and colour inconsistencies that often arise during the physical dyeing process of real fabrics.
- The psychophysical experiments conducted using the Leeds Fabric Tactile Database applied the method of categorical judgement. Participants were asked to rate the samples on a 9-point Likert scale. This approach allows the database to be continuously expanded, with newly added images and real fabrics evaluated individually and seamlessly integrated into the existing database. With more data, the prediction of visual-tactile and tactile perception will be possibly improved.
- The database holds the potential for applications in various research fields. For example, the high-resolution flat fabric images in the database may enable the development of algorithms for the efficient and accurate analysis of woven and knitted fabric structures. Moreover, the flat fabric images can be considered as colour patches with added texture, making the database a valuable resource for studying textured colour perception. The draped fabric images and fabric rotation videos also support the investigations into

the perception of colour on 3D objects. The effect of texture and shape will be possibly investigated using the database.

- Analyses across the Chapters in the thesis were interconnected and compared, providing a cohesive and comprehensive evaluation of the findings.
- The analyses were demonstrated in an interpretable way. Since the evaluation was conducted on a 9-point Likert scale, the effects of fabric structure, colour, and experiment conditions on tactile perceptual ratings were quantified within the 9-point range. Additionally, model performance was also presented in the same scale. Each point on the 9-point scale corresponded to specific description, making the whole study particularly consumer-friendly. The results can be easily translated into understandable information about tactile perception, helping consumers make informed decisions about fabric choices based on clear, descriptive ratings, regarding the background of consumers in the market.

8.8 Future work

The present study used five pairs of tactile descriptors: flexible-stiff, smooth-rough, soft-firm, spongy-crisp, and warm-cool, in the psychophysical experiments. The selection of tactile descriptors is based on the use in previous studies listed in Table 2.2. However, the description of fabric tactile properties is more than the 5 pairs. Tactile properties such as stretchiness (Mahar et al., 2013), fullness (Mahar et al., 2013; Sun et al., 2018), and sticky/slippery, uniform/regular (Mehta et al., 2014) etc., have not been evaluated under the comprehensive experiment conditions designed in the present study. The evaluation of such tactile properties can be studied in the future.

As discussed in Chapter 7, one of the limitations of the database is that the number of real fabrics is not very large. 15 and 118 real fabrics were included in database Part I and Part II, respectively. The correlation analyses and model

development were conducted based on the current database. Models predicting the visual-tactile and tactile perception achieved good results by adopting regression methods. The future study could involve more real fabrics and corresponding images and videos. With a larger-scale psychophysical experiment to collect more observation data, the models could be more robust by using a larger training dataset and independent testing dataset. Advanced modelling techniques, such as neural network, deep learning, and AI could be adopted to improve the predictive performance.

The effect of individual fabrics and fabric structures has been investigated in the fabric visual-tactile and tactile perception. Significant differences were found among individual fabrics and between woven and knitted fabrics. Given that fabrics can be used on multiple categories of products, such as sofa, garment, curtain, and carpet, the future study could involve one or more specific categories of fabric products, investigating the effect of fabric products and the interactive effect between fabric products and fabrics. A more targeted and comprehensive understanding of visual-tactile and tactile perception could be achieved by focusing on specific categories of fabric products.

The effect of colour on visual-tactile and tactile perception has been investigated in the present study. Even though colour showed a limited effect, the present study only included fabrics in a single colour, without involving multicoloured or patterned fabrics. Human perception of the aesthetics of fabric appearance is inherently complicated, suggesting that the future study could benefit from the inclusion of fabrics in multiple colours and various patterns.

Reference

- Ackerley, R., Saar, K., McGlone, F., & Backlund Wasling, H. 2014. Quantifying the Sensory and Emotional Perception of Touch: Differences Between Glabrous and Hairy Skin. *Frontiers in Behavioral Neuroscience*. [Online]. **8**, article no: 34. [Accessed 18 February 2025]. Available from: <https://doi.org/10.3389/fnbeh.2014.00034>
- Adobe. 2024. *What is White Balance?*. [Online]. [Accessed 10 February 2025]. Available from: <https://www.adobe.com/uk/creativecloud/video/discover/white-balance.html>
- Agresti, A. 2010. *Analysis of Ordinal Categorical Data*. 2nd ed. Hoboken, NJ: Wiley.
- Aron, A., Coups, E. J., & Aron, E. 2013. *Statistics for Psychology*. 6th ed. Boston, MA; London: Pearson.
- Atav, R., & Keskin, S. 2024. Investigation of the effects of colour on the user's fabric handle perception and warm/cool feeling. *Coloration Technology*. [Online]. **140**(6), pp. 913-924. [Accessed 25 February 2025]. Available from: <https://doi.org/10.1111/cote.12756>
- Bacci, L., Camilli, F., Drago, S., Magli, M., Vagnoni, E., Mauro, A., & Predieri, S. 2012. Sensory Evaluation and Instrumental Measurements to Determine Tactile Properties of Wool Fabrics. *Textile Research Journal*. [Online]. **82**(14), pp. 1430–1441. [Accessed 16 February 2025]. Available from: <https://doi.org/10.1177/0040517512438125>
- Bala, R. 2003. *Device Characterization*. In: Sharma, G. ed. *Digital Color Imaging Handbook*. Boca Raton, FL: CRC Press
- Baumgartner, E., Wiebel, C. B., & Gegenfurtner, K. R. 2013. Visual and Haptic Representations of Material Properties. *Multisensory Research*. [Online]. **26**(5), pp. 429–455. [Accessed 16 February 2025]. Available from: <https://doi.org/10.1163/22134808-00002429>

- Bergmann Tiest, W.M. and Kappers, A.M.L. 2006. Analysis of haptic perception of materials by multidimensional scaling and physical measurements of roughness and compressibility. *Acta Psychologica*. [Online]. **121**(1), pp.1–20. [Accessed 9 March 2025]. Available from: <https://doi.org/10.1016/j.actpsy.2005.04.005>
- Berns, R. S. 1996. Methods for Characterizing CRT Displays. *Displays*. [Online]. **16**(4), pp. 173-182. [Accessed 14 February 2025]. Available from: [https://doi.org/10.1016/0141-9382\(96\)01011-6](https://doi.org/10.1016/0141-9382(96)01011-6)
- Berns, R. S. 2019. *Numerical Color Specification: Colorimetry*. In: *Principles of Color Technology*. 4th ed. Hoboken, NJ: Wiley, pp. 51-84.
- Berns, R. S., Gorzynski, M. E., & Motta, R. J. 1993. CRT Colorimetry. Part II: Metrology. *Color Research & Application*. [Online]. **18**(5), pp. 315–325. [Accessed 15 February 2025]. Available from: <https://doi.org/10.1002/col.5080180505>
- Bertaux, E., Lewandowski, M., & others. 2007. Relationship between Friction and Tactile Properties for Woven and Knitted Fabrics. *Textile Research Journal*. [Online]. **77**(6), pp. 387–396X. [Accessed 21 February 2025]. Available from: <https://doi.org/10.1177/0040517507074165>
- Bhatta, S. R., Tiippana, K., Vahtikari, K., Hughes, M., & Kyttä, M. 2017. Sensory and Emotional Perception of Wooden Surfaces Through Fingertip Touch. *Frontiers in Psychology*. [Online]. **8**, article no: 367. [Accessed 18 February 2025]. Available from: <https://doi.org/10.3389/fpsyg.2017.00367>
- Bouman, K. L., Xiao, B., & Battaglia, P. 2013. Estimating the Material Properties of Fabric from Video. In: IEEE. ed. *Proceedings of the IEEE International Conference on Computer Vision (ICCV), 1–8 December 2013, Sydney, Australia*. New York: IEEE, pp. 1984–1991.
- Breen, D.E., & House, D.H. 2001. *Cloth Modeling and Animation*. Natick, MA: A K Peters.
- Brigham, E. O. 1988. *The Fast Fourier Transform and Its Applications*. Englewood Cliffs, NJ: Prentice-Hall.

- British Standards Institution. 1973. BS 5058:1973. *Methods for assessment of drape of fabrics*. London: BSI.
- Cabral, I., Santiago, D., & Steffens, F. 2023. Chromic Textiles: Colour Fastness Properties and Irreversible Colour Change Behaviour of Textiles Screen Printed with Thermochromic, Photochromic and Hydrochromic Colourants. *Coloration Technology*. [Online]. **139**(3). [Accessed 14 February 2025]. Available from: <https://doi.org/10.1111/cote.12660>
- Carrera-Gallissa, E., Capdevila, X., Álvarez, J. and Sainz, V. 2017. Evaluating drape shape in woven fabrics. *Journal of the Textile Institute*. [Online]. **108**(3), pp.325-336. [Accessed 9 March 2025]. Available from: <https://doi.org/10.1080/00405000.2016.1166804>.
- Chae, Y. 2024. Spectrophotometric and Calculative Determination Methods of Textile Color-Difference Threshold Considering the Observing Condition. *Research Journal of Textile and Apparel*. [Online]. **28**(1). [Accessed 14 February 2025]. Available from: <https://doi.org/10.1108/rjta-05-2024-0075>
- Chae, Y. & Lee, E. 2021. Color Inconstancy of Chromatic and Achromatic Textile Fabrics with Changes in the Correlated Color Temperature and Luminance of the Light Source. *Fibers and Polymers*. [Online]. **22**(10), pp. 2672-2772. [Accessed 14 February 2025]. Available from: <https://doi.org/10.1007/s12221-021-0769-4>
- Chae, Y., Lee, M., & Cho, G. 2011. Mechanical Properties and Tactile Sensation of Naturally Colored Organic Cotton Fabrics. *Fibers and Polymers*. [Online]. **12**, pp. 1042–1047. [Accessed 21 February 2025]. Available from: <https://doi.org/10.1007/s12221-011-1042-z>
- Chan, C., & Pang, G.K.H. Fabric defect detection by Fourier analysis. *IEEE Transactions on Industry Applications*. [Online]. **36**(5), pp.1267-1276. [Accessed 24 February 2025]. Available from: <https://ieeexplore.ieee.org/abstract/document/871274>
- Chang, T., & Kuo, C.C.J. 1993. Texture analysis and classification with tree-structured wavelet transform. *IEEE Transactions on Image Processing*.

- [Online]. **2**(4), pp. 429-441. [Accessed 24 February 2025]. Available from: <https://ieeexplore.ieee.org/abstract/document/242353/>
- Choi, C.J., Kim, H.J., Jin, Y.C., & Kim, H.S. 2009. Objective wrinkle evaluation system of fabrics based on 2D FFT. *Fibers and Polymers*. [Online]. **10**, pp. 260-265. [Accessed 24 February 2025]. Available from: <https://link.springer.com/article/10.1007/s12221-009-0260-0>
- Chromaxion. 2025. *ColorChecker DC*. [Online]. [Accessed 13 February 2025]. Available from: https://www.chromaxion.com/information/colorchecker_dc.html
- Chu, C.C., Cummings, C.L., and Teixeira, N.A. 1950. Mechanics of elastic performance of textile materials: Part V: A study of the factors affecting the drape of fabrics—the development of a drape meter. *Textile Research Journal*. [Online]. **20**(8), pp.539-548. [Accessed 9 March 2025]. Available from: <https://journals.sagepub.com/doi/abs/10.1177/004051755002000802>
- Chu, V., McMahon, I., Riano, L., McDonald, C. G., He, Q., Martinez Perez-Tejada, J., Arrigo, M., & Others. 2013. Using Robotic Exploratory Procedures to Learn the Meaning of Haptic Adjectives. In: IEEE. ed. *Proceedings of the IEEE International Conference on Robotics and Automation (ICRA 2013), 6–10 May 2013, Karlsruhe, Germany*. Piscataway, NJ: IEEE, pp. 3048–3055. [Accessed 10 February 2025]. Available from: <https://doi.org/10.1109/ICRA.2013.6631000>
- CIE. 2018. *Colorimetry*. 4th ed. United CIE Pub. No.015. DOI: 10.25039/TR.015.2018
- Clarke, F. J., MacDonald, R., & Rigg, B. 1984. Modification of the JPC79 Colour-Difference Formula. *Journal of the Society of Dyers and Colourists*. [Online]. **100**(4), pp. 128-132. [Accessed 20 February 2025]. Available from: <https://doi.org/10.1111/j.1478-4408.1984.tb00969.x>
- Cui, G., Luo, M. R., Rhodes, P. A., & Rigg, B. 2003. Grading Textile Fastness. Part 1: Using a Digital Camera System. *Coloration Technology*. [Online]. **119**(5), pp. 212-218. [Accessed 14 February 2025]. Available from:

<https://doi.org/10.1111/j.1478-4408.2003.tb00174.x>

Cusick, G.E. 1968. 21—The measurement of fabric drape. *Journal of the Textile Institute*. [Online]. **59**(6), pp.253-260. [Accessed 9 March 2025]. Available from:

https://www.tandfonline.com/doi/abs/10.1080/00405006808659985?casa_token=hufsxEBWUNkAAAAA:HIjkJz33cSbA_QAnrk9z4wyFNIhPIb0D9SBqP3spjR6X1N0HO-qqSIbmRZAjU6v3b1Kqm3obsSPo-A.

Datacolor. 2025. *Datacolor 200*. [Online]. [Accessed 14 February 2025]. Available from: <https://www.datacolor.com/business-solutions/product/datacolor-200/>

Drewing, K., Ramisch, A., & Bayer, F. 2009. Haptic, Visual and Visuo-Haptic Softness Judgments for Objects with Deformable Surfaces. In: IEEE. ed. *Proceedings of the IEEE World Haptics Conference, 18–20 March 2009, Salt Lake City, USA*. Piscataway, NJ: IEEE, pp. 640–645.

Elkharraz, G., Thumfart, S., & Akay, D. 2013. Making Tactile Textures with Predefined Affective Properties. *IEEE Transactions on Haptics*. [Online]. **5**(1), pp. 57–70. [Accessed 21 February 2025]. Available from: <https://ieeexplore.ieee.org/abstract/document/6626305/>

Fairchild, M. D. 2013. *Color Appearance Models*. 3rd ed. Chichester, UK: Wiley.

Feick, M., Degraen, D., & Hupperich, F. 2023. MetaReality: Enhancing tactile experiences using actuated 3D-printed metamaterials in virtual reality. *Frontiers in Virtual Reality*. [Online]. **4**. Article no: 1172381. [Accessed 25 February 2025]. Available from: <https://www.frontiersin.org/articles/10.3389/frvir.2023.1172381/full>

Fenko, A., Schifferstein, H. N. J., & Hekkert, P. 2010. Looking Hot or Feeling Hot: What Determines the Product Experience of Warmth? *Materials & Design*. [Online]. **31**(3), pp. 1325-1331. [Accessed 10 February 2025]. Available from: <https://www.sciencedirect.com/science/article/pii/S0261306909004932>

Fradin, J., Haliyo, S., & Gueorguiev, D. 2023. Humans struggle to perceive

- congruence in visuo-haptic textures. In: IEEE. ed. *Proceedings of the 2023 IEEE World Haptics Conference, 10-13 July 2023, Delft, Netherlands*. NJ: IEEE, pp. 128-133.
- Friedman, J., Hastie, T. and Tibshirani, R. 2010. Regularization paths for generalized linear models via coordinate descent. *Journal of Statistical Software*. [Online]. **33**, pp.1–22. [Accessed 9 March 2025]. Available from: <https://www.jstatsoft.org/article/view/v033i01>.
- Gao, Y., Hendricks, L. A., Kuchenbecker, K. J., & Darrell, T. 2016. Deep Learning for Tactile Understanding from Visual and Haptic Data. In: IEEE. ed. *Proceedings of the IEEE International Conference on Robotics and Automation (ICRA 2016), 16–21 May 2016, Stockholm, Sweden*. Piscataway, NJ: IEEE, pp. 536–543. [Accessed 16 February 2025]. Available from: <https://doi.org/10.1109/ICRA.2016.7487176>
- Gescheider, G. A. 1997. *Psychophysics: The Fundamentals*. 3rd ed. Mahwah, NJ: Lawrence Erlbaum Associates.
- Glombikova, V. and Kus, Z. 2014. Drape evaluation by the 3D drape scanner. *Textile and Apparel*. [Online]. **24**(3), pp.279-285. [Accessed 9 March 2025]. Available from: <https://dergipark.org.tr/en/pub/tekstilvekonfeksiyon/issue/23645/251860>
- Guest, S., Dessirier, J. M., Mehrabyan, A., McGlone, F., Essick, G., Gescheider, G., Fontana, A., Xiong, R., Ackerley, R., & Blot, K. 2011. The Development and Validation of Sensory and Emotional Scales of Touch Perception. *Attention, Perception, & Psychophysics*. [Online]. **73**(2), pp. 531–550. [Accessed 16 February 2025]. Available from: <https://doi.org/10.3758/s13414-010-0037-y>
- Haleem, N., Liu, X., Hurren, C. and Gordon, S. 2019. Investigating the cotton ring spun yarn structure using micro computerized tomography and digital image processing techniques. *Textile Research Journal*. [Online]. **89**(15), pp.3007-3023. [Accessed 9 March 2025]. Available from: <https://doi.org/10.1177/0040517518805387>.

- Haralick, R. M., Shanmugam, K., & Dinstein, I. 1973. Textural Features for Image Classification. *IEEE Transactions on Systems, Man, and Cybernetics*. [Online]. **(6)**, pp. 610–621. [Accessed 21 February 2025]. Available from: <https://doi.org/10.1109/TSMC.1973.4309314>
- Hassan, W., Joolee, J. B., & Jeon, S. 2023. Establishing Haptic Texture Attribute Space and Predicting Haptic Attributes from Image Features Using 1D-CNN. *Scientific Reports*. [Online]. **13**(1), article no:11684. [Accessed 21 February 2025]. Available from: <https://doi.org/10.1038/s41598-023-38929-6>
- Hastie, T., Tibshirani, R., & Friedman, J. 2009. *The Elements of Statistical Learning: Data Mining, Inference, and Prediction*. 2nd ed. New York: Springer.
- Havenith, G. 1999. Heat balance when wearing protective clothing. *Annals of Occupational Hygiene*. [Online]. **43**(5), pp.339-346. [Accessed 9 March 2025]. Available from: <https://doi.org/10.1093/annhyg/43.5.289>
- He, R., Xiao, K., Pointer, M., & Bressler, Y. 2022. Development of an Image-Based Measurement System for Human Facial Skin Colour. *Color Research & Application*. [Online]. **47**(4), pp. 943–957. [Accessed 13 February 2025]. Available from: <https://doi.org/10.1002/col.22737>
- Hong, G., Luo, M. R., & Rhodes, P. A. 2001. A Study of Digital Camera Colorimetric Characterization Based on Polynomial Modeling. *Color Research & Application*. [Online]. **26**(1), pp. 76–84. [Assessed 13 February 2025]. Available from [https://doi.org/10.1002/1520-6378\(200102\)26:1<76::AID-COL8>3.0.CO;2-3](https://doi.org/10.1002/1520-6378(200102)26:1<76::AID-COL8>3.0.CO;2-3)
- Howitt, D., & Cramer, D. 2011. *Introduction to Statistics in Psychology*. 5th ed. Harlow, UK: Pearson.
- Hu, G.H., Wang, Q.H., & Zhang, G.H. 2015. Unsupervised defect detection in textiles based on Fourier analysis and wavelet shrinkage. *Applied Optics*. [Online]. **54**(10), pp. 2963-2980. [Accessed 23 February 2025]. Available from: <https://opg.optica.org/abstract.cfm?uri=ao-54-10-2963>

- Hu, J. 2004. *Structure and Mechanics of Woven Fabrics*. Cambridge: Woodhead Publishing Ltd.
- Hunt, R. W. G. & Pointer, M. R. 2011. *Measuring Colour*. 4th ed. Chichester, UK: Wiley.
- International Organization for Standardization. 2005. ISO 139:2005. *Standard atmosphere for conditioning and testing*. Geneva: ISO.
- Jeguirim, S., Dhouib, A. B., & Others. 2010. Sensory and Instrumental Techniques Evaluating the Effect of Structure Parameters on the Tactile Properties of Knitted Fabrics. *Journal of Texture Studies*. [Online]. **41**(5), pp. 714–735 [Accessed 21 February 2025]. Available from: <https://doi.org/10.1111/j.1745-4603.2010.00251.x>
- JETI. 2025. *specbos 1211-2 Spectroradiometer*. [Online]. [Accessed 14 February 2025]. Available from: <https://www.jeti.com/Products/Spectroradiometer/specbos1211-2>
- Ji, F., Li, R., and Qiu, Y. 2006. Simulate the Dynamic Draping Behavior of Woven and Knitted Fabrics. *Journal of Industrial Textiles*. [Online]. **35**(3), pp. 201–215. [Accessed 6 March 2025]. Available from: <https://doi.org/10.1177/1528083706055753>
- Jiao, J., Zhang, Y., Wang, D., & Guo, X. 2019. HapTex: A Database of Fabric Textures for Surface Tactile Display. In: IEEE. ed. *Proceedings of the 2019 IEEE World Haptics Conference, 9-12 July 2019, Tokyo, Japan*. Piscataway, NJ: IEEE, pp. 331–336.
- Kampouris, C., Zafeiriou, S., Ghosh, A., & Malassiotis, S. 2016. Fine-Grained Material Classification Using Micro-Geometry and Reflectance. In: Leibe, B., Matas, J., Sebe, N., & Welling, M. (eds.) *Proceedings of the 14th European Conference on Computer Vision (ECCV 2016), 11-14 October 2016, Amsterdam, Netherlands*. Cham, Switzerland: Springer, pp. 778–792.
- Kang Z, Yuan C, Yang Q. 2013. The fabric defect detection technology based on wavelet transform and neural network convergence. In: IEEE. ed. *Proceedings of the 2013 IEEE International Conference on Information and*

- Automation (ICInfA)*, 26-28 August 2013, Yinchuan, China. IEEE, pp. 597-601.
- Kawabata, S. 1984. Development of the objective measurement of fabric handle. *Journal of Industrial Fabrics*. [Online]. 4, pp.4-31. [Accessed 9 March 2025]. Available from: <https://cir.nii.ac.jp/crid/1573387449960038784>.
- Kenkare, N., Lamar, T.A.M., and Pandurangan, P. 2008. Enhancing accuracy of drape simulation. Part I: Investigation of drape variability via 3D scanning. *Journal of the Textile Institute*. [Online]. **99**(3), pp.211-218. [Accessed 9 March 2025]. Available from: <https://www.tandfonline.com/doi/abs/10.1080/00405000701489222>.
- Kikuchi, K., Mizokami, Y., & Egawa, M. 2020. Development of an Image Evaluation Method for Skin Color Distribution in Facial Images and its Application: Aging Effects and Seasonal Changes of Facial Color Distribution. *Color Research & Application*. [Online]. **45**(6), pp. 1243–1253. [Accessed 13 February 2025]. Available from: <https://doi.org/10.1002/col.22469>
- Konica Minolta. 2025a. *CS-2000 Spectroradiometer*. [Online]. [Accessed 14 February 2025]. Available from: <https://sensing.konicaminolta.us/us/products/cs-2000-spectroradiometer/>
- Konica Minolta. 2025b. *CM-700d Spectrophotometer*. [Online]. [Accessed 14 February 2025]. Available from: <https://sensing.konicaminolta.us/us/products/cm-700d-spectrophotometer/>
- Kumah, C., Zhang, N., Raji, R. K., & Pan, R. 2019. Color Measurement of Segmented Printed Fabric Patterns in Lab Color Space from RGB Digital Images. *Journal of Textile Science and Technology*. [Online]. **5**(3), pp. 1-18. [Accessed 14 February 2025]. Available from: <https://www.scirp.org/journal/paperinformation.aspx?paperid=90206>
- Kuo, C. F. J., & Tsai, C. C. 2006. Automatic Recognition of Fabric Nature by Using the Approach of Texture Analysis. *Textile Research Journal*. [Online]. **76**(5), pp. 375–382. [Accessed 21 February 2025]. Available from:

<https://doi.org/10.1177/0040517506063917>

- Leung, T. and Malik, J. 1999. Recognizing surfaces using three-dimensional textures. In: IEEE. ed. *Proceedings of the Seventh IEEE International Conference on Computer Vision, 20-27 September 1999, Kerkyra, Greece*. Los Alamitos, CA: IEEE Computer Society, pp.1010-1017.
- Li, P., Zhang, H., Jing, J., Li, R., & Zhao, J. 2015. Fabric defect detection based on multi-scale wavelet transform and Gaussian mixture model method. *The Journal of The Textile Institute*. [Online]. **106**(6), pp.587-592. [Accessed 25 February 2025]. Available from: <https://www.tandfonline.com/doi/abs/10.1080/00405000.2014.929790>
- Li, Q., Zhang, F., Jin, X., & Zhu, C. 2014. Optimal Yarn Colour Combination for Full-Colour Fabric Design and Mixed-Colour Chromaticity Coordinates Based on CIE Chromaticity Diagram Analysis. *Coloration Technology*. [Online]. **130**(2), pp. 437-444. [Accessed 14 February 2025]. Available from: <https://doi.org/10.1111/cote.12117>
- Lee, W.Y., Luo, M.R. and Ou, L.C. 2009. Assessing the affective feelings of two- and three-dimensional objects. *Color Research & Application*. [Online]. **34**(1), pp.75–83. [Accessed 9 March 2025]. Available from: <https://doi.org/10.1002/col.20464>
- Luo, L., Shen, H. L., Shao, S. J., & Xin, J. H. 2016. Colour Matching Comparison Between Spectrophotometric and Multispectral Imaging Measurements. *Coloration Technology*. [Online]. **132**(4), pp. 282–291. [Accessed 14 February 2025]. Available from: <https://doi.org/10.1111/cote.12191>
- Luo, L., Zhang, M., Yang, Y., and Zhang, Y. 2015. A multispectral imaging approach to colour measurement and colour matching of single yarns without winding. *Coloration Technology*. [Online]. **131**(4), pp.342-351. [Accessed 9 March 2025]. Available from: <https://doi.org/10.1111/cote.12162>.
- Luo, M. R., Cui, G., & Rigg, B. 2001. The Development of the CIE 2000 Colour-Difference Formula: CIEDE2000. *Color Research & Application*. [Online].

- 26**(5), pp. 340–350. [Accessed 20 February 2025]. Available from <https://doi.org/10.1002/col.1049>
- Luo, S., Yuan, W., Adelson, E., & Cohn, A. G. 2018. ViTac: Feature Sharing Between Vision and Tactile Sensing for Cloth Texture Recognition. In: IEEE. ed. *Proceedings of the IEEE International Conference on Robotics and Automation (ICRA 2018), 21–25 May 2018, Brisbane, Australia*. Piscataway, NJ: IEEE, pp. 2722–2727.
- Mahmood, T., Ashraf, R., & Faisal, C.M.N. 2023. An efficient scheme for the detection of defective parts in fabric images using image processing. *The Journal of The Textile Institute*. [Online]. **114**(7), pp.1041-1049. [Accessed 25 February 2025]. Available from: <https://www.tandfonline.com/doi/abs/10.1080/00405000.2022.2105114>
- Mahar, T. J., Wang, H., & Postle, R. 2013. A Review of Fabric Tactile Properties and Their Subjective Assessment for Next-to-Skin Knitted Fabrics. *Journal of the Textile Institute*. [Online]. **104**(6), pp. 572–589. [Accessed 16 February 2025]. Available from: <https://doi.org/10.1080/00405000.2013.774947>
- Malek, A.S., Drean, J.Y., & Bigue, L. 2013. Optimization of automated online fabric inspection by fast Fourier transform (FFT) and cross-correlation. *Textile Research Journal*. [Online]. **83**(3), pp. 256-268. [Accessed 24 February 2025]. Available from: <https://doi.org/10.1177/0040517512458340>
- Mao, N. 2014. Towards Objective Discrimination & Evaluation of Fabric Tactile Properties: Quantification of Biaxial Fabric Deformations by Using Energy Methods. In: *Proceedings of the 14th AUTEX World Textile Conference, 26–28 May 2014, Bursa, Turkey*. AUTEX.
- Mazzuchetti, G., Demichelis, R., Songia, M. B., & Others. 2008. Objective Measurement of Tactile Sensitivity Related to a Feeling of Softness and Warmth. *Fibres & Textiles in Eastern Europe*. [Online]. **16**(4), pp. 67–71. [Accessed 18 February 2025]. Available from:

http://www.fibtex.lodz.pl/69_17_67.pdf

- McCullough, E.A., Eckels, S. and Harms, C. 2009. Determining temperature ratings for children's cold weather clothing. *Applied Ergonomics*. [Online]. **40**(5), pp.870–877. [Accessed 9 March 2025]. Available from: <https://doi.org/10.1016/j.apergo.2008.12.004>
- Mehta, S., Holásková, I., & Walker, M. 2024. Tactile Sensitivity Alters Textile Touch Perception. *PLOS ONE*. [Online]. **19**(9), article no: e0308957. [Accessed 19 February 2025]. Available from: <https://journals.plos.org/plosone/article?id=10.1371/journal.pone.0308957>
- Mei, Z., Shen, W., Wang, Y., Yang, J., Zhou, T. and Zhou, H. 2015. Unidirectional fabric drape testing method. *PLOS ONE*. [Online]. **10**(11), article no: e0143648. [Accessed 9 March 2025]. Available from: <https://journals.plos.org/plosone/article?id=10.1371/journal.pone.0143648>.
- Minazio, G.P. 1995. FAST-fabric assurance by simple testing. *International Journal of Clothing Science and Technology*. [Online]. **7** (2/3) , pp.43-48. [Accessed 9 March 2025]. Available from: <https://www.emerald.com/insight/content/doi/10.1108/09556229510087146/full/html>.
- Mirjalili, F. & Hardeberg, J. Y. 2019. Appearance Perception of Textiles: A Tactile and Visual Texture Study. In: *Color and Imaging Conference (CIC27)*, 21–25 October 2019, Paris, France. Springfield, VA: Society for Imaging Science and Technology, pp. 43–48.
- Morovic, J. 1998. *To Develop a Universal Gamut Mapping Algorithm*. PhD thesis, University of Derby.
- Muck, D., Tomc, H. G., Elesini, U. S., Ropret, M., & Leskovšek, M. 2021. Colour Fastness to Various Agents and Dynamic Mechanical Characteristics of Biocomposite Filaments and 3D Printed Samples. *Polymers*. [Online]. **13**(21). Article no: 3738. [Accessed 14 February 2025]. Available from: <https://doi.org/10.3390/polym13213738>

- Ou, L.C. and Luo, M.R. 2006. A colour harmony model for two-colour combinations. *Color Research & Application*. [Online]. **31**(3), pp.191–204. [Accessed 9 March 2025]. Available from: <https://doi.org/10.1002/col.20208>
- Ou, L.C., Luo, M.R., Sun, P.L., Hu, N.C., Chen, H.S., Lin, H.S., Lai, C.H., Hsieh, S.H., Wei, M.S., Weng, C.H., et al. 2012. A cross-cultural comparison of colour emotion for two-colour combinations. *Color Research & Application*. [Online]. **37**(1), pp.23–43. [Accessed 9 March 2025]. Available from: <https://doi.org/10.1002/col.20648>
- Ou, L.C., Luo, M.R., Woodcock, A., & Wright, A. 2004. A study of colour emotion and colour preference. Part I: Colour emotions for single colours. *Color Research & Application*. [Online]. **29**(3), pp. 232-240. [Accessed 25 February 2025]. Available from: <https://doi.org/10.1002/col.20010>
- Oxford University Press. 2025a. *Oxford English Dictionary*. [Online]. [Accessed 9 March 2025]. Available from: <https://www.oed.com/?tl=true>.
- Oxford University Press. 2025b. *Oxford English Dictionary: “stiff”*. [Online]. [Accessed 9 March 2025]. Available from: <https://www.oed.com/search/dictionary/?scope=Entries&q=stiff>.
- Pan, N. 2006. Quantification and Evaluation of Human Tactile Sense Towards Fabrics. *International Journal of Design & Nature and Ecodynamics*. [Online]. **1**(1), pp. 48–60. [Accessed 16 February 2025]. Available from: <https://doi.org/10.2495/D&N-V1-N1-48-60>
- Pantone. 2025a. *Skintone Guide Limited Edition*. [Online]. [Accessed 13 February 2025]. Available from: <https://www.pantone.com/uk/en/products/fashion-home-interiors/skintone-guide-limited-edition>
- Pantone. 2025b. *Fashion, Home + Interiors Color Guide*. [Online]. [Accessed 13 February 2025]. Available from: <https://www.pantone.com/uk/en/products/fashion-home-interiors/fashion-home-interiors-color-guide>

- Phillips, J. B. & Eliasson, H. 2018. *Camera Image Quality Benchmarking*. Cham, Switzerland: Springer.
- Popa, S., Radulescu-Grad, M. E., Perdivara, A., & Others. 2021. Aspects Regarding Colour Fastness and Adsorption Studies of a New Azo-Stilbene Dye for Acrylic Resins. *Scientific Reports*. [Online]. **11**, article no: 5889. [Accessed 14 February 2025]. Available from: <https://doi.org/10.1038/s41598-021-85452-7>
- Robertson, A.R. 1978. CIE guidelines for coordinated research on colour-difference evaluation. *Color Research & Application*. [Online]. **3**(3), pp.149-151. [Accessed 9 March 2025]. Available from: <https://doi.org/10.1002/j.1520-6378.1978.tb00001.x>
- Rombaldoni, F., Demichelis, R., & Others. 2010. Prediction of Human Psychophysical Perception of Fabric Crispness and Coolness Hand from Rapidly Measurable Low-Stress Mechanical and Thermal Parameters. *Journal of Sensory Studies*. [Online]. **25**(6), pp. 899-916. [Accessed 18 February 2025]. Available from: <https://doi.org/10.1111/j.1745-459X.2010.00312.x>
- Sanad, R.A. and Cassidy, T. 2015. Fabric objective measurement and drape. *Textile Progress*. [Online]. **47**(4), pp. 317-406. [Accessed 9 March 2025]. Available from: <https://www.tandfonline.com/doi/abs/10.1080/00405167.2015.1117243>
- Siegel, S. & Castellan, N. J. 1988. *Nonparametric Statistics for the Behavioral Sciences*. 2nd ed. New York: McGraw-Hill.
- Sifuzzaman, M., Islam, M.R. & Ali, M.Z. 2009. Application of wavelet transform and its advantages compared to Fourier transform. *Journal of hysical Science*. [Online]. **13**, pp.121-134. [Accessed 10 February 2025]. Available from: <https://ir.vidyasagar.ac.in/handle/123456789/779>
- Silvestre-Blanes, J., Albero-Albero, T., Miralles, I., & Ferris, R. 2019. A Public Fabric Database for Defect Detection Methods and Results. *Autex Research Journal*. [Online]. **19**(4), pp. 363–374. [Accessed 10 February

- 2025]. Available from: <https://doi.org/10.2478/aut-2019-0035>
- Soufflet, I., Calonnier, M., & Dacremont, C. 2004. A Comparison Between Industrial Experts' and Novices' Haptic Perceptual Organization: A Tool to Identify Descriptors of the Handle of Fabrics. *Food Quality and Preference*. [Online]. **15**(7–8), pp. 689-699. [Accessed 19 February 2025]. Available from: <https://www.sciencedirect.com/science/article/pii/S0950329304000370>
- Stevens, S. S. 1946. On the Theory of Scales of Measurement. *Science*. [Online]. **103**(2684), pp. 677-680. [Accessed 12 February 2025]. Available from: <https://doi.org/10.1126/science.103.2684.677>.
- Strazdiene, E. 2011. Textiles Objective and Sensory Evaluation in Rapid Prototyping. *Materials Science*. [Online]. **17**(4), pp. 407–412. [Accessed 18 February 2025]. Available from: <https://www.matssc.ktu.lt/index.php/MatSc/article/view/778>
- Sun, F., Du, Z., & Naebe, M. 2018. Determination of Model Parameters for Predicting Handle Characteristics of Wool-Rich Suiting Woven Fabrics Based on the Wool HandleMeter and KES-F. *The Journal of The Textile Institute*. [Online]. **109**(2), pp. 147-159. [Accessed 18 February 2025]. Available from: <https://doi.org/10.1080/00405000.2017.1334308>
- Sun, J. 2012. Fabric Wrinkle Characterization and Classification Using Modified Wavelet Coefficients and Support-Vector-Machine Classifiers. Master's thesis, The University of Texas at Austin.
- Suzuki, Y., & Sukigara, S. 2013. Mechanical and Tactile Properties of Plain Knitted Fabrics Produced from Rayon Vortex Yarns. *Textile Research Journal*. [Online]. **83**(7), pp. 740-751. [Accessed 21 February 2025]. Available from: <https://doi.org/10.1177/0040517512467132>
- Sztandera, L. M., Cardello, A. V. & Others. 2013. Identification of the Most Significant Comfort Factors for Textiles from Processing Mechanical, Handfeel, Fabric Construction, and Perceived Tactile Comfort Data. *Textile Research Journal*. [Online]. **83**(1), pp. 34–43. [Accessed 15 February 2025].

Available

from:

<https://journals.sagepub.com/doi/abs/10.1177/0040517512438121>

- Takahashi, K., & Tan, J. 2019. Deep Visuo-Tactile Learning: Estimation of Tactile Properties from Images. In: IEEE. ed. *Proceedings of the 2019 International Conference on Robotics and Automation (ICRA), 20–24 May 2019, Montreal, Canada*. Piscataway, NJ: IEEE, pp. 8951–8957.
- Talu, M.F., Hanbay, K., & Varjovi, M.H. 2022. CNN-based fabric defect detection system on loom fabric inspection. *Textile and Apparel*. [Online]. **32**(3), pp.208-219. [Accessed 25 February 2025]. Available from: <https://dergipark.org.tr/en/pub/tekstilvekonfeksiyon/issue/72837/1032529>
- THE FABRICS DATABASE, Imperial College London. 2016. *Fabrics Dataset - iBUG Group*. [Online]. [Accessed 15 February 2025]. Available from: <https://ibug.doc.ic.ac.uk/resources/fabrics/>
- Thurstone, L.L. 1927. A law of comparative judgment. *Psychological Review*. **34**(4), pp.273–286.
- Topliss, J., Lukosch, S., Coutts, E., & Piumsomboon, T. 2023. Manipulating underfoot tactile perceptions of flooring materials in augmented virtuality. *Applied Sciences*. [Online]. **13**(24), Article no: 13106. [Accessed 25 February 2025]. Available from: <https://www.mdpi.com/2076-3417/13/24/13106>
- Torgerson, W.S. 1958. *Theory and methods of scaling*. New York: Wiley.
- VeriVide. 2025. *DigiEye System*. [Online]. [Accessed 13 February 2025]. Available from: <https://www.verivide.com/product-category/verivide-products/digieye-system/>
- Wang, F., Li, Y., Tao, L., Wu, J., & Others. 2023. A Human-Like Siamese-Based Visual-Tactile Fusion Model for Object Recognition. *IEEE Transactions on Cognitive and Developmental Systems*. [Online]. **16**(3), pp. 850-863. [Accessed 22 February 2025]. Available from: <https://ieeexplore.ieee.org/abstract/document/10239300/>.
- Wang, J., Shi, K., Wang, L., & Pan, R. 2020. A computer vision system for

- objective fabric smoothness appearance assessment with an ensemble classifier. *Textile Research Journal*. [Online]. **90**(9-10), pp. 333-343. [Accessed 24 February 2025]. Available from: <https://doi.org/10.1177/0040517519866951>
- Wang, X., & Georganas, N. D. 2009. GLCM Texture Based Fractal Method for Evaluating Fabric Surface Roughness. In: IEEE. ed. *Proceedings of the 2009 Canadian Conference on Computer and Robot Vision (CRV)*, 25–27 May 2009, Kelowna, Canada. Piscataway, NJ: IEEE, pp. 104-107.
- Westland, S., Ripamonti, C., & Cheung, V. 2012. *Computational Colour Science Using MATLAB*. 2nd ed. Chichester, UK: Wiley.
- Wijntjes, M. W. A., Xiao, B., & Volcic, R. 2019. Visual Communication of How Fabrics Feel. *Journal of Vision*. [Online]. **19**(4), article no: 4. [Accessed 16 February 2025]. Available from: <https://doi.org/10.1167/19.2.4>
- X-Rite. 2025a. *ColorChecker Classic*. [Online]. [Accessed 13 February 2025]. Available from: <https://www.xrite.com/categories/calibration-profiling/colorchecker-classic>
- X-Rite. 2025b. *ColorChecker Digital SG*. [Online]. [Accessed 13 February 2025]. Available from: <https://www.xrite.com/categories/calibration-profiling/colorchecker-digital-sg>
- Xiao, B., Bi, W., Jia, X., Wei, H., & Adelson, E. H. 2016. Can You See What You Feel? Color and Folding Properties Affect Visual–Tactile Material Discrimination of Fabrics. *Journal of Vision*. [Online]. **16**(3). Article no: 34. [Accessed 16 February 2025]. Available from: <https://doi.org/10.1167/16.3.34>
- Xu, S., Xu, H., Mao, F., Ji, M., & Yang, W. 2024. Visual and Corresponding Tactile Dataset of Flexible Material for Robots and Cross-Modal Perception. *Data in Brief*. [Online]. **52**, article no: 109755. [Accessed 16 February 2025]. Available from: <https://doi.org/10.1016/j.dib.2024.109755>
- Yenket, R., & Chambers IV, E. 2007. Color Has Little Effect on Perception of Fabric Handfeel Tactile Properties in Cotton Fabrics. *Journal of Sensory*

- Studies*. [Online]. **22**(3), pp. 336-352. [Accessed 18 February 2025]. Available from: <https://onlinelibrary.wiley.com/doi/abs/10.1111/j.1745-459X.2007.00109.x>
- Yim, K. Y., & Kan, C. W. 2014. A Comparison Study of Fabric Objective Measurement (FOM) Using KES-FB and PhabrOmeter System on Warp Knitted Fabrics Handle – Smoothness, Stiffness and Softness. *International Journal of Chemical, Molecular, Nuclear, Materials and Metallurgical Engineering*. [Online]. **8**(8), pp. 789-792. [Accessed 18 February 2025]. Available from: <https://citeseerx.ist.psu.edu/document?repid=rep1&type=pdf&doi=5e7b1877b4a8286b069f6bda0b61ccc1e2321c28>
- Yuan, W., Mo, Y., Wang, S., & Others. 2018. Active Clothing Material Perception Using Tactile Sensing and Deep Learning. In: IEEE. ed. *Proceedings of the IEEE International Conference on Robotics and Automation (ICRA 2018), 21–25 May 2018, Brisbane, Australia*. Piscataway, NJ: IEEE, pp. 4842–4849.
- Zhang, C., Feng, S., Wang, X., & Others. 2020. ZJU-LEAPER: A Benchmark Dataset for Fabric Defect Detection and a Comparative Study. *IEEE Transactions on Artificial Intelligence*. [Online]. **1**(3), pp. 219–232. [Accessed 16 February 2025]. Available from: <https://doi.org/10.1109/TII.2020.2975732>
- Zhang, J., Xin, B., and Wu, X. 2013. A review of fabric identification based on image analysis technology. *Textiles and Light Industrial Science and Technology*. [Online]. **2**(3), pp.120-130. [Accessed 9 March 2025]. Available from: https://www.academia.edu/download/47742690/TLIST10073_2_3_120_130.pdf
- Zhang, P., Wang, D., & Zhang, Y. 2017. Analysis of Correlation Between Image Texture and Friction Coefficient of Materials. In: IEEE. ed. *Proceedings of the IEEE International Conference on Systems, Man, and Cybernetics, 18-*

20 October 2017, Beijing, China. Piscataway, NJ: IEEE, pp. 1–6.

List of Abbreviations

2D FFT	2-Dimensional Fast Fourier Transform
AIC	Akaike Information Criterion
AWB	Auto White Balance
BIC	Bayesian Information Criterion
CIE	Commission Internationale de L' Éclairage (International Commission on Illumination)
CIELAB	CIE 1976 (L*a*b*) Colour Space
CLM	Cumulative Link Model
CLMM	Cumulative Link Mixed Model
CMFs	Colour matching functions
CNN	Convolutional Neural Network
CWT	Continuous Wavelet Transform
DFT	Discrete Fourier Transform
DOF	Depth Of Field
DSLR	Digital Single-Lens Reflex camera
DWT	Discrete Wavelet Transform
EMMs	Estimated Marginal Means
EN	The Elastic Net Regression
FAST	Fabric Assurance by Simple Testing
FFT	Fast Fourier Transform
GLCM	Grey-level Co-occurrence Matrix
GOG	Gain-Offset-Gamma
IQR	Interquartile Range
ISP	Image Signal Processor
KES-F	Kawabata Evaluation System for Fabric
LASSO	Least Absolute Shrinkage and Selection Operator Regression
LCD	Liquid Crystal Display
LRT	Likelihood Ratio Test

LUFHES	Leeds University Fabric Handle Evaluation System
OLS	Ordinary Least Squares Regression (OLS)
RMS	Root Mean Squares
RMSE	Root Mean Square Error
RR	The Ridge Regression
RSS	Residual sum of squares
SCE	Specular excluded
SCI	Specular included
SD	Standard Deviation
SPD	Spectral power distribution
TPT	Touch Perception Task
VLB	X-Rite® Virtual Lighting Booth
WT	Wavelet Transform

Appendix A: the fabric materials in Leeds Fabric Tactile Database

Part I

Fabric 1	Coated cotton duck PK44 white
Fabric 2	Polyester crepe back satin white
Fabric 3	Kova wool sateen white
Fabric 4	Cotton satin medium white
Fabric 5	Milk till white
Fabric 6	Coated cotton twill SG78 white
Fabric 7	Coated twill silk heavy (PL80) white
Fabric 8	Plain cotton white
Fabric 9	Polyester voile white
Fabric 10	Fusible H616 polyester white
Fabric 11	Polyester jersey troon white
Fabric 12	Viscos/cotton rib Siberia natural
Fabric 13	Fabric collected in Testing lab in Schol of Design, University of leeds
Fabric 14	Fabric collected in Testing lab in Schol of Design, University of leeds
Fabric 15	Fabric collected in Testing lab in Schol of Design, University of leeds

Part II

Fabric 1	92% Merino 8% Nylon
Fabric 2	100% Merino
Fabric 3	100% Merino
Fabric 4	100% Merino
Fabric 5	55% Poly/45% Wool

Fabric 6	100% Merino
Fabric 7	95% Merino 5% Nylon
Fabric 8	85% Merino 15% Other Fibres
Fabric 9	100% Merino
Fabric 10	100% Merino
Fabric 11	100% Merino
Fabric 12	100% Merino
Fabric 13	100% Merino
Fabric 14	100% Merino
Fabric 15	100% Merino
Fabric 16	95% Merino / 5% Nylon
Fabric 17	85 lambswool/ 15% cashmere
Fabric 18	100% Merino
Fabric 19	100% Merino
Fabric 20	100% Merino
Fabric 21	70% Viscose, 30% Linen
Fabric 22	100% Viscose
Fabric 23	100% Viscose
Fabric 24	52% Polyester, 48% Viscose
Fabric 25	87% Cotton, 13% Polyester
Fabric 26	45% Viscose, 55% Linen
Fabric 27	100% Linen
Fabric 28	100% Linen
Fabric 29	50% Polyester, 47% Viscose, 3% Spandex
Fabric 30	60% Cotton, 40% Polyester
Fabric 31	100% Organic cotton
Fabric 32	96% Viscose, 4% Spandex
Fabric 33	100% Cotton
Fabric 34	90% Polyester, 10% Spandex

Fabric 35	85% Polyester, 12% metal-coated polyester, 3% Spandex
Fabric 36	100% Cotton
Fabric 37	80% Polyester, 16% Viscose, 4% Spandex
Fabric 38	100% Viscose
Fabric 39	75% Viscose, 25% Linen
Fabric 40	Cosy hand, light, fleecy, Horizontal Stretch, soft
Fabric 41	100% Polyester
Fabric 42	92% Polyester, 8% Polyamide
Fabric 43	70% Polyacrylic, 30% Polyester
Fabric 44	100% Polyester
Fabric 45	100% Organic cotton
Fabric 46	77% Viscose, 20% Polyester, 3% Spandex
Fabric 47	80% Viscose, 18% Nylon, 2% Spandex
Fabric 48	100% Cotton
Fabric 49	55% Cotton, 40% Polyester, 5% Spandex
Fabric 50	96% Cotton, 4% Spandex
Fabric 51	65% Cotton, 35% Polyester
Fabric 52	50% Polyester, 48% Cotton, 2% Spandex
Fabric 53	100% Organic cotton
Fabric 54	100% Cotton
Fabric 55	92% Merino 8% Nylon
Fabric 56	100% Merino
Fabric 57	100% Merino
Fabric 58	100% Merino
Fabric 59	55% Poly/45% Wool
Fabric 60	100% Merino
Fabric 61	95% Merino 5% Nylon
Fabric 62	85% Merino 15% Other Fibres
Fabric 63	100% Merino

Fabric 64	100% Merino
Fabric 65	100% Merino
Fabric 66	100% Merino
Fabric 67	100% Merino
Fabric 68	100% Merino
Fabric 69	100% Merino
Fabric 70	95% Merino / 5% Nylon
Fabric 71	85 lambswool/ 15% cashmere
Fabric 72	100% Merino
Fabric 73	100% Merino
Fabric 74	100% Merino
Fabric 75	70% Viscose, 30% Linen
Fabric 76	100% Viscose
Fabric 77	100% Viscose
Fabric 78	52% Polyester, 48% Viscose
Fabric 79	87% Cotton, 13% Polyester
Fabric 80	45% Viscose, 55% Linen
Fabric 81	100% Linen
Fabric 82	100% Linen
Fabric 83	50% Polyester, 47% Viscose, 3% Spandex
Fabric 84	60% Cotton, 40% Polyester
Fabric 85	100% Organic cotton
Fabric 86	96% Viscose, 4% Spandex
Fabric 87	100% Cotton
Fabric 88	90% Polyester, 10% Spandex
Fabric 89	85% Polyester, 12% metal-coated polyester, 3% Spandex
Fabric 90	100% Cotton
Fabric 91	80% Polyester, 16% Viscose, 4% Spandex
Fabric 92	100% Viscose

Fabric 93	75% Viscose, 25% Linen
Fabric 94	Cosy hand, light, fleecy, Horizontal Stretch, soft
Fabric 95	100% Polyester
Fabric 96	92% Polyester, 8% Polyamide
Fabric 97	70% Polyacrylic, 30% Polyester
Fabric 98	100% Polyester
Fabric 99	100% Organic cotton
Fabric 100	77% Viscose, 20% Polyester, 3% Spandex
Fabric 101	80% Viscose, 18% Nylon, 2% Spandex
Fabric 102	100% Cotton
Fabric 103	55% Cotton, 40% Polyester, 5% Spandex
Fabric 104	96% Cotton, 4% Spandex
Fabric 105	65% Cotton, 35% Polyester
Fabric 106	50% Polyester, 48% Cotton, 2% Spandex
Fabric 107	100% Organic cotton
Fabric 108	100% Cotton
Fabric 109	92% Merino 8% Nylon
Fabric 110	100% Merino
Fabric 111	100% Merino
Fabric 112	100% Merino
Fabric 113	55% Poly/45% Wool
Fabric 114	100% Merino
Fabric 115	95% Merino 5% Nylon
Fabric 116	85% Merino 15% Other Fibres
Fabric 117	100% Merino
Fabric 118	100% Merino

Appendix B: Ethical approval for the experiment

Phase I and Phase II.

Phase I:

Dear Qinyuan

LTDESN-159 - Visual and handle judgement of the tactile properties of the fabrics.

NB: All approvals/comments are subject to compliance with current University of Leeds and UK Government advice regarding the Covid-19 pandemic.

I am pleased to inform you that your proportionate touch research ethics application has been reviewed by the Faculty of Arts, Humanities and Cultures Research Ethics Committee (AHC) and I can confirm this has received a favourable ethical opinion based on the documentation received at date of this email.

The reviewers had some comments for your consideration, these do not impact your approval. If you decide to update any documents in response to these comments please submit these to this email address for storage:

1. **The information sheet or advertising materials should explain how participants will be compensated for their time.**
2. **The question about how participants will be identified (and recruited) hasn't been addressed fully. If participants are students, please follow the guidance on using students as research participants.**

Please retain this email as evidence of approval in your study file.

Please notify the committee if you intend to make any amendments to the original research as submitted and approved to date. This includes recruitment methodology; all changes must receive ethical approval prior to implementation. Please see <https://ris.leeds.ac.uk/research-ethics-and-integrity/applying-for-an-amendment/> or contact the Research Ethics Administrator for further information (ahcresearchethics@leeds.ac.uk) if required.

Ethics approval does not infer you have the right of access to any member of staff or student or documents and the premises of the University of Leeds. Nor does it imply any right of access to the premises of any other organisation, including clinical areas. The committee takes no responsibility for you gaining access to staff, students and/or premises prior to, during or following your research activities.

Please note: You are expected to keep a record of all your approved documentation, as well as documents such as sample consent forms, risk assessments and other documents relating to the study. This should be kept in your study file, which should be readily available for audit purposes. You will be given a two week notice period if your project is to be audited.

It is our policy to remind everyone that it is your responsibility to comply with Health and Safety, Data Protection and any other legal and/or professional guidelines there may be.

I hope the study goes well.

Very best wishes,
George

On behalf of Professor Robert Jones (AHC REC Chair)

Georgina Hough, Administrative Assistant, The Secretariat, University of Leeds, LS2 9NL, g.hough1@leeds.ac.uk

Please note I currently work with Research Ethics (Mon, Tue, Thur, Fri) and QA CTIMPs (Wed).

Phase II:

Dear Qinyuan,

LTDESN-159 Amendment 1 Feb 2024 - Visual and handle judgement of the tactile properties of the fabrics

We are pleased to inform you that your amendment to your research ethics application has been reviewed by the Faculty of Arts, Humanities & Cultures Research Ethics Committee (AHC REC) and we can confirm that ethics approval is granted based on the documentation received at date of this email.

Please retain this email as evidence of approval in your study file.

Please notify the committee if you intend to make any further amendments to the research as submitted and approved to date. This includes recruitment methodology; all changes must receive ethical approval prior to implementation. Please see <https://secretariat.leeds.ac.uk/research-ethics/how-to-apply-for-research-ethics-amendment/> or contact the Research Ethics team for further information ahcresearchethics@leeds.ac.uk if required.

Ethics approval does not infer you have the right of access to any member of staff or student or documents and the premises of the University of Leeds. Nor does it imply any right of access to the premises of any other organisation, including clinical areas. The committee takes no responsibility for you gaining access to staff, students and/or premises prior to, during or following your research activities.

Please note: You are expected to keep a record of all your approved documentation, as well as documents such as sample consent forms, risk assessments and other documents relating to the study. This should be kept in your study file, which should be readily available for audit purposes. You will be given a two week notice period if your project is to be audited.

It is our policy to remind everyone that it is your responsibility to comply with Health and Safety, Data Protection and any other legal and/or professional guidelines there may be.

I hope the study continues to go well.

Best wishes,

Taylor Haworth, Phoenix Lead, Research Ethics, Secretariat

On behalf of Dr Rach Cosker-Rowland, Chair, Faculty Research Ethics Committee